

ANAEROBIC OXIDATION OF METHANE IN COLD SEEPS AND GAS HYDRATES:
RESPONSIBLE MICROORGANISMS, RATES OF ACTIVITY, AND INTERACTIONS
WITH OTHER PROCESSES

by Beth! N. Orcutt

(under the supervision of Samantha B. Joye)

ABSTRACT

This work utilized a multidisciplinary approach to explore the microbial biogeochemistry of methane cycling in the marine environment with the aim of identifying which processes were occurring and which microorganisms were involved, focusing on two methane-rich systems: oil-laden, gas hydrate-bearing and/or brine-charged cold seeps in the Gulf of Mexico and the Hydrate Ridge deep biosphere. The research presented here expands our knowledge of microbially-mediated anaerobic oxidation of methane (AOM) and associated process such as sulfate reduction (SR) and methanogenesis in surficial and deep methane-rich environments. This work confirmed that the ANME-1 and -2 clades of methanotrophic archaea are responsible for AOM in surficial sediments in the Gulf of Mexico and was the first to demonstrate that the ANMEs are also involved in the production of methane, although at a fraction of the rate of AOM. Our work was the first to directly document microbial activity within gas hydrate material collected from the Gulf of Mexico, which suggests that microbial activity may impact the biogeochemical cycling of methane within the unique gas hydrate niche. Active populations of both *Bacteria* and *Archaea* were observed in a methane-rich deep biosphere environment, in contrast to previous studies which suggest that one or the other domain is dominant. In methane-rich areas of the deep subsurface, ANME were detected for the first time in an area where sulfate levels were elevated, although AOM may be limited in the deep biosphere by the availability of

sulfate coupled with slow growth rates. Unlike at other cold seeps which have been studied to date, SR in Gulf of Mexico surficial sediments is often uncoupled from AOM and is also fueled by other endogenous hydrocarbons and petroleum derivatives; the identity of the microorganisms which mediate sulfate-dependent hydrocarbon oxidation *in situ* is unclear but likely includes members of the seep-endemic *Deltaproteobacteria* sulfate reducing bacterial (SRB) clades. Modeling approaches to determine the potential intermediate compound exchanged within consortia of ANME and SRB to sustain AOM and SR revealed that hydrogen, acetate and formate cannot sustain rates of activity that match measured values due to diffusion-limited removal of the intermediate compound.

INDEX WORDS: Anaerobic oxidation of methane, Sulfate Reduction, Methanogenesis, Biogeochemistry, Molecular Ecology, Lipid biomarkers, Gas hydrate, Cold seeps, Gulf of Mexico, Oil, Reaction transport model, Deep biosphere, Hydrate Ridge, Thermodynamics, Archaea, Ocean Drilling Program

ANAEROBIC OXIDATION OF METHANE IN COLD SEEPS AND GAS HYDRATES:
RESPONSIBLE MICROORGANISMS, RATES OF ACTIVITY, AND INTERACTIONS
WITH OTHER PROCESSES

by

BETH! NOELLE ORCUTT

B.S. Interdisciplinary Studies, University of Georgia, 2002

A Dissertation Submitted to the Graduate Faculty of the University of Georgia in Partial
Fulfillment of the Requirements for the Degree

DOCTOR OF PHILOSOPHY

ATHENS, GEORGIA

2007

© 2007

Beth! N. Orcutt

All Rights Reserved

ANAEROBIC OXIDATION OF METHANE IN COLD SEEPS AND GAS HYDRATES:
RESPONSIBLE MICROORGANISMS, RATES OF ACTIVITY, AND INTERACTIONS
WITH OTHER PROCESSES

by

BETH! NOELLE ORCUTT

Major Professor:

Samantha B. Joye

Committee:

Antje Boetius
Christof Meile
Mary Ann Moran
Stuart Wakeham
William Whitman

Electronic Version Approved:
Maureen Grasso
Dean of the Graduate School
The University of Georgia
May 2007

ACKNOWLEDGEMENTS

There are many people I would like to thank for helping make this dissertation possible, either for helping me with my work or for offering support, encouragement and good jokes, or both. I am so thankful for my advisor, Mandy Joye, for giving me the opportunity as an undergraduate to explore the fascinating world of environmental microbial biochemistry, for providing incredible research opportunities, for inspiring me to pursue a career in science, and for being a friend. None of this would have been possible without the initial support of Steve Carini, who brought me into the lab and taught me much of what I know. Many thanks to my other UGA labmates – Steve Bell, Meaghan Bernier, Marshall Bowles, Jon Clark, Matty Erickson, Kim Hunter, Rosalynn Lee, Bill Porubsky, Kate Segarra, and Nat Weston – for keeping the energy level high and the machines working. There are others at UGA who have helped me along the way that I would like to thank – Jen Fisher, Tim Hollibaugh, Christof Meile, Mary Ann Moran, Rachel Poretsky, Stuart Wakeham and Barny Whitman.

I owe a huge debt of gratitude to Antje Boetius, my home-away-from-home advisor in Bremen, Germany. Thank you so much for supporting my many visits to your labs, for encouraging me to push the boundaries of what I can do, and for being a fabulous role model. To everyone at the MPI who helped me out over the years – Viola Beier, Imke Busse, Marcus Elvert, Niko Finke, Katrin Knittel, Tina Lösekann, Jochen Neuster, Helge Niemann, and Tina Treude – thank you, especially to my office mate and chaos girl Nina Knab.

To the RCOM Organic Geochemistry Group in Bremen, thanks for offering one of the friendliest and most inspiring working environments. Much of my lipid biomarker work would not have been possible without Kai-Uwe Hinrichs allowing me to work in his lab – thank you. Thanks again to Marcus Elvert for always being there with advice and for never relenting in

telling me to learn German. Julius Lipp has been a great working partner for the deep biosphere project – thanks for putting up with my overseas requests! Daniel Birgel, Solveig Bühring, Verena Heuer, Xavi Prieto, Pamela Rossel, Flo Schübotz, and Julio Sepúlveda – I can't thank you enough for your encouragement and your enduring friendship.

I consider myself blessed to have friends far and wide that share my enthusiasm for understanding the world and trying to make it a better place. Jelte Harnmeijer, I will never forget our adventures. Emily Fleming, you are welcome to stay on a couch I sell out from under you anytime. John Spear, your compassionate instruction in the field, in the lab, in the classroom, and in general render you an invaluable role model in my book.

Thanks to the unknown reviewers of my NSF graduate research fellowship application – I couldn't have done half of what I did without the support their decision led to.

And finally, thanks to my high school chemistry teacher – Mr. Lanham – for sparking my imagination and setting me on the path of the pursuit of truth.

TABLE OF CONTENTS

	Page
ACKNOWLEDGEMENTS.....	vi
LIST OF TABLES.....	viii
LIST OF FIGURES.....	x
CHAPTER	
1 INTRODUCTION AND LITERATURE REVIEW.....	1
2 MICROBIAL BIOGEOCHEMISTRY OF SULFATE REDUCTION, METHANOGENESIS AND THE ANAEROBIC OXIDATION OF METHANE AT GULF OF MEXICO COLD SEEPS.....	37
3 IMPACT OF OIL AND HIGHER HYDROCARBONS ON MICROBIAL DIVERSITY, DISTRIBUTION AND ACTIVITY IN GULF OF MEXICO SEDIMENTS.....	88
4 ON THE RELATIONSHIP BETWEEN METHANE PRODUCTION AND OXIDATION BY ANAEROBIC METHANOTROPHIC COMMUNITIES FROM COLD SEEPS OF THE GULF OF MEXICO.....	131
5 LIFE AT THE EDGE OF METHANE ICE: MICROBIAL CYCLING OF CARBON AND SULFUR IN GULF OF MEXICO GAS HYDRATES.....	162
6 <i>BACTERIA</i> AND <i>ARCHAEA</i> AND THEIR ACTIVITY IN HYDRATE- BEARING DEEP SUBSURFACE SEDIMENTS OF HYDRATE RIDGE (CASCADIA MARGIN, ODP LEG 204).....	194

7	CONSTRAINTS ON MECHANISMS AND RATES OF ANAEROBIC OXIDATION OF METHANE BY ANME-2 CONSORTIA.....	249
8	CONCLUSIONS.....	284

LIST OF TABLES

	Page
Table 2.1: Concentrations of sulfide and chloride, total cell abundance, and percentage of cells that were <i>Bacteria</i> , <i>Archaea</i> , of the ANME-1 clade of <i>Euryarchaeota</i> , of the ANME-2 clade of <i>Euryarchaeota</i> , or of the <i>Desulfosarcina/Desulfococcus</i> spp. clades of δ -proteobacteria in sediments from the Gulf of Mexico.....	67
Table 2.2: Isotopic composition of various carbon compounds from gas hydrate and brine pool sites in the Gulf of Mexico.....	68
Table 2.3A: Abundance and isotopic composition of select lipid biomarkers extracted from sediments at a brine influence site in the Gulf of Mexico.....	69
Table 2.3B: Abundance and isotopic composition of select lipid biomarkers extracted from sediments at a gas hydrate site in the Gulf of Mexico.....	70
Table 3.1: Gulf of Mexico site and sample descriptions.....	116
Table 3.2: Integrates rates of sulfate reduction, the anaerobic oxidation of methane, methanogenesis from carbon dioxide or from acetate, and acetate oxidation and estimated turnover times of the methane, sulfate, and acetate pools for hydrocarbon-rich sediments from the Gulf of Mexico.....	117
Table 3.3: Overview of 16S gene sequences obtained from Gulf of Mexico sediments.....	118
Table 4.1: Site descriptions for the Gulf of Mexico sediments used in these experiments.....	152
Table 4.2: Abundance of ANME groups in sediments.....	153
Table 5.1: Average hydrocarbon gases of hydrate material and vent gas.....	183
Table 5.2: Rates of AOM and SR in gas hydrate material collected from two sites in the Gulf of Mexico.....	184

	Page
Table 6.1: Southern Hydrate Ridge (ODP Leg 204) site characteristics.....	226
Table 6.2: Primers used for specific amplification of SRB.....	227
Table 6.3: Composition of bacterial and archaeal apolar and polar lipids and relative composition of microbial community in Hydrate Ridge deep biosphere sediments (ODP Leg 204).....	228
Table 6.4: Overview of 16S rRNA gene sequences obtained from Hydrate Ridge sediment using general archaeal and bacterial primers.....	229
Table 6.5: Rates of AOM and OC degradation activity and corresponding energy yields and requirements for microbial communities in the Southern Hydrate Ridge deep biosphere sediments (ODP Leg 204).....	230
Table 7.1: Potential coupled reactions of AOM and SR and the corresponding standard free energy yield of the reactions.....	271
Table 7.2: Survey of available data on AOM/SR-mediating consortia sizes, cell sizes, and cell ratios.....	272
Table 7.3: Properties of compounds considered in the model.....	273
Table 7.4: Model parameters.....	274
Table 7.5: Consortia size, abundance and rates of activity measured in ANME2/DSS aggregates.....	275

LIST OF FIGURES

	Page
Figure 1.1: Reservoirs of methane on Earth.....	3
Figure 1.2: Sources of methane to the atmosphere.....	4
Figure 1.3: Production and consumption of methane in various systems.....	6
Figure 1.4: Simplified phylogenetic tree of archaea, including known methanogens and groups involved in AOM or methane cycling.....	8
Figure 1.5: Methanogenic pathways from CO ₂ and acetate.....	11
Figure 1.6: Structures of select archaeal and bacterial lipid biomarkers.....	14
Figure 2.1: Composite profiles of geochemistry, rates of microbial processes, microorganism diversity and abundance, and abundance and isotopic composition of select lipid biomarkers in sediments collected from underneath a bacterial mat at a brine pool cold seep in the Gulf of Mexico.....	74
Figure 2.2: Composite profiles of geochemistry, rates of microbial processes, microorganism diversity and abundance, and abundance and isotopic composition of select lipid biomarkers in sediments collected from underneath a bacterial mat at a gas hydrate cold seep in the Gulf of Mexico.....	75
Figure 2.3: Photomicrographs of microorganisms in Gulf of Mexico sediments identified using CARD-FISH.....	76
Figure 2.4: Schematic illustrating the interactions between AOM, SR and MOG, the geochemical, and the geological environment at the two cold seep environments.....	77
Figure 3.1: Study sites and sediment types in the Gulf of Mexico.....	119

Figure 3.2: Composite profiles of geochemical species and rates of microbial processes measured in sediments collected from Station 87/Site GC234, Station 140/Site Chapopote, Station 156/Site GC185, Station 161/Site GC415 and Dive 4463/Site GC232 in the Gulf of Mexico.....	120
Figure 3.3: C ₁₅₊ chromatograms of saturated hydrocarbons indicate the loss of distinguishable isoprenoids and alkanes in the heavily biodegraded oils in Station 140 sediments as compared to Station 87 sediments.....	122
Figure 3.4: Concentration profiles of C ₁ (methane), C ₂ (ethane), C ₃ (propane), iC ₄ (<i>iso</i> -butane), and C ₄ (<i>n</i> -butane) alkanes in sediments from the Gulf of Mexico.....	123
Figure 3.5: Phylogenetic tree showing the affiliations of Gulf of Mexico 16S rRNA gene sequences to selected reference sequences of the <i>Deltaproteobacteria</i>	124
Figure 3.6: Phylogenetic tree showing the affiliations of Gulf of Mexico 16S rRNA gene sequences to selected reference sequences of the <i>Archaea</i>	125
Figure 4.1: Study sites in the Gulf of Mexico from SO-174.....	154
Figure 4.2: Microbial activity of sulfate reduction, anaerobic oxidation of methane, and methanogenesis measured in experiment 1.....	155
Figure 4.3: Rates of microbial activity in slurried sediment from Station 156 in relation to various methane concentrations.....	156
Figure 4.4: Rates of microbial activity in slurries amended with hydrogen and with or without methane.....	157
Figure 5.1: Layers of Gulf of Mexico gas hydrate used in these experiments.....	185
Figure 5.2: An underwater photo of a surface-breaching hydrate.....	186

	Page
Figure 5.3: Microscopic images of microorganisms stained with AO from material from the interface sediment and interior hydrate.....	187
Figure 5.4: Rates of AOM and SR in hydrate material collected from Gulf of Mexico hydrate sites in 2001 and 2002.....	188
Figure 6.1: Geochemical characteristics and microbial activity in sediments collected from Site 1249 at the summit of Southern Hydrate Ridge (ODP Leg 204).....	232
Figure 6.2: Geochemical characteristics and microbial activity in sediments collected from Site 1250 at the summit of Southern Hydrate Ridge (ODP Leg 204).....	233
Figure 6.3: Comparison of the stable carbon isotopic composition of sedimentary methane, TOC and DIC with select polar- and apolar- derived lipid biomarkers for archaea.....	234
Figure 6.4: Geochemical characteristics and microbial activity in sediments collected from Site 1251 on the eastern slope basin of Southern Hydrate Ridge (ODP Leg 204).....	235
Figure 6.5: CARD FISH micrograph of ANME-1 cells.....	236
Figure 6.6: Phylogenetic tree showing the affiliations of Site 1249 54 mbsf, and 1250 24 mbsf, 16S rRNA gene sequences to selected sequences of the <i>Archaea</i>	237
Figure 6.7: 16S rRNA phylogenetic tree showing the affiliations of the detected groups of sulfate-reducing bacteria at Sites 1249, 54 mbsf and 1250, 24 mbsf, to selected sequences of the <i>Deltaproteobacteria</i>	238
Figure 7.1: AOM and SR mediating consortia.....	278
Figure 7.2: Values of F_{TAOM} in a 25 μm OD aggregate for various combinations of k_{AOM} and k_{SR} (units of $\text{nmol cell}^{-1} \text{d}^{-1}$) when K_{mH_2} equals 10 nM or 0.1 nM.....	279

Figure 7.3: Values of F_{TAOM} for various combinations of k_{AOM} and k_{SR} when K_{mH_2} equals 1 nM and the size of the consortia is 4, 12 or 25 $\mu\text{m OD}$	280
Figure 7.4: Values of F_{TAOM} for a 3 $\mu\text{m OD}$ consortia when K_{mH_2} for SRB is 0.1 nM, H_2 equals 10 nM and the environmental boundary is placed at 2 or 10 μm	281
Figure 7.5: Values of F_T for a 3 $\mu\text{m OD}$ consortia when K_{mH_2} for SRB is 0.1 nM and the environmental concentration of hydrogen is forced to be 0.1, 1 or 10 nM.....	282
Figure 7.6: Values of F_{TAOM} for a 25 $\mu\text{m OD}$ aggregate and a 3 $\mu\text{m OD}$ aggregate under no gradient conditions when $K_{mAc} = 1, 10$ or 100 nM.....	283

CHAPTER 1

INTRODUCTION and LITERATURE REVIEW

The following introduction explains why methane is a compound worthy of study from a microbial biogeochemical perspective and explores the current body of knowledge regarding microbially-mediated methane dynamics. The first sections provide an overview of the chemical and physical properties of methane as well as the importance of methane as a greenhouse gas, exploring how atmospheric methane has changed over geologic time. The next sections summarize the contemporary global methane budget with a focus on sources and sinks. The oceanic sources and sinks of methane are then discussed in more detail, detailing the processes and microorganism responsible for methane consumption or production. The variety of methane-rich habitats in the ocean is explained and new frontiers of methane cycling research are described. Finally, the last sections outline the main objectives of this work.

METHANE'S PROPERTIES AND IMPORTANCE AS A GREENHOUSE GAS

Methane is simultaneously the most reduced form of carbon and the simplest organic molecule, consisting of one carbon atom covalently bonded to four hydrogen atoms. Since it is a non-polar molecule, methane is only slightly soluble in water (saturation at atmospheric pressure is ~1.4 mM in seawater); salinity and temperature have a negative effect on methane solubility (YAMAMOTO et al., 1976).

As a greenhouse gas, methane can absorb and re-emit infrared radiation. Being roughly 25 times more effective at trapping heat than carbon dioxide (LELIEVELD et al., 1998), another

greenhouse gas, methane concentration in the atmosphere can significantly influence the energy budget of the Earth. Estimates indicate that methane is responsible for 20% of contemporary global warming (WUEBBLES and HAYHOE, 2002). Currently, the atmosphere has a methane concentration of almost 1.8 ppmv, which is a ~150% increase since pre-industrial times (IPCC, 2001).

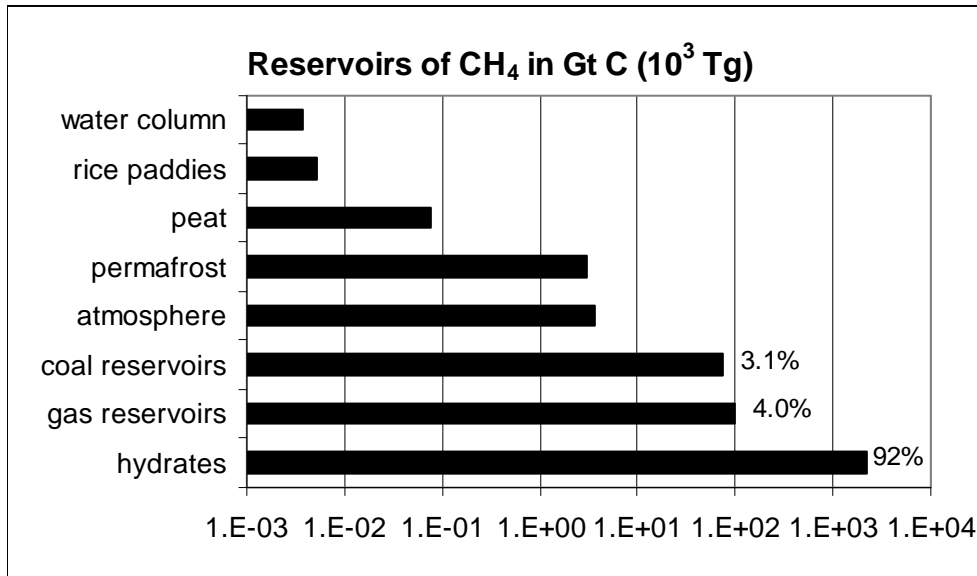
Throughout Earth's history, changes in the inventory of methane in the atmosphere have positively co-varied with increases in temperature (KASTING, 2004). The rise in concentration of methane likely contributed to the warming experienced during those periods. Some researchers suggest that large releases of methane from the ocean floor may have triggered the increase in atmospheric methane concentrations and thus driven temperature increases (DICKENS et al., 1995; KENNETT et al., 2000; THOMAS et al., 2002).

RESERVOIRS, SOURCES AND SINKS FOR METHANE

There are several reservoirs or 'standing stocks' of methane on Earth. A summary of the sizes of the reservoirs has been described previously (WHITICAR, 1990), although more recent evaluations have adjusted some pool sizes up or down. By far the largest reservoir of methane (92%) occurs buried in the seafloor in the form of gas hydrates or methane clathrates (Fig.1). Methane clathrates are ice-like structures which trap methane and other gases within a rigid lattice of ice cages that form under specific temperature and pressure conditions when sufficient methane and water are available (KVENVOLDEN, 1993). Some reports estimate that over 50% of organic matter (i.e. 10,000 gigatons of carbon, GtC) on Earth occurs as methane trapped in hydrate (KVENVOLDEN, 1993). More recent estimates, however, suggest that hydrate-bound methane accounts for 5-22% of Earth's organic matter (MILKOV et al., 2005). Gas hydrates are

typically found on outer continental margins; these areas are characterized by low temperature, high pressure and sufficient methane supply from decomposing organic matter.

The next largest stocks of methane (7% of the total) are found in natural gas, oil, and coal deposits. Methane in these deposits can originate either from thermal degradation of other hydrocarbons and organic matter or from biological production. Permafrost, or terrestrial



hydrates, contain 3 Gt C worldwide; although this is only 0.12% of the total methane pool, melting of permafrost would double the atmospheric methane burden.

Figure 1.1. Reservoirs of methane on Earth, modified from (WHITICAR, 1990)

Standing stocks of methane in peat, rice paddies, and in the water columns of the world's oceans and lakes make up a trivial fraction (0.003%) of the global methane pool. The last reservoir of methane occurs in the atmosphere.

Although the concentration of methane in the atmosphere is relatively low compared to other compounds like water vapor or carbon dioxide, it is the most abundant organic compound in the atmosphere, and as mentioned previously, is an important factor in Earth's greenhouse warming. The burden of methane in the atmosphere is ~5000 Tg CH₄ which is 0.15% of

Earth's methane reservoir (IPCC, 2000). The average residence time of methane in the atmosphere is ~8 years (LELIEVELD et al., 1998).

The flux of methane in and out of the atmospheric reservoir is dynamic and in transition. The most recent calculations estimate that ~600 Tg C of methane enters the atmosphere annually (IPCC, 2001; KVENVOLDEN and ROGERS, 2005; REEBURGH, 1996). Hydroxyl molecules in the atmosphere scavenge the methane and convert it to carbon dioxide and water at the rate of 450 Tg C yr⁻¹ (CICERONE and OREMLAND, 1996).

Aerobic methane oxidizers in soil also consume a fraction of atmospheric methane. The flux of methane into the atmosphere is currently greater than the removal of methane through scavenging and consumption, leading to an average increase of methane in the atmosphere of 1% per year (IPCC, 2001).

Currently, anthropogenic factors are cumulatively the largest source of methane to

the atmosphere (Fig. 1.2). Global food production is a major contributor: release of methane from rice cultivation contributes 18% (110 Tg C) to the flux; effluent from enteric/ruminant animals such as cows contributes an additional 19% (115 Tg C). Incomplete oxidation of burning biomass is another significant anthropogenic source (7%) as is the release of methane from organic matter degradation in landfills (9%). Finally, production of oil, gas and coal

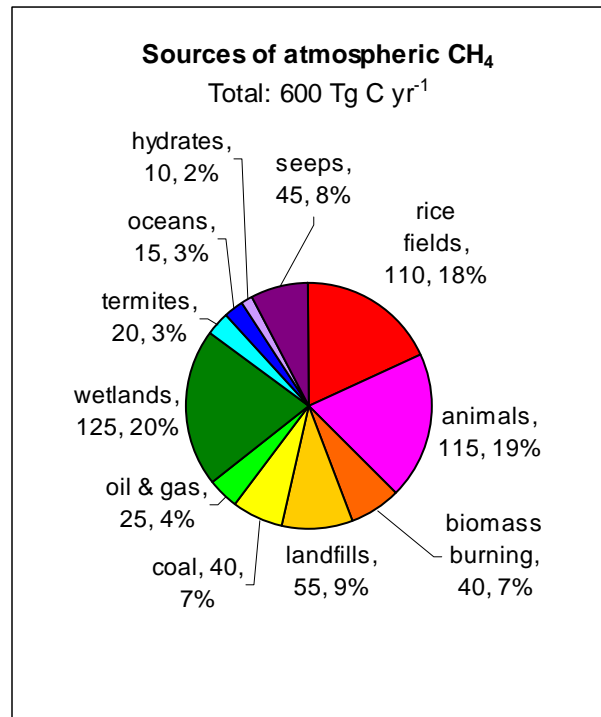


Figure 1.2. Sources of methane to the atmosphere. Middle value indicates magnitude of source in Tg C per year, percentage value indicates percent of total source. Modified from (IPCC, 2001; REEBURGH, 1996)

deposits for human energy demands results in the release of 65 Tg C (11%) to the atmosphere annually. Altogether, human activities result in a flux of 385 Tg C yr⁻¹ or 64.2% of the total source terms.

Release of methane from wetlands, including bogs, swamps, ponds and tundra, make up the largest natural source of methane to the atmosphere at 125 Tg C yr⁻¹ (Fig. 1.2). Termites are another smaller natural source of methane, formed from the breakdown of cellulosic materials by gut methanogens. The final natural sources of methane derive from oceanic and geological sources such as terrestrial and marine mud volcanoes, mid-ocean ridges, gas hydrates and cold seeps. The contribution of seeps as a source of atmospheric methane has been revised upward to 45 Tg C yr⁻¹ (8% of sources) in the past few years as more data has become available on the extent and magnitude of methane seepage in the world's oceans (KVENVOLDEN and ROGERS, 2005).

What are the processes that lead to these sources of methane to the atmosphere? To understand these source terms, and how they might change, we must look at the production and consumption of methane in each of these systems (Fig. 1.3). 577 Tg C of methane is produced in rice paddies annually (Fig. 1.3A) due to the development of anoxic conditions from flooding the paddies and enhanced transport of the methane from the rhizosphere through the aerenchyma of the rice plants (SEILER, 1984). Although aerobic microorganisms in the rice paddies consume a large portion of the produced methane, nearly 20% of the methane escapes to the atmosphere (Fig. 1.3B). All the methane produced by husbanded animals and biomass burning enters the atmosphere (Fig. 1.3A). 30% of the methane produced in landfills is re-oxidized (Figs. 3A, 3B); new technologies are being developed and implemented to capture landfill methane for re-use as

an energy source. Only 20% of the methane generated in wetlands is re-oxidized. Half of the methane produced by termites is re-oxidized in the surrounding soils.

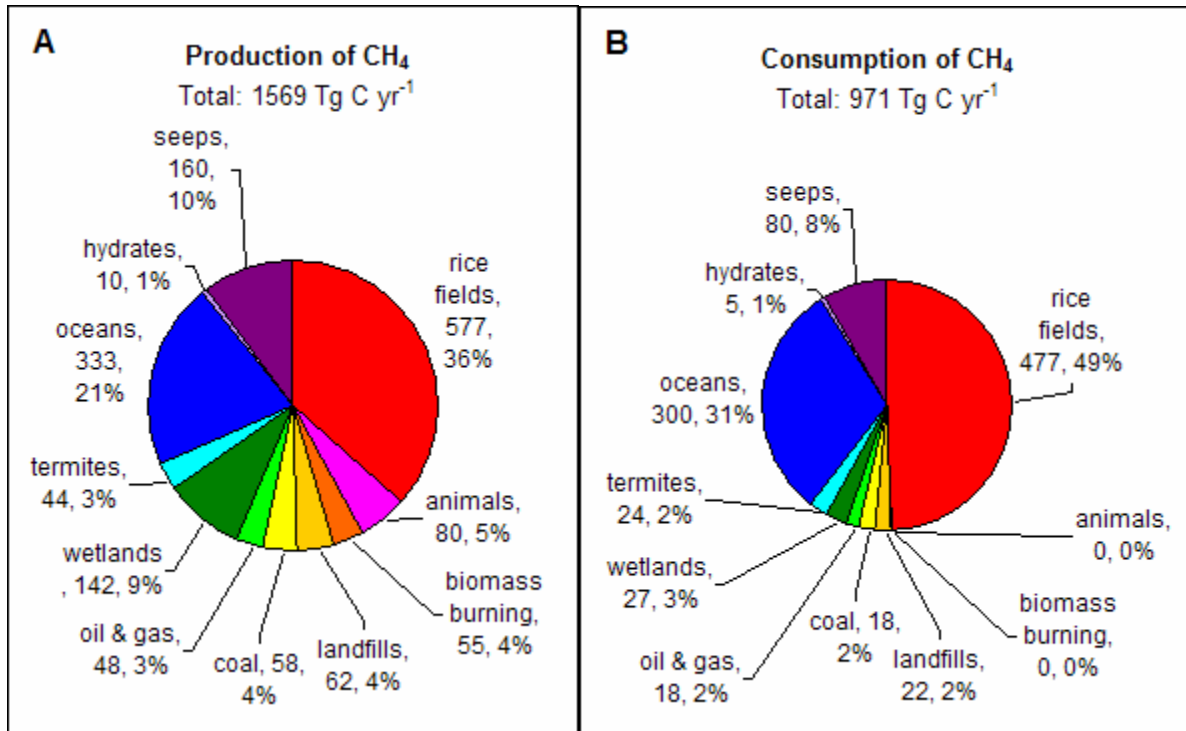


Figure 1.3. Production and consumption of methane in various systems. Modified from (HINRICHS and BOETIUS, 2002; REEBURGH, 1996; REEBURGH et al., 1993)

Finally, 50% of methane released from marine gas seeps and hydrates, and 90% of other oceanic methane sources, are microbially consumed (HINRICHS and BOETIUS, 2002; REEBURGH et al., 1993). The escape rate can be higher at seeps because methane can be advected out of the system before microorganisms have a chance to consume it. It is striking that oceanic seeps are not a larger source of methane to the atmosphere, as more than 92% of methane occurs below the ocean floor. The small magnitude of the oceanic seep source is due to efficient microbial consumption of methane in the environment (see below), preventing the release of methane to the hydro- or atmosphere. It should be noted that the methane flux from the ocean is poorly

constrained, as there are few data about the spatial extent and magnitude of methane flux at the various seepage features.

METHANE PRODUCTION IN THE MARINE ENVIRONMENT

Methane in marine sediments originates from abiotic and biotic sources. Abiotically, methane can be generated in the marine environment either by the thermal degradation of buried organic matter (LOLLAR et al., 2002) or by the reaction of H₂ and CO₂ during serpentinization reactions of peridotite rocks (KELLEY and FRÜH-GREEN, 1999). Organic matter deposited at the seafloor serves as an electron donor for a cascade of microbially-mediated redox reactions in the sediments, where the most energy rich electron acceptors (i.e. oxygen > nitrate > metal oxides > sulfate > CO₂) are consumed in a predictable serial fashion based on free energy yields of the reactions (FROELICH et al., 1979). In sediment diagenesis, the organic matter is decomposed to smaller and smaller organic compounds, eventually being “remineralized” back to inorganic CO₂. At the end of the redox chain, methane is formed biologically from CO₂ and other low molecular weight organic compounds by methanogenic archaea. Averaged globally, methanogenesis is responsible for about 5% of total organic carbon remineralization, although locally methanogenesis can be much a more important remineralization process, especially when sedimentation rates are high (CANFIELD et al., 2005; CRILL and MARTENS, 1986).

The ability to biologically produce methane is restricted to the strictly anaerobic methanogens which are divided into five different orders of the archaeal kingdom *Euryarchaeota* – *Methanobacteriales*, *Methanococcales*, *Methanomicrobiales*, *Methanosarcinales*, and *Methanopyrus* (CANFIELD et al., 2005; WHITMAN et al., 1999)(Fig. 1.4).

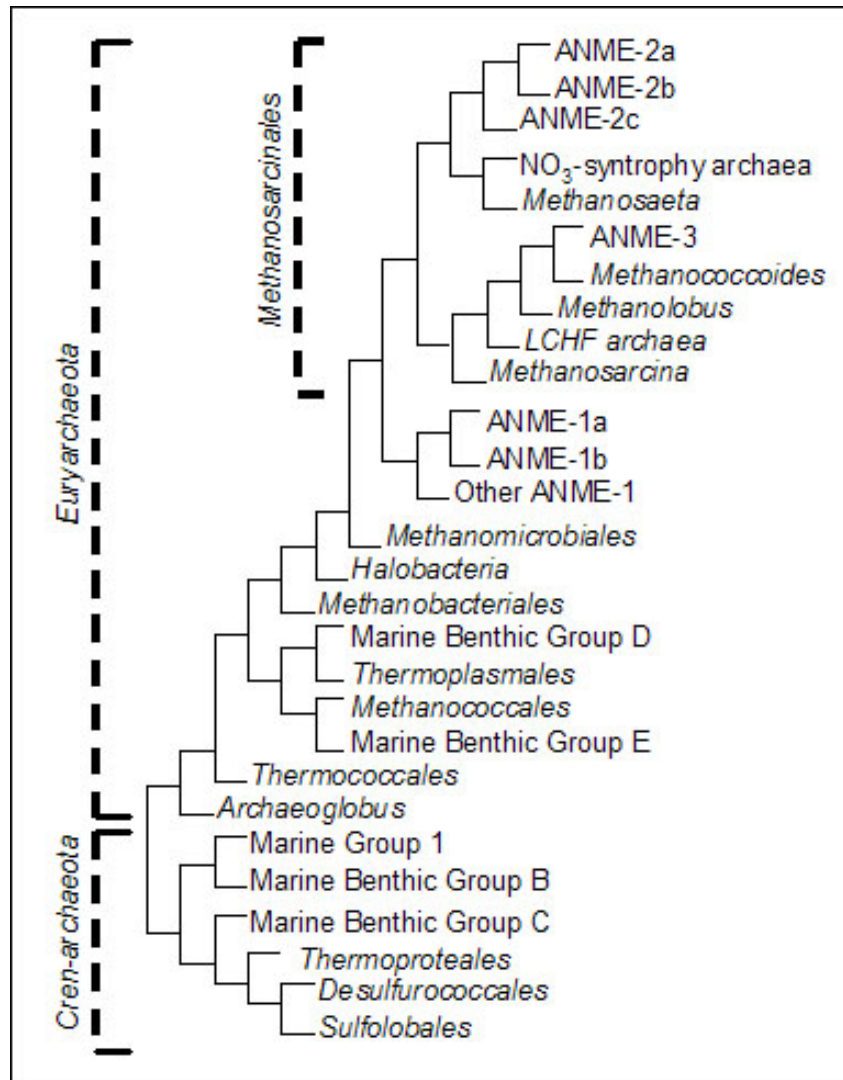
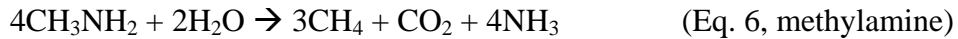


Figure 1.4. Simplified phylogenetic tree of archaea, including known methanogens and groups involved in AOM or methane cycling. Modified from (KNITTEL et al., 2005; RAGHOEBARSING et al., 2006; SCHRENK et al., 2004)

The substrates for methanogenesis include one carbon (C_1) compounds which are reduced by H_2 (Eq. 1) or alcohols to methane as well as carbon compounds (including formate (Eq. 2), acetate (Eq. 3), carbon monoxide (Eq. 4), methanol (Eq. 5), methylamines (Eq. 6), and methylsulfides (Eq. 7)) which are disproportionated to methane and CO_2 :





Comparison of the stable carbon isotopic compositions of methane and methanogenic substrate end-members provides a useful measurement of the relative contribution of the various methanogenic pathways. In nature, methane occurs in three isotopic forms – the stable isotopes ^{12}C and ^{13}C as well as the radioisotope ^{14}C . Biological reactions typically discriminate against the heavier stable isotope (^{13}C) and select for ^{12}C ; the resulting products are enriched in ^{12}C relative to ^{13}C . The degree of deviation ($\delta^{13}\text{C}$) is quantified versus a known standard (Pee Dee Belemnite, PDB) in the following manner:

$$\delta^{13}\text{C} = ([(^{13}\text{C}/^{12}\text{C})_{\text{sample}} \div (^{13}\text{C}/^{12}\text{C})_{\text{PDB}}] - 1) * 10^3 \quad (\text{Eq. 8})$$

The $\delta^{13}\text{C}$ value is reported in per mil (‰) notation; compounds depleted in ^{13}C relative to the standard have negative $\delta^{13}\text{C}$ values. Methanogenesis from CO_2 is typically associated with a strong discrimination against ^{13}C , as is methanogenesis from methylated-compounds, while methanogenesis from acetate has a weaker fractionation effect (KRZYCKI et al., 1987; WHITICAR, 1999). Based on the average stable carbon isotopic composition of methane in sedimentary environments (-50 to -100‰ vs. PDB), CO_2 is the most common substrates for methanogenesis (although many members of the *Methanosarcinales* do not use this compound) followed by acetate, which is the dominant substrate in freshwater environments (CANFIELD et al., 2005; LOVLEY and KLUG, 1986; WHITICAR, 1999). Methanogens must compete with sulfate reducers for some substrates like H_2 and acetate (i.e. the sulfate reducers are able to keep the

concentrations of these compounds too low to yield energy for methanogenesis), while methylated compounds are thought to be non-competitive (OREMLAND and POLCIN, 1982).

Methanogenesis is mediated by a complex series of enzymes and cofactors (Fig. 1.5), many of which were thought to be unique to methanogens but are now being found in other nonmethanogenic bacteria and archaea (HEDDERICH and WHITMAN, 2006). Although the carbon source yielding the methyl group may differ between the various methanogens, the final biochemical step in methane production is the same in all known methanogens (FERRY, 1999; THAUER, 1998). Beforehand, the methyl group is transferred to coenzyme M by the action of methyltetrahydromethanopterin:coenzyme M methyltransferase (if the methyl group originates from carbon dioxide or acetate) or by other methyltransferases (if the methyl group originates from methylated compounds). Methyl-coenzyme M reductase (*mcr*) then catalyzes the reaction of methyl-coenzyme M with coenzyme B by fostering the nucleophilic attack on the methyl group by the Ni-containing cofactor F₄₃₀. The end result is the production of methane and the disulfide coenzyme M:coenzyme B complex and energy conservation.

MICROBIAL CONSUMPTION OF METHANE IN MARINE SEDIMENTS

As mentioned previously, only a small fraction of the methane generated in the marine subsurface escapes into the water column or into the atmosphere. Oxygen is typically consumed quickly in sediments by diagenetic reactions and is therefore not available to fuel aerobic methane oxidation by methanotrophic bacteria. The first evidence of the anaerobic oxidation of methane (AOM) came from biogeochemical surveys of marine sediments, where it was observed that methane accumulation began just after sulfate depletion and that methane consumption

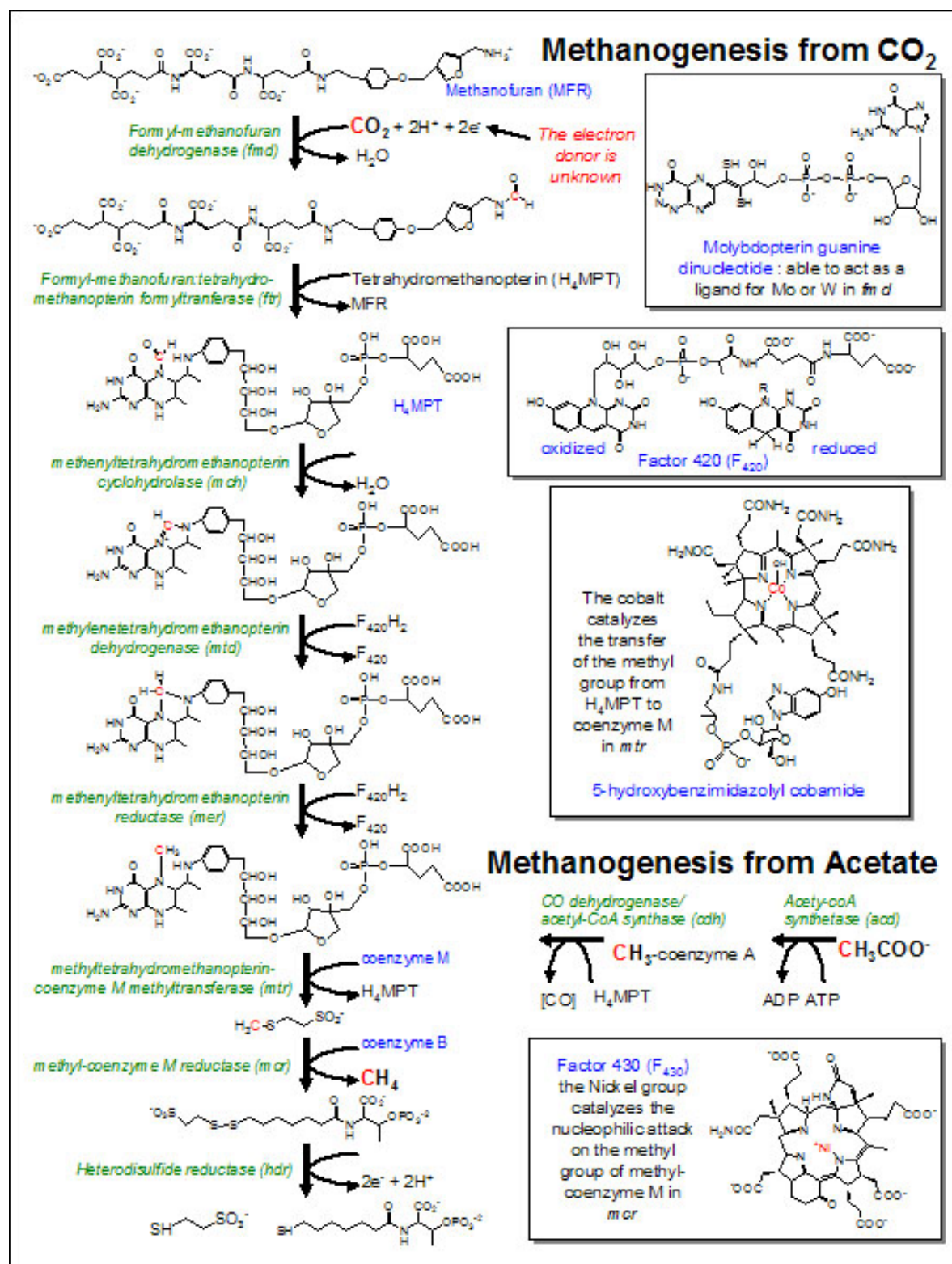
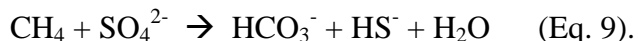


Figure 1.5. Methanogenic pathways from CO₂ and acetate. Enzymes labeled in green. Modified from (BUCKEL, 1999; FERRY, 1999; HEDDERICH and WHITMAN, 2006)

occurred at that interface (BARNES and GOLDBERG, 1976; IVERSEN and BLACKBURN, 1981; IVERSEN and JØRGENSEN, 1985; MARTENS and BERNER, 1974; REEBURGH, 1980; REEBURGH and HEGGIE, 1977). Stoichiometric relationships showed that methane and sulfate reduction were coupled according to the following net reaction (BARNES and GOLDBERG, 1976):



Subsequent surveys indicate that AOM and SR are coupled nearly 1:1 in “normal” diffusive sediments at the sulfate methane transition zone (SMTZ), although SR is also fueled by other carbon sources at shallower depths. Integrated over the depth of SR, AOM accounts for roughly 10% of SR in these settings (HINRICHS and BOETIUS, 2002). The magnitude of AOM can be much higher, and the ratio versus total SR greater, at areas with high methane content, such as cold gas seeps, mud volcanoes, gas-charged sediments, permanently anoxic water columns, and at hydrothermal vents (for example, (JOYE et al., 2004; MICHAELIS et al., 2002; NIEMANN et al., 2006; TREUDE et al., 2003)). In fact, in some areas with high methane flux, methane can also be a nutritive source for macrofauna in addition to fueling microbial growth – for example, multiple forms of clams, mussels and worms sustain growth from symbiotic relationships with aerobic, methane-oxidizing bacteria (CARY et al., 1988; CAVANAUGH, 1993; FISHER, 1990; FISHER et al., 2000).

Initially, it was proposed that sulfate reducing bacteria (SRB) used methane as an additional carbon source to fuel sulfate reduction (SR). However, no SRB has been found to mediate this process. Instead, growing evidence supports the hypothesis put forward by Hoehler et al. (1994) that the reaction is mediated via a syntrophic relationship between a methane-consuming organism and a sulfate-reducing organism. The methane-consuming microorganism was identified first by applying culture-independent techniques to sediments from methane cold

seeps (HINRICHS et al., 1999). Biomarkers typically associated with archaea, namely archaeol and hydroxyarchaeol, were found to be highly depleted in ^{13}C , which could be explained by the incorporation of “light”, ^{13}C -depleted methane (HINRICHS et al., 1999); contemporaneous studies discovered other highly depleted archaeal lipids (i.e. crocetane and 2,6,10,15,19-pentamethyleicosane) at other cold seeps where AOM occurred (ELVERT et al., 1999). These and other lipids commonly found in AOM-environments or discussed in this dissertation are shown in Fig. 1.6. Using 16S rRNA-based clone libraries, the archaeon was determined to be phylogenetically distantly related to the methanogenic order *Methanosarcinales*, forming a unique cluster named ANME-1 (for Anaerobic Methanotrophic; Fig. 1.4) (HINRICHS et al., 1999). The involvement of SRB in methane cycling was also confirmed by lipid biomarker approaches – non-isoprenoidal glycerol ethers and fatty acids attributable to SRB were also depleted in ^{13}C (HINRICHS et al., 2000). Using 16S rRNA-based fluorescence in situ hybridization (FISH) approaches, Boetius et al. (2000) were the first to visualize organized consortia of SRB and archaea in sediments with high AOM potential, where a shell of SRB belonging to the *Desulfosarcina/Desulfococcus* group of delta-proteobacteria surrounded an inner core of another archaeal group related to the *Methanosarcinales*, the ANME-2 (Fig. 1.4). The participation of both SRB and ANME in methane cycling was further supported by analyzing the stable carbon isotopic composition of whole cell material from the various ANME and SRB using FISH coupled with secondary-ion mass spectrometry (FISH-SIMS) – materials from both groups were highly depleted in ^{13}C (ORPHAN et al., 2001a; ORPHAN et al., 2001b; ORPHAN et al., 2002). The function of the syntrophic consortia has been confirmed by multiple *in vitro* experiments in which a 1:1 stoichiometry of AOM to SR is observed, as would be expected from Eq. 8 (NAUHAUS et al., 2006; NAUHAUS et al., 2002; NAUHAUS et al., 2005).

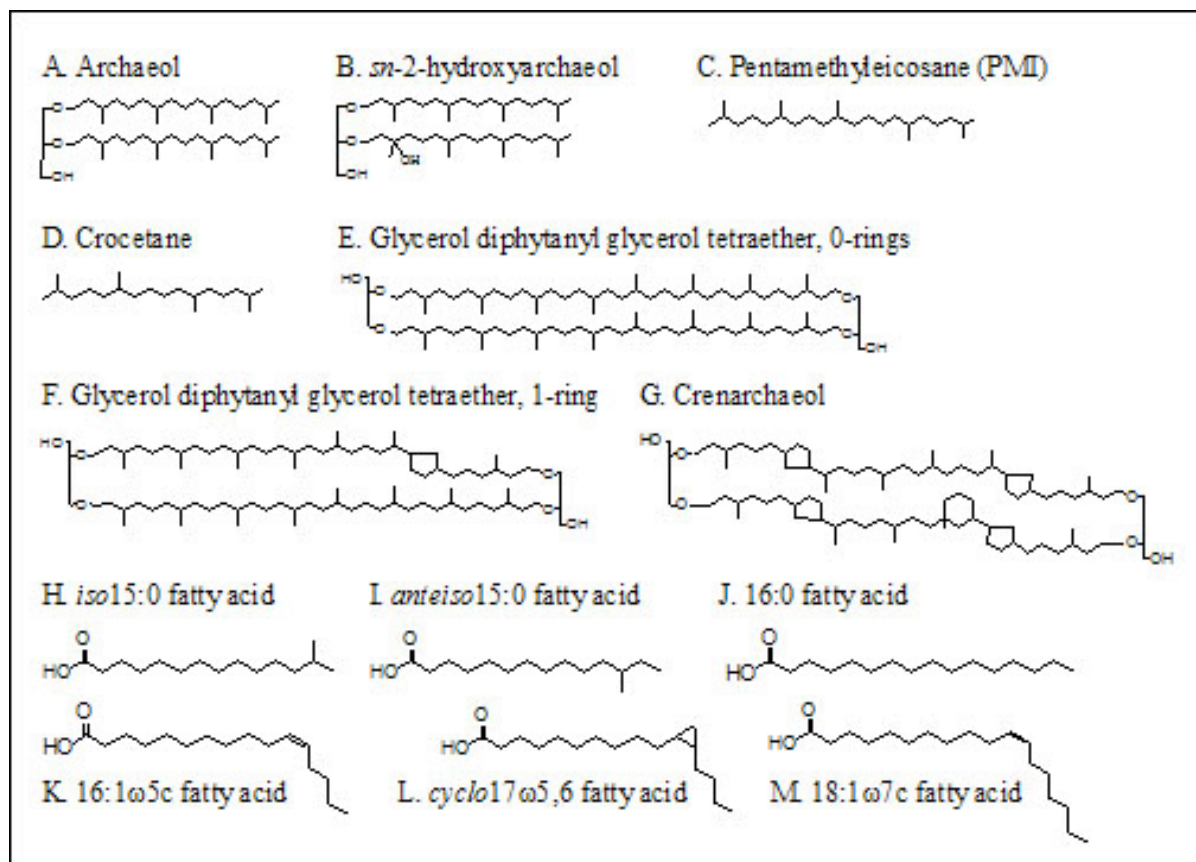


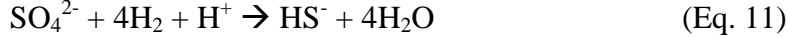
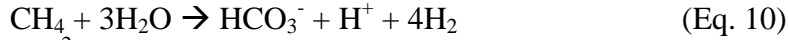
Figure 6. Structures of select archaeal (A-G) and bacterial (H-M) lipid biomarkers referred to in this dissertation. See chapters 2 and 6 for extended descriptions of these compounds.

Although it is evident that ANME and SRB mediate AOM in the environment, it is still unclear how the reaction proceeds. Under typical environmental conditions, the free energy yield of AOM coupled to SR is meager (i.e. -20 to -40 kJ/mol), and this net energy must be split between at least two partners. Traditional views hold that the minimum free energy threshold for bacteria is around -20 kJ/mol (i.e. the amount of energy needed to generate ATP/mole H^+ ; (SCHINK, 1997)); how was it possible that AOM coupled to SR could proceed? More recent investigations suggest that some microorganisms have evolved mechanisms to sustain growth at near chemical equilibrium (JACKSON and MCINERNEY, 2002); thus, it is possible that the AOM/SR syntrophy utilizes similar mechanisms.

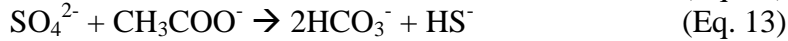
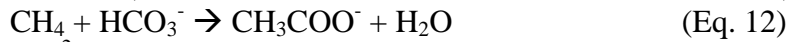
Another unknown in the AOM/SR syntrophy is how exactly the two processes are coupled. It is unclear what the individual AOM and SR reactions are. AOM is thought to proceed via a ‘reversal’ of methanogenic pathways as proposed by Hoehler and Alperin (1996).

Some proposed reactions couples that lead to the net reaction in Eq. 9:

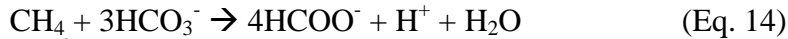
Hydrogen transfer (HOEHLER et al., 1994; ZEHNDER and BROCK, 1980):



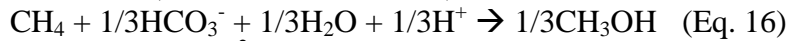
Acetate transfer (HOEHLER et al., 1994; ZEHNDER and BROCK, 1980):



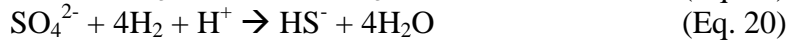
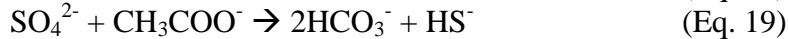
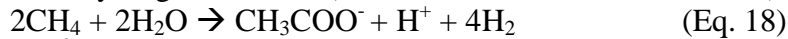
Formate transfer (SØRENSEN et al., 2001):



Methanol transfer (SØRENSEN et al., 2001):



Acetate and Hydrogen Transfer (VALENTINE and REEBURGH, 2000)



These couples allow for exchange of compounds that (1) are already known to be consumed by sulfate reducers, (2) allow for free energy to be gained from the methane-oxidizing organism at environmentally relevant concentrations, and (3) allow for interspecies carbon transfer (with the exception of Eqs. 10-11) to explain how SRB cell material is depleted in ^{13}C . In regards to the second point, the syntrophy would be advantageous as the SRB could keep the concentration of exchangeable species low enough as to thermodynamically favor AOM. So far, however, none of the proposed exchangeable species have been verified. *In vitro* experiments attempting to uncouple SR from AOM by addition of the proposed intermediates,

thereby short-cutting the need for syntrophy by the SRB, did not show enhanced SR rates as would be expected (NAUHAUS et al., 2002; NAUHAUS et al., 2005). Theoretical calculations of the allowable exchangeable species based on the free energy yields associated with diffusive concentration gradients between two cells indicate that hydrogen is not a possible intermediate, although acetate or formate could be at high methane concentrations (SØRENSEN et al., 2001; STROUS and JETTEN, 2004; VALENTINE, 2002).

Although it is still unclear which particular mechanism is used by anaerobic methanotrophs, support for the concept of ANME using a general ‘reverse’ methanogenic pathway comes from environmental metagenomic surveys of systems naturally enriched in AOM-mediating microorganisms. A majority of genes for enzymes typically associated with methanogenesis (see Fig. 1.5 above), many of which are easily reversible, have been found in ANME genomic library sets (CHISTOSERDOVA et al., 2005; HALLAM et al., 2004; MEYERDIERKS et al., 2005). A modified form of *mcr* is thought to catalyze the first step of the AOM reaction as it has structural modifications that would prevent mechanistic inhibition of the activation of methane (KRÜGER et al., 2003; SHIMA and THAUER, 2005); indeed, extracts of the modified enzyme from methanotrophic microbial mats from the Black Sea mediated AOM in proteomic experiments (KRÜGER et al., 2003).

MARINE METHANE SEEPS AND OTHER METHANE-RICH HABITATS

From methane production and consumption budgets it is clear that methane dynamics in the ocean realm are important. There are a variety of methane-rich environments in the ocean, ranging in terms of the dominant methane source (ie. biogenic, abiogenic, thermogenic) as well

as production and flux rates. The following is a general description of the various methane-rich habitats found in the marine environment.

Diffusive sediments

In “normal” marine sediments, diffusion is the sole mechanism of transport of methane upward from the zone of methane production. The relatively slow advance of methane towards the sediment water interface (SWI) gives ample time for AOM-mediating microorganisms to consume the rising methane at the SMTZ, which is generally meters below the SWI, leading to an extremely efficient removal of methane (FOSSING et al., 2000; IVERSEN and BLACKBURN, 1981; IVERSEN and JØRGENSEN, 1985; NIEWÖHNER et al., 1998). Although the total production and consumption of methane in diffusive systems is relatively low in magnitude on a local scale, the aerial extent of these systems globally increase their importance as a methane sink (HINRICHS and BOETIUS, 2002).

Gas-charged coastal sediments

In coastal zones with high organic matter input, such as estuaries, the magnitude of organic matter decomposition, including methanogenesis, is elevated. The rapid production rates of methane lead to supersaturation and formation of methane bubbles (HOEHLER et al., 1994; MARTENS et al., 1999; MARTENS et al., 1986). This can lead to the formation of bubble fronts in the sediment as well as the ebullition of methane gas. Although these systems may not be highly advective, the rapid formation of methane leads to a shallowing of the SMTZ.

“Cold” gas seeps

As opposed to hydrothermal vents, cold seeps are characterized by the advection of colder fluids which are charged with gas. The gas, typically dominated by methane but also commonly including other higher hydrocarbons and/or carbon dioxide, can originate from deep

thermogenic reservoirs or from the dissociation of abundant gas hydrates, which occur at cold seeps under conditions of high methane availability and pressure and low temperature. Methanogenesis is another source of methane in these environments. Fluid flux rates at cold seeps vary temporally and spatially; however, the presence of abundant and long-lived macrofauna (on the order of hundreds of years; (FISHER et al., 1997)) that are nutritionally supported by methane or AOM/SR byproducts (i.e. sulfide; including tubeworms, mussels, and clams with endosymbiotic sulfide oxidizing bacteria), indicates that cold seeps are quasi-permanent features. Fault features facilitate the movement of fluid in these systems; the fault networks are dynamic as old conduits become blocked by the precipitation of carbonates or gas hydrates (CHEN et al., 2004). Several cold seeps have been well-documented – for instance, at Hydrate Ridge and the Cascadia Convergent Margin off the western coast of the USA and Canada (BOETIUS and SUESS, 2004; KASTNER et al., 1995; KULM et al., 1986; SUESS et al., 1999); on the shelves, slopes and in deep water in the Gulf of Mexico (JOYE et al., 2004; MACDONALD et al., 2004; MACDONALD et al., 1994; PAULL et al., 1984; ROBERTS et al., 1990); off the California coast in the Eel River and Santa Barbara Basins (HINRICHS et al., 1999; ORPHAN et al., 2004); and in the North Sea at the Tommeliten seep area (NIEMANN et al., 2005). A special type of cold seep – the brine seep – occurs when buoyant salt plumes intersect the SWI, leading to the formation of surficial “pools” of highly saline water where gas release occurs (JOYE et al., 2005; MACDONALD et al., 1990; MEDINAUT/MEDINETH, 2000; ROBERTS and CARNEY, 1997). Rates of methane consumption are relatively high at cold seeps, although the efficiency of methane removal may vary if methane rapidly transits through the system (HINRICHS and BOETIUS, 2002; JOYE et al., 2004; TREUDE et al., 2003).

Pockmarks

Pockmarks, rounded depressions at the SWI varying in size from meters to hundreds of meters, are a surficial expression of a different methane-rich habitat. Pockmarks result when sediment overpressure resulting from the build-up of methane or other fluids under impermeable layers is released, causing the surficial sediment to sink from the decreased pressure (HOVLAND et al., 2002). Gas and fluid seepage may continue after pockmark formation as the buried reservoir continues to release; pockmarks may also represent an inactive seepage site if the reservoir was depleted during the outburst that formed the pockmark. Pockmarks appear to be a widespread feature on continental shelves and slopes.

Mud volcanoes

Like cold gas seeps, mud volcanoes represent a high methane habitat with strong advection. Localized expressions of rapid but intermittent fluid expulsion are generated by tectonic activity (i.e. accretion, faulting) or by salt or shale compression of sediments (i.e. buoyant movement of buried salt, slope failures), often coinciding with areas of high sedimentation rates (reviewed in (MILKOV, 2000)). Unlike gas seeps, fluidized mud is also expelled along with gas and water, leading to the formation of ‘volcanoes’. Methane-cycling dynamics of several mud volcanoes have been described – for example, in the Gulf of Mexico (JOYE et al., 2005; JOYE et al., in preparation); in the northern Atlantic (NIEMANN et al., 2006; PIMENOV et al., 1999); and at accretionary prisms in the Mediterranean Sea (HAESE et al., 2003; WERNE et al., 2004).

Hydrothermal methane seeps

Three types of hydrothermal systems with high methane content have been described: (1) thermogenically-sourced methane-rich hydrothermal seeps in an area of high organic matter

deposition in the Guaymas Basin in the Gulf of California (SIMONEIT and LONSDALE, 1982; TESKE et al., 2002), (2) abiogenically-sourced methane produced from serpentinization reactions at the Lost City Hydrothermal Field (LCHF) (KELLEY et al., 2001; KELLEY et al., 2005); and (3) thermogenically-produced methane from water-rock reactions at high temperatures at hydrothermal vents such as the Endeavor Field on the Juan de Fuca ridge (BAROSS et al., 1982; DE ANGELIS et al., 1993). The AOM-mediating microorganisms from the thermogenically-sourced methane habitat appear to be phylogenetically closely related to organisms from cold seeps (i.e. ANME-1 and ANME-2; Fig. 1.4) although with modified lipid membranes to withstand high environmental temperatures (DHILLON et al., 2005; SCHOUTEN et al., 2003; TESKE et al., 2002). At the LCHF, a distinct clade related to the *Methanosarcinales* order of methanogenic order but unaffiliated with ANME-1, -2, or -3 (Fig. 1.4) dominates the archaeal community and is likely involved in methane cycling (BRAZELTON et al., 2006; SCHRENK et al., 2004).

NEW FRONTIERS IN METHANE-CYCLING RESEARCH

Recent discoveries have broadened the horizon of potential habitats, mechanisms and diversity of organisms involved in methane consumption.

AOM in the Deep Biosphere

With the application of deep-sea drilling technologies, a window into the deep marine subsurface (sediments below 10 cm) has been opened, raising questions about the activity and diversity of microorganisms in the “deep biosphere”. Although this zone receives low inputs of organic matter from primary production, rough estimates based on available data suggest that the

deep marine subsurface contains 55 - 85 % of Earth's microbial population (WHITMAN et al., 1998), representing between 10-30 % of Earth's total biomass (PARKES et al., 2000; WHITMAN et al., 1998). Profiles of methane and sulfate in these environments as well as activity measurements indicate that AOM occurs, although it is presently unclear which microorganisms mediate these processes. Microbial groups typically found in surficial methane-consuming zones (i.e. the ANME-1, -2, and -3 clades of anaerobic methanotrophic archaea and sulfate-reducing bacteria related to *Desulfosarcina/Desulfococcus* or *Desulfobulbus* spp.; (KNITTEL et al., 2003; KNITTEL et al., 2005) are conspicuously absent from all 16S rRNA clone libraries constructed from deep biosphere samples to date, with the exception of one study conducted on capped borehole fluid collected one year after drilling, where ANME-1 related sequences were retrieved (LANOIL et al., 2005). Instead, certain groups of Crenarchaeota, namely the Marine Crenarchaea Group I (MCGI) and the combined Marine Benthic Group B (MBGB)/Deep Sea Archaeal Group (DSAG; Fig. 1.4), are present in a wide range of deep biosphere samples (BIDDLE et al., 2006; INAGAKI et al., 2006; INAGAKI et al., 2003; SØRENSEN et al., 2004; SØRENSEN and TESKE, 2006; TESKE, 2006). Measurement of stable isotopic composition of whole cells and lipid material in samples where these Crenarchaea are suggested to be abundant indicate that they do not incorporate methane-derived carbon into cellular material and are instead heterotrophic (BIDDLE et al., 2006). Determining which microorganisms consume methane in the deep biosphere is still an active field of investigation.

AOM coupled to other electrons acceptors

Until recently, AOM-mediating communities had only been found associated with sulfate-reduction, making sulfate the electron acceptor for methane oxidation. Other electron

acceptors, including nitrate and iron oxides, could theoretically be coupled with methane oxidation based on potential free energy yields (ZEHNDER and BROCK, 1980). A recent study (RAGHOEBARSING et al., 2006) discovered AOM-mediating archaea associated with denitrifying bacteria in freshwater sediments; they occurred in consortia arrangements similar to those seen for ANME/DSS (KNITTEL et al., 2005). The archaea are distantly related to the described ANME-2 group within the *Methanosarcinales* order (Fig. 1.4)(RAGHOEBARSING et al., 2006). Comparing the biochemistry of this new group of methanotrophs with the ANME may help elucidate the mechanism of anaerobic methane consumption and shed light on the syntrophic requirements of AOM-mediating communities. Further investigation is also required to explore natural systems to document the global biogeochemical importance of this new methane consuming pathway and to uncover AOM linked to other electron acceptors.

METHANE CYCLING: AN ANCIENT MICROBIAL PATHWAY?

Increasing evidence (HINRICHS, 2002; SHEN and BUICK, 2004) suggests that the microbially-mediated processes of sulfate reduction (SR), methanogenesis, and methane oxidation were predominant metabolic pathways on early Earth. Stable isotopic analyses suggest that SR was active by at least 3.5 Ga in localized, high sulfate environments (SHEN et al., 2001), although the timing of globally-distributed bacterial SR across habitats is debatable (CANFIELD et al., 2000; SHEN et al., 2001). During the late Archean, when the larger ocean basins were likely depleted in sulfate (FARQUHAR et al., 2002; HABICHT et al., 2002), methanogenic pathways would have been thermodynamically favorable. A biosignature of methanogenesis, and possibly methanotrophy, exists in late Archean rocks in the form of isotopically depleted kerogens (HAYES, 1994). Although this signature was originally ascribed to aerobic methanotrophs

(HAYES, 1983; HAYES, 1994), anaerobic oxidation of biogenically-produced methane, presumably coupled to SR, provides a more robust explanation (HINRICHS, 2002), as oxygen was likely limiting during this time (DES MARAIS, 2000). Given the antiquity of these anaerobic carbon and sulfur biogeochemical cycles, an understanding of the interactions and associations of contemporary microorganisms mediating these processes is necessary for understanding their evolutionary history on early Earth.

OBJECTIVES OF THE FOLLOWING DISSERTATION

A variety of methane-rich habitats - from the deep marine subsurface to cold seeps featuring mud volcanoes, brine pools, and gas hydrates - were investigated using a multidisciplinary approach to gain a systematic understanding of microbially-mediated methane dynamics in the marine subsurface. Building from other's investigations, this work focuses on systems that have not been fully characterized – Gulf of Mexico oil-laden cold seeps and the Hydrate Ridge deep biosphere; environmental surveys as well as enrichment experiments and modeling are used to explore AOM. These studies aim to define how the marine microbial methane filter operates – identifying which processes, microorganisms, and factors are involved. Other questions addressed include:

- How are AOM and SR linked together, and how tightly?
- Is AOM influenced by other processes such as methanogenesis?
- What factors influence the diversity and distribution of AOM-mediating microorganisms?
- What is the range of environments where AOM occurs, and why (what are the factors controlling AOM)?

Results of these studies are presented in the following six chapters (2-7) as publishable manuscripts. The final chapter (8) summarizes the findings of this work.

References

- Barnes R. O. and Goldberg E. D. (1976) Methane production and consumption in anaerobic marine sediments. *Geology* **4**, 297-300.
- Baross J. A., Lilley M. D., and Gordon L. I. (1982) Is the CH₄, H₂ and CO venting from submarine hydrothermal systems produced by thermophilic bacteria? *Nature* **298**, 366-368.
- Biddle J. F., Lipp J. S., Lever M., Lloyd K. G., Sørensen K. B., Anderson K., Fredricks H. F., Elvert M., Kelly T. J., Schrag D. P., Sogin M. L., Brechley J. E., Teske A., House C. H., and Hinrichs K.-U. (2006) Heterotrophic Archaea dominate sedimentary subsurface ecosystems off Peru. *Proceedings of the National Academy of Science U.S.A.* **103**(10), 3846-3851.
- Boetius A., Ravensschlag K., Schubert C. J., Rickert D., Widdel F., Gieseke A., Amann R., Jørgensen B. B., Witte U., and Pfannkuche O. (2000) A marine microbial consortium apparently mediating anaerobic oxidation of methane. *Nature* **407**, 623-626.
- Boetius A. and Suess E. (2004) Hydrate Ridge: a natural laboratory for the study of microbial life fueled by methane from near-surface gas hydrates. *Chemical Geology* **204**.
- Brazelton W. J., Schrenk M. O., Kelley D. S., and Baross J. A. (2006) Methane- and sulfur-metabolizing microbial communities dominate the Lost City Hydrothermal Field ecosystem. *Applied and Environmental Microbiology* **72**(9), 6257-6270.
- Buckel W. (1999) Anaerobic Energy Metabolism. In *Biology of the Prokaryotes* (ed. J. W. Lengeler, G. Drews, and H. G. Schlegel), pp. 278-342. Georg Thieme Verlag/Blackwell Science.
- Canfield D. E., Habicht K. S., and Thamdrup B. (2000) The Archean sulfur cycle and the early history of atmospheric oxygen. *Science* **288**, 658-661.
- Canfield D. E., Kristensen E., and Thamdrup B. (2005) *Aquatic Geomicrobiology*. Elsevier Academic Press.
- Cary S. C., Fisher C. R., and Felback H. (1988) Mussel growth supported by methane as sole carbon and energy source. *Science* **240**, 78-80.

- Cavanaugh C. M. (1993) Methanotroph-invertebrate symbioses in the marine environment: ultrastructural, biochemical and molecular studies. In *Microbial Growth on C₁ Compounds* (ed. J. C. Murrell and D. P. Kelly), pp. 315-328. Intercept Ltd.
- Chen D. F., Cathles III L. M., and Roberts H. H. (2004) The geochemical signatures of variable gas venting at gas hydrate sites. *Marine and Petroleum Geology* **21**, 317-326.
- Chistoserdova L., Vorholt J. A., and Lidstrom M. E. (2005) A genomic view of methane oxidation by aerobic bacteria and anaerobic archaea. *Genome Biology* **6**, 208.
- Cicerone R. J. and Oremland R. S. (1996) Biogeochemical aspects of atmospheric methane. *Global Biogeochemical Cycles* **2**, 299-327.
- Crill P. M. and Martens C. S. (1986) Methane production from bicarbonate and acetate in an anoxic marine sediment. *Geochimica et Cosmochimica Acta* **50**(9), 2089-2097.
- de Angelis M. A., Lilley M. D., Olson E. J., and Baross J. A. (1993) Methane oxidation in deep-sea hydrothermal plumes of the Endeavor Segment of the Juan de Fuca Ridge. *Deep-Sea Research I* **40**(6), 1169-1186.
- Des Marais D. J. (2000) When did photosynthesis emerge on Earth? *Science* **289**(1703-1705).
- Dhillon A., Lever M., Lloyd K. G., Albert D. B., Sogin M. L., and Teske A. (2005) Methanogen diversity evidenced by molecular characterization of methyl coenzyme M reductase A (*mcrA*) genes in hydrothermal sediments of Guaymas Basin. *Applied and Environmental Microbiology* **71**(8), 4592-4601.
- Dickens G. R., O'Neil J. R., Rea D. K., and Owen R. M. (1995) Dissociation of oceanic methane hydrate as a cause of the carbon excursion at the end of the Paleocene. *Paleoceanography* **10**(6), 965-971.
- Elvert M., Suess E., and Whiticar M. J. (1999) Anaerobic methane oxidation associated with marine gas hydrates: super-light C-isotopes from saturated and unsaturated c-20 and c-25 irregular isoprenoids. *Naturwissenschaften* **86**, 295-300.
- Farquhar J., Wing B. A., McKeegan K. D., Harris J. W., Cartigny P., and Thiemens M. H. (2002) Mass-independent sulfur of inclusions in diamond and sulfur recycling on early earth. *Science* **298**(5602), 2369-2372.
- Ferry J. G. (1999) Enzymology of one-carbon metabolism in methanogenic pathways. *FEMS Microbiology Reviews* **23**, 13-38.

- Fisher C. R. (1990) Chemoautotrophic and methanotrophic symbioses in marine invertebrates. *Reviews in Aquatic Sciences* **2**(3,4), 399-436.
- Fisher C. R., MacDonald I. R., Sassen R., Young C. M., Macko S. A., Hourdez S., Carney R., Joye S. B., and McMullin E. (2000) Methane ice worms: *Hesiocaeca methanicola* colonizing fossil fuel reserves. *Naturwissenschaften* **87**, 184-187.
- Fisher C. R., Urcuyo I. A., Simkins M. A., and Nix E. (1997) Life in the slow lane: Growth and longevity of cold-seep vestimentiferans. *Marine Ecology* **18**, 83-94.
- Fossing H., Ferdelman T. G., and Berg P. (2000) Sulfate reduction and methane oxidation in continental margin sediments influenced by irrigation (South-East Atlantic off Namibia). *Geochimica et Cosmochimica Acta* **64**, 897-910.
- Froelich P. N., Klinkhammer G. P., Bender M. L., Luedtke N. A., Heath G. R., Cullen D., Dauphin P., Hammond D. E., Hartmann B., and Maynard V. (1979) Early oxidation of organic matter in pelagic sediments of the eastern equatorial Atlantic suboxic diagenesis. *Geochimica et Cosmochimica Acta* **43**, 1075-1088.
- Habicht K. S., Gade M., Thamdrup B., Berg P., and Canfield D. E. (2002) Calibration of sulfate levels in the archaean ocean. *Science* **298**, 2372-2374.
- Haese R. R., Meile C., van Cappellen P., and de Lange G. (2003) Carbon geochemistry of cold seeps: Methane fluxes and transformation in sediments from Kazan mud volcano, eastern Mediterranean Sea. *Earth and Planetary Science Letters* **212**, 361-375.
- Hallam S. J., Putnam N., Preston C. M., Detter J. C., Rokhsar D., Richardson P. M., and Delong E. F. (2004) Reverse methanogenesis: Testing the hypothesis with environmental genomics. *Science* **305**, 1457-1462.
- Hayes J. M. (1983) Geochemical evidence bearing on the origin of aerobiosis, a speculative hypothesis. In *Earth's Earliest Biosphere, Its Origin and Evolution* (ed. J. W. Schopf), pp. 291-301. Princeton University Press.
- Hayes J. M. (1994) Global methanotrophy at the Archean-Proterozoic transition. In *Early Life on Earth*, Vol. 84 (ed. S. Bengtson), pp. 220-236. Columbia Press University.
- Hedderich R. and Whitman W. B. (2006) Physiology and biochemistry of the methane-producing archaea. *Prokaryotes* **2**, 1050-1079.
- Hinrichs K.-U. (2002) Microbial fixation of methane carbon at 2.7Ga: was an anaerobic mechanism possible? *Geochemistry, Geophysics, Geosystems* **3**.

- Hinrichs K.-U. and Boetius A. (2002) The anaerobic oxidation of methane: New insights in microbial ecology and biogeochemistry. In *Ocean Margin Systems* (ed. G. Wefer, D. Billett, D. Hebbeln, B. B. Jørgensen, M. Schlueter, and T. C. E. van Weering), pp. 457-477. Springer-Verlag.
- Hinrichs K.-U., Hayes J. S., Sylva S. P., Brewer P. G., and Delong E. F. (1999) Methane-consuming archaeobacteria in marine sediments. *Nature* **398**, 802-805.
- Hinrichs K.-U., Summons R. E., Orphan V. J., Sylva S. P., and Hayes J. M. (2000) Molecular and isotopic analysis of anaerobic methane-oxidizing communities in marine sediments. *Organic Geochemistry* **31**, 1651-1701.
- Hoehler T. M. and Alperin M. J. (1996) Anaerobic methane oxidation by methanogen-sulfate reducer consortium: geochemical evidence and biochemical considerations. In *Microbial Growth on C₁ compounds* (ed. M. E. Lidstrom and R. F. Tabita), pp. 326-333. Kluwer Academic Publishing.
- Hoehler T. M., Alperin M. J., Albert D. B., and Martens C. S. (1994) Field and laboratory studies of methane oxidation in an anoxic marine sediment - evidence for a methanogen-sulfate reducer consortium. *Global Biogeochemical Cycles* **8**, 451-463.
- Hovland M., Gardner J., and Judd A. (2002) The significance of pockmarks to understanding fluid flow processes and geohazards. *Geofluids* **2**(2), 127-136.
- Inagaki F., Nunoura T., Nakagawa T., Teske A., Lever M., Lauer A., Suzuki M., Takai K., Delwiche M. E., Colwell F. S., Nealson K. H., Horikoshi K., D'Hondt S., and Jørgensen B. B. (2006) Biogeographical distribution and diversity of microbes in methane hydrate-bearing deep marine sediments on the Pacific Ocean Margin. *Proceedings of the National Academy of Science U.S.A.* **103**(8), 2815-2820.
- Inagaki F., Suzuki M., Takai K., Oida H., Sakamoto T., Aoki K., Nealson K. H., and Horikoshi K. (2003) Microbial communities associated with geological horizons in coastal subseafloor sediments from the Sea of Okhotsk. *Applied and Environmental Microbiology* **69**(12), 7224-7235.
- IPCC. (2000) Land Use, Land-Use Change, and Forestry. A Special Report of the Intergovernmental Panel on Climate Change (IPCC) (ed. R. T. Watson, I. R. Noble, B. Bolin, N. H. Ravindranath, D. J. Verardo, and D. J. Dokken). Cambridge University Press.
- IPCC I. P. o. C. C. (2001) Climate Change 2001 - The Scientific Basis, pp. 881. Cambridge University Press.

- Iversen N. and Blackburn H. T. (1981) Seasonal rates of methane oxidation in anoxic marine sediments. *Applied and Environmental Microbiology* **41**, 1295-1300.
- Iversen N. and Jørgensen B. B. (1985) Anaerobic methane oxidation rates at the sulfate-methane transition in marine sediments from Kattegat and Skagerrak (Denmark). *Limnology and Oceanography* **30**, 944-955.
- Jackson B. E. and McInerney M. J. (2002) Anaerobic microbial metabolism can proceed close to thermodynamic limits. *Nature* **415**, 454-456.
- Joye S. B., MacDonald I. R., Montoya J. P., and Peccini M. B. (2005) Geophysical and geochemical signatures of Gulf of Mexico seafloor brines. *Biogeosciences* **2**, 295-309.
- Joye S. B., Orcutt B. N., Boetius A., Montoya J. P., Schulz H., Erickson M. J., and Lugo S. K. (2004) The anaerobic oxidation of methane and sulfate reduction in sediments from at Gulf of Mexico cold seeps. *Chemical Geology* **205**(3-4), 219-238.
- Joye S. B., Samarkin V. A., Orcutt B. N., Hinrichs K.-U., MacDonald I. R., Meile C. D., Elvert M., and Montoya J. P. (in preparation) Deeply sourced brines fuel microbial activity along the seafloor in the Gulf of Mexico. *Science*.
- Kasting J. K. (2004) When methane made climate. In *Scientific American*, pp. 78-85.
- Kastner M., Sample J. C., Whiticar M. J., Hovland M., Cragg B. A., and Parkes R. J. (1995) Geochemical evidence for fluid flow and diagenesis at the Cascadia convergent margin. In *Proceedings of the Ocean Drilling Program, Scientific Results*, Vol. 146 (ed. B. Carson, G. K. Westbrook, R. J. Musgrave, and E. Suess), pp. 375-384. Ocean Drilling Program.
- Kelley D. S. and Früh-Green G. (1999) Abiogenic methane in deep-seated mid-ocean ridge environments: Insights from stable isotope analyses. *Journal of Geophysical Research-Solid Earth* **104**(B5), 10439-10460.
- Kelley D. S., Karson J. A., Blackman D. K., Früh-Green G. L., Butterfield D. A., Lilley M. D., Olson E. J., Schrenk M. O., Roe K., Lebon G. T., Rivizzigno P., and Party t. A.-S. (2001) An off-axis hydrothermal vent field near the Mid-Atlantic Ridge at 30° N. *Nature* **412**, 145-149.
- Kelley D. S., Karson J. A., Früh-Green G. L., Yoerger D. R., Shank T., Butterfield D. A., Hayes J. M., Schrenk M. O., Olson E. J., Proskurowski G., Jakuba M., Bradley A., Larson B., Ludwig K. A., Glickson D., Buckman K., Bradley A. S., Brazelton W. J., Roe K., Elend M. J., Delacour A., Bernasconi S. M., Lilley M. D., Baross J. A., Summons R. E., and

- Sylva S. P. (2005) A serpentine-hosted ecosystem: the Lost City Hydrothermal Field. *Science* **307**, 1428-1434.
- Kennett J. P., Cannariato K. G., Hendy J. L., and Behl R. J. (2000) Carbon isotopic evidence for methane hydrate instability during quaternary interstadials. *Science* **288**, 128-133.
- Knittel K., Boetius A., Lemke A., Eilers H., Lochte K., Pfannkuche O., and Linke P. (2003) Activity, distribution, and diversity of sulfate reducers and other bacteria in sediments above gas hydrate (Cascadia Margin, Oregon). *Geomicrobiology Journal* **20**, 269-294.
- Knittel K., Lösekann T., Boetius A., Kort R., and Amann R. (2005) Diversity and Distribution of Methanotrophic Archaea at Cold Seeps. *Applied and Environmental Microbiology* **71**(1), 467-479.
- Krüger M., Meyerdiecks A., Glockner F. O., Amann R., Widdel F., Kube M., Reinhardt R., Kahnt R., Bocher R., Thauer R. K., and Shima S. (2003) A conspicuous nickel protein in microbial mats that oxidize methane anaerobically. *Nature* **426**, 878-881.
- Krzycki J. A., Kenealy W. R., DeNiro M. J., and Zeikus J. G. (1987) Stable isotope fractionation by *Methanosarcina barkeri* during methanogenesis from acetate, methanol, or carbon dioxide-hydrogen. *Applied and Environmental Microbiology* **53**, 2597-2599.
- Kulm L. D., Suess E., Moore J. C., Carson S., Lewis B. T., Ritger S. D., Kadko D. C., Thornburg T. M., Embley R. W., Rugh W. D., Massoth G. J., Langseth M. G., Cochrane G. R., and Scamman R. L. (1986) Oregon subduction zone: venting, fauna, and carbonates. *Science* **231**, 561-566.
- Kvenvolden K. A. (1993) Gas hydrates - geological perspective and global change. *Reviews of Geophysics* **31**, 173-187.
- Kvenvolden K. A. and Rogers B. W. (2005) Gaia's breath - global methane exhalations. *Marine and Petroleum Geology* **22**, 579-590.
- Lanoil B. D., La Duc M. T., Wright M., Kastner M., Nealson K. H., and Bartlett D. (2005) Archaeal diversity in ODP legacy borehole 892b and associated seawater and sediments of the Cascadia Margin. *FEMS Microbiology Ecology* **54**, 167-177.
- Lelieveld J., Crutzen P. J., and Dentener F. J. (1998) Changing concentration, lifetime and climate forcing of atmospheric methane. *Tellus* **50B**, 128-150.
- Lollar B. S., Westgate T. D., Ward J. A., Slater G. F., and Lacrampe-Couloume G. (2002) Abiogenic formation of alkanes in the Earth's crust as a minor source for global hydrocarbon reservoirs. *Nature* **416**, 522-524.

- Lovley D. R. and Klug D. D. (1986) Model for the distribution of sulfate reduction and methanogenesis in fresh-water sediment. *Geochimica et Cosmochimica Acta* **50**(1), 11-18.
- MacDonald I. R., Bohrmann G., Escobar E., Abegg F., Blanchon P., Blinova V., Bruckmann W., Drews M., Eisenhauer A., Han X., Heeschen K., Meier F., Mortera C., Naehr T., Orcutt B. N., Bernard B., Brooks J. M., and de Farago M. (2004) Asphalt volcanism and chemosynthetic life in the Campeche Knolls, Gulf of Mexico. *Science* **304**, 999-102.
- MacDonald I. R., Guinasso N. L., Sassen R., Brooks J. M., Lee L., and Scott K. T. (1994) Gas hydrate that breaches the sea-floor on the continental slope of the Gulf of Mexico. *Geology* **22**, 699-702.
- MacDonald I. R., Reilly Jr. J. F., Guinasso N. L., Brooks J. M., Carney R., Bryant W. A., and Bright T. (1990) Chemosynthetic mussels at a brine-filled pockmark in the Northern Gulf of Mexico. *Science* **248**, 1096-1099.
- Martens C. S., Albert D. B., and Alperin M. J. (1999) Stable isotope tracing of anaerobic methane oxidation in the gassy sediments of Eckernforde Bay, German Baltic Sea. *American Journal of Science* **299**, 589-610.
- Martens C. S. and Berner R. A. (1974) Methane production in the interstitial waters of sulfate-depleted marine sediments. *Science* **185**, 1167-1169.
- Martens C. S., Blair N. E., and Green C. D. (1986) Seasonal variations in the stable carbon isotopic signature of biogenic methane in a coastal sediment. *Science* **233**, 1300-1303.
- MEDINAUT/MEDINETH S. S. P. (2000) Linking Mediterranean brine pools and mud volcanism. *EOS, Transactions of the American Geophysical Union* **81**, 625.
- Meyerdierks A., Kube M., Lombardot T., Knittel K., Bauer M., Glöckner F. O., Reinhardt R., and Amann R. (2005) Insights into the genomes of archaea mediating the anaerobic oxidation of methane. *Environmental Microbiology* **7**(12), 1937-1951.
- Michaelis W., Seifert R., Nauhaus K., Treude T., Thiel V., Blumenberg M., Knittel K., Gieseke A., Peterknecht F., Pape T., Boetius A., Amann R., Jørgensen B. B., Widdel F., Peckmann J., Pimenkov N., and Gulin M. B. (2002) Microbial reefs in the Black Sea fueled by anaerobic methane oxidation. *Science* **297**, 1013-1015.
- Milkov A. V. (2000) Worldwide distribution of submarine mud volcanoes and associated gas hydrates. *Marine Geology* **167**, 29-42.

- Milkov A. V., Claypool G. E., Lee Y.-J., and Sassen R. (2005) Gas hydrate systems at Hydrate Ridge offshore Oregon inferred from molecular and isotopic properties of hydrate-bound and void gases. *Geochimica et Cosmochimica Acta* **69**(4), 1007-1026.
- Nauhaus K., Albrecht M., Elvert M., Boetius A., and Widdel F. (2006) *In vitro* cell growth of marine archaeal-bacterial consortia during anaerobic oxidation of methane. *Environmental Microbiology* doi:10.1111/j.1462-2920.2006.01127.x.
- Nauhaus K., Boetius A., Krüger M., and Widdel F. (2002) *In vitro* demonstration of anaerobic oxidation of methane coupled to sulfate reduction from a marine gas hydrate area. *Environmental Microbiology* **4**, 296-305.
- Nauhaus K., Treude T., Boetius A., and Krüger M. (2005) Environmental regulation of the anaerobic oxidation of methane a comparison of ANME-1 and ANME-II communities. *Environmental Microbiology* **7**(1), 98-106.
- Niemann H., Elvert M., Hovland M., Orcutt B. N., Judd A., Suck I., Gutt J., Joye S. B., Damm E., Finster K., and Boetius A. (2005) Methane emission and consumption at a North Sea gas seep (Tommeliten area). *Biogeosciences* **2**(4), 335-351.
- Niemann H., Lösekann T., de Beer D., Elvert M., Nadalig T., Knittel K., Amann R., Sauter E., Schlüter M., Klages M., Foucher J.-P., and Boetius A. (2006) Novel microbial communities of the Haakon Mosby mud volcano and their role as a methane sink. *Nature* **443**, 854-858.
- Niewöhner C., Hensen C., Kasten S., Zabel M., and Schulz H. D. (1998) Deep sulfate reduction completely mediated by anaerobic methane oxidation in sediments of the upwelling area off Namibia. *Geochimica et Cosmochimica Acta* **62**, 455-464.
- Oremland R. S. and Polcin S. (1982) Methanogenesis and sulfate reduction - competitive and noncompetitive substrates in estuarine sediments. *Applied and Environmental Microbiology* **44**(6), 1270-1276.
- Orphan V. J., Hinrichs K.-U., Ussler W., III, Paull C. K., Taylor L. T., Sylva S. P., Hayes J. M., and Delong E. F. (2001a) Comparative analysis of methane-oxidizing archaea and sulfate-reducing bacteria in anoxic marine sediments. *Applied and Environmental Microbiology* **67**(4), 1922-1934.
- Orphan V. J., House C. H., Hinrichs K.-U., McKeegan K. D., and Delong E. F. (2001b) Methane-consuming archaea revealed by directly coupled isotopic and phylogenetic analysis. *Science* **293**, 484-487.

- Orphan V. J., House C. H., Hinrichs K.-U., McKeegan K. D., and Delong E. F. (2002) Multiple archaeal groups mediate methane oxidation in anoxic cold seep sediments. *Proceedings of the National Academy of Science U.S.A.* **99**, 7663-7668.
- Orphan V. J., Ussler W., III, Naehr T., House C. H., Hinrichs K.-U., and Paull C. K. (2004) Geological, geochemical, and microbiological heterogeneity of the seafloor around methane vents in the Eel River Basin, offshore California. *Chemical Geology* **204**, 265-289.
- Parkes R. J., Cragg B. A., and Wellsbury P. (2000) Recent studies on bacterial populations and processes in sub seafloor sediments: a review. *Hydrogeology Journal* **8**, 11-28.
- Paull C. K., Hecker B., Commeau R., Freeman-Lynde R. P., Neumann C., Corso W. P., Hook J. E., Sikes E., and Curray J. (1984) Biological communities at the Florida Escarpment resemble hydrothermal vent taxa. *Science* **226**, 965-967.
- Pimenov N., Savvichev A., Rusanov I., Egorov A. V., Gebruk A., Moskalev L., and Vogt P. R. (1999) Microbial processes of carbon cycle as the base of food chain of Haakon Mosby mud volcano benthic community. *Geo-Marine Letters* **19**(1-2), 89-96.
- Raghoebarsing A. A., Pol A., van de Pas-Schoonen K. T., Smolders A. J. P., Ettwig K. F., Rijpstra W. I. C., Schouten S., Sinninghe Damste J. S., Op den Camp H. J. M., Jetten M. S. M., and Strous M. (2006) A microbial consortium couples anaerobic methane oxidation to denitrification. *Nature* **440**, 918-921.
- Reeburgh W. S. (1980) Anaerobic methane oxidation: rate depth distributions in Skan Bay sediments. *Earth and Planetary Science Letters* **47**, 345-352.
- Reeburgh W. S. (1996) "Soft Spots" in the global methane budget. In *Microbial Growth on C₁ Compounds* (ed. M. E. Lidstrom and R. F. Tabita), pp. 334. Kluwer Academic Publishers.
- Reeburgh W. S. and Heggie D. T. (1977) Microbial methane consumption reactions and their effect on methane distributions in freshwater and marine environments. *Limnology and Oceanography* **22**, 1-9.
- Reeburgh W. S., Whalen S. C., and Alperin M. J. (1993) The role of methylotrophy in the global methane budget. In *Microbial Growth on C₁ Compounds* (ed. J. C. Murrell and D. P. Kelly), pp. 1-14. Intercept Ltd.
- Roberts H. H., Aharon P., Carney R., Larkin J., and Sassen R. (1990) Sea floor responses to hydrocarbon seeps, Louisiana continental slope. *Geo-Marine Letters* **10**, 232-243.

- Roberts H. H. and Carney R. (1997) Evidence of episodic fluid, gas, and sediment venting on the northern Gulf of Mexico slope. *Economic Geology* **92**, 863-879.
- Schink B. (1997) Energetics of syntrophic cooperation in methanotrophic degradation. *Microbial Molecular Biology Review* **61**, 262-280.
- Schouten S., Wakeham S. G., Hopmans E. C., and Sinninghe Damste J. S. (2003) Biogeochemical evidence that thermophilic archaea mediate the anaerobic oxidation of methane. *Applied and Environmental Microbiology* **69**(3), 1680-1686.
- Schrenk M. O., Kelley D. S., Bolton S. A., and Baross J. A. (2004) Low archaeal diversity linked to subsurface geochemical processes at the Lost City Hydrothermal Field, Mid-Atlantic Ridge. *Environmental Microbiology* **6**(10), 1086-1095.
- Seiler W. (1984) Contribution of biological processes to the global budget of CH₄ in the atmosphere. In *Current perspectives in microbial ecology* (ed. M. J. Klug and C. A. Reddy). American Society for Microbiology.
- Shen Y. A., Buick R., and Canfield D. E. (2001) Isotopic evidence for microbial sulphate reduction in the early Archaean era. *Nature* **410**(6824), 77-81.
- Shen Y. N. and Buick R. (2004) The antiquity of microbial sulfate reduction. *Earth-Science Reviews* **64**(3-4), 243-272.
- Shima S. and Thauer R. K. (2005) Methyl-coenzyme M reductase and the anaerobic oxidation of methane in methanotrophic Archaea. *Current Opinion in Microbiology* **8**, 643-648.
- Simoneit B. and Lonsdale P. F. (1982) Hydrothermal petroleum in mineralized mounds at the seabed of Guaymas Basin. *Nature* **295**, 198-202.
- Sørensen K. B., Finster K., and Ramsing N. B. (2001) Thermodynamic and kinetic requirements in anaerobic methane oxidizing consortia exclude hydrogen, acetate, and methanol as possible electron shuttles. *Microbial Ecology* **42**, 1-10.
- Sørensen K. B., Lauer A., and Teske A. (2004) Archaeal phylotypes in a metal-rich and low-activity deep subsurface sediment of the Peru Basin, ODP Leg 201, Site 1231. *Geobiology* **2**, 151-161.
- Sørensen K. B. and Teske A. (2006) Stratified communities of active archaea in deep marine subsurface sediments. *Applied and Environmental Microbiology* **72**(7), 4596-4603.
- Strous M. and Jetten M. S. M. (2004) Anaerobic oxidation of methane and ammonium. *Annual Reviews of Microbiology* **2004**(58), 99-117.

- Suess E., Torres M., Bohrmann G., Collier R. W., Greinert J., Linke P., Rehder G., Trehu A., Wallmann K., Winckler G., and Zuleger E. (1999) Gas hydrate destabilization: enhanced dewatering, benthic material turnover and large methane plumes at the Cascadia convergent margin. *Earth and Planetary Science Letters* **170**(1-2), 1-15.
- Teske A. (2006) Microbial communities of deep marine subsurface sediments: Molecular and cultivation surveys. *Geomicrobiology Journal* **23**, 357-368.
- Teske A., Hinrichs K.-U., Edgecomb V., de Vera Gomez A., Kysela D., Sylva S. P., Sogin M. L., and Jannasch H. W. (2002) Microbial diversity of hydrothermal sediments in the Guaymas Basin: Evidence for anaerobic methanotrophic communities. *Applied and Environmental Microbiology* **68**(4), 1994-2007.
- Thauer R. K. (1998) Biochemistry of methanogenesis: A tribute to Marjory Stephenson. *Microbiology-UK* **144**, 2377-2406.
- Thomas D. N., Zachos J. C., Bralower T. J., Thomas E., and Bohaty S. (2002) Warming the fuel for the fire: evidence for the thermal dissociation of methane hydrate during the Paleocene-Eocene thermal maximum. *Geology* **30**(12), 1067-1070.
- Treude T., Boetius A., Knittel K., Wallmann K., and Jørgensen B. B. (2003) Anaerobic oxidation of methane above gas hydrates at Hydrate Ridge, NE Pacific Ocean. *Marine Ecological Progress Series* **264**, 1-14.
- Valentine D. L. (2002) Biogeochemistry and microbial ecology of methane oxidation in anoxic environments: a review. *Antonie van Leeuwenhoek* **81**, 271-282.
- Valentine D. L. and Reeburgh W. S. (2000) New perspectives on anaerobic methane oxidation. *Environmental Microbiology* **2**(5), 477-484.
- Werne J. P., Haese R. R., Zitter T., Aloisi G., Bouloubassi I., Heijs S., Fiala-Médioni A., Pancost R. D., Sinninghe Damsté J. S., de Lange G., Forney L. J., Gottschal J. C., Foucher J.-P., Mascle J., Woodside J., and Parties t. M. a. M. S. S. (2004) Life at cold seeps: a synthesis of biogeochemical and ecological data from Karzan mud volcano, eastern Mediterranean Sea. *Chemical Geology* **204**, 367-390.
- Whiticar M. J. (1990) A geochemical perspective of natural gas and atmospheric methane. *Organic Geochemistry* **16**(1-3), 531-547.
- Whiticar M. J. (1999) Carbon and hydrogen isotope systematics of bacterial formation and oxidation of methane. *Chemical Geology* **161**, 291-314.

- Whitman W. B., Bowen T. L., and Boone D. R. (1999) The methanogenic bacteria. In *The Prokaryotes*, Vol. release 3.0 (ed. M. Dworkin, A. Balows, H. G. Trüper, W. Harder, and K.-H. Schleifer). Springer.
- Whitman W. B., Coleman D. C., and Wiebe W. J. (1998) Prokaryotes: The unseen majority. *Proceedings of the National Academy of Science U.S.A.* **95**, 6578-6583.
- Wuebbles D. J. and Hayhoe K. (2002) Atmospheric methane and global change. *Earth Science Review* **57**(3-4), 177-210.
- Yamamoto S., Alcauskas J. B., and Crozier T. E. (1976) Solubility of methane in distilled water and seawater. *Journal of Chemical Engineering Data* **21**, 78-81.
- Zehnder A. J. B. and Brock T. D. (1980) Anaerobic methane oxidation: Occurrence and Ecology. *Applied and Environmental Microbiology* **39**(1), 194-204.

CHAPTER 2

MOLECULAR BIOGEOCHEMISTRY OF SULFATE REDUCTION, METHANOGENESIS AND THE ANAEROBIC OXIDATION OF METHANE AT GULF OF MEXICO COLD SEEPS¹

¹ Orcutt, B!, A. Boetius, M. Elvert, V. Samarkin, S.B. Joye. 2005. *Geochimica et Cosmochimica Acta*. 69: 4267-4281. Reprinted here with permission of the publisher.

Abstract

The anaerobic oxidation of methane in aquatic environments is a globally significant sink for a potent greenhouse gas. Significant gaps remain in our understanding of the anaerobic oxidation of methane because data describing the distribution and abundance of putative anaerobic methanotrophs in relation to rates and patterns of anaerobic oxidation of methane activity are rare. An integrated biogeochemical, molecular ecological and organic geochemical approach was used to elucidate interactions between the anaerobic oxidation of methane, methanogenesis, and sulfate reduction in sediments from two cold seep habitats (one brine site, the other a gas hydrate site) along the continental slope in the Northern Gulf of Mexico. The results indicate decoupling of sulfate reduction from anaerobic oxidation of methane and the contemporaneous occurrence of methane production and consumption at both sites.

Phylogenetic and organic geochemical evidence indicate that microbial groups previously suggested to be involved in anaerobic oxidation of methane coupled to sulfate reduction were present and active. The distribution and isotopic composition of lipid biomarkers correlated with microbial distributions, although concrete assignment of microbial function based on biomarker profiles was complicated given the observed overlap of competing microbial processes.

Contemporaneous activity of anaerobic oxidation of methane and bicarbonate-based methanogenesis, the distribution of methane-oxidizing microorganisms, and lipid biomarker data suggest that the same microorganisms may be involved in both processes.

1. Introduction

A substantial increase in atmospheric methane concentration over the past two centuries has contributed to present-day global warming (IPCC, 2000). Additional evidence links atmospheric methane concentrations with global-scale climate change throughout geologic time (HESSELBO et al., 2000; KATZ et al., 1999; THOMAS et al., 2002). Though the largest known reservoirs of methane occur in marine sediments as methane hydrate (KVENVOLDEN, 1988), the contribution of this reservoir to the atmospheric methane pool is moderated by the anaerobic oxidation of methane (AOM). Rate measurements, geochemical profiles and reaction-transport modeling results indicate methane is consumed anaerobically using sulfate as electron acceptor according to the following net equation (BARNES and GOLDBERG, 1976; DEVOL et al., 1984; HOEHLER et al., 1994; IVERSEN and JØRGENSEN, 1985; REEBURGH, 1976):



Although the correlation between AOM and sulfate reduction (SR) has been observed in a variety of environments, the biogeochemical mechanism behind AOM remains to be determined (HOEHLER et al., 1994; NAUHAUS et al., 2002; SØRENSEN et al., 2001; VALENTINE and REEBURGH, 2000). Phylogenetic and organic geochemical data have identified a putative syntrophic consortia of anaerobic methanotrophs and sulfate reducing bacteria that mediate AOM, but the metabolic intermediate(s) exchanged between the participating microbes is unknown (BOETIUS et al., 2000; ELVERT et al., 1999; HINRICHS et al., 2000; HOEHLER et al., 1994; ORPHAN et al., 2001b). The anaerobic methanotrophs (named ANME) are phylogenetically related to methanogenic archaea, while the sulfate reducing bacteria are associated with the *Desulfosarcina/Desulfococcus* cluster (BOETIUS et al., 2000; KNITTEL et al., 2003; ORPHAN et al., 2001a). Additional molecular data suggest the involvement of multiple

archaeal and bacterial groups in AOM (HINRICHS et al., 2000; ORPHAN et al., 2001a; ORPHAN et al., 2002; PANCOST et al., 2000; TESKE et al., 2002; THOMSEN et al., 2001). Available 16S clone library evidence suggests that classical methanogens are rare in ANME communities, with the exception of the hydrothermally-heated sediments of the Guaymas Basin (Teske et al. 2002). Recent genomic and proteomic data from samples naturally enriched in ANME microorganisms showed that they contained modified methanogenic genes and enzymes, suggesting that the biochemical mechanism of AOM is a reversal of the bicarbonate-based methanogenesis (Bi-MOG) pathway (HALLAM et al., 2003; HALLAM et al., 2004; KRÜGER et al., 2003). The question remains as to whether ANME microorganisms switch between AOM and methanogenesis (MOG) as a function of environmental conditions.

The processes of AOM, MOG and SR may interact in a variety of ways but no previous work has documented patterns of these processes in comparison to microbiological and geochemical variables. While a number of studies of surficial sediments have focused on interactions between SR and AOM (HANSEN et al., 1998; HOEHLER et al., 1994; JOYE et al., 2004) or SR and MOG (LOVLEY and KLUG, 1986; OREMLAND and POLCIN, 1982), few have investigated potential interaction(s) between AOM and MOG. Available data show that rates of MOG vary considerably in comparison to AOM rates. In sediments from a barrier lagoon, (Cape Lookout Bight, USA), AOM occurred in sulfate-depleted sediments at ~10% the rate of Bi-MOG; both AOM and Bi-MOG were stimulated when sediments were amended with sulfate (HOEHLER et al., 1994). In contrast, in sediments from another coastal environment (Eckernförde Bay, Germany), AOM was limited to sulfate-containing sediments, and Bi-MOG rates were ~40-50% of AOM rates (TREUDE et al., submitted). In benthic microbial mats from the Black Sea, Bi-MOG rates were comparable to AOM and SR rates (TREUDE, 2003); the

majority of archaeal biomass in these mats was associated with ANME-1 and ANME-2 (based on 16S clone libraries and FISH; (KNITTEL et al., 2005)). Thus, the activity of AOM and MOG exhibit variability with respect to the geochemical environment, being restricted to sulfate-depleted sediments in one case and sulfate-replete sediments in another, and the relative magnitude of rates of MOG to those of AOM spanned a considerable range, from 10 to 100% of AOM rates. The observed variation in patterns of methanotrophic and methanogenic activities could result from variability in geochemical factors, microbial community structure, or additional, unknown factors.

To further understand why the processes of AOM and SR appear to be tightly coupled in some cases (HINRICHS and BOETIUS, 2002) but only loosely coupled in others (JOYE et al., 2004), and to document the interaction between AOM and MOG, we investigated these processes in two types of cold seep habitats on the continental slope in the Northern Gulf of Mexico. One site featured a brine pool, the absence of surficial gas hydrates, and a fluid flux of methane-saturated brine; the second site was characterized by surficial and deep gas hydrates and contemporaneous seepage of methane, other alkanes and oil. We used an integrated biogeochemical, molecular biological and organic geochemical approach to holistically characterize the environment. ¹⁴C- and ³⁵S-based radiotracer assays revealed weak coupling between AOM and SR (e.g., <1:1 stoichiometry as would be expected from Eq. 1) and contemporaneous activity of AOM and Bi-MOG, with Bi-MOG rates amounting to about 10% of AOM rates. Microbial distribution and lipid biomarker data illustrated the abundance of putative methanotrophic Archaea, but these data were insufficient to determine concretely the metabolic role of these microbes since AOM and MOG activity overlapped.

2. Methods

2.1. Study Sites and Sample Collection

Along the continental slope in the northern Gulf of Mexico, salt tectonics generate fault networks that act as natural migration pathways for oil, gas, and brine fluid from deep reservoirs to surficial sediments (AHARON, 1994; BEHRENS, 1988; KENNICUTT et al., 1988). When pressure and temperature conditions on the bottom are suitable, high gas fluxes result in gas hydrate formation (DICKENS, 2001; KVENVOLDEN, 1993; MILKOV and SASSEN, 2000; SLOAN, 1990). Seepage of gas charged brine versus oil and gas support distinct cold seep environments dominated by brine pools and mud volcanoes (in the former case) or gas hydrates (in the latter case). Both types of cold seeps are characterized by abundant chemosynthetically-based communities of free-living bacteria (e.g., *Beggiatoa*, *Thioploca*, *Thiomargarita*) and symbiotic macrofauna (e.g. *Lamellibranchia* sp. and *Escarpia* sp. tube worms with thiotrophic symbionts, and *Bathymodoilius*-like mussels with methanotrophic symbionts; (MACDONALD et al., 1989; MACDONALD et al., 1994; MACDONALD et al., 2003; SASSEN and MACDONALD, 1994; SASSEN et al., 2001).

Samples were collected during dives of the manned submersible *Johnson Sea Link II* operated from the *R/V Seward Johnson II* (Harbor Branch Oceanographic Institute) during the summer of 2002 using methods described previously (JOYE et al., 2004). One suite of samples was collected at a brine-influenced seep (GC233; 27:43.3844N, 91:16.6054W, 650m water depth). Seepage was dominated by gas-charged brine; no gas hydrate or oil seepage was evident (MACDONALD et al., 1990a; SASSEN et al., 1994). At this site, a brine pool (~190 m²; (MACDONALD et al., 1990b)) was surrounded by concentric rings (3-7 m wide) of densely-packed mussels (MACDONALD et al., 2003). Sediment cores were collected along the outer edge

of the mussel bed, approximately 3-5m from the edge of the brine pool, where microbial mats dominated by a *Thiomargarita namibiensis*-relative (KALENETRA et al., 2005) were abundant. The second suite of samples was collected from a hydrocarbon-influenced seep in lease block GC232 (27:44.4566N, 91:18.9812W, 504m water depth). The GC232 site lies approximately 4 km west of GC233 (DE BEUKELAER et al., 2003; SAGER et al., 2003) and was characterized by abundant, large (~2m in diameter) surficial gas hydrate mounds and seepage of methane and oil. The sediment surface was covered by a plush mat of vacuolate sulfide-oxidizing bacteria (*Beggiatoa* spp.). Sediment push cores (7cm I.D., ~30 cm core tube length, average recovery of ~15cm of sediment) were collected carefully using the robotic arm of the submersible. Upon return to the surface, cores were transferred immediately to an environmental lab held at bottom water temperature (~ 8 °C) where all subsequent processing was conducted.

2.2 Core sectioning, porewater collection and analysis

Several replicate cores were recovered from an area of about 1 m². One replicate core was used for each of the following procedures: 1. porewater and solid phase analyses, 2. AOM and SR rates, molecular ecology and lipid biomarkers samples, and 3. MOG rates. For porewater and solid phase sample collection, each core tube was fitted with a piston (black rubber stopper) and mounted on a hydraulic extruder. The sediment was extruded at 2 cm intervals into an Argon-filled glove bag in a cold room. At each depth interval, a 2 mL sub-sample was collected into a cut-off syringe for dissolved methane quantification. The sediment was transferred immediately to a 6 mL helium-purged serum vial that contained 2 mL of helium-purged 2M NaOH, which served to arrest biological activity in the sample, and crimp sealed with a butyl rubber stopper. Another 1 mL sub-sample was collected into pre-weighed and pre-

combusted glass vial for determination of porosity (determined by the change in weight after drying at 80°C to a constant weight). The remaining material was transferred into a PVC cup for attachment to a Reeburgh-type squeezer for porewater extraction (JOYE et al., 2004). Sample fixation and analyses for quantifying dissolved methane (CH₄), sulfide (HS⁻), sulfate (SO₄), chloride (Cl⁻) and bicarbonate (DIC or HCO₃⁻) followed the methods of Joye et al. (2004). Samples for volatile fatty acids analysis, primarily for acetate (CH₃COO⁻), were filtered (0.2 μm) and stored frozen until quantification using HPLC (ALBERT and MARTENS, 1997).

2.3 Rate Measurements

To determine AOM and SR rates, 1 to 6 sub-cores (30 cm long x 2.54 cm i.d.) were collected from a core (7 cm i.d.) by manual insertion. Each plexiglass sub-core had pre-drilled, silicone-sealed injection ports at 1 cm intervals along one side of the core. The water phase overlying the core was maintained during sub-coring and the ends of the core tubes were sealed securely with black rubber stoppers. For AOM, 100 μL of dissolved ¹⁴CH₄ tracer (about 35,000 dpm in slightly alkaline milliQ water) was injected into each silicone-filled port. Cores were incubated for 12 hours at bottom water temperature (8° C). Following incubation, cores were extruded and sub-samples were collected at 1 cm intervals and immediately transferred to 20 mL glass vials containing 2 mL of 2M NaOH (which served to arrest biological activity and fix ¹⁴C-CO₂ and ¹⁴C-HCO₃⁻). Each vial was sealed with a teflon-lined screw cap, vortexed to mix the sample and base, and immediately frozen. Time zero samples were fixed immediately after tracer injection. The specific activity of the tracer (¹⁴CH₄) was determined by injecting 100 μL directly into scintillation cocktail (Scintiverse BD) followed by liquid scintillation counting (JOYE et al., 1999). The accumulation of ¹⁴C product (¹⁴CO₂) was determined by acid digestion

following the method of Joye et al. (1999; 2004). The AOM rate was calculated using equation 2:

$$AOM\ Rate = [CH_4] \times \alpha_{CH_4} / t \times (a^{-14}CO_2 / a^{-14}CH_4) \quad (Eq. 2)$$

Here, the *AOM Rate* is expressed as nmol CH₄ oxidized per cm³ sediment per day (nmol cm⁻³ d⁻¹), $[CH_4]$ is the methane concentration (μM), α_{CH_4} is the isotope fractionation factor for AOM (1.06; (ALPERIN and REEBURGH, 1988)), t is the incubation time (d), $a^{-14}CO_2$ is the activity of the product pool, and $a^{-14}CH_4$ is the activity of the substrate pool.

For SR rate measurements, each port was injected with 100 μL of slightly alkaline milliQ water containing about 2 μCi of Na₂³⁵SO₄. Cores were incubated and sectioned as described above. Each section was transferred to a 50 mL centrifuge tube containing 10 mL of 20% zinc acetate to halt microbial activity and fix H₂³⁵S as Zn³⁵S. The accumulation of H₂³⁵S product was recovered in a one-step hot chromous acid digestion (CANFIELD et al., 1986; FOSSING and JØRGENSEN, 1989). The activity of ZnS and sulfate fractions was determined by scintillation counting. The sulfate reduction rate was calculated using equation 3:

$$SR\ Rate = [SO_4] \times \alpha_{SO_4} / t \times (a-H_2^{35}S / a^{-35}SO_4) \quad (Eq. 3)$$

The *SR rate* is expressed as nmol SO₄ reduced cm⁻³ d⁻¹, α_{SO_4} is the isotope fractionation factor for sulfate reduction (1.06; (JØRGENSEN, 1978)), $[SO_4]$ is the pore water sulfate concentration (mM), t is incubation time (d), $a-H_2^{35}S$ is the activity of the product pool, and $a^{-35}SO_4$ is the activity of the substrate pool.

Rates of Bi-MOG and acetoclastic methanogenesis (Ac-MOG) were determined by incubating samples in gas-tight, closed-tube vessels without headspace, to prevent the loss of gaseous ¹⁴CH₄ product during sample manipulation. For collection of sub-samples, a polycarbonate manifold containing 8 pre-drilled holes that were slightly larger than the diameter

of the sample tubes was placed on top of the sediment core. The sediment was extruded into the manifold at 2cm intervals and then a stainless steel blade was inserted at the base of the device to isolate the section from the remaining sediment. Next, 6-8 glass tubes (20ml Pyrex[®] Hungate culture tubes with the rounded end removed) were inserted through the pre-drilled holes into the sediment, stopping at the blade. Tubes were sealed using custom-designed plungers (black Hungate stoppers with the lip removed containing a plastic “tail” that was run through the stopper) were inserted at the base of the tube; the sediment was then pushed via the plunger to the top of the tube until a small amount protruded through the tube opening. A butyl rubber septa was then eased into the tube opening to displace sediment in contact with the atmosphere and close the tube, which was then sealed with a open-top screw cap. The rubber materials used in these assays were boiled in 1N NaOH for 1 hour, followed by several rinses in boiling milliQ[®], to leach potentially toxic substances.

A volume of radiotracer solution (100 μ L of $^{14}\text{C-HCO}_3^-$ tracer ($\sim 1 \times 10^7$ dpm in slightly alkaline milliQ[®] water) or 1,2- $^{14}\text{C-CH}_3\text{COO}^-$ tracer ($\sim 5 \times 10^6$ dpm in slightly alkaline milliQ[®] water)) was injected into each sample. Samples were incubated as described above and then 2 ml of 2N NaOH was injected through the top stopper into each sample to terminate biological activity (time zero samples were fixed prior to tracer injection). Samples were mixed to evenly distribute NaOH through the sample. Production of $^{14}\text{CH}_4$ was quantified by stripping methane from the tubes with an air carrier, converting the $^{14}\text{CH}_4$ to $^{14}\text{CO}_2$ in a combustion furnace, and subsequent trapping of the $^{14}\text{CO}_2$ in NaOH as carbonate (CRAGG et al., 1990; CRILL and MARTENS, 1986). Activity of $^{14}\text{CO}_2$ was measured subsequently by liquid scintillation counting. The rates of Bi-MOG and Ac-MOG rates were calculated using equations 4 and 5, respectively:

$$\text{Bi-MOG Rate} = [\text{HCO}_3^-] \times \alpha_{\text{HCO}_3^-} / t \times (a\text{-}^{14}\text{CH}_4 / a\text{-H}^{14}\text{CO}_3^-) \quad (\text{Eq. 4})$$

$$Ac-MOG\ Rate = [CH_3COO^-] \times \alpha_{CH_3COO^-} / t \times (a^{-14}CH_4 / a^{-14}CH_3^{14}COO^-) \quad (Eq. 5)$$

Both rates are expressed as nmol HCO₃⁻ or CH₃COO⁻, respectively, reduced cm⁻³ d⁻¹, $\alpha_{HCO_3^-}$ and $\alpha_{CH_3COO^-}$ are the isotope fractionation factors for MOG (assumed to be 1.06; (GELWICKS et al., 1994; KRZYCKI et al., 1987)). $[HCO_3^-]$ and $[CH_3COO^-]$ are the pore water bicarbonate (mM) and acetate (μ M) concentrations, respectively, t is incubation time (d), $a^{-14}CH_4$ is the activity of the product pool, and $a-H^{14}CO_3$ and $a-^{14}CH_3^{14}COO$ are the activities of the substrate pools.

2.4. Microbial Distribution

The abundance and associations of specific microbial groups were evaluated using fluorescence in situ hybridization (FISH) techniques that targeted 16S rRNA (PERNTHALER et al., 2002). Due to high background fluorescence from oil in sediment preparations (for example, see Fig. 2.3A), mono-labeled fluorescent oligonucleotide probes were not sensitive enough for robust detection of microbes; thus, an immunochemical-based FISH protocol was used to increase signal intensity (PERNTHALER and AMANN, 2004). In catalyzed reporter deposition FISH (CARD-FISH; also described elsewhere as the tyramide signal amplification (TSA) system; (SCHÖNHUBER et al., 1997)), multiple copies of fluorescently-labeled tyramide molecules bind to oligonucleotide probes bound with horseradish peroxidase (HRP), which increases the fluorescent label per copy of rRNA in the target cells relative to mono-labeled FISH.

Sediment samples for cell counts and FISH were fixed in 3.7% formaldehyde buffered in 1xPBS (140mM NaCl, 10mM sodium phosphate, pH 7.6) for 4-8 hours at 4°C, washed in 1xPBS, and subsequently stored in 1:1 1xPBS:ethanol (EtOH) at -20°C until analysis (BOETIUS et al., 2000). Immobilization of cells on filters for hybridization followed methods described previously (BOETIUS et al., 2000). Total cell abundance of single cells and cells in aggregates

(estimated by dividing aggregate size by average size of spherical cells in aggregate) was determined using acridine orange direct counting (ORCUTT et al., 2004).

The application of FISH probes and amplification of the fluorescence signal followed the methods of Pernthaler et al. (2002), as modified for sediment applications. Hybridization filters were covered in a thin layer of 0.1% (wt/vol) low-melting point agarose (MetaPhor, Bioproducts, Rockland, Maine), dried at 46°C for 1 hour, dehydrated with 80% EtOH and dried at room temperature (RT). Endogenous peroxidases in fixed cells were inactivated by incubating filters in 0.01M HCl for 10 min. at RT. Permeabilization of microbial cell walls was required to permit passage of the large HRP-labeled rRNA probes into the cells; these procedures did not compromise the integrity of the cell structure. Filters were briefly washed in 1xPBS, incubated in SDS solution (0.5% [wt/vol] sodium dodecyl sulfate in 1xPBS) for 8 min. at RT, washed again in 1xPBS, incubated in fresh lysozyme solution (0.05M EDTA, 0.1M Tris (pH 8), 10 mg ml⁻¹ lysozyme) for 1 hour at 37°C, serially washed in 1xPBS, MilliQ water, and 80% EtOH and then dried at RT. This permeabilization strategy resulted in robust enumeration of sediment *Archaea* and *Bacteria* with minimal increase in background fluorescence, loss of target cells, or unspecific binding of rRNA probes (data not shown).

Hybridization protocols were performed as described previously (PERNTHALER et al., 2002). Filter sections were incubated in appropriate hybridization buffers (900mM NaCl, 20mM Tris-HCl, varying concentrations of formamide (FA; 99.9% molecular biology grade, see below for percentage used), 1% blocking reagent (Roche, Basel, Switzerland), 10% [wt./vol] dextran sulfate) with HRP-labeled probes (Thermo Biosciences GmbH, Germany; ~27 pmol ml⁻¹ final concentration) at 35°C for 2 hours with gentle mixing. Probes and corresponding FA concentrations in hybridization buffers used were as follows: EUB338 I-III (DAIMS et al., 1999)

for *Bacteria* (55% FA), ARCH915 (AMANN et al., 1990) for *Archaea* (55% FA), ANME1-350 (BOETIUS et al., 2000) for the ANME1 clade of *Euryarchaeota* (40% FA), EelMSX932 (BOETIUS et al., 2000) for the ANME2 clade of *Euryarchaeota* (40% FA), DSS658 (MANZ et al., 1998) for the *Desulfosarcina* spp./*Desulfococcus* spp./*Desulfofrigus* spp./*Desulfofaba* spp. clades of sulfate reducing δ -Proteobacteria (55% FA), and NON338 (WALLNER et al., 1993) as a non-sense negative control probe to check for unspecific binding (55% FA). Background signal from the nonsense probe NON338 was negligible, and thus, is not reported. Probe specificity was verified by hybridization in samples of defined microbial composition. Synthesis of fluorescently-labeled (Cy3, carboxyfluorescein, Alexa₅₄₆ and Alexa₄₈₈ dyes) tyramides followed the method of Hopman et al. (1998); application of tyramide to hybridized samples followed the method of Pernthaler et al. (2002). To simultaneously visualize multiple microbial groups, hybridization and fluorescence labeling was carried out in sequence using probes labeled with different fluorescent dyes. Each probe was applied, hybridized, and then signal amplified. Then, the HRP-label was inactivated by incubating in 0.01M HCl for 10 min. at RT followed by a 1xPBS wash. The next hybridization was performed in a similar manner.

Hybridized filters were covered with 4',6'-diamidino-2-phenylindole (DAPI)-amended mounting solution (1 part 1xPBS, 5.5 parts Citifluor mountant, 1 part Vecta Shield mountant, 2 $\mu\text{g ml}^{-1}$ DAPI) for total cell enumeration. Cell counts using DAPI was comparable to measurements using AODC (data not shown). Roughly 40 fields (1000-1600 DAPI cells) were examined for each sample/probe combination to determine average cell counts. Percentages of each microbial group were determined by the representative proportion of hybridized cells to DAPI cells per field. Samples were visualized under 1000x oil-immersion magnification using an Axioplan II Zeiss epifluorescence microscope equipped with an HBO 100-W Hg vapor lamp,

with appropriate filters sets for Cy3 and Alexa₅₄₆ (Chroma, Brattleborough, Conn.), carboxyfluorescein and Alexa₄₈₈ (Zeiss09; Zeiss, Germany), and DAPI (Zeiss01; Zeiss, Germany) fluorescence.

2.5. Lipid biomarkers

Lipid biomarkers were extracted from ~1.4 g wet sediment and analyzed according to previously described methods (BOETIUS et al., 2000; ELVERT et al., 2003; ELVERT et al., 2001). Briefly, total lipids were extracted following ultrasonification in methanol/dichloromethane. The total lipid extract (TLE) was saponified with 6% KOH in methanol; neutral lipids were removed from the saponified TLE by extraction with *n*-hexane. Fatty acids were obtained from the remaining TLE phase by acidification to pH 1 and subsequent extraction with *n*-hexane. Carboxylic (fatty) acid methyl esters (FAMES) were generated from the fatty acids by reaction with 14% BF₃ in methanol and subsequent re-extraction with *n*-hexane. Alcohol lipid fractions were obtained from the neutral lipid extract using liquid chromatography separation on a column of activated silica suspended in dichloromethane. Alcohol derivatives were generated by reaction with pyridine and BSTFA. Lipid biomarkers were identified by coupled gas chromatography-mass spectrometry (GC-MS) using a Thermoquest Trace GC interfaced to a Finnigan Trace MS. Compounds were identified by comparison with mass spectra from known compounds. Carbon isotopic compositions of individual biomarkers were determined by coupled gas chromatography-isotope ratio mass spectrometry (GC-IRMS) using HP 6890 Series GC interfaced via a Finnigan Combustion Interface III to a Finnigan Delta plus mass spectrometer. The reported biomarker $\delta^{13}\text{C}$ values have an analytical error of ± 1.0 ‰ and have been corrected for the introduction of additional carbon atoms during derivitization.

3. Results

3.1. Methane turnover and sulfate reduction

In sediments collected from a microbial mat at the edge of the brine pool (GC233, (MACDONALD et al., 2003)), methane concentrations were well below saturation ($<30\mu\text{M}$; Fig. 2.1A) and AOM rates were very low ($<2\text{ nmol cm}^{-3}\text{ d}^{-1}$; Fig. 2.1A), despite high turnover rates for ^{14}C -methane ($\sim 10\%$ turnover in 12 hours). Dissolved inorganic carbon (HCO_3^-) concentration increased steadily with depth, reaching a maximum of 14 mM between 10-12 cm (Fig. 2.1B). Rates of Bi-MOG increased with depth but were low ($<0.4\text{ nmol cm}^{-3}\text{ d}^{-1}$; Fig. 2.1B). Both acetate concentrations and rates of Ac-MOG were also low in these sediments (Fig. 2.1C). The SR rates, in contrast, were extremely high between 2 and 8 cm ($>3.5\text{ }\mu\text{mol cm}^{-3}\text{ d}^{-1}$; Fig. 2.1D). The sulfate concentration decreased from 26 to 15 mM over 10 cm (Fig. 2.1D). Sulfide (H_2S) gradually increased from 0.2 mM at the surface to 7 mM at 11 cm (Table 2.1). Although these sediments were collected from a brine seep, the pore water chlorinity (Cl) did not increase markedly with depth (Table 2.1), showing that the core did not penetrate into brine. Averaged over the top 10 cm, AOM and SR rates were 0.1 and $154\text{ mmol m}^{-2}\text{ d}^{-1}$, respectively, and the Bi-MOG rate was $4.8\text{ }\mu\text{mol m}^{-2}\text{ d}^{-1}$.

In contrast to the brine site, sediments collected from a gas hydrate site (GC232) contained significant concentrations of methane ($<1.5\text{ mM}$; Fig. 2.2A), though still below *in situ* saturation values ($\sim 80\text{ mM}$). The peak in methane concentration at 5-7 cm coincided with the peak in AOM ($\sim 160\text{ nmol cm}^{-3}\text{ d}^{-1}$; Fig. 2.2A) and Bi-MOG ($\sim 30\text{ nmol cm}^{-3}\text{ d}^{-1}$; Fig. 2.2B). The HCO_3^- concentration increased rapidly from the surface ($<2\text{ mM}$) to 5-7 cm where concentrations were $\sim 30\text{ mM}$ (Fig. 2.2B). Acetate concentration, in contrast, remained fairly

constant ($<12 \mu\text{M}$) down to 5-7 cm, then increased dramatically to $\sim 400 \mu\text{M}$ at 15 cm (Fig. 2.2C). Similarly, Ac-MOG was negligible ($<0.1 \text{ nmol cm}^{-3} \text{ d}^{-1}$) above 5-7 cm, but increased gradually to $>50 \text{ nmol cm}^{-3} \text{ d}^{-1}$ by 15 cm (Fig. 2.2C). Sulfate was rapidly consumed within 0-4 cm from 28 mM to $\sim 6 \text{ mM}$ and then gradually decreased between 4 and 10 cm (Fig. 2.2D). Rates of SR ranged from 80-640 $\text{nmol cm}^{-3} \text{ d}^{-1}$ in the upper 10 cm, and were usually greater than AOM rates (Fig. 2.2D). The SR rates in deeper sediments were extremely high ($>3.3 \mu\text{mol cm}^{-3} \text{ d}^{-1}$; Fig. 2.2D). Overall concentrations of H_2S were high ($>11 \text{ mM}$) throughout the core, with a peak in concentration ($\sim 20 \text{ mM}$) at 5 cm (Table 2.1). A noticeable decrease in Cl^- from 557 mM at the surface to 421 mM at 7 cm (Table 2.1) in the core suggests freshening of the porewater, possibly via gas hydrate dissociation during core recovery. Aerial AOM and SR rates at GC232 in the upper 10 cm were 6.4 and $\sim 30 \text{ mmol m}^{-2} \text{ d}^{-1}$, respectively; Bi-MOG and Ac-MOG rates were ~ 380 and $93.2 \mu\text{mol m}^{-2} \text{ d}^{-1}$, respectively.

3.2. Distribution and diversity of microorganisms

Using CARD-FISH, we evaluated the abundance patterns of five groups of prokaryotes. Total cell counts via AODC were higher in brine sediments ($5.6 \pm 0.7 \times 10^9 \text{ cells ml}^{-1}$) than in gas hydrate sediments ($2.7 \pm 0.7 \times 10^9 \text{ cells ml}^{-1}$; Table 2.1). In brine sediments, *Bacteria* dominated the surficial microbial community; however, below 5 cm, *Archaea* abundance increased significantly, accounting for nearly 50% of the total microbial population at 9 cm (Table 2.1). In contrast, *Bacteria* were dominant over depth in hydrate sediments, although the proportion of *Archaea* increased with depth (Table 2.1).

CARD-FISH with group specific primers revealed high numbers of putative methanotrophic archaea (i.e. ANME-1 and ANME-2; Figs. 1E, 2E; Table 2.1), although the

abundance patterns were noticeably different between sites. At the brine site, ANME-1 dominated the archaeal microbial population below 3 cm, increasing from 12 to 46% of the total microbial community (70-95% of *Archaea*) within the zone where peak SR activity was observed (Fig. 2.1E). Typically, ANME-1 occurred as short rods (2-3 μm in length) or as segmented rod chains consisting of 2-8 cells up to 20 μm in length (Fig. 2.3C); mono-specific clusters of ANME-1 up to 25 μm in diameter were also observed (Fig. 2.3D). Although not present in high abundance, ANME-2 archaea were typically found in shell-type consortia with sulfate reducing bacteria (SRB) of the *Desulfosarcina/Desulfococcus* spp. (DSS) taxon (Figs. 1E, 3E). Clusters ranged from 5 to 25 μm in diameter. ANME-1 occasionally formed loose clusters with other microorganisms, including DSS and other unidentified bacteria. DSS-type cells were most often found associated with ANME-2 cells in shell-type consortia.

In gas hydrate sediments, ANME-1 was also the dominant archaeal group (Fig. 2.2E; Table 2.1), accounting for up to 20% of the total microbial population and 78% of total *Archaea* at depth. Shell-type consortia of the ANME-2/DSS were more abundant and generally larger in size at the gas hydrate site. DSS-targeted cells were often found unassociated with either of the ANME groups; these microbes had a vibrio-like morphology in contrast to the more coccoid-like DSS-SRB that were observed in the ANME consortia. ANME-2 were not observed in shell-type consortia with non-DSS cells, although they were occasionally observed in loose arrangements without associated DSS (Fig. 2.3F). Both ANME populations increased around the depth where rates of AOM and Bi-MOG peaked; DSS increased in the same interval (Fig. 2.2E). At this depth, combined numbers of ANME-1 and ANME-2 comprised >96% of the total *Archaea*.

3.3. Distribution and C isotopic signatures of lipid biomarkers

The abundance and C isotopic composition of signature lipid biomarkers were evaluated to infer carbon flow through the microbial population. Unraveling carbon flow in such complex systems requires knowledge of the isotopic values of various carbon pools (for example, methane, carbon dioxide, organic acids, organic matter, etc.; Table 2.2). The $\delta^{13}\text{C}$ -methane at the brine site was ~14-30‰ lighter than that observed at the hydrate site. Values of $\delta^{13}\text{C}$ for acetate or other labile organic acids (common substrates for sulfate reducers) are, to our knowledge, unknown at either site.

Lipid biomarkers diagnostic for the putative methanotrophic archaea (i.e., archaeol and *sn*-2-hydroxyarchaeol, (ELVERT et al., 1999; HINRICHS et al., 1999; ORPHAN et al., 2002) were present at low concentration at both sites (Figs. 1F, 2F, Tables 3A, 3B). These biomarkers were very depleted in ^{13}C , with $\delta^{13}\text{C}$ values of -90.7 to -114.5‰ at the brine site (Fig. 2.1G, Table 2.3A) and -83.9 to -104.6‰ at the gas hydrate site (Fig. 2.2G, Table 2.3B). Generally, stronger ^{13}C -depletions and higher concentrations were detected for *sn*-2-hydroxyarchaeol at both sites with the exception of two depths at the brine site, where archaeol was more ^{13}C -depleted. Other forms of hydroxyarchaeol were not detected at either site. Signature archaeal hydrocarbon lipids could not be analyzed due to weak signal-to-noise resolution of lipids against a strong background of an unresolved complex mixture (UCM; (ZHANG et al., 2002)). Other important membrane lipids such as glycerol dialkyl glycerol diethers (GDGTs) and their biphytanic hydrocarbon degradation products (BLUMENBERG et al., 2004; HINRICHS et al., 2000; PANCOST et al., 2001) were not targeted by the methods employed here.

In brine sediments, the most abundant bacterial fatty acid, *cis*-11 octadecanoate (18:1 ω 7c; Table 2.3A), had $\delta^{13}\text{C}$ values ranging from -39.8‰ at the surface to -79.2‰ at 10 cm.

After the generic bacterial biomarker hexadecanoate (16:0), the unsaturated lipids cis-11 hexadecanoate (16:1 ω 5c) and cis-9 hexadecanoate (16:1 ω 7c) were most abundant (Table 2.3A). 16:1 ω 5c, a biomarker diagnostic for DSS in the AOM consortia (ELVERT et al., 2003), had $\delta^{13}\text{C}$ values ranging from -62.6‰ at the surface to -90.4‰ at depth (Figs 1H, 1I, Table 2.3A). The branched chain 13-methyltetradecanoate (ai-15:0) and 12-methyltetradecanoate (i-15:0) fatty acids (Fig. 2.1H, 1I, Table 2.3A), both considered generally diagnostic for sulfate reducing bacteria (TAYLOR and PARKES, 1985), also exhibited ^{13}C depletion with increasing depth (down to -83.7‰ for ai-15:0 and -68.9‰ for i-15:0). Although in low abundance, two additional fatty acids showed significant depletion in ^{13}C with depth: the cyclopropane fatty acid 11,12-methylene-hexadecanoic acid (cy17:0 ω 5,6) exhibited $\delta^{13}\text{C}$ values from -73.8 to -112.4‰ and cis-11 heptadecanoate (17:1 ω 6c) exhibited a $\delta^{13}\text{C}$ range of -54.4 to -79.6‰ (Table 2.3A). Both of these lipids are suggested to be indicative of the DSS involved in AOM (ELVERT et al., 2003). Recent evidence suggests that the occurrence of 16:1 ω 7c, 16:1 ω 5c, and cy17:0 ω 5,6 fatty acids may also be indicative of DSS associated with ANME-2 ('ANME-2-type DSS'), while isotopically ^{13}C -depleted ai15:0 and i15:0 lipids derive from DSS associated with ANME-1 ('ANME-1-type DSS'; (BLUMENBERG et al., 2004). The branched chain 15-methylhexadecanoate (ai-17:0) and 14-methylhexadecanoate (i-17:0) fatty acids were in very low abundance, and their values are not reported here.

Overall patterns of lipid abundance were similar in gas hydrate sediments, with a few notable exceptions. 16:1 ω 7c was the most abundant biomarker, followed by 18:1 ω 7c; both showed depletion in ^{13}C with depth (Table 2.3B). Of the biomarkers supposedly diagnostic for SRB, ai-15:0, 16:1 ω 5c, and i-15:0 were the most abundant (Fig. 2.2H, Table 2.3B). As at the brine site, these fatty acids generally exhibited lighter $\delta^{13}\text{C}$ values with depth, with 16:1 ω 5c

having the strongest depletion (-67.6‰; Fig. 2.2I, Table 2.3B). Cy17:0 ω 5,6 was more abundant at the gas hydrate site and was the most ¹³C depleted (down to -79.6‰ at 4-6 cm depth; Figs. 2H, 2I, Table 2.3B). In general, both the bacterial fatty acids and the archaeal alcohol biomarkers were heavier at the hydrate- site than at the brine site (Tables 3A, 3B).

4. Discussion

This study presents the first data set from two distinct cold seeps comparing results from radiotracer-based measurements of AOM, MOG, and SR with geochemical, microbial diversity, and lipid biomarker data. We observed decoupling of SR from AOM as well as the contemporaneous production of methane from bicarbonate and the oxidation of methane to bicarbonate in sediments from gas hydrate and brine sites. Phylogenetic and organic geochemical evidence indicate that microbial groups associated with AOM coupled to SR (i.e., ANME-1, ANME-2, and DSS; (BOETIUS et al., 2000; HINRICHS et al., 2000; MICHAELIS et al., 2002; ORPHAN et al., 2001b)) were present in these sediments and ANMEs dominated the archaeal community. We suggest that both types of ANMEs were responsible for the observed ¹⁴C-methane consumption and that one or both of the ANMEs were responsible for the observed methane production.

A schematic of physical and geochemical characteristics of the sites, highlighting the differences between the two cold seep environments, is presented in Figure 4. Interactions between AOM, SR and MOG occurring in sediments underlying microbial mats are illustrated in the inset of Figure 4. The oxidation of methane by ANME microorganisms is linked to sulfate reduction activity, although the specific intermediate coupling these processes is unknown. Other *Archaea*, perhaps ANME microorganisms, produce methane within the same environment,

though the mechanism of potential coupling between MOG and AOM is unclear. Oxidation of oil and other alkanes may also fuel sulfate reduction activity, particularly at the gas hydrate site.

4.1. Brine-dominated cold seeps

The geochemical profiles in brine sediments (e.g., low methane and high sulfate concentrations at depth) showed that the “traditional” sulfate-methane interface, which demarcates the AOM zone, was not penetrated in this core. However, SR rates were extremely high ($>3.5 \mu\text{mol cm}^{-3} \text{ d}^{-1}$, $154 \text{ mmol m}^{-2} \text{ d}^{-1}$ for the upper 10cm), similar to previous SR rates documented in the Gulf of Mexico (ARVIDSON et al., 2004; JOYE et al., 2004) and higher than rates observed at other methane seeps (AHARON and FU, 2003; BOETIUS et al., 2000; HANSEN et al., 1998; PIMENOV et al., 1999; TREUDE, 2003; TREUDE et al., 2003; WEBER and JØRGENSEN, 2002). High SR and low AOM suggests that the majority of SR activity was fueled by organic carbon sources other than methane (JOYE et al., 2004).

Despite the observed low rates of AOM in brine sediments, turnover of the methane pool was rapid ($\sim 10\% \text{ d}^{-1}$; Fig. 2.1A), suggesting a considerable potential for AOM during periods of increased methane fluxes/concentrations. The conspicuously dominant ANME-1 population increased rapidly within and below the depth of maximal AOM and Bi-MOG rates. Given the observed low rate of AOM, the large size of the ANME population is surprising, suggesting that this population either used another metabolic strategy (see inset of Fig. 2.4), was supported by the measured (low) AOM rates, or reflected a previous high methane flux/methane oxidation activity period. The presence and ^{13}C depletion of archaeal lipids indicated an active, or recently active, AOM-mediating population. Fluid flow through cold seep sediments is transient in both space and time (BROWN et al., 1996; LINKE et al., 1994; TORRES et al., 2002a; TYRON et al.,

1999). Currently, it is unclear how long populations of AOM-associated microbes can survive during periods of low methane flux. Available data indicate that anaerobic methanotrophs grow slowly (doubling time of several months; (NAUHAUS et al., 2002), even under relatively high methane concentrations, inferring that the modest energy yield of AOM results in low anabolic rates.

Though AOM rates were low, SR rates were extremely high. To reconcile the observed sulfate profile with the high SR rates (Fig. 2.1D) requires a sulfate source in addition to diffusion (ARVIDSON et al., 2004). Brine advection through the sediments would reduce the sulfate penetration depth since the brine contains no sulfate (JOYE et al., 2005) and, at present, no fluid flux rates are available for this site. However, it is possible that brine advection generates convection cells that drive seawater percolation through sediments at the edge of the brine pool, increasing sulfate availability at least in some areas. Modeling of geochemical profiles at gas hydrate sites indicated that organism-sediment interactions replenish subsurface sulfate via bioirrigation and/or in situ recycling via anaerobic sulfide oxidation (ARVIDSON et al., 2004) but tubeworms are not abundant at this brine pool. Some sulfide oxidizing microbes (e.g., *Thiovulum*) common to sulfide-rich sediments generate structures (e.g., veils) that influence flow through the sediments to optimize geochemical conditions for their activity (FENCHEL and GLUD, 1998). *Beggiatoa* at Gulf of Mexico cold seeps also form complex surface veils that may influence fluid flow through sediments. The surface sediments at the brine site were covered by a dense mat of a giant sulfide oxidizing bacteria closely related to *Thiomargarita namibiensis* (0.51 mm³ cm⁻³ biovolume; (KALENETRA et al., 2005). However, because 99% of the sulfide oxidizing bacterial biomass was found in the upper 2 cm of sediment (KALENETRA et al., unpublished data) and because *Thiomargarita*-like microbes are not motile, it is unlikely that

they supplied sulfate to depths > 5 cm. One possible explanation for the increased sulfate concentration at depth is barite dissolution. Authigenic barite is abundant at cold seeps in the Gulf of Mexico (FU et al., 1994) and elsewhere (PAYTAN et al., 2002; TORRES et al., 2003; TORRES et al., 2002b). Similar increases in sulfate concentration at depth in cold seep sediments in the Sea of Okhotsk were linked to barite dissolution (GREINERT et al., 2002). We hypothesize that barite dissolution is responsible for generating the increased sulfate concentration observed at depth and plan to address this possibility in future studies.

The abundance of *Thiomargarita*-related bacteria correlated with the lipid biomarker profiles of the sediments. The 18:1 ω 7c and 16:1 ω 7c fatty acids likely derive from *Beggiatoa* spp. (CANTU et al., 2003; ELVERT et al., 2003). In the brine sediments, 18:1 ω 7c and 16:0, both having similar $\delta^{13}\text{C}$ -values of $\sim -40\text{‰}$, were the dominant fatty acids; 16:1 ω 7c (-43‰) was less common. Since *Beggiatoa* spp. were almost two orders of magnitude less abundant than the dominant *Thiomargarita namibienses*-relative (KALENETRA et al., 2005), the 18:1 ω 7c > 16:1 ω 7c trend may reflect a biosignature of this abundant microbe.

Although the SR rate was high in brine sediments, the total number of SRB detected with CARD-FISH was low: less than 7% of cells were DSS (compared with 40-50% ANME-1; Fig. 2.1E). The DSS 658 probe may not have targeted the dominant SRB in these sediments; however, hybridization with other FISH probes specific for putative seep-endemic SRB (probe DSR 651, *Desulforhopalus* spp.; probe 660, *Desulfobulbus* spp.; (KNITTEL et al., 2003)) revealed that these microorganisms were rare (<5% and 1%, respectively, of the total population; data not shown). Previous work at Gulf of Mexico gas hydrate sites (LANOIL et al., 2001; MILLS et al., 2003; MILLS et al., 2004) indicated that a significant fraction (32.4%) of δ -*Proteobacteria* sequences in sediments (based on 16S complementary rDNA clone libraries; (MILLS et al.,

2004)) fall within the coverage of the DSS 658 probe, although ~49% of *δ-Proteobacteria* sequences (MILLS et al., 2004) group with the “SEEP-SRB2/Eel-2 group” of SRB (KNITTEL et al., 2003; ORPHAN et al., 2001a), which is not targeted by the DSS 658 probe (KNITTEL et al., 2003) or any other published probe. To our knowledge, no *δ-Proteobacteria* sequences have been published for Gulf of Mexico brine sediments; therefore, the SRB at these sites could be divergent from known groups and thus were not targeted by the FISH probes we used.

The DSS-cells observed in the brine sediments occurred almost exclusively in consortia arrangements with ANME-2 microorganisms. This association was also evident in the lipid biomarker profiles: in the upper depths of the sediment, the ANME-2-type DSS signature lipids (BLUMENBERG et al., 2004; ELVERT et al., 2003) were abundant and significantly depleted in ¹³C. However, ANME-1-type DSS appeared to become more prevalent with depth (based on decreasing abundance of ANME-2-type DSS signature lipids and depletion of ¹³C of ANME-1-type DSS signature lipids; Figs. 1H, 1I, Table 2.3A). The concentration ratio of *sn*-2-hydroxyarchaeol to archaeol in the upper sediments indicates that the ANME-2 may be the dominant producer of these lipids (BLUMENBERG et al., 2004; ELVERT et al., 2005). In the upper sediment layers, ANME-2-type consortia carry the strongest AOM-derived signal, followed by ANME-1 with depth, a pattern consistent with other observations (ELVERT et al., 2005; ORPHAN et al., 2004).

4.2. Gas hydrate-dominated cold seeps

In gas hydrate site sediments, the coincident occurrence of AOM and Bi-MOG was observed between 5 and 9 cm (Figs. 2A, 2B). As observed at the brine site, total Bi-MOG rates were roughly 10% of AOM rates, although rates of both processes were 2 orders of magnitude

higher at the hydrate site, where methane concentrations were also higher. Within the zone of elevated AOM and MOG, the populations of ANME-1, and to a lesser degree ANME-2, increased as based on CARD-FISH observations; together they comprised nearly 92% of the identified *Archaea* (Fig. 2.2E, Table 2.2). A study of sediments collected at a nearby gas hydrate site (GC234, 9.5 km from GC232) indicated that only the ANME-2 group was metabolically active (based on complementary rDNA clone libraries; (MILLS et al., 2004)), even though ANME-1 comprised a significant portion of archaeal 16S rRNA clone libraries (17.2%, (LANOIL et al., 2001); 19.8%, (MILLS et al., 2003)). Since FISH methods are based on the presence of rRNA, a molecule that degrades rapidly in dead or dying microbial cells, our data suggest that both groups are metabolically active at these sites.

The higher abundance of ai15:0 and i15:0 in the hydrate site sediments suggest the association of DSS with ANME-1 (BLUMENBERG et al., 2004; ELVERT et al., 2005). Similarly, the abundance and ¹³C-depletion of 16:1 ω 5c and cy17:0 ω 5,6 lipids may imply associations of DSS with ANME-2. Although the branched chain fatty acids were present in high concentration in the gas hydrate site sediments (specifically ai15:0 and i15:0), they were not the most ¹³C depleted fatty acids observed (Fig. 2.2H, Table 2.3B), contrary to previous reports for Gulf of Mexico cold seep sediments (ZHANG et al., 2002). The differences in lipid distributions and isotopic composition of bacterial biomarkers between brine and hydrate sediments most likely reflects the variability between the SRB populations (e.g., ANME-1-type or ANME-2-type DSS or other sulfate reducers), metabolism (e.g., involvement in AOM versus oil, hydrocarbon or other DOM oxidation), and/or differences in available organic carbon substrates (e.g., absence of oil and higher alkanes at the brine site). Overall, the isotopic composition of DSS lipids are

relatively heavy at the hydrate site, which is consistent with the incorporation of carbon derived from heavier thermogenic methane or fractionation during lipid biosynthesis.

In contrast to the brine sediments, in gas hydrate site sediment, DSS-type SRB were abundant ($\leq 20\%$ with depth, Fig. 2.2E). Many of the observed DSS were attached to ANME-2 archaea in consortia of various sizes (Fig. 2.3E); however, the majority occurred alone or in loose association with ANME-1 or other unidentified bacteria. The unattached DSS-SRB typically had a vibrio-like morphology when compared to the coccoid DSS-SRB noted in consortia with ANME-2, suggesting that distinct subpopulations of DSS-type SRB inhabited the gas hydrate site sediment. As observed in brine sediments, only a few cells could be visualized with FISH probes for other non-DSS SRB (i.e. *Desulforhopalus*, *Desulfobulbus* spp.; data not shown). The unattached DSS-SRB and possibly other SRBs likely contributed to the high SR observed; the excess SR activity (relative to AOM) was probably coupled to oxidation of higher hydrocarbons or oil (JOYE et al., 2004).

In the surficial sediments from the hydrate site, which were covered by a mat containing white *Beggiatoa* and other sulfide oxidizing bacteria (Fig. 2.4), 16:1 ω 7c and 18:1 ω 7c were by far the most abundant fatty acids, with 16:1 ω 7c almost three times as abundant as 18:1 ω 7c (Table 2.3B). These lipids are suggested to be derived from sulfide oxidizing bacteria (CANTU et al., 2003; ELVERT et al., 2003). However, the lighter isotopic composition of 16:1 ω 7c (-63‰) compared to 18:1 ω 7c (-30‰) suggest that these fatty acids are derived from at least two different bacterial sources.

4.3. Are methane production and oxidation linked in AOM zones?

Although there are substantial geochemical and geological differences between the two sites investigated in this study (highlighted in Fig. 2.4), similar trends of AOM and MOG activity were observed. In sediments from both sites, rates of Bi-MOG were roughly 10% of measured AOM rates within the zones of maximal activity. This contemporaneous occurrence of AOM and MOG, coupled with the observation that ANME-1, and to a lesser degree ANME-2, microorganisms dominated the archaeal community, suggests that one or both of the ANME groups catalyzes both processes (inset of Fig. 2.4). Previous studies with methanogenic cultures and methanogenic coastal sediments showed low rates of AOM relative to Bi-MOG (~1% to 10% respectively, (HOEHLER et al., 1994; ZEHNDER and BROCK, 1980). The coincident occurrence of AOM and Bi-MOG in sediments dominated by ANME's has been observed elsewhere (e.g., ANME-1 dominated Black Sea mats and ANME-2 dominated estuarine sediments, (TREUDE, 2003), suggesting that the involvement of ANME's in AOM and MOG is widespread. Previous evidence suggests that ANME-1 may occur without associated sulfate reducing bacterial partners (ORPHAN et al., 2002) and the results presented here suggests that ANMEs may mediate MOG.

Recent evidence suggests that the ANME archaea contain genes involved in the methanogenic pathway and that expression of these genes generates catalytically active enzymes (HALLAM et al., 2003; HALLAM et al., 2004; KRÜGER et al., 2003). These data help explain the biochemical machinery necessary to allow ANME's to oxidize methane (i.e., by reversing the methanogenic enzymatic machinery). However, if the enzymatic machinery is reversible, it is possible that the observed rates of MOG occur via enzymatic back-reaction (e.g., equilibrium enzyme effects). While it is highly unlikely that a single microorganism would both oxidize and

produce methane for energy generation, it is possible that separate but similar microbes exploit opposing methanogenic/methanotrophic machinery depending on environmental geochemical cues and/or the association of syntrophic partners. An enzymatic back reaction with one pathway being dominant and the other representing a small fraction of the other could occur, as has been demonstrated in methanogens that oxidize methane slowly (~1%) relative to the rate of MOG (HOEHLER et al., 1994; ZEHNDER and BROCK, 1980). Availability of labile organic carbon, hydrogen, and other possible intermediates represent chemical cues that could influence the patterns of AOM coupled to MOG and SR. Determining which cues drive AOM-associated microbes to be net methanogenic versus net methanotrophic is imperative in order to understand interactions between the microbes involved in AOM.

The observation that ANME-type microorganisms dominate the archaeal community in areas with coincident AOM and Bi-MOG raises questions about the function(s) of these microorganisms in the environment. Previous work (ORPHAN et al., 2001a; ORPHAN et al., 2002; ORPHAN et al., 2004; PANCOST et al., 2000; TESKE et al., 2002) suggests that multiple and diverse groups of microorganisms are involved in AOM; the data presented here suggests that these microorganisms utilize multiple and diverse metabolic strategies (i.e. ANME-1 may be involved in MOG; Fig. 2.4). Presumably, microorganisms involved in AOM survive on the edge of thermodynamic limits since the energy yield of the net process is small (HOEHLER et al., 1994; SØRENSEN et al., 2001), thus, it would be advantageous if they were able to utilize multiple metabolic strategies as a function of local environmental conditions. If ANME microorganisms mediate AOM by a reversal of the methanogenic pathway (Fig. 2.4; (HALLAM et al., 2003; HALLAM et al., 2004; HOEHLER et al., 1994; ZEHNDER and BROCK, 1980)), the key, then, is to determine the factors that trigger the enzymatic processes to result in net methanotrophy versus

net methanogenesis. Achieving this goal requires additional research in a variety of environments where AOM occurs.

Acknowledgements

The authors thank the crew of the *R/V Seward Johnson II* and the *Johnson Sea Link II* submersible and the science party of the LExEn 2002 research cruise for their help in collecting and processing samples. We thank M. Erickson, K. Kalenetra, T. Lösekann, N. Finke, A. Pernthaler, and R. Amann for providing analytical assistance and expertise, J. Montoya for assistance with the conceptual development of Figure 4, and J. Harnmeijer and two anonymous reviewers for providing useful comments on this manuscript. This research was supported by the National Science Foundation Life in Extreme Environments Program (OCE-0085549) and by the American Chemical Society (PRF-36834-AC2). The U.S. Department of Energy and the NOAA-National Undersea Research Program provided funding for submersible operations. Financial support for B. Orcutt was provided by a University of Georgia graduate recruiting fellowship and by a National Science Foundation graduate fellowship.

Table 2.1. Concentrations of sulfide (H₂S) and chloride (Cl⁻), total cell abundance, and percentage of cells (as determined by CARD-FISH) that were *Bacteria* (EUB), *Archaea* (ARC), of the ANME-1 clade of *Euryarchaeota* (ANME1), of the ANME-2 clade of *Euryarchaeota* (ANME2), or of the *Desulfosarcina/Desulfococcus* spp. clades of δ -proteobacteria (DSS) in sediments from the Gulf of Mexico.

<i>parameter:</i>	depth	H ₂ S	Cl ⁻	cells	EUB	ARC	ANME1	ANME2	DSS
<i>unit:</i>	cmbsf	mM	mM	10 ⁹ ml ⁻¹	% cells				
<u>Site + Dive</u>									
GC233	1	0.2	544.9	5.4	64.5	5.6	2.7	4.6	10.0
(brine pool)	3	1.0	531.4	4.8	55.3	16.9	11.8	7.4	9.9
Dive 4458	5	2.9	571.1	5.5	28.9	41	36.1	4.4	7.0
	7	4.6	-	5.4	22.8	37.6	33.4	6.9	4.4
	9	-	509.5	6.8	11.7	48.3	45.9	2.4	4.6
	11	7.0	-	-	-	-	-	-	-
GC232	1	11.9	556.7	3.7	78.5	4.4	2.5	0.0	18.8
(hydrate)	3	18.9	544.4	2.5	79.5	4.1	1.0	0.1	16.9
Dive 4459	5	20.1	535.3	2.2	79	12	3.7	1.0	12.2
	7	17.4	421.9	2.2	74	24.5	19.1	3.0	25.9
	9	17.8	468.6	-	-	-	-	-	-
	11	14.5	511.0	-	-	-	-	-	-

- : no data

Table 2.2. Isotopic composition of various carbon compounds from gas hydrate and brine pool sites in the Gulf of Mexico.

Compound	Gas Hydrate	Brine Pool
Methane	$\delta^{13}C$ (‰) ^a	$\delta^{13}C$ (‰)
vent gas	-48.5 ^b	-63.8 to -80 ^h
hydrate-bound	-47.5 ^b	
Porewater	-49.3 ^b	
Particulate Organic Matter	-25 ^c	-25 ⁱ
Sedimentary Carbonate	-15 to -26 ^d	-10 ⁱ
Dissolved Inorganic Carbon	-30 ^b	
C ₂₂ – C ₃₀ alkanes (average)	-30.1 ^e	
Photic Zone Organic Matter	-20.6 ^f	
Crude Oil	-27 ^g	

a: isotopic composition versus the Vienna Pee Dee belemnite standard

b: from site GC234, ~9.5km from the site in this study; (SASSEN et al., 2004)

c: from site GC185; (JOYE et al., 2004)

d: from site GC234; (FORMOLO et al., 2004; JOYE et al., 2004)

e: (JAHNKE et al., 1995)

f: (CLAYPOOL and KAPLAN, 1974)

g: (KENNICUTT et al., 1988)

h: same brine pool as this study, GC233; (MACDONALD, 2002; MACDONALD et al., 1990b)

i: same brine pool as this study, GC233; (JOYE et al., 2004)

Table 2.3A. Abundance (expressed as $\mu\text{g lipid g}^{-1}$ sediment) and isotopic composition ($\delta^{13}\text{C}$ vs. PDB standard) of select lipid biomarkers extracted from sediments at a brine influence site in the Gulf of Mexico. See text for explanation of lipid nomenclature.

Location	LIPID	0-2cm		2-4cm		4-6cm		6-8cm		8-10cm	
		$\mu\text{g/g}$	$\delta^{13}\text{C}$								
GC233	14:0 ^a	10.5	-45.3	5.7	-58.5	2.5	-55.7	1.2	-55.5	0.9	-44.9
	i15:0	5.3	-41.9	2.3	-48.0	1.2	-58.9	0.9	-62.9	0.5	-68.9
Brine pool	a15:0	9.6	-41.5	5.0	-57.1	3.1	-74.0	3.2	-79.9	2.9	-83.7
	15:0	2.1	-45.2	1.3	-56.3	0.6	-61.1	0.7	-83.3	0.4	-57.5
	16:1 ω 7c	11.5	-43.4	4.6	-47.4	10.2	-55.6	6.4	-66.4	2.7	-71.9
	16:1 ω 5c	20.7	-62.6	11.0	-65.8	3.3	-72.1	2.7	n.m.	1.1	-90.4
	16:0	41.2	-40.6	19.5	-40.4	7.4	-37.7	7.0	-31.3	4.7	-35.9
	10Me16:0	5.3	-53.1	3.5	-64.3	0.7	-62.6	0.5	-65.1	n.d.	n.d.
	17:1 ω 6c	1.7	-54.4	1.1	-69.0	1.0	-79.6	1.0	-76.1	0.5	-79.1
	cy17:0 ω 5,6	0.7	-112.4	1.1	-82.6	0.5	-81.7	0.5	-73.8	n.d.	n.d.
	17:0	1.2	-36.2	0.7	-39.1	0.3	-32.4	0.3	-32.9	0.2	n.m.
	18:1 ω 9c	6.1	-37.4	2.9	-39.7	1.2	-40.2	2.0	-46.2	1.1	-38.3
	18:1 ω 7c	43.8	-39.8	21.2	-48.3	9.3	-68.6	8.5	-71.8	5.2	-79.2
	18:0	9.2	-25.4	6.7	-23.6	3.9	-20.7	4.5	-22.5	3.1	-22.2
	archaeol ^b	0.5	-100.5	0.3	-114.5	0.3	-109.5	n.d.	n.d.	0.3	-93.2
sn-2-hydroxy	1.1	-113.3	0.6	-109.2	0.7	-114.5	n.d.	n.d.	0.2	-90.7	

a: bacterial fatty acids

b: archaeal alcohol lipids

n.d.: not detected

n.m.: not measurable due to low signal to noise ratio

Table 2.3B. Abundance (expressed as $\mu\text{g lipid g}^{-1}$ sediment) and isotopic composition ($\delta^{13}\text{C}$ vs. PDB standard) of select lipid biomarkers extracted from sediments at a gas hydrate site in the Gulf of Mexico. See text for explanation of lipid nomenclature.

Location	LIPID	0-2cm		2-4cm		4-6cm		6-8cm		8-10cm	
		$\mu\text{g/g}$	$\delta^{13}\text{C}$	$\mu\text{g/g}$	$\delta^{13}\text{C}$	$\mu\text{g/g}$	$\mu\text{g/g}$	$\delta^{13}\text{C}$	$\mu\text{g/g}$	$\delta^{13}\text{C}$	$\mu\text{g/g}$
GC232	14:0 ^a	18	-30.1	13.2	-38.4	14.1	-50.1	14.6	-56.5	2.2	-40.2
	i15:0	16.9	-30.7	11.2	-32.8	9.4	-36.7	8.3	-52.8	1.1	-42.8
Gas hydrate	a15:0	31.5	-30.4	28.1	-35.2	22.9	-39.3	21.4	-53.2	3.6	-43
	15:0	5.4	-31.4	3.8	-36.8	3.6	-44.2	4.8	-56.7	0.7	-41.4
	16:1 ω 7c	344	-62.5	63.3	-43.8	51.8	-44.0	36.1	-61.0	4.1	-59.9
	16:1 ω 5c	26.8	-47.8	15.2	-45.9	15.7	-54.6	16.2	-67.6	2.3	-57.9
	16:0	87	-33	40.4	-38.1	29.9	-39.9	26.5	-46.1	8.6	-27.4
	10Me16:0	3.1	-30.7	2.9	-45.0	5.2	-64.9	4.5	-51.1	0.4	-49.2
	17:1 ω 6c	3.4	-30.4	2.4	-45.0	2.1	-63.4	5.6	-54.1	0.9	-54.2
	cy17:0 ω 5,6	0.8	-46.6	1.5	-56.0	2.9	-79.6	5.4	-55.3	1.2	-52.3
	17:0	3.4	-35.3	1.9	-31.1	1.5	-30.1	1.5	n.m.	0.5	-25.5
	18:1 ω 9c	14.6	-24.7	9.7	-32.4	6.5	-32.6	5.2	-45.5	1.3	-34.7
	18:1 ω 7c	124.2	-30.2	31.6	-43.8	27.1	-46.8	32.0	-63.6	6.2	-70.1
	18:0	17.1	-25.3	13.7	-26.9	9.1	-23.2	8.1	-28.3	11	-19.6
	archaeol ^b	n.d.	n.d.	1.2	-83.9	1.9	-83.9	3.2	-99.8	1.9	-89.3
	sn-2-hydroxy	n.d.	n.d.	1.7	-102.6	1.3	-97	9.3	-101.5	2.9	-104.6

a: bacterial fatty acids

b: archaeal alcohol lipids

n.d.: not detected

n.m.: not measurable due to low signal to noise ratio

Figure Captions

Figure 1. Composite profiles of geochemistry, rates of microbial processes, microorganism diversity and abundance, and abundance and isotopic composition of select lipid biomarkers in sediments collected from underneath a bacterial mat at a brine pool cold seep (GC233) in the Gulf of Mexico. In (A)-(D), filled symbols represent the concentration while open symbols represent the rate. In (F)-(I), abbreviated names of lipids are presented in legends; see text for explanation of abbreviations. (A) Methane (CH_4) concentration and AOM rate; (B) dissolved inorganic carbon (HCO_3^-) concentration and the rate of autotrophic methanogenesis (Bi-MOG); (C) acetate concentration and the rate of acetoclastic methanogenesis (Ac-MOG); (D) sulfate (SO_4^{2-}) concentration and SR rate; (E) total abundance of specific groups of microorganisms as determined by CARD-FISH; (F) abundance of select archaeal lipid biomarkers extracted from sediment; (G) $\delta^{13}\text{C}$ isotopic composition of same select archaeal lipid biomarkers (legend given in (F)); (H) abundance of select bacterial lipid biomarkers extracted from sediment; (I) $\delta^{13}\text{C}$ isotopic composition of same select bacterial lipid biomarkers (legend given in (H)). All panels scaled to the same depth axis (given in (A) and (E) in cm below seafloor).

Figure 2. Composite profiles of geochemistry, rates of microbial processes, microorganism diversity and abundance, and abundance and isotopic composition of select lipid biomarkers in sediments collected from underneath a bacterial mat at a gas hydrate cold seep (GC232) in the Gulf of Mexico. Panels and symbols identical to those presented in Figure 1.

Figure 3. Photomicrographs of microorganisms in Gulf of Mexico sediments identified using CARD-FISH. Scale bars represent various lengths. (A) Oil autofluorescence prevented robust

usage of mono-labeled FISH probes. Arrow indicates a cell targeted by a general *Archaeal* rRNA FISH probe labeled with a green fluorescent dye to illustrate difficulty in separating signal from oil autofluorescence. **(B)** Representation of microbial morphologies present. Cells stained with DAPI (blue). **(C)** Loose cluster of rods targeted with green-fluorescent probe specific for the ANME-1 group of Archaea. Other rod-shaped cells in the image (stained with DAPI, blue) may be ANME with a low cellular rRNA content, making these cells fall below the threshold of detection for FISH. **(D)** Mono-specific cluster of microorganisms targeted with a green-fluorescent probe specific for the ANME-1 group of Archaea. No SRB of the *Desulfosarcina/Desulfococcus* group, which were targeted with a red-fluorescent probe, were visible in this cluster. **(E)** Organized consortia of ANME-2 (targeted with a group specific green-fluorescent probe) and *Desulfosarcina/Desulfococcus* spp. (targeted with a group-specific red-fluorescent probe). ANME-2 were typically found in organized consortia with these SRB. **(F)** Loose cluster of ANME-2 cells (green) surrounded by other microorganisms which were not related to the *Desulfosarcina/Desulfococcus* spp. (which would have been labeled red).

Figure 4. Schematic illustrating the interactions between AOM, SR and MOG, the geochemical, and the geological environment at the two cold seep environments. Not drawn to scale.

Macrofaunal and microbial mat communities are indicated by specific symbols labeled in the figure. The left-hand side of the diagram depicts a gas hydrate site (GC232) fed by methane and oil migrating through faults and fractures. The carbon isotopic composition of the mostly thermogenic source methane at this site is taken from Sassen et al. (2004). Surficial chemosynthetic communities at this site include *Beggiatoa* spp. and other sulfide oxidizing bacterial mats, tube worms and mussels. The right-hand side of the diagram illustrates a brine

pool site (GC233), characterized by the migration of biogenic methane (MACDONALD, 2002) and brines, with a surface chemosynthetic community composed of mussels and *Thiomargarita*-type sulfide oxidizing bacterial mats. The inset shows a magnified view of hypothesized cycling of methane and sulfur occurring in subsurface sediments mediated by ANME-type microorganisms (**ANME**), methanogenic archaea (**ARCH**; which could also be ANME, see text for explanation), sulfate reducing bacteria (**SRB**), and giant vacuolated sulfide oxidizing bacteria (**VSB**); arrows indicate the flow of various compounds between microorganisms and the environment.

Figure 2.1.

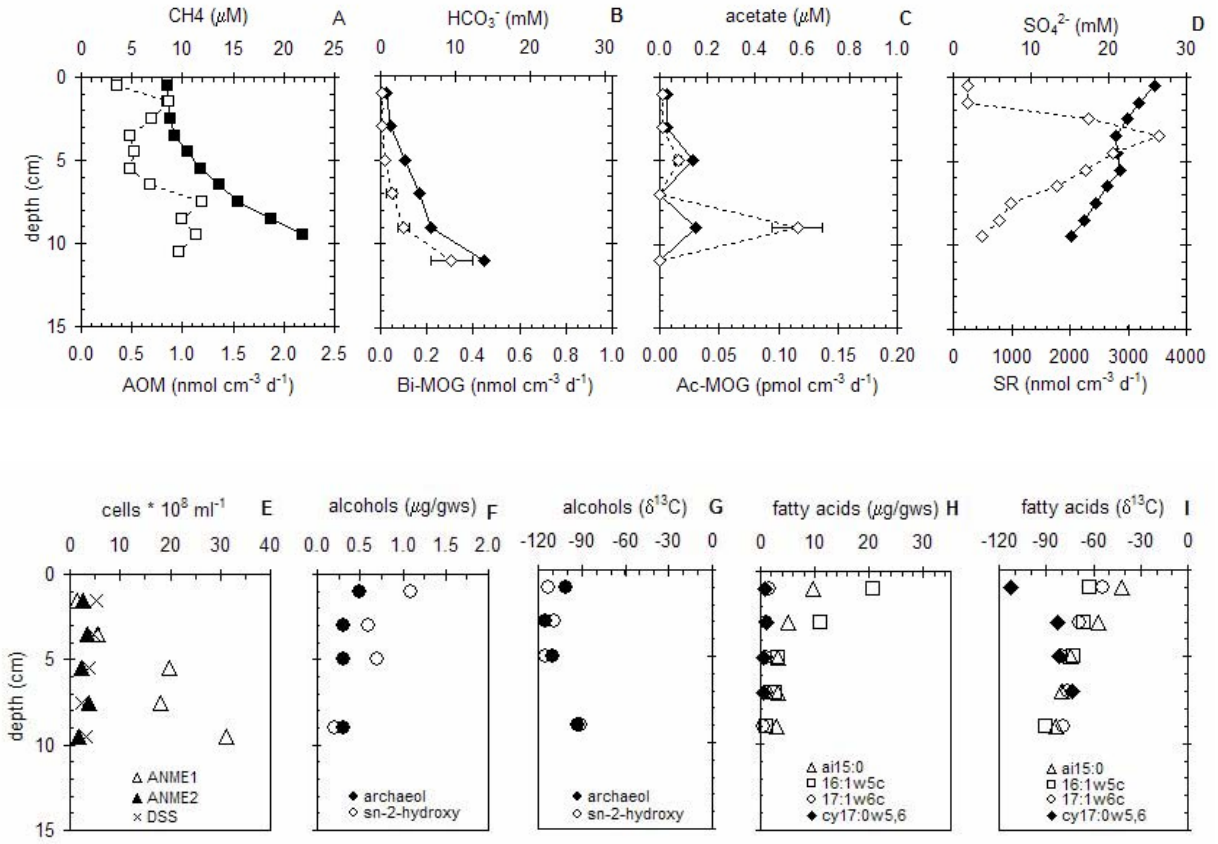


Figure 2.2.

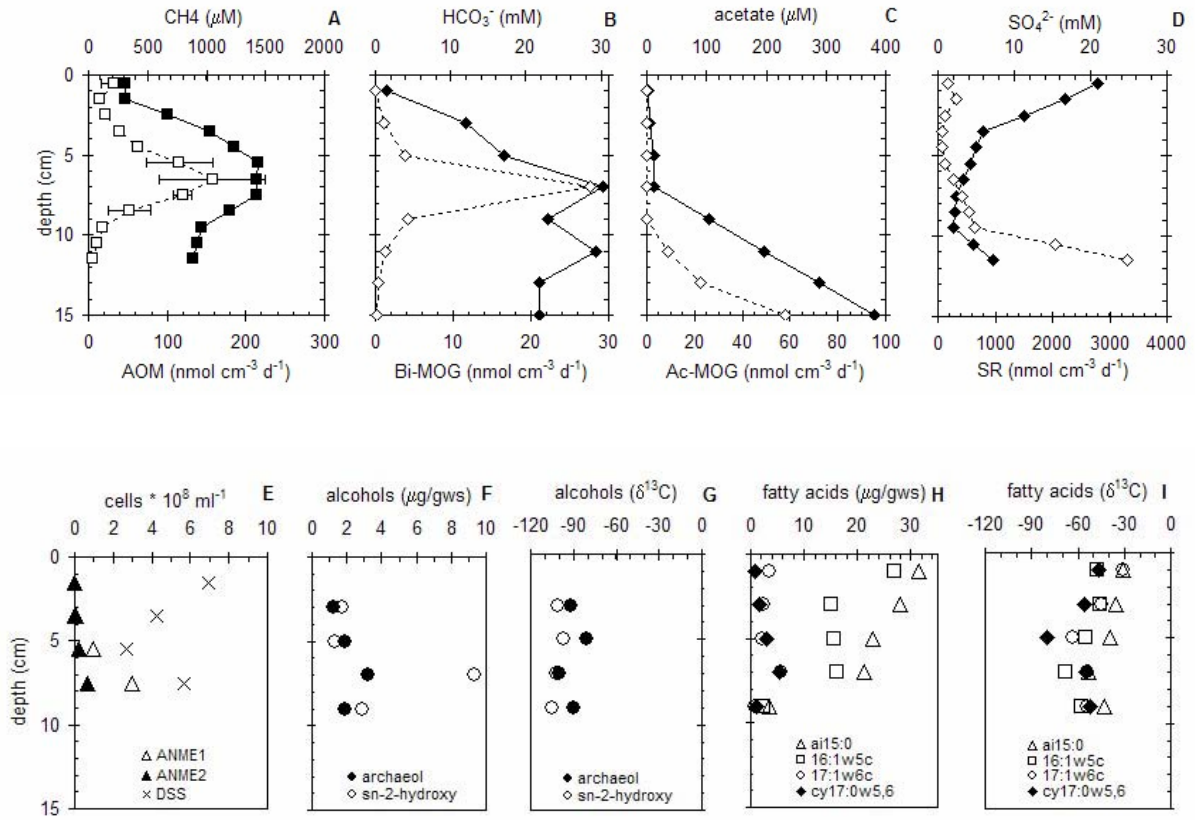


Figure 2.3.

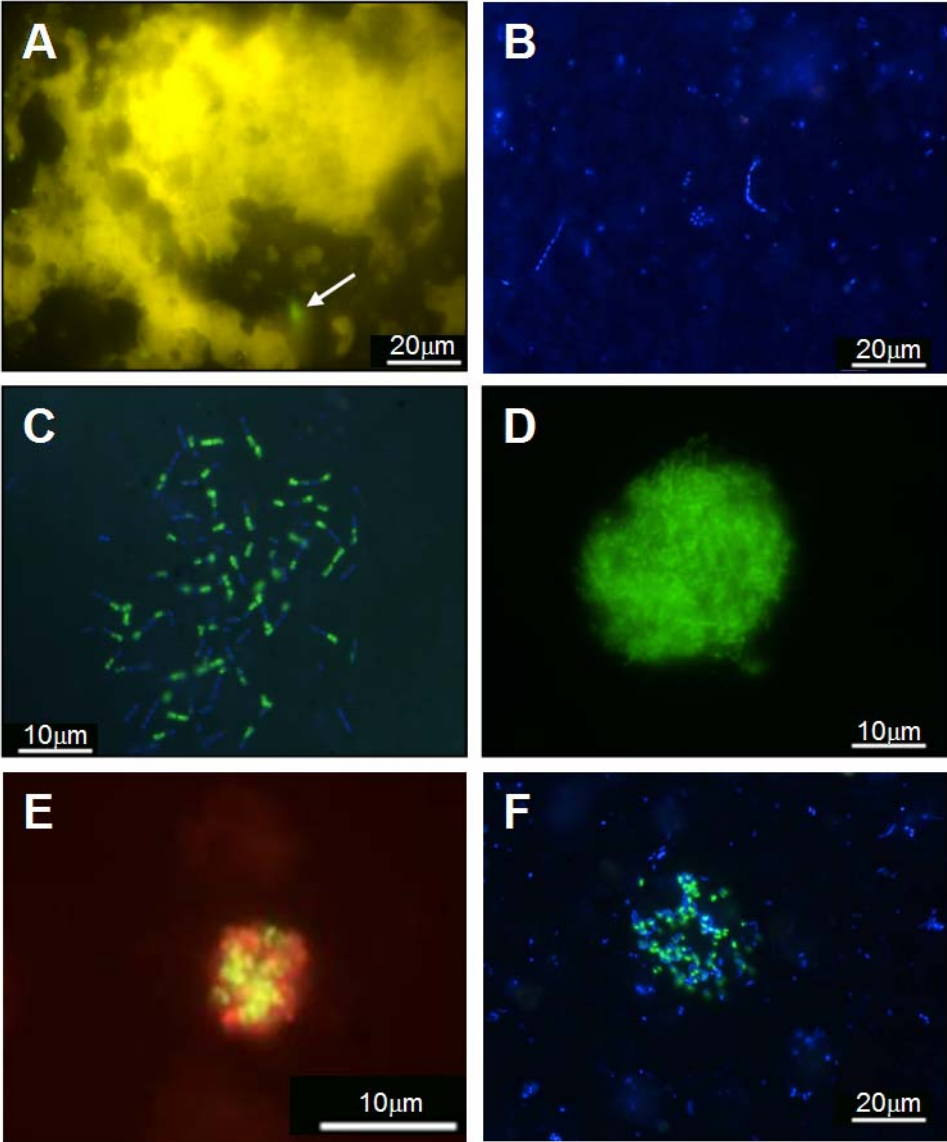
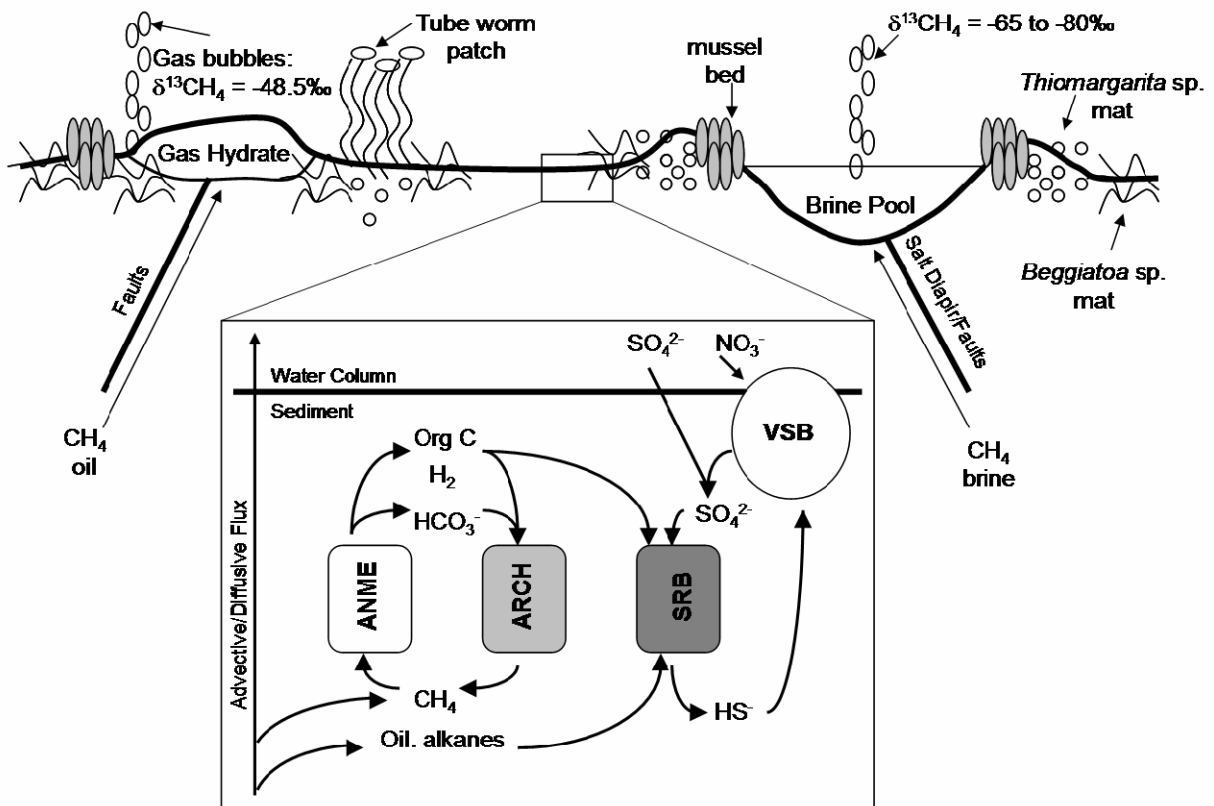


Figure 2.4.



References

- Aharon P. (1994) Geology and biology of modern and ancient submarine hydrocarbon seeps and vents: an introduction. *Geo-Marine Letters* **14**, 69-73.
- Aharon P. and Fu B. (2003) Sulfur and oxygen isotopes of coeval sulfate-sulfide in pore fluids of cold seep sediments with sharp redox gradients. *Chemical Geology* **195**, 201-218.
- Albert D. B. and Martens C. S. (1997) Determination of low-molecular-weight organic acid concentrations in seawater and porewater samples via HPLC. *Marine Chemistry* **56**, 27-37.
- Alperin M. J. and Reeburgh W. S. (1988) Carbon and hydrogen isotope fractionation resulting from anaerobic methane oxidation. *Global Biogeochemical Cycles* **2**(3), 279-288.
- Amann R., Krumholz L., and Stahl D. A. (1990) Fluorescent-oligonucleotide probing of whole cells for determinative, phylogenetic, and environmental studies in microbiology. *Journal of Bacteriology* **172**, 762-770.
- Arvidson R. S., Morse J. W., and Joye S. B. (2004) The sulfur biogeochemistry of chemosynthetic cold seep communities, Gulf of Mexico, USA. *Marine Chemistry* **87**, 97-119.
- Barnes R. O. and Goldberg E. D. (1976) Methane production and consumption in anaerobic marine sediments. *Geology* **4**, 297-300.
- Behrens E. Q. (1988) Geology of a continental slope oil seep, northern Gulf of Mexico. *Bulletin of the American Association of Petroleum Geologists* **72**, 105-114.
- Blumenberg M., Seifert R., Reitner J., Pape T., and Michaelis W. (2004) Membrane lipid patterns typify distinct anaerobic methanotrophic consortia. *Proceedings of the National Academy of Science U.S.A.* **101**(30), 11111-11116.
- Boetius A., Ravensschlag K., Schubert C. J., Rickert D., Widdel F., Gieseke A., Amann R., Jørgensen B. B., Witte U., and Pfannkuche O. (2000) A marine microbial consortium apparently mediating anaerobic oxidation of methane. *Nature* **407**, 623-626.
- Brown K. M., Bangs N. L., Froelich P. N., and Kvenvolden K. A. (1996) The nature, distribution and origin of gas hydrate in the Chile Triple Junction region. *Earth and Planetary Science Letters* **19**, 471-483.

- Canfield D. E., Raiswell R., Westrich J. T., Reaves C. M., and Berner R. A. (1986) The use of chromium reduction in the analysis of reduced inorganic sulfur in sediments and shale. *Chemical Geology* **54**, 149-155.
- Cantu J., Zhang C. L., Huang Z., Pancost R. D., Lyons T. W., Formolo M. J., and Sassen R. (2003) Biogeochemical signatures and community structure of a microbial (*Beggiatoa*) mat in the gas hydrate system of Gulf of Mexico. *Geological Society of America Annual Meeting 2003, Abstract with Programs*, 619.
- Claypool G. E. and Kaplan I. R. (1974) The origin and distribution of methane in marine sediments. In *Natural Gases in Marine Sediments* (ed. I. R. Kaplan), pp. 99-139. Plenum.
- Cragg B. A., Parkes R. J., Fry J. C., Herbert R. A., Wimpenny J. W. T., and Getliff J. M. (1990) Bacterial biomass and activity profiles within deep sediment layers. In *Proceedings of the Ocean Drilling Program, Scientific Results, Leg 112*, Vol. 112 (ed. E. Suess and R. von Huene), pp. 607-619. Ocean Drilling Program.
- Crill P. M. and Martens C. S. (1986) Methane production from bicarbonate and acetate in an anoxic marine sediment. *Geochimica et Cosmochimica Acta* **50**(9), 2089-2097.
- Daims H., Bruhl A., Amann R., Schleifer K.-H., and Wagner M. (1999) The domain-specific probe EUB338 is insufficient for the detection of all Bacteria: development and evaluation of a more comprehensive probe set. *Systematic Applied Microbiology* **22**, 434-444.
- De Beukelaer S. M., MacDonald I. R., Guinasso N. L., and Murrery J. A. (2003) Distinct side-scan sonar, RADARSAT SAR, and acoustic profiler signatures of gas and oil seeps on the Gulf of Mexico slope. *Geo-Marine Letters* **23**(3-4), 177-186.
- Devol A. H., Anderson J. J., Kuivila K., and Murrery J. W. (1984) A model for coupled sulfate reduction and methane oxidation in the sediments of Saanich Inlet. *Geochimica et Cosmochimica Acta* **48**, 993-1004.
- Dickens G. R. (2001) The potential volume of oceanic methane hydrates with variable external conditions. *Organic Geochemistry* **32**(10), 1179-1193.
- Elvert M., Boetius A., Knittel K., and Jørgensen B. B. (2003) Characterization of specific membrane fatty acids as chemotaxonomic markers for sulfate-reducing bacteria involved in anaerobic oxidation of methane. *Geomicrobiology Journal* **20**, 403-419.
- Elvert M., Greinert J., Suess E., and Whiticar M. J. (2001) Carbon isotopes of biomarkers derives from methane-oxidizing microbes at Hydrate Ridge, Cascadia convergent margin. In *Natural Gas Hydrates: Occurrence, Distribution, and Dynamics*, Vol. 124 (ed. C. K. Paull and W. P. Dillon), pp. 115-129. American Geophysical Union.

- Elvert M., Hopmans E. C., Treude T., Boetius A., and Suess E. (2005) Spatial variations of methanotrophic consortia at cold methane seeps: Implications from a high resolution molecular and isotopic approach. *Geobiology* **3**, 195-209.
- Elvert M., Suess E., and Whiticar M. J. (1999) Anaerobic methane oxidation associated with marine gas hydrates: super-light C-isotopes from saturated and unsaturated c-20 and c-25 irregular isoprenoids. *Naturwissenschaften* **86**, 295-300.
- Fenchel T. and Glud R. N. (1998) Veil architecture in a sulphide-oxidizing bacterium enhances countercurrent flux. *Nature* **394**, 367-369.
- Formolo M. J., Lyons T. W., Zhang C. L., Kelley C., Sassen R., Horita J., and Cole D. R. (2004) Quantifying carbon sources in the formation of authigenic carbonates at gas hydrate sites in the Gulf of Mexico. *Chemical Geology* **205**, 253-264.
- Fossing H. and Jørgensen B. B. (1989) Measurement of bacterial sulfate reduction in sediments - evaluation of a single-step chromium reduction method. *Biogeochemistry* **8**, 205-222.
- Fu B., Aharon P., Byerly G. R., and Roberts H. H. (1994) Barite chimneys on the Gulf of Mexico continental slope: Initial report on their petrography and geochemistry. *Geo-Marine Letters* **14**(2-3), 81-87.
- Gelwicks J. T., Risatti J. B., and Hayes J. M. (1994) Carbon-isotope effects associated with acetoclastic methanogenesis. *Applied and Environmental Microbiology* **60**(2), 467-472.
- Greinert J., Bollwerk S. M., Derkachev A., Bohrmann G., and Suess E. (2002) Massive barite deposits and carbonate mineralization in the Derugin Basin, Sea of Okhotsk: Precipitation processes at cold seep sites. *Earth and Planetary Science Letters* **203**, 165-180.
- Hallam S. J., Girguis P. R., Preston C. M., Richardson P. M., and Delong E. F. (2003) Identification of methyl coenzyme M reductase A (*mcrA*) genes associated with methane-oxidizing archaea. *Applied and Environmental Microbiology* **69**(9), 5483-5491.
- Hallam S. J., Putnam N., Preston C. M., Detter J. C., Rokhsar D., Richardson P. M., and Delong E. F. (2004) Reverse methanogenesis: Testing the hypothesis with environmental genomics. *Science* **305**, 1457-1462.
- Hansen L. B., Finster K., Fossing H., and Iversen N. (1998) Anaerobic methane oxidation in sulfate depleted sediments: effects of sulfate and molybdate additions. *Aquatic Microbial Ecology* **14**, 195-204.

- Hesselbo S. P., Groecke D. R., Jenkyns H. C., Bjerrum C. J., Farrimond P., Morgans Bell H. S., and Green O. R. (2000) Massive dissociation of gas hydrate during a Jurassic oceanic anoxic event. *Nature* **406**, 392-395.
- Hinrichs K.-U. and Boetius A. (2002) The anaerobic oxidation of methane: New insights in microbial ecology and biogeochemistry. In *Ocean Margin Systems* (ed. G. Wefer, D. Billett, D. Hebbeln, B. B. Jørgensen, M. Schlüter, and T. C. E. van Weering), pp. 457-477. Springer-Verlag.
- Hinrichs K.-U., Hayes J. S., Sylva S. P., Brewer P. G., and Delong E. F. (1999) Methane-consuming archaeobacteria in marine sediments. *Nature* **398**, 802-805.
- Hinrichs K.-U., Summons R. E., Orphan V. J., Sylva S. P., and Hayes J. M. (2000) Molecular and isotopic analysis of anaerobic methane-oxidizing communities in marine sediments. *Organic Geochemistry* **31**, 1651-1701.
- Hoehler T. M., Alperin M. J., Albert D. B., and Martens C. S. (1994) Field and laboratory studies of methane oxidation in an anoxic marine sediment - evidence for a methanogen-sulfate reducer consortium. *Global Biogeochemical Cycles* **8**, 451-463.
- Hopman A. H., Ramaekers F. C., and Speel E. J. (1998) Rapid synthesis of biotin-, digoxigenin-, trinitrophenyl-, and fluorochrome-labeled tyramides and their application for In situ hybridization using CARD amplification. *Journal of Histochemical Cytochemistry* **46**(6), 771-777.
- IPCC. (2000) Land Use, Land-Use Change, and Forestry. A Special Report of the Intergovernmental Panel on Climate Change (IPCC) (ed. R. T. Watson, I. R. Noble, B. Bolin, N. H. Ravindranath, D. J. Verardo, and D. J. Dokken). Cambridge University Press.
- Iversen N. and Jørgensen B. B. (1985) Anaerobic methane oxidation rates at the sulfate-methane transition in marine sediments from Kattegat and Skagerrak (Denmark). *Limnology and Oceanography* **30**, 944-955.
- Jahnke L. L., Summons R. E., Dowling L. M., and Zahirais K. D. (1995) Identification of methanotrophic lipid biomarkers in cold-seep mussel gills: chemical and isotopic analysis. *Applied and Environmental Microbiology* **61**(2), 576-582.
- Jørgensen B. B. (1978) A comparison of methods for quantification of bacterial sulfate reduction in coastal marine sediments. I. Measurements with radiotracer techniques. *Geomicrobiology Journal* **1**, 11-28.

- Joye S. B., Connell T., Miller L. G., Oremland R. S., and Jellison R. (1999) Oxidation of ammonia and methane in an alkaline, saline lake. *Limnology and Oceanography* **44**, 178-188.
- Joye S. B., MacDonald I. R., Montoya J. P., and Peccini M. B. (2005) Geophysical and geochemical signatures of Gulf of Mexico seafloor brines. *Biogeosciences* **2**, 295-309.
- Joye S. B., Orcutt B. N., Boetius A., Montoya J. P., Schulz H., Erickson M. J., and Lugo S. K. (2004) The anaerobic oxidation of methane and sulfate reduction in sediments from at Gulf of Mexico cold seeps. *Chemical Geology* **205**(3-4), 219-238.
- Kalenetra K., Joye S. B., Sunseri N. R., and Nelson D. (2005) Novel, large vacuolate, nitrate-accumulating sulfur bacteria discovered in the Gulf of Mexico reproduce by reductive division in three dimensions. *Environmental Microbiology*.
- Katz M. E., Pak D. K., Dickens G. R., and Miller K. G. (1999) The source and fate of massive carbon input during the latest paleocene thermal maximum. *Science* **286**, 1531-1533.
- Kennicutt M. C., Brooks J. M., and Denoux G. J. (1988) Leakage of deep reserved petroleum to the near surface of the Gulf of Mexico continental slope. *Marine Chemistry* **24**, 39-59.
- Knittel K., Boetius A., Lemke A., Eilers H., Lochte K., Pfannkuche O., and Linke P. (2003) Activity, distribution, and diversity of sulfate reducers and other bacteria in sediments above gas hydrate (Cascadia Margin, Oregon). *Geomicrobiology Journal* **20**, 269-294.
- Knittel K., Lösekann T., Boetius A., Kort R., and Amann R. (2005) Diversity and Distribution of Methanotrophic Archaea at Cold Seeps. *Applied and Environmental Microbiology* **71**(1), 467-479.
- Krüger M., Meyerdiecks A., Glockner F. O., Amann R., Widdel F., Kube M., Reinhardt R., Kahnt R., Bocher R., Thauer R. K., and Shima S. (2003) A conspicuous nickel protein in microbial mats that oxidize methane anaerobically. *Nature* **426**, 878-881.
- Krzycki J. A., Kenealy W. R., DeNiro M. J., and Zeikus J. G. (1987) Stable isotope fractionation by *Methanosarcina barkeri* during methanogenesis from acetate, methanol, or carbon dioxide-hydrogen. *Applied and Environmental Microbiology* **53**, 2597-2599.
- Kvenvolden K. A. (1988) Methane hydrates and global change. *Global Biogeochemical Cycles* **2**(3), 221-229.
- Kvenvolden K. A. (1993) Gas hydrates - geological perspective and global change. *Reviews of Geophysics* **31**, 173-187.

- Lanoil B. D., Sassen R., La Duc M. T., Sweet S. T., and Neilson K. H. (2001) *Bacteria and Archaea* physically associated with Gulf of Mexico gas hydrates. *Applied and Environmental Microbiology* **67**(11), 5143-5153.
- Linke P., Suess E., Torres M., Martens V., Rugh W. D., Ziebis W., and Kulm L. D. (1994) *In situ* measurements of fluid flow from cold seeps at active continental margins. *Deep-Sea Research I* **41**(4), 721-739.
- Lovley D. R. and Klug D. D. (1986) Model for the distribution of sulfate reduction and methanogenesis in fresh-water sediment. *Geochimica et Cosmochimica Acta* **50**(1), 11-18.
- MacDonald I. R. (2002) *Stability and Change in Gulf of Mexico Chemosynthetic Communities. Volume II: Technical Report*. U.S. Department of the Interior, Minerals Management Service, Gulf of Mexico OCS Region.
- MacDonald I. R., Boland G. S., Baker J. S., Brooks J. M., Kennicutt M. C., and Bidigare R. R. (1989) Gulf of Mexico hydrocarbon seep communities II: spatial distribution of seep organisms and hydrocarbons at Bush Hill. *Marine Biology* **101**, 235-247.
- MacDonald I. R., Guinasso N. L., Reilly Jr. J. F., Brooks J. M., Callender W. R., and Gabrielle S. G. (1990a) Gulf of Mexico hydrocarbon seep communities: VI. Patterns of community structure and habitat. *Geo-Marine Letters* **10**, 244-252.
- MacDonald I. R., Guinasso N. L., Sassen R., Brooks J. M., Lee L., and Scott K. T. (1994) Gas hydrate that breaches the sea-floor on the continental slope of the Gulf of Mexico. *Geology* **22**, 699-702.
- MacDonald I. R., Reilly Jr. J. F., Guinasso N. L., Brooks J. M., Carney R., Bryant W. A., and Bright T. (1990b) Chemosynthetic mussels at a brine-filled pockmark in the Northern Gulf of Mexico. *Science* **248**, 1096-1099.
- MacDonald I. R., Sager W. W., and Peccini M. B. (2003) Gas hydrate and chemosynthetic biota in mounded bathymetry at mid-slope hydrocarbon seeps: Northern Gulf of Mexico. *Marine Geology* **198**, 133-158.
- Manz W., Eisenbrecher M., Neu T. R., and Szewzyk U. (1998) Abundance and spatial organization of gram negative sulfate-reducing bacteria in activated sludge investigated *in situ* probing with specific 16S rRNA targeted oligonucleotides. *FEMS Microbiology Ecology* **25**, 43-61.
- Michaelis W., Seifert R., Nauhaus K., Treude T., Thiel V., Blumenberg M., Knittel K., Gieseke A., Peterknecht F., Pape T., Boetius A., Amann R., Jørgensen B. B., Widdel F.,

- Peckmann J., Pimenkov N., and Gulin M. B. (2002) Microbial reefs in the Black Sea fueled by anaerobic methane oxidation. *Science* **297**, 1013-1015.
- Milkov A. V. and Sassen R. (2000) Thickness of the gas hydrate stability zone, Gulf of Mexico continental slope. *Marine Petroleum Geology* **17**, 981-991.
- Mills H. J., Hodges C., Wilson K., MacDonald I. R., and Sobecky P. A. (2003) Microbial diversity in sediments associated with surface-breaching gas hydrate mounds in the Gulf of Mexico. *FEMS Microbiology Ecology* **46**(1), 39-52.
- Mills H. J., Martinez R. J., Story S., and Sobecky P. A. (2004) Identification of members of the metabolically active microbial populations associated with *Beggiatoa* species mat communities from Gulf of Mexico cold-seep sediments. *Applied and Environmental Microbiology* **70**(9), 5447-5458.
- Nauhaus K., Boetius A., Krüger M., and Widdel F. (2002) *In vitro* demonstration of anaerobic oxidation of methane coupled to sulfate reduction from a marine gas hydrate area. *Environmental Microbiology* **4**, 296-305.
- Orcutt B. N., Boetius A., Lugo S. K., MacDonald I. R., Samarkin V. A., and Joye S. B. (2004) Life at the edge of methane ice: microbial cycling of carbon and sulfur in Gulf of Mexico gas hydrates. *Chemical Geology* **205**(3-4), 239-251.
- Oremland R. S. and Polcin S. (1982) Methanogenesis and sulfate reduction - competitive and noncompetitive substrates in estuarine sediments. *Applied and Environmental Microbiology* **44**(6), 1270-1276.
- Orphan V. J., Hinrichs K.-U., Ussler W., III, Paull C. K., Taylor L. T., Sylva S. P., Hayes J. M., and Delong E. F. (2001a) Comparative analysis of methane-oxidizing archaea and sulfate-reducing bacteria in anoxic marine sediments. *Applied and Environmental Microbiology* **67**(4), 1922-1934.
- Orphan V. J., House C. H., Hinrichs K.-U., McKeegan K. D., and Delong E. F. (2001b) Methane-consuming archaea revealed by directly coupled isotopic and phylogenetic analysis. *Science* **293**, 484-487.
- Orphan V. J., House C. H., Hinrichs K.-U., McKeegan K. D., and Delong E. F. (2002) Multiple archaeal groups mediate methane oxidation in anoxic cold seep sediments. *Proceedings of the National Academy of Science U.S.A.* **99**, 7663-7668.
- Orphan V. J., Ussler W., III, Naehr T., House C. H., Hinrichs K.-U., and Paull C. K. (2004) Geological, geochemical, and microbiological heterogeneity of the seafloor around

- methane vents in the Eel River Basin, offshore California. *Chemical Geology* **204**, 265-289.
- Pancost R. D., Bouloubassi I., Aloisi G., Sinninghe Damste J. S., and Party M. S. S. (2001) Three series of non-isoprenoidal dialkyl glycerol diethers in cold-seep carbonate crusts. *Organic Geochemistry* **32**, 695-707.
- Pancost R. D., Sinninghe Damste J. S., de Lint S., van der Maarel M. J. E. C., Gottschal J. C., and Party M. S. S. (2000) Biomarker evidence for widespread anaerobic methane oxidation in Mediterranean sediments by a consortium of methanogenic archaea and bacteria. *Applied and Environmental Microbiology* **66**, 1126-1132.
- Paytan A., Mearon S., Cobb K., and Kastner M. (2002) Origin of marine barite deposits: Sr and S isotope characterization. *Geology* **30**, 747-750.
- Pernthaler A. and Amann R. (2004) Simultaneous fluorescence in situ hybridization of mRNA and rRNA in environmental bacteria. *Applied and Environmental Microbiology* **70**(9), 5426-5433.
- Pernthaler A., Pernthaler J., and Amann R. (2002) Fluorescence in situ hybridization and catalyzed reporter deposition for the identification of marine bacteria. *Applied and Environmental Microbiology* **68**(6), 3094-3101.
- Pimenov N., Savvichev A., Rusanov I., Egorov A. V., Gebruk A., Moskalev L., and Vogt P. R. (1999) Microbial processes of carbon cycle as the base of food chain of Haakon Mosby mud volcano benthic community. *Geo-Marine Letters* **19**(1-2), 89-96.
- Reeburgh W. S. (1976) Methane consumption in Cariaco Trench waters and sediments. *Earth and Planetary Science Letters* **28**, 337-344.
- Sager W. W., MacDonald I. R., and Hou R. (2003) Geophysical signatures of mud mounds at hydrocarbon seeps on the Louisiana continental slope, northern Gulf of Mexico. *Marine Geology* **198**, 97-132.
- Sassen R. and MacDonald I. R. (1994) Evidence of structure H hydrate, Gulf of Mexico continental slope. *Organic Geochemistry* **23**, 1029-1032.
- Sassen R., MacDonald I. R., Requejo A. G., Guinasso N. L., Kennicutt M. C., Sweet S. T., and Brooks J. M. (1994) Organic geochemistry of sediments from chemosynthetic communities, Gulf of Mexico slope. *Geo-Marine Letters* **14**, 110-119.
- Sassen R., Roberts H. H., Carney R., Milkov A. V., DeFreitas A., Lanoil B. D., and Zhang C. L. (2004) Free hydrocarbon gas, gas hydrate, and authigenic minerals in chemosynthetic

- communities of the northern Gulf of Mexico continental slope: relation to microbial processes. *Chemical Geology* **205**, 195-217.
- Sassen R., Sweet S. T., DeFreitas A., Morelos J. A., and Milkov A. V. (2001) Gas hydrate and crude oil from the Mississippi Fan foldbelt, downdip Gulf of Mexico Salt Basin: significance to petroleum system. *Organic Geochemistry* **32**, 999-1008.
- Schönhuber W., Fuchs B., Juretschko S., and Amann R. (1997) Improved sensitivity of whole-cell hybridization by the combination of horseradish peroxidase-labeled oligonucleotides and tyramide signal amplification. *Applied and Environmental Microbiology* **63**(8), 3268-3273.
- Sloan E. D. (1990) *Clathrate hydrates of natural gases*. Marcel Drekker Inc.
- Sørensen K. B., Finster K., and Ramsing N. B. (2001) Thermodynamic and kinetic requirements in anaerobic methane oxidizing consortia exclude hydrogen, acetate, and methanol as possible electron shuttles. *Microbial Ecology* **42**, 1-10.
- Taylor J. and Parkes R. J. (1985) Identifying different populations of sulphate-reducing bacteria within marine sediment systems using fatty acid biomarkers. *Journal of General Microbiology* **131**, 631-642.
- Teske A., Hinrichs K.-U., Edgecomb V., de Vera Gomez A., Kysela D., Sylva S. P., Sogin M. L., and Jannasch H. W. (2002) Microbial diversity of hydrothermal sediments in the Guaymas Basin: Evidence for anaerobic methanotrophic communities. *Applied and Environmental Microbiology* **68**(4), 1994-2007.
- Thomas D. N., Zachos J. C., Bralower T. J., Thomas E., and Bohaty S. (2002) Warming the fuel for the fire: evidence for the thermal dissociation of methane hydrate during the Paleocene-Eocene thermal maximum. *Geology* **30**(12), 1067-1070.
- Thomsen T. R., Finster K., and Ramsing N. B. (2001) Biogeochemical and molecular signatures of anaerobic methane oxidation in a marine sediment. *Applied and Environmental Microbiology* **67**, 1646-1656.
- Torres M., Bohrmann G., Dubé T. E., and Poole F. G. (2003) Formation of modern and Paleozoic stratiform barite at cold methane seeps on continental margins. *Geology* **31**(10), 897-900.
- Torres M., McManus J., Hammond D. E., de Angelis M. A., Heeschen K., Colbert S. L., Tyron M. D., Brown K. M., and Suess E. (2002a) Fluid and chemical fluxes in and out of sediments hosting methane hydrate deposits on Hydrate Ridge, OR. I: hydrological provinces. *Earth and Planetary Science Letters* **201**, 525-540.

- Torres M., McManus J., and Huh C.-A. (2002b) Fluid seepage along the San Clemente Fault scarp: basin-wide impact on barium cycling. *Earth and Planetary Science Letters* **203**, 181-194.
- Treude T. (2003) Anaerobic oxidation of methane in marine sediments. Ph.D. dissertation, University of Bremen.
- Treude T., Boetius A., Knittel K., Wallmann K., and Jørgensen B. B. (2003) Anaerobic oxidation of methane above gas hydrates at Hydrate Ridge, NE Pacific Ocean. *Marine Ecological Progress Series* **264**, 1-14.
- Treude T., Krüger M., Boetius A., and Jørgensen B. B. (submitted) Environmental control on anaerobic oxidation of methane in the gassy sediments of Eckernförde Bay (German Baltic). *Limnology and Oceanography*.
- Tyron M. D., Brown K. M., Torres M., Trehu A., McManus J., and Collier R. W. (1999) Measurements of transience and downward fluid flow near episodic methane gas vents, Hydrate Ridge, Cascadia. *Geology* **27**(1075-1078).
- Valentine D. L. and Reeburgh W. S. (2000) New perspectives on anaerobic methane oxidation. *Environmental Microbiology* **2**(5), 477-484.
- Wallner G., Amann R., and Beisker W. (1993) Optimizing fluorescent in situ hybridization with rRNA-targeted oligonucleotide probes for flow cytometric identification of microorganisms. *Cytometry* **14**, 136-143.
- Weber A. and Jørgensen B. B. (2002) Bacterial sulfate reduction in hydrothermal sediments of the Guaymas Basin, Gulf of California, Mexico. *Deep-Sea Research I* **49**, 827-841.
- Zehnder A. J. B. and Brock T. D. (1980) Anaerobic methane oxidation: Occurrence and Ecology. *Applied and Environmental Microbiology* **39**(1), 194-204.
- Zhang C. L., Li Y., Wall J. D., Larsen L., Sassen R., Huang Y., Wang Y., Peacock A., White D. C., Horita J., and Cole D. R. (2002) Lipid and carbon isotopic evidence of methane-oxidizing and sulfate-reducing bacteria in association with gas hydrates from the Gulf of Mexico. *Geology* **30**(3), 239-242.

CHAPTER 3

IMPACT OF OIL AND HIGHER HYDROCARBONS ON MICROBIAL DIVERSITY, DISTRIBUTION AND ACTIVITY IN GULF OF MEXICO COLD SEEP SEDIMENTS¹

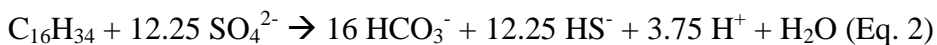
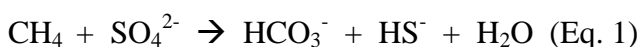
¹ Orcutt, B!, K. Knittel, V. Smarkin, T. Treude, A. Retiz, A. Boetius, S.B. Joye. In preparation for *Applied and Environmental Microbiology*.

Abstract

Due to the variable composition and magnitude of fluid and gas flux, hydrocarbon cold seeps in the Gulf of Mexico comprise a natural laboratory for investigating the effects of natural oils and non-methane hydrocarbons on microbial activity, diversity and distribution in marine surficial sediments. Though some sediments were characterized by high relative quantities of oil, which may be toxic to some microorganisms, high rates of sulfate reduction (SR, up to 27.9 ± 14.7 mmol m⁻² d⁻¹), anaerobic oxidation of methane (AOM, up to 16.15 ± 6.7 mmol m⁻² d⁻¹), and acetate oxidation (up to 2.74 ± 0.76 mmol m⁻² d⁻¹) were observed using radiotracer measurements. Analysis of 16S rDNA gene clone libraries revealed that the sediments were phylogenetically diverse although dominated by phylotypes of sulfate reducing bacteria (SRB) and anaerobic methanotrophs of the ANME-1 and ANME-2 varieties. The microorganisms responsible for sulfate-dependent non-methane hydrocarbon oxidation are unclear but likely include members of seep-endemic SRB clades.

Introduction

Sulfate reduction (SR) is the dominant pathway for organic matter mineralization in ocean margin sediments, accounting for up to 50% of total CO₂ production in these areas (CANFIELD et al., 1993; JØRGENSEN, 1982). In normal marine sediments, SR in upper organic carbon-rich layers is fueled largely by the fermentation products of degraded organic matter (i.e. H₂ and organic acids). At depth (i.e. in the sulfate methane transition zone (SMTZ)), some SR is fueled by coupling with the anaerobic oxidation of methane (AOM). Under diffusive regimes that characterize most ocean sediments, methane derived from the deeper methanogenic strata is consumed by sulfate reduction within the SMTZ. Hence, the ratio between AOM and SR is usually 1 in the SMTZ, but AOM accounts for only about 10% of the total integrated SR in the sulfate containing sediments (HINRICHS and BOETIUS, 2002). “Hot spots” of SR, where sulfate reduction rates are extremely high (>1 μmol cm⁻³ d⁻¹ range as opposed to low nmol cm⁻³ d⁻¹ range in normal marine sediments), occur at marine hydrocarbon seeps (BOETIUS et al., 2000; JOYE et al., 2004; TREUDE et al., 2003). Here, SR is coupled to the AOM (Eq. 1) or to the oxidation of higher hydrocarbons and oil-derivatives (Eq. 2, e.g., hexane oxidation (WIDDEL and RABUS, 2001)):



In methane-dominated sediments, methane oxidation activity is nearly equivalent to sulfate reduction, resulting in an approximate 1:1 coupling between the two processes. In sediments characterized by an abundance of methane and other non-methane hydrocarbons (e.g. alkanes) and/or petroleum-derivatives, SR rates significantly exceed methane oxidation rates, illustrating that other non-methane hydrocarbons support significant rates of SR *in situ* (JOYE et

al., 2004; ORCUTT et al., 2005). A number of sulfate reducing bacteria (SRB) can couple SR to the oxidation of short- and long- chain alkanes, complex aromatics and aliphatics, toluene, benzene, or bulk oil (HEIDER et al., 1999; KNIEMEYER et al., In press; PHELPS et al., 1998; RABUS et al., 1993; RUETER et al., 2001; SPORMANN and WIDDEL, 2000). Sediments from cold seeps often are depleted in 'labile' oil components (i.e. *n*-alkanes and branched chain isoprenoids) relative to source oil, indicating preferential microbial oxidation of these compounds (SASSEN et al., 1994), although it is unclear what fraction of this microbial oxidation *in situ* is attributable to SRB. Additionally, *in situ* microbial oxidation of 'labile' hydrocarbons like propane and *n*-butane can be inferred by the enriched (i.e. relatively heavy in ¹³C in comparison with a standard) stable carbon isotopic composition of these compounds dissolved in sediment porewater versus source gases, which indicates preferential microbial oxidation of the lighter ¹²C-containing isomers (SASSEN et al., 2004).

Methane dependent sulfate reduction is mediated by a limited assemblage of microorganisms. Methane is oxidized by anaerobic methanotrophic archaea which are grouped into three distinct clades (i.e. ANME-1, -2, and -3); these clades are distant relatives of *Methanosarcinales*-type methanogenic archaea (BOETIUS et al., 2000; KNITTEL et al., 2005; ORPHAN et al., 2002; TESKE et al., 2002). These archaea are typically associated with sulfate reducing bacteria (SRB) of the *Desulfosarcina/Desulfococcus* or *Desulfobulbus* genera of the *DeltaProteobacteria*, presumably in a syntrophic relationship (BOETIUS et al., 2000; KNITTEL et al., 2003; ORPHAN et al., 2001). Other *Desulfobacteriaceae*- and *Desulfobulbaceae*-family related SRB are commonly and exclusively found at cold seeps, especially when non-methane hydrocarbons are present (DHILLON et al., 2003; KNITTEL et al., 2003; MILLS et al., 2004; ORPHAN et al., 2001; TESKE et al., 2002). The carbon compounds supporting the growth of these

other seep-exclusive SRB groups are speculative, but may include methane as well as non-methane hydrocarbons. Additionally, exceptionally high concentrations of dissolved organic carbon can fuel SR at brine seeps (JOYE et al., in preparation; ORCUTT et al., 2005). The parameters that influence differential growth of the various SR and SR-AOM communities are unconstrained but may include methane flux, non-methane reduced-carbon flux, temperature, and/or oxygen sensitivity (KNITTEL et al., 2005; NAUHAUS et al., 2005).

Cold seeps on the continental slope in the Gulf of Mexico (GOM) comprise a natural system for studying the impact of oil and non-methane hydrocarbons on microbial community diversity, distribution and activity in marine sediments. These seeps are commonly associated with natural oil-slicks visible from space, indicating the seepage of oil in addition to methane (MACDONALD et al., 2004; MACDONALD et al., 1996); more than 20,000 m³ yr⁻¹ of natural oil seepage occurs in the GOM (MACDONALD et al., 1993). Some GOM sediments are replete with petroleum-associated compounds, including C₂-C₅ alkanes, hexadecane, naphthalene, phenanthrene, toluene, and crude oil (KENNICUTT et al., 1988; SASSEN et al., 1994). The *in situ* stable carbon isotopic signature of some of these compounds indicate biological degradation (i.e. compounds are enriched in ¹³C, indicating preferential oxidation of the lighter ¹²C isomers (SASSEN et al., 2004)), although it is unclear which microbes are responsible. Surveys of SR in GOM sediments indicate that a significant fraction of SR is fueled by non-methane hydrocarbons (JOYE et al., 2004; ORCUTT et al., 2005). Studies with oil-rich sediments from the GOM indicate that SR can be stimulated by aliphatic compounds, and sulfate-reducing bacteria which grow solely on butane and propane were recently cultivated from GOM sediments (KNIEMEYER et al., In press). These findings indicate that the endemic sulfate-reducing microbial community is capable of consuming these compounds *in situ*.

The objective of this study was to gain a better understanding of the distribution and activity of sulfate reducing bacteria and methanotrophic archaea in hydrocarbon-rich seep sediments of the GOM. Sediments from different hydrocarbon-rich habitats were investigated using biogeochemical and molecular ecological techniques to determine which microorganisms dominated each habitat. Surveys comparing sediments with tight coupling of AOM and SR to those with looser coupling allowed us to investigate which microbial groups were involved in non-methane hydrocarbon degradation, methane oxidation or organic matter mineralization.

Materials and Methods

Sample Collection

Cold seeps in the northern and southern Gulf of Mexico (Fig. 3.1A) were visited during two oceanographic cruises: (1) aboard the *R.V. Seward Johnson II* (cruise LExEn 2002) using the *Johnson SeaLink* research submersible (Harbor Branch Oceanographic Institution) in July 2002, and (2) aboard *R.F. SONNE* (cruise OTEGA II SO174) in October/November of 2003 (BOHRMANN et al., 2004). Areas of seepage were identified by the presence of an overlying microbial mat, exposed carbonate crusts or visible gas/oil seepage, which indicated advection of reduced metabolites to the sediment surface. An area of $\sim 1 \text{ m}^2$ of seafloor was cored by the submersible's robot arm (LExEn 2002 cruise), by a video-guided box-corer (SO174 cruise), or by a video-guided multiple-corer device capable of retrieving up to 6 cores of 10 cm inner diameter each (SO174 cruise). A description of the cold seep sites visited and the condition of the cores retrieved is given in Table 3.1. Sediments are described hereafter in reference to the station-number (SO174 cruise) or dive-number (LExEn 2002) of the cruises.

Station 87 (SO174): Cores were collected from site GC234 (550 m water depth) on the continental slope in the northern GOM directly adjacent to a large aggregation of tubeworms (see ref (BOHRMANN et al., 2004; MACDONALD et al., 2003) for site details). The retrieved sediment was overlain with a dense mat of sulfide oxidizing bacteria (SOB; mainly orange but some white *Beggiatoa* spp., Fig. 3.1C) and visibly contained oil and carbonate nodules but no gas hydrate.

Station 140 (SO174): Sediments around a carbonate outcrop near the recently discovered *Chapopote* asphalt volcano in the Campeche Knolls region of the southern GOM (2900 m water depth; (BOHRMANN et al., 2004; MACDONALD et al., 2004)) were sampled using the box coring device (Fig. 3.1D). Upon recovery, dissociation of hydrate and degassing resulted in sediment expansion. Push cores were manually inserted into the expanded sediment. There were no noticeable SOB or asphalt pieces associated with the disturbed sediment but there were numerous oil-coated casings from tube worms and clams; gas hydrate, oil, and carbonate nodules were dispersed throughout the sediment.

Station 156 (SO174): Cores were collected from a white SOB mat that was located between a large population of *Lamellibrachia* spp. tubeworms (Fig. 3.1E) and an outcrop of gas hydrate from a gas hydrate site on the northern slope, GC185. (550m water depth; see (BOHRMANN et al., 2004; MACDONALD et al., 2005; MACDONALD et al., 1994; MACDONALD et al., 2003) for site details).

Station 161 (SO174): Sediment cores were collected from an area with carbonate outcrops and white/grey SOB mats (Fig. 3.1F) using the multiple-corer at GC415, a deep water (950 m) cold seep (BOHRMANN et al., 2004; MACDONALD, 2004). Upon insertion of the push cores, a vigorous stream of gas bubbles and oil droplets erupted from the seafloor for about 15 minutes while the multicorer was left in place, indicating that a carbonate cap or hydrate lens had

been punctured. The recovered sediment was highly disturbed, saturated with oil, and contained disseminated hydrate and carbonate nodules. The disturbance of the sediment collection prevented completion of a full suite of analyses (no acetate concentration, methanogenesis or acetate oxidation samples were collected).

Dive 4463 (LExEn 2002): This dive visited site GC232 (500 m water depth; see (ORCUTT et al., 2005; SAGER et al., 2003) for site details), near GC234 and GC185 on the northern slope, and collected oil-laden sediment cores from a patch of gray/white SOB mat (Fig. 3.1B). A stream of bubbles emanated from the sediment during coring operations. Due to the small number of sediment cores collected, not all analyses were possible with these sediments (no acetate concentrations, methanogenesis, acetate oxidation or CARD FISH measurements data are available).

Sample manipulation and geochemistry analysis

Upon retrieval, sediment cores were transferred to a 4 °C cold room and processed within a few hours under a stream of Argon gas. Duplicate cores from each station were processed to obtain samples for AOM, SR and methanogenesis rate analyses; porewater and solid phase geochemistry and hydrocarbon concentration determination; and DNA- and RNA-based molecular analysis. Cores from Dive 4463 were sectioned and analyzed as described previously (ORCUTT et al., 2005). Cores from S0174 stations were sectioned at 2 cm intervals with the aid of a plastic manifold fitted to the core and a stationary plunger. For C₁-C₄ hydrocarbon gas quantification, a 2 mL sub-sample was collected into a cut-off syringe, transferred immediately to and sealed in either a 9 or 16 mL helium-purged serum vial that contained 2 mL of helium-purged 2M NaOH, which served to arrest biological activity in the sample. For fluorescence in

situ hybridization analysis, 1 ml of sediment was fixed in 3.7% formaldehyde in phosphate buffered saline. Sediments for DNA samples were collected by sterile metal spatula, transferred to pre-combusted glass jars sealed with dichloromethane-cleaned (to remove organics) Teflon[®] caps, and stored frozen at -20°C until analysis. Porewater was collected by centrifuging 25 mL of sediment in a 50 mL plastic Falcon tube except for Station 161, where porewater was retrieved by squeezing using a pressure filtration system (0.2 µm cellulose acetate filters) at pressures up to 5 bars. Sample fixation and analyses for quantifying dissolved hydrocarbon gases (methane, ethane, propane, *iso*-butane, butane and pentane), sulfide (HS⁻), sulfate (SO₄), chloride (Cl⁻), bicarbonate (DIC or HCO₃⁻) and volatile fatty acids (primarily acetate) followed previously described methods (JOYE et al., 2004; ORCUTT et al., 2004). Sediments for total carbon, organic carbon and carbonate contents were stored frozen until processing and analysis. Total carbon content was measured directly on aliquots of untreated, dried sediments in tin capsules on a ThermoFinnigan Flash elemental analyzer. Inorganic carbon was removed from parallel samples stored in silver capsules following acidification by concentrated HCl vapors in an enclosed chamber; acidified samples were then analyzed on the elemental analyzer to determine the remaining organic carbon content. The analytical procedures and methods to determine the named sediment parameters are documented in detail at http://www.ifm-geomar.de/index.php?id=mg_analytik&L=1.

Sediments preserved for C₁-C₄ hydrocarbon analysis (above) were subsequently used for analyzing total solvent-extractable organic matter (i.e. C₁₅₊ hydrocarbon) content (KENNICUTT et al., 1988; SASSEN et al., 1994). Fixed sediments were extracted in dichloromethane and methanol with sonification using a modified Bligh and Dyer method (ORCUTT et al., 2005). The total extract was evaporated to dryness to calculate the total weight of extracted material then

diluted in hexane and analyzed by gas chromatography using a Hewlett Packard 6890 chromatograph equipped with a 30 m HP-5 capillary column. As noted elsewhere (SASSEN et al., 1994), chromatograms of extracts from oil-laden sediments with active microbial degradation of oil by-products are often characterized both by an unresolved complex mixture (UCM) of organic compounds present as a broad “hump” in the baseline and by the absence of *n*-alkane and isoprenoid compounds which are abundant in unaltered oils.

Microbial activity measurements

Samples for AOM, SR, bicarbonate-based methanogenesis (Bi-MOG), acetoclastic methanogenesis (Ace-MOG) and acetate oxidation (Ace-Ox) were collected in modified cut-end glass tubes and incubated with radiotracer following previously described methods (ORCUTT et al., 2005) with the exception of AOM and SR samples from Dive 4463 which were collected and incubated in whole sub-cores as described previously (JOYE et al., 2004). Rate samples were incubated in triplicate; rates are expressed as the average \pm standard deviation ($n=3$). For acetate metabolism, after $^{14}\text{CH}_4$ produced during the incubation was stripped from the ^{14}C -acetate amended tubes (to determine Ace-MOG), the remaining sediment was used for the analysis of Ace-Ox (i.e. oxidation of ^{14}C -labeled acetate to $^{14}\text{CO}_2$). Sediment was transferred from the tubes to 250 ml distillation flasks and mixed with 30 ml of milli-Q[®] water. 5 ml of 20% zinc acetate (ZnAc) was added to samples to minimize volatilization of ^{14}C -acetate which would contaminate the $^{14}\text{CO}_2$ distillate. Distillation flasks were attached to a “hot” distillation system using a water-cooled condenser for stripping and capture of $^{14}\text{CO}_2$ product released after acidification of the sample with 15 ml of 12M HCl (final concentration of HCl \sim 10%). Samples were distilled for 15 min. without heating following by 25 min. of heating to a slow boil and finally another 20

min. without heat. A secondary acetate-vapor trap comprised of 10 ml of acidified (to pH 1) 5% ZnAc was installed before two base traps (10 ml of 1N NaOH), which serially captured $^{14}\text{CO}_2$. After distillation, the base trap solutions were combined and a 2 ml aliquot of the solution was mixed with Ultima Gold scintillation cocktail and counted on an LS 6500 Beckmann counter. The acetate oxidation rates were calculated as follows:

$$\text{Ace-Ox Rate} = [\text{acetate}] \times \alpha_{\text{CH}_3\text{COO-}/t} \times (a\text{-}^{14}\text{CO}_2/a\text{-}^{14}\text{C-acetate}) \quad (\text{Eq. 2})$$

where the rate is expressed as nmol acetate reduced $\text{cm}^{-3} \text{d}^{-1}$; $[\text{acetate}]$ is the pore water acetate concentration corrected for porosity (nmol cm^{-3}); $\alpha_{\text{CH}_3\text{COO-}}$ is the isotope fractionation factor (assumed to be 1.06 as for Ace-MOG; (GELWICKS et al., 1994; KRZYCKI et al., 1987)); t is incubation time (d); $a\text{-}^{14}\text{CO}_2$ is the activity of the product pool; and $a\text{-}^{14}\text{C-acetate}$ is the activity of the substrate pool.

Microbial diversity measured with 16S rRNA gene libraries

16S rRNA gene libraries were constructed from Station 140, Station 161 and Dive 4463 sediments. Although clone libraries were not constructed from Station 87 or Station 156 sediments, other researchers have previously characterized the bacterial and archaeal communities in sediments that originate from the same sites and similar environmental settings (MILLS et al., 2003; MILLS et al., 2004). Total DNA was extracted directly from 5-10 g of frozen sediment following the method of Zhou et al. (1996). Crude DNA was purified with the Wizard DNA Clean-Up Kit (Promega, Madison, WI). Archaeal and bacterial 16S rDNA clone libraries were constructed for each sample using the primer sets Arch20f (MASSANA et al., 1997)/Uni1392R (LANE et al., 1985) and ARCH20f/ARCH958R (DELONG, 1992) for archaea and EUB008f/EUB1492R; (KANE et al., 1993; MUYZER et al., 1995) for bacteria. Polymerase

chain reaction (PCR) products were purified with the QiaQuick PCR Purification Kit using the manufacturer's protocol (Qiagen, Hilden, Germany). Clone libraries were constructed in pGEM-T-Easy (Promega, Madison, WI, USA) or the TOPO pCR4 vector (Invitrogen, Karlsruhe, Germany) according to the manufacturer's recommendations. Sequencing was performed by *Taq* cycle sequencing with a model ABI377 sequencer (Applied Biosystems). The presence of chimeric sequences in the clone libraries was determined with the CHIMERA_CHECK program of the Ribosomal Database Project II (Center for Microbial Ecology, Michigan State University, <http://rdp.cme.msu.edu/html/analyses.html>). Potential chimeras were eliminated before phylogenetic trees were constructed. Sequence data were analyzed with the ARB software package (LUDWIG et al., 2004). Phylogenetic trees of 16S rRNA gene sequences were calculated by parsimony, neighbor-joining, and maximum-likelihood analysis with different sets of filters. For tree calculation, only nearly full-length sequences were considered. Partial sequences were inserted into the reconstructed tree by parsimony criteria without allowing changes in the overall tree topology. Using different treeing methods, tree topology did not result in a stable branching order for all groups; consequently, some branches are displayed as multifurcated to reflect the instability.

Results

Biogeochemistry

Station 87: Samples from the GC234 shallow gas hydrate site were covered by a dense mat of orange SOB and exhibited slight depth gradients in geochemistry and relatively low rates of microbial activity (Fig. 3.2A). Chloride values throughout the core (~550 mM) were

comparable to those expected in seawater. The sediment organic carbon content was relatively low (~2 carbon weight percent, Cwt%) while the carbonate carbon wt% was relatively high at depth (20-40 % from 15-30 cm). The sediments contained 8.5 mg cm^{-3} solvent-extractable organic matter and C_{15+} chromatograms of the extract revealed a shallow UCM with defined *n*-alkane and isoprenoid compound peaks (Fig. 3.3). Methane was slightly elevated (up to $44 \text{ } \mu\text{m}$) in the upper 10 cm of the core and decreased to $3\text{-}4 \text{ } \mu\text{m}$ below 10 cm (Fig. 3.2A); higher alkanes (i.e. ethane (C_2), propane (C_3), *iso*-butane (iC_4) and *n*-butane (C_4)) were below detection. In the upper 10 cm, sulfide was elevated from background values (0.1 mM) up to $\sim 1.5 \text{ mM}$. Acetate varied from zero to $2 \text{ } \mu\text{M}$ above 15 cm and increased to $26 \text{ } \mu\text{M}$ by 30 cm. There was no obvious sulfate methane transition zone (SMTZ) in this core. Although the sulfate gradient did not indicate net consumption, significant SR rates were measured throughout the core, ranging from 11 ± 1.2 to $800 \pm 560 \text{ nmol cm}^{-3} \text{ d}^{-1}$ with several peaks in activity observed at 7, 17 and 29 cm. The highest rates of AOM (up to $5.7 \pm 3.8 \text{ nmol cm}^{-3} \text{ d}^{-1}$) occurred in the upper 6 cm, with minimal activity below. In contrast, Bi-MOG rates became measurable below 6 cm and maintained a relatively constant rate of $0.1 \pm 0.02 \text{ nmol cm}^{-3} \text{ d}^{-1}$ until 29 cm depth. At this depth, Ace-MOG was detectable at $0.21 \pm 0.06 \text{ nmol cm}^{-3} \text{ d}^{-1}$ but Ace-MOG activity was near zero at shallower depths. The oxidation of acetate (Ace-Ox) was a greater sink for acetate, ranging from 0.5 ± 0.1 to $3.1 \pm 0.2 \text{ nmol cm}^{-3} \text{ d}^{-1}$ throughout the sediment column.

Station 140: Sediments from a gas hydrate-rich area of the *Chapopote* asphalt volcano were oil-laden and had the highest levels of organic carbon ($>20 \text{ Cwt\%}$ at the surface; Fig. 3.2B) and solvent-extractable organic matter (149 mg cm^{-3}) measured in this survey. The extracted C_{15+} hydrocarbons were highly degraded – the chromatogram contained no discernable *n*-alkane or isoprenoid peaks and a broad UCM (Fig. 3.3). Chloride was elevated nearly 2x greater than

background values at 9 cm (1066 mM) but was slightly fresher than seawater elsewhere in the core (512-545 mM, Fig. 3.2B). Carbonate content ranged from 3.1 to 32.0 Cwt% with the highest value at 12 cm. Sulfate was depleted throughout the core, ranging from 1.1 to 3.5 mM, although it is possible that higher sulfate values existed near the sediment-water interface, which was undetectable at the 2 cm resolution of the sampling. Sulfide values were quite high throughout the core, ranging from 3.4 to 10.7 mM with a broad peak from 5 to 11 cm. Methane ranged from 1.6 to 3.1 mM, with the highest values observed near the surface. Acetate was also highest at the surface (405 μ M) and remained relatively constant (105 to 130 μ M) with depth. Although the methane concentration was relatively constant with depth, higher alkanes (C_2 - C_4) exhibited depletion centered around 9 cm depth and again at 15 cm (Fig. 3.4A). From the surface to 9 cm, ethane decreased from 313 to 57 μ M, propane decreased the most from 781 to 29 μ M, *iso*-butane dropped from 184 to 7 μ M and *n*-butane ranged from 31 to 2 μ M. Over the depths sampled, the ratio of iC_4/C_4 ranged from 3.5 to 6.1 and $C_1/(C_1 + C_2)$ varied from 0.91-0.98. Rates of SR, AOM and Bi-MOG were lower by at least an order of magnitude in St. 140 sediment when compared to the other sites (Fig 2B). SR and AOM were highest in the top layer of sediment at 0.9 ± 1.3 and 1.3 ± 0.01 $\text{nmol cm}^{-3} \text{d}^{-1}$, respectively; Ace-Ox also peaked in this zone and was higher than either SR or AOM at 10.4 ± 3.4 $\text{nmol cm}^{-3} \text{d}^{-1}$. Bi-MOG activity peaked at 0.02 ± 0.001 $\text{nmol cm}^{-3} \text{d}^{-1}$ at 7 cm and was absent above this depth. Ace-MOG rates increased just below this depth and peaked at 13 cm at 0.4 ± 0.2 $\text{nmol cm}^{-3} \text{d}^{-1}$; the highest rate of Ace-MOG in the sediments surveyed.

Station 156: Sediments collected from a microbial mat near a hydrate outcrop and a tube-worm bush exhibited some of the highest microbial activity rates of the sediments surveyed in this study and a strong SMTZ observed between 5 and 7 cm (Fig. 3.2C). Chloride remained

constant with depth at seawater values. The organic carbon content of the sediment increased slightly from ~6.5 to 8.5 Cwt% over depth (Fig. 3.2C) and the sediments contained 23.3 mg cm⁻³ of solvent-extractable organic matter comprised on a broad UCM with no discernable *n*-alkane or isoprenoid compounds (data not shown). Carbonate carbon content varied from 12.3 to 18.3 Cwt% with a subsurface peak around 6 cm depth (Fig. 3.2C). Sulfate decreased rapidly from seawater values at the sediment water interface to 4.7 mM at 7 cm and decreased gradually thereafter to 1.1 mM at the deepest depth sampled (13 cm). Sulfide peaked at 7 cm at 10.6 mM, decreasing to 4.8 mM at the surface and 5.8 mM at depth. Methane concentrations were also highest (3.3 mM) at 7 cm; methane concentration decreased to 0.2 mM at the surface and to 1.3 mM at depth. Ethane showed a similar pattern of distribution, although the highest concentration reached was 242 μM; other higher alkanes were below detection limit (Fig. 3.4B). The C₁/(C₁ + C₂) ratio ranged from 0.93 at the depth of highest ethane concentration to 0.99 elsewhere in the core. Acetate was present in relatively high concentration throughout the core, ranging from 67 to 472 μM with a general increasing trend with depth. Sulfate reduction rates were extremely variable and were highest in the sediment above 7 cm, ranging from 48 ± 58 to 118 ± 102 nmol cm⁻³ d⁻¹, and decreased to values below 1 nmol cm⁻³ d⁻¹ at depth (Fig. 3.2C). AOM activity was highest at 7 cm at 470 ± 0.5 nmol cm⁻³ d⁻¹ and decreased to <100 ± 0.1 nmol cm⁻³ d⁻¹ within 4 cm below or above that zone. The highest rates of Bi-MOG (8.9 ± 2.0 nmol cm⁻³ d⁻¹) occurred in the upper 2 cm and decreased to <2 nmol cm⁻³ d⁻¹ below that depth. Although acetate concentrations were highest in these sediments, the rates of Ace-MOG were the lowest measured. Elevated Ace-MOG activity (0.03 ± 0.02 nmol cm⁻³ d⁻¹) occurred in the upper 3 cm and the highest rates were found at 13 cm (0.07 ± 0.05 nmol cm⁻³ d⁻¹). Ace-Ox rates were

highest in these sediments, ranging from 11.7 ± 1.0 to 36.0 ± 13.8 $\text{nmol cm}^{-3} \text{ d}^{-1}$ with the maximum value occurring at 7 cm.

Station 161: Sediment collected from GC415 was highly disturbed due to the vigorous release of oil and gas from the seafloor during collection. The sediments were oil-rich and had high organic carbon content (up to 2.6 Cwt%), very high carbonate content (up to 57.6 Cwt%) and the highest alkane concentrations measured in this survey in the upper layers of sediment (Figs. 2D, 3C). The sediments contained 12.5 mg cm^{-3} of solvent-extractable organic matter characterized both by a broad UCM and strong *n*-alkane and isoprenoid peaks (data not shown). Chloride was elevated above background throughout the core, increasing from 612 mM at the surface to 3058 mM (5.5x background values) at 13 cm (Fig. 3.2D). Sulfate was lower than seawater values at the surface (19.8 mM) and decreased to 3.9 mM by 13 cm. The steepest gradient in sulfate occurred from 1-5 cm where methane concentration increased from 3 to 38 mM. Ethane ranged from 245-3612 μM , propane from 386-6921 μM , *iso*-butane from 241-2071 μM , and *n*-butane from 115-1138 μM (Fig. 3.4C). The $i\text{C}_4/\text{C}_4$ ratio in these sediments ranged from 1.5-2.1 and the ratio of $\text{C}_1/\text{C}_1 + \text{C}_2$ ranged from 0.82-0.89. A mixture of sediment from 0-10 cm exhibited SR and AOM rates of 559 ± 294 and 216 ± 43 $\text{nmol cm}^{-3} \text{ d}^{-1}$, respectively (data not shown). Sediment below 10 cm had comparable rates of SR (676 ± 198 $\text{nmol cm}^{-3} \text{ d}^{-1}$) and AOM (162 ± 50 $\text{nmol cm}^{-3} \text{ d}^{-1}$; data not shown).

Dive 4463: Porewater and microbial activity patterns in sediments collected from a microbial mat from site GC232 were similar to those measured from sediments from GC185 (Station 156; Fig. 3.2E). Chloride decreased from background values at the surface to 'fresher' values at depth (down to 430 mM), probably due to sublimation of gas hydrate during recovery. The organic carbon content varied between 4.2 and 7.4 Cwt% with a peak at 7 cm; carbonate

carbon content was relatively low (2.0-3.9 Cwt%) and peaked at 3 cm (Fig. 3.2E). The sediments contained 30.3 mg cm^{-3} solvent-extractable organic matter characterized by a broad UCM with no distinguishable *n*-alkane or isoprenoid peaks (data not shown). The steepest gradients of sulfate and methane occurred in the SMTZ between 3 and 7 cm (Fig. 3.2E). Sulfate decreased from seawater values at the surface to 3 mM by 7 cm and to 1.6 mM by 11 cm. Methane peaked at 1 mM at 7 cm. Sulfide had a broad peak in concentration from 13.6 to 15.6 mM from 5-9 cm and displayed high values throughout the sediment column. SR rates were highest ($183 \text{ nmol cm}^{-3} \text{ d}^{-1}$) near the surface with a secondary peak in activity ($130 \text{ nmol cm}^{-3} \text{ d}^{-1}$) between 8 and 10 cm; AOM also peaked near the surface at $120 \text{ nmol cm}^{-3} \text{ d}^{-1}$. As with Station 156 sediments, ethane distribution mirrored the methane distribution but was present at lower concentration (1.6-9.0 μM); the $C_1/(C_1 + C_2)$ ratio was >0.99 throughout the sediment and higher alkanes ($>C_3$) were not detectable (Fig. 3.4D).

The highest integrated rates of AOM and SR in the upper 10 cm were found in sediments collected from shallow- to mid-water depth ($<1000 \text{ m}$) gas hydrate sites in areas covered with white/grey sulfide-oxidizing bacterial mats (Stations 156, 161 and Dive 4463; Table 3.2). SR often exceeded the rate of AOM in the sediments surveyed (Stations 87, 161, Dive 4463) although there were cases where AOM overall exceeded SR (Stations 140, 56). SR and AOM rates exceeded the rates of other processes in all sediments except at Station 140, which had much higher acetate consumption rates than SR and AOM. With the exception of Station 140 sediments, which had extremely low rates of AOM and SR activity and very long estimated turnover times for the methane and sulfate pools (tens to hundreds of years), the estimated turnover time for the methane pool in these sediments averaged tens of days while the

estimated time for turnover for the sulfate pool averaged at hundreds to thousands of days. The oxidation of acetate could turnover the entire acetate pool in tens of days (Table 3.2).

Microbial diversity and abundance

A total of 162, 212, and 166 16S gene clones were screened from Station 140, Station 161 and Dive 4463 sediments, respectively (Table 3.3). The 16S rRNA gene libraries obtained for the *Bacteria* and *Archaea* were phylogenetically diverse and included numerous cultivated and uncultivated lineages (Figs. 5,6). Substantial differences in sequence diversity between the samples investigated were apparent. For instance, the JS1 group of Bacteria dominated the bacterial clone library from Station 140 sediments (40% of bacterial clones, n=83) but only made up 11% and 3% of the bacterial clones of Station 161 (n=118) and Dive 4463 (n=64) sediments, respectively (Table 3.3).

SRB within the *Deltaproteobacteria* constituted a substantial fraction (35-41%) of the bacterial clone libraries from these sediments (Table 3.3, Fig. 3.5). Clones from seep-related SRB groups (i.e. *Desulfosarcina* related spp., SEEP-SRB1, SEEP-SRB2, SEEP-SRB3) were the most abundant, although the proportion varied between sites (Table 3.3, Fig. 3.5). In Station 140 sediments, the majority of SRB clones grouped with the SEEP-SRB1 and -SRB2. Members of the SEEP-SRB1 within the *Desulfosarcina/Desulfococcus* group are known to be involved in AOM in partnership with the ANME-2 archaea (KNITTEL et al., 2003; ORPHAN et al., 2001). Clones for the SEEP-SRB3 group within the *Desulfobulbaceae* were the most abundant SRB phylotypes (31%, n=42) in the Station 161 sediments; sequences related to the *Desulfosarcina* and *Desulfobacterium anilini* were the second most abundant phylotypes observed (19% each). The SEEP-SRB4 phylotype was only observed in the Station 161 sediments. No particular SRB

phylotype dominated the Dive 4463 sediments from GC232, which had strong representation of the *Desulfosarcina*, SEEP-SRB2, *Desulfuromonas*, and *Desulfuromusa* spp. groups.

The ANME-1 phylotype dominated (49-53% of sequences) the archaeal clone libraries from all of the samples investigated (Table 3.3, Fig. 3.6). The ANME-2c phylotype was abundant in the Station 140 (25%, n=79) and Dive 4463 (10%, n=102) and was the only ANME-2 phylotype recovered from the Station 161 sediments. Station 140 sediments also had sequences that grouped with the ANME-2b cluster whereas Dive 4463 sediments contained ANME-2a related sequences. The ANME-3 group of AOM-mediating archaea was not detected in any of the samples. Station 161 was the only site to have sequences group with the GOM ARC1 phylotype (LLOYD et al., 2006) which is most closely affiliated with the recently discovered ANME that mediates AOM in concert with denitrification (RAGHOEBARSING et al., 2006). All of the sites contained sequences that clustered within the *Methanomicrobiales* as well as sequences that grouped with the Marine Benthic Group D phylotype. The Marine Benthic Group B of the Crenarchaeota phylotype was only found in the sediments from Dive 4463.

Sediments similar to those from Stations 87 and 156 (Sites GC234 and GC185, respectively) have been analyzed previously for microbial diversity (MILLS et al., 2003; MILLS et al., 2004). Those studies revealed that the SEEP-SRB1, SEEP-SRB2, SEEP-SRB3 and SEEP-SRB4 phylotypes were present in the bacterial clone libraries, as well as sequences related to *Desulfobacterium anilini* (other Gulf of Mexico sequences labeled in Fig. 3.5). The ANME-1 and ANME-2 phylotypes are also present in the GC234 and GC185 sediments, but not the ANME-3 phylotype (Fig. 3.6).

In a parallel study (ORCUTT et al., in preparation), the abundance of particular microbial groups within the sediments was quantified using catalyzed reporter deposition fluorescence in

situ hybridization. Small (average 3 μm diameter) ANME-2/DSS consortia were detected in sediments from Stations 87, 140 and 161, although not in high abundance. Larger (up to 15 μm) and more abundant ANME-2/DSS aggregates were observed in Station 156 sediments in both shell- and mixed-type configurations. ANME-1 cells were abundant (>20% of total cells) in Station 87, 140 and 161 sediments but were nearly absent in Station 156 sediments. Sediments from Dive 4463 were unfortunately not preserved for analysis.

Discussion

To the best of our knowledge, this work represents the first survey of the impact of natural, endogenous oil and non-methane hydrocarbons on the rates of microbial activity and microbial community structure in surficial sediments from marine cold seeps. As sulfate reduction and anaerobic oxidation of methane are dominant microbial metabolisms at cold seeps, we focused on these processes but also examined the coupling with methane production and acetate cycling. Our results show that (1) significant rates of SR were supported by endogenous non-methane hydrocarbons in these sediments; (2) that acetate, possibly derived from oil-degradation, was rapidly consumed by acetate oxidation; and (3) that the input of oil and higher hydrocarbons may have influenced the microbial community structure in sediments.

As described previously (AHARON and FU, 2000; ARVIDSON et al., 2004; JOYE et al., 2004; ORCUTT et al., 2005) and supported by this study, AOM and SR activities in GOM seep sediments are relatively high in comparison with sediments from other cold seep sites (BOETIUS et al., 2000; HINRICHS and BOETIUS, 2002; NIEMANN et al., 2006; SAHLING et al., 2002; TREUDE et al., 2003). *In vitro* enrichment experiments with sediments from a variety of methane cold seeps showed that sediments from GOM gas hydrate sites had the highest methane-fueled sulfate

reduction potential per gram of sediment (KRÜGER et al., 2005). This elevated activity may be related to higher AOM and SR-associated biomass in Gulf of Mexico sediments as compared to other sites (KRÜGER et al., 2005). In this study, AOM and SR rates exhibited high variability between replicates in some instances; again indicating that significant small scale spatial variability exists *in situ*, as suggested previously (ORCUTT et al., 2005; TREUDE et al., 2003). The impact of macrofaunal pumping may also have significant local impacts on rates of sedimentary microbial activity (CORDES et al., 2005). It is possible that the high rates of SR observed at depth and the relatively flat profile of SO_4^{2-} concentrations in Station 87 sediments (Fig. 3.2A) may have been influenced by pumping activity of the ‘roots’ of tubeworms, which are abundant at GC234 (MACDONALD et al., 2003), as the multicorer for this sample collection was placed directly beside a large tubeworm aggregation.

Sulfate reduction often exceeded AOM in these GOM sediments, in some cases by up to two orders of magnitude (Fig. 3.1, Table 3.2). For example, SR was consistently higher than AOM in oil-rich sediments from GC415, a 950 m deep site. Non-methane hydrocarbons supported the observed sulfate reducing activity. The ratios of $i\text{C}_4/\text{C}_4$ in these sediments, where *iso*-butane is consistently higher than *n*-butane, indicate that the more ‘labile’ higher hydrocarbons (i.e. *n*-butane) were consumed *in situ* (SASSEN et al., 1994; SASSEN et al., 1988). Interestingly, a comparison of the turnover times for the sulfate and methane pools (i.e. hundreds of days versus tens of days; Table 3.2) indicates that SRBs associated with AOM may be methane limited.

Sediments from the shallower (500-600 m water depth) gas hydrate sites (Station 87, 156, Dive 4463) were comprised of 10% or less organic carbon, contained 30 mg cm^{-3} or less solvent-extractable organic matter which was characterized by a weak to moderate UCM of biodegraded

material, and contained 1-3 orders of magnitude more methane than other hydrocarbon gases. These sediments contained a mixture of ANME-1 and ANME-2 communities and a relatively high diversity of SRB. In contrast, oily sediments from the *Chapopote* asphalt volcano (MACDONALD et al., 2004) which were characterized by high organic content (149 mg cm⁻³ highly biodegraded solvent-extractable organic matter and 10-20% organic carbon) and high proportions of C₂-C₄ hydrocarbon gases were less diverse, with abundant ANME-1, very few ANME-2, and dominance of the SRB phylotypes by the SEEP-SRB1/DSS and SEEP-SRB2 groups. Additionally, the mid-water depth Site GC415 sediments (Station 161), which had relatively low quantities of less biodegraded solvent-extractable organic matter but high organic carbon content and C₂-C₄ gas concentrations contained multiple phylotypes which were not observed in the other sediments, including the SEEP-SRB4, *Desulfocapsa* related species, *Acidobacteria*, *Nitrospina*, *Actinobacteria* groups of bacteria and the GOM ARC1 group of Archaea which are most closely related to ANME archaea which partner with denitrifying bacteria instead of sulfate reducing bacteria (RAGHOEBARSING et al., 2006). Notably, the Station 161 sediments did not contain any SEEP-SRB2 related sequences. Phylotypes closely related to the recently cultivated anaerobic butane oxidizing SRB (KNIEMEYER et al., In press) were also not observed in any of the sediments investigated.

Unlike previous findings with GOM cold seep sediments (ORCUTT et al., 2005), there was not a clear relationship between AOM and Bi-MOG in the GOM sediments investigated in this survey (Fig. 3.2). Previous work suggested that ANMEs may mediate Bi-MOG in addition to AOM, as Bi-MOG was found to repeatedly occur at 10% of the rate of AOM in sediments and microbial mats where ANMEs dominated the archaeal community (ORCUTT et al., 2005; TREUDE et al., In press). As ANMEs are thought to oxidize methane by 'reversing' methanogenic

enzymes (i.e. ANMEs contain most of the genes of known methanogenic pathways; (HALLAM et al., 2003; HALLAM et al., 2004; MEYERDIERKS et al., 2005; SHIMA and THAUER, 2005)); it is reasonable to assume that the enzymes could also work in ‘forward’ mode to generate methane. In this study, there were no obvious overlaps in the zones of peak AOM and Bi-MOG activity *ex situ*. In fact, in Station 87 sediments the zones of peak AOM, Bi-MOG and Ace-MOG were distinct; Bi-MOG occurred at <4% the rate of AOM in the zone of highest AOM (Fig. 3.2A). In sediments from the *Chapopote* asphalt volcano (Station 140), although Bi-MOG and Ace-MOG were spatially separated, AOM occurred throughout the core; in one zone Bi-MOG occurred at most at $7 \pm 0.5\%$ the rate of AOM and at <2% elsewhere (Fig. 3.2B). In the zone of maximum AOM activity in sediments from the GC185 gas hydrate site (Station 156), Bi-MOG was <2% of the AOM rate (Fig. 3.2C). Although the *ex situ* patterns did not indicate a 10% coupling of Bi-MOG to AOM, *in vitro* enrichment experiments with these same sediments documented Bi-MOG occurring at ~10% the rate of AOM in the presence of methane and sulfate (ORCUTT et al., in preparation); the observed difference between *ex situ* and *in vitro* incubations could reflect high spatial variability in the original sediments.

Station 140 sediments had anomalously low rates of SR and AOM activity considering the availability of hydrocarbons in the sediments (Fig. 3.2, Table 3.2). It is possible that benzene or other petroleum-derived compounds in these oil-rich sediments were at toxic levels that inhibited microbial activity. Although the diversity in Station 140 sediments was lower than at the other sites (Table 3.3), a substantial community of ANME-1 cells was observed in the sediments, suggesting that the high organic content of the sediments did not preclude the existence of those microorganisms. Sulfate concentrations were low (~1 mM) throughout the core; it is possible that AOM and AOM-related SR were limited by the availability of sulfate as

the electron acceptor sulfate. Previous work has shown that limitation of AOM occurs when sulfate is in the low mM (1-2 mM) range (TREUDE, 2003). To our knowledge, fluid flux rates for the *Chapopote* asphalt volcano are unknown, although persistent observation of oil slicks above the site indicate that substantial fluid flow occurs (MACDONALD et al., 2004). It is possible that advection of reduced, sulfate-free fluids from the site leads to low sulfate availability within the sediment, thus prohibiting high rates AOM and SR. Interestingly, the high carbonate content, a typical sedimentary signature of AOM, in the Station 140 sediments indicates that over longer periods of time hydrocarbon-fueled SR may be a significant process. It is possible that SR activity in these sediments corresponds to fluid flux variations (i.e. SR occurs when sulfate is available at >1 mM).

Conclusions

Due to the variability of fluid flow and composition, the Gulf of Mexico hosts a spectrum of hydrocarbon seep sites, ranging from methane-dominated systems to those with high relative proportions of C₂₊ alkanes and oils. The microbial communities at these sites utilize the electron acceptor sulfate to oxidize the available hydrocarbons, although low sulfate availability (~1 mM) may limit consumption and activity in some settings. Sulfate reducing bacteria comprise a significant proportion of the phylotypes observed in the sediments, regardless of the oil, hydrocarbon or organic carbon content. The phylogenetic affiliations of the microorganisms responsible for the oxidation of non-methane hydrocarbons may vary and are unclear from this survey; future studies which utilize stable carbon isotopic analysis of lipid biomarkers may help elucidate the key players in these processes.

Acknowledgments

This work would not have been possible without the generous assistance of the LExEn 2002 and OTEGA SO-174 scientific parties. In particular, we acknowledge I. Busse, L. Hmelo, and M. Erickson for help with sediment sampling and analysis; F. Abegg, T. Schott, and A. Petersen for assistance with sediment collection and machinery operation; I. MacDonald for sharing data for site selections and for providing sediment surface pictures; and G. Bohrmann for expert leadership at sea. We thank the crews of the *R/V Seward Johnson II* and *R/F SONNE* and the pilots and crew of the *Johnson SeaLink* for their expertise in sample collection, V. Beier for assistance with molecular phylogenetic analysis, and K. Loftis for assistance with solvent-extraction hydrocarbon analysis. The U.S. National Science Foundation (grant OCE-0085549 to SBJ and Graduate Research Fellowship to BO), the Max Planck Society, and programs “Gas Hydrate in the Geosystem” (OTEGA II project) and “Geotechnology” (MUMM project) of the German Federal Ministry for Education and Research (BMBF) provided funding for this work. We thank reviewers for providing critical comments that helped improve this manuscript.

Figure Captions

Figure 3.1. Study sites and sediment types in the Gulf of Mexico. (A) Map of locations visited. Site from the LExEn 2002 cruise listed by dive number and marked with white dot; sites from the SONNE 174 2003 cruise listed by station number and indicated with black dots. Contour lines in 500 m intervals. Map created using Online Mapping Tool available at <www.aquarius.geomar.de>. (B) Photo of the sediment surface sampled at GC232, taken with a submersible-mounted Nikon® camera. (C)-(F) Photos of sediment surfaces as captured by a Nikon® camera mounted on an OFOS video sled.

Figure 3.2. Composite profiles of geochemical species and rates of microbial processes measured in sediments collected from (A) Station 87/Site GC234, (B) Station 140/Site Chapopote, (C) Station 156/Site GC185, (D) Station 161/Site GC415 and (E) Dive 4463/Site GC232 in the Gulf of Mexico. Error bars represent one standard deviation of the mean (n=3). See text for explanation of terms.

Figure 3.3. C₁₅₊ chromatograms of saturated hydrocarbons indicate the loss of distinguishable isoprenoids and alkanes in the heavily biodegraded oils in Station 140 sediments as compared to Station 87 sediments.

Figure 3.4. Concentration profiles of C₁ (methane), C₂ (ethane), C₃ (propane), iC₄ (*iso*-butane), and C₄ (*n*-butane) alkanes in sediments from the Gulf of Mexico. (A) Station 140 (*Chapopote*) core; (B) Station 156 (*GC185*) core; (C) Station 161 (*GC415*); and (D) Dive 4463 (*GC232*).

Note concentrations (in μM) are plotted on logarithmic scale; legend in panel (C) applies to all panels. Dashed lines in (D) signify that concentrations are approximate as they are averaged over 5 cm intervals.

Figure 3.5. Phylogenetic tree showing the affiliations of Gulf of Mexico 16S rRNA gene sequences to selected reference sequences of the *Deltaproteobacteria*. The tree was calculated on a subset of 174 nearly full length sequences by maximum-likelihood analysis in combination with filters, which considered only 50% conserved regions of the 16S rRNA of *Deltaproteobacteria* to exclude the influence of highly variable positions. A total of 1380 positions were used for analysis. Partial sequences (ca. 500-1000 bp: AY211737, AY211747, AY324502, AY542603, AY542618, AY542577, AY542255, AY542232, AY324495, AY324519, GoM161_Bac52 and GoM140_Bac26) have been inserted into the existing tree by parsimony criteria with global/local optimization, without allowing changes in the overall tree topology. Cloned 16S rRNA gene sequences from Gulf of Mexico sediments are shown in green (station 140), blue (station 161), and red (station 4463). The bar represents 10% estimated phylogenetic divergence.

Figure 3.6. Phylogenetic tree showing the affiliations of Gulf of Mexico 16S rRNA gene sequences to selected reference sequences of the *Archaea*. The tree was calculated on a subset of 174 nearly full length sequences by maximum-likelihood analysis in combination with filters, which considered only 50% conserved regions of the 16S rRNA of Archaea to exclude the influence of highly variable positions. A total of 1208 positions were used for analysis. Partial sequences (ca. 550-850 bp: AY542216, AY542175, AY324526, AY542625, AY542583,

AY54252, DQ521773, DQ521769, DQ521768, DQ521764, DQ521759, DQ521755-DQ521757, AY211727, AY211714, AY211710, AY211709, AY211707, AY211704, AY211703, AY211700, AY211700, AY211696, AY211691, AY211690, AY211687, AY211685) have been inserted into the existing tree by parsimony criteria with global/local optimization, without allowing changes in the overall tree topology. Cloned 16S rRNA gene sequences from Gulf of Mexico sediments are shown in green (station 140), blue (station 161), and red (station 4463). The bar represents 10% estimated phylogenetic divergence.

Table 3.1. Gulf of Mexico site and sample descriptions.

Stations	Sample Description	Site Name	Coordinates (Lat./Long.)	Water depth (m)
87	orange <i>Beggiatoa</i> spp. SOB ¹	GC234	27°44.73 / 91°13.33	552
156	white SOB, hydrate	GC185	27°46.95 / 91°30.47	546
140	oil, hydrate, carbonate nodules, disturbed during retrieval	<i>Chapopote</i>	21°54.00 / 93°26.4	2902
161	white SOB ¹ , oil, hydrate, carbonate nodules, disturbed during retrieval	GC415	27°33.48 / 90°58.86	950
4463	white and gray SOB ¹ , hydrate	GC232	27°44.48 / 91°19.04	504

1: SOB, sulfide oxidizing bacteria living in a 'mat' on the surface of the sediment

Table 3.2. Integrated rates of sulfate reduction (SR), the anaerobic oxidation of methane (AOM), methanogenesis from carbon dioxide (BiMOG) or from acetate (AceMOG), and acetate oxidation (AceOx) and estimated turnover times of the methane (from AOM), sulfate (from SR), and acetate (from AceOx) pools for hydrocarbon-rich sediments from the Gulf of Mexico.

Station	Site	Integrated rate (mmol m ⁻² d ⁻¹) ^a					Turnover time		
		SR	AOM	BiMOG	AceMOG	AceOx	CH ₄	SO ₄	Acetate
87	GC234	2.22 ± 1.1	0.19 ± 0.01	0.004 ± 0.001	0.002 ± 10 ⁻⁵	0.093 ± 0.014	5-53 d	28-2460 d	4-7 d
140	<i>Chapopote</i>	0.04 ± 0.06	0.08 ± 0.01	0.0005 ± 10 ⁻⁵	0.386 ± 0.002	0.38 ± 0.15	4.4-24.4 a	3.5-530 a	27-159 d
156	GC185	5.59 ± 4.6	16.15 ± 6.7	0.28 ± 0.07	0.001 ± 0.001	2.74 ± 0.76	5-13 d	91-2379 d	4-15 d
161	GC415	27.9 ± 14.7	10.8 ± 2.2	n.m. ^b	n.m.	n.m.	6-12 d	6-35 d	n.a. ^c
4463	GC232	10.10	4.22	n.m.	n.m.	n.m.	7-15 d	2-264 d	n.a.

a: integrated over a depth of 0-10 cm

b: n.m. not measured

c: n.a. not applicable

Table 3.3. Overview of 16S gene sequences obtained from Gulf of Mexico sediments.

Phylogenetic Group		Station 140	Station 161	Dive 4463	
Bacteria	Alphaproteobacteria	0	2	0	
	Gammaproteobacteria	2	4	2	
	Epsilonproteobacteria	2	17	2	
	Deltaproteobacteria	<i>Desulfosarcina</i> rel.	3	8	4
		SEEP-SRB1	12	2	1
		<i>Desulfobacter/Desulfotignum</i>	2	0	2
		SEEP-SRB4 (<i>Desulforhopalus</i> rel.)	0	4	0
		<i>Desulfocapsa</i> rel.	0	3	0
		SEEP-SRB3 (<i>Desulfobulbus</i> rel.)	2	13	2
		SEEP-SRB2 (<i>Desulfoarculus</i> rel.)	7	0	5
		<i>Desulfobacterium anilini</i> rel.	0	8	2
		<i>Syntrophus</i> rel.	4	4	0
		<i>Desulfiromonas</i> rel.	0	0	5
	<i>Desulfiromusa</i> rel.	0	0	4	
	<i>Bdellovibrio</i>	0	0	1	
	Fusobacteria	0	1	3	
	Sprichoeta	3	0	1	
	Bacteroidetes	2	14	11	
	JS1	33	13	2	
Gemmatimonadales	1	0	0		
Acidobacteria	0	1	0		
Nitrospina	0	1	0		
Planctomycetes	2	5	0		
Deferribacteres	1	2	0		
Firmicutes	0	0	11		
Actinobacteria	0	1	0		
Cyanobacteria	0	1	0		
Thermomicrobia	3	12	3		
OD1	1	4	2		
WS1	0	0	1		
OP5	3	0	0		
Archaea	ANME-1	42	45	52	
	ANME-2a	0	0	8	
	ANME-2b	2	0	0	
	ANME-2c	20	6	10	
	ANME-3	0	0	0	
	GoM ARC1 (ANME-nitrate related)	0	3	0	
	Methanosaeta	1	2	1	
	<i>Methanogenium/Methanofollis</i> etc rel.	0	10	0	
	<i>Methanogenium/Methanofollis</i> distantly rel.	11	19	8	
	Marine Benthic Group D	3	7	14	
Marine Benthic Group B	0	0	9		

Figure 3.1.

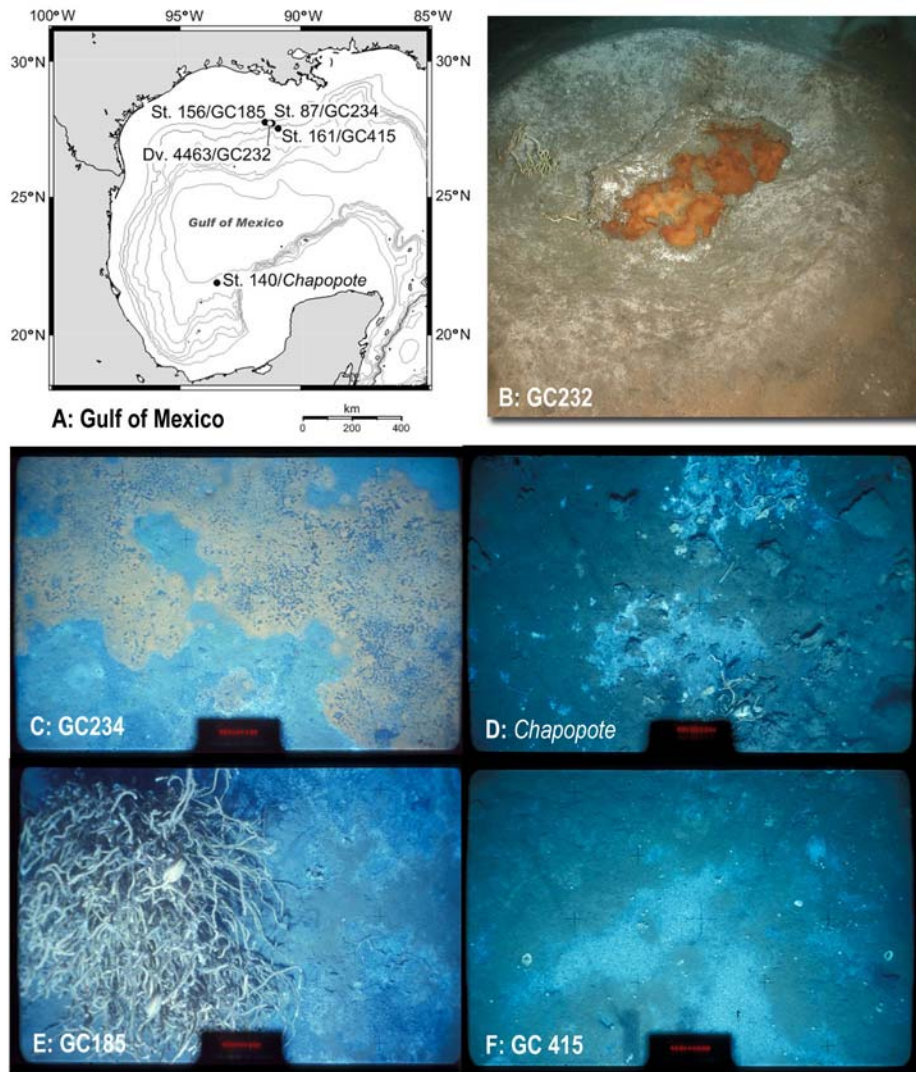
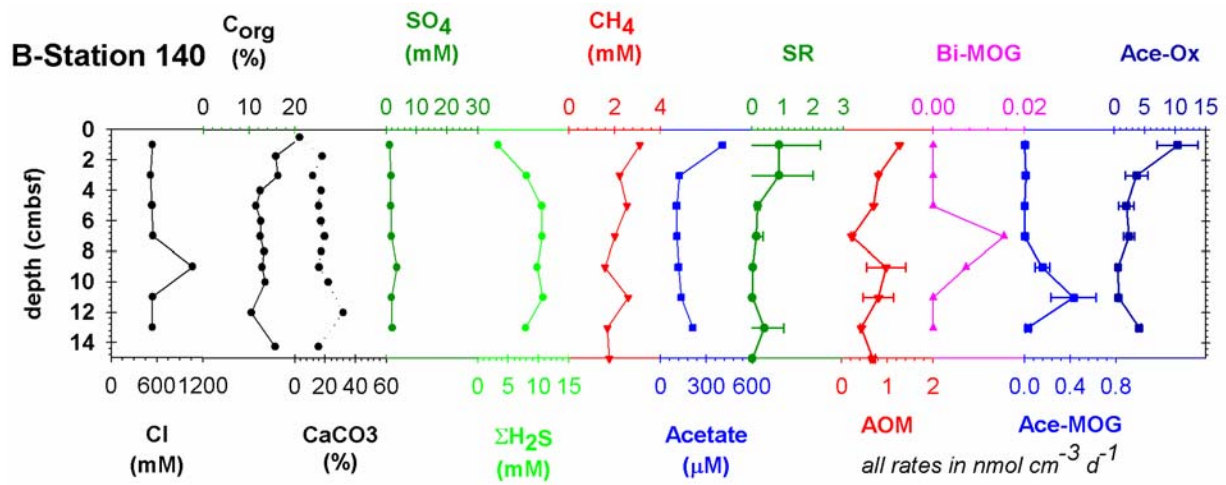
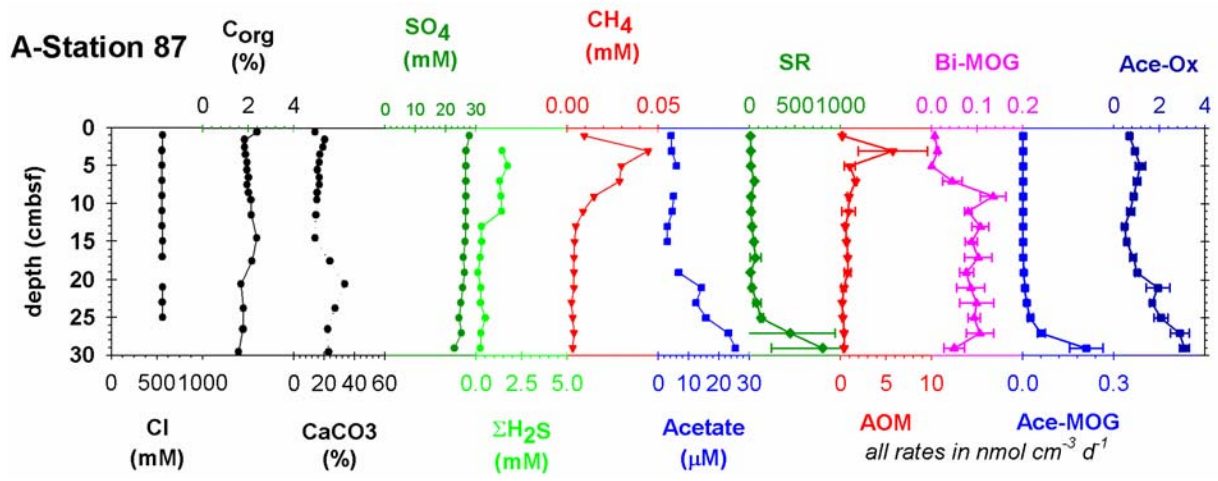


Figure 3.2.



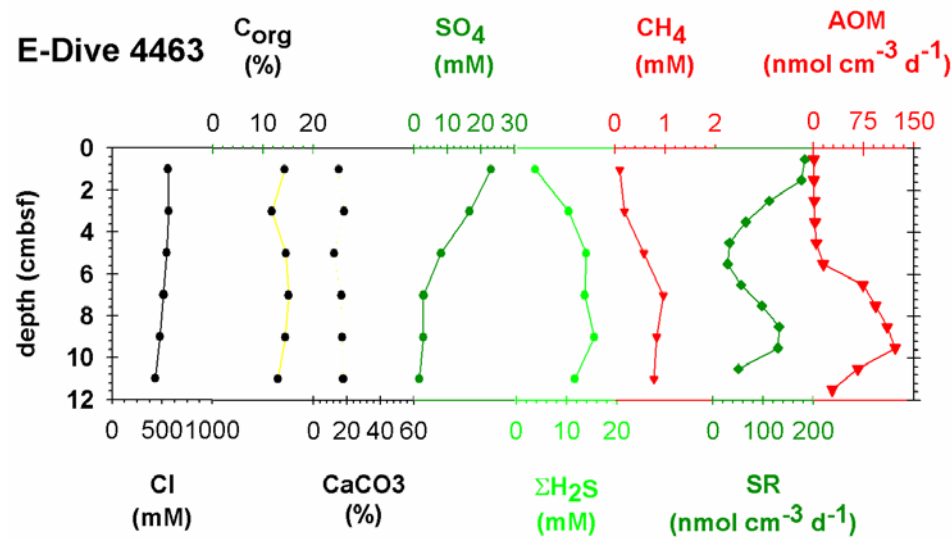
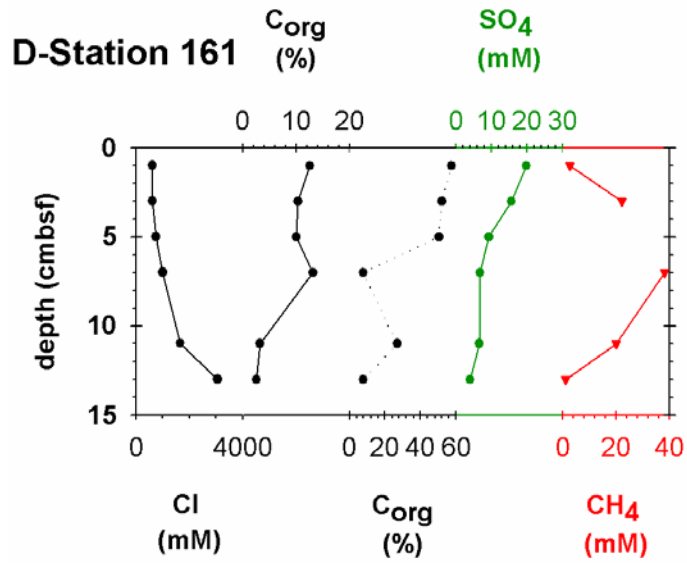
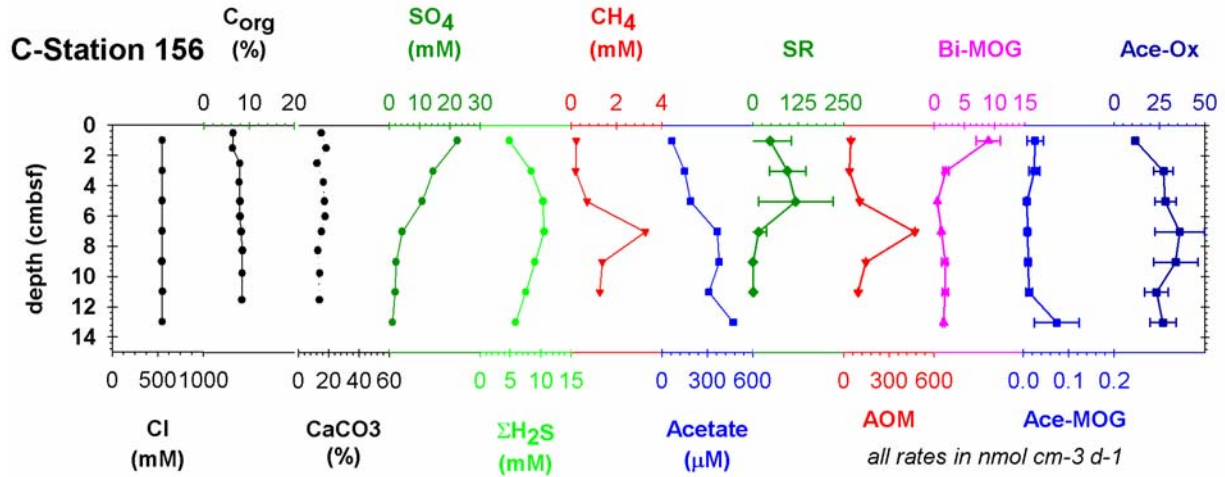


Figure 3.3.

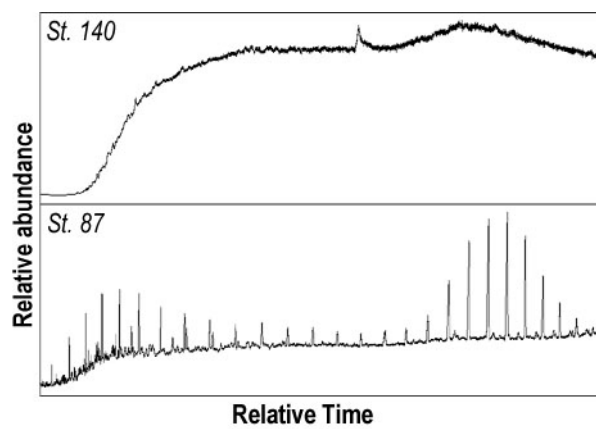


Figure 3.4.

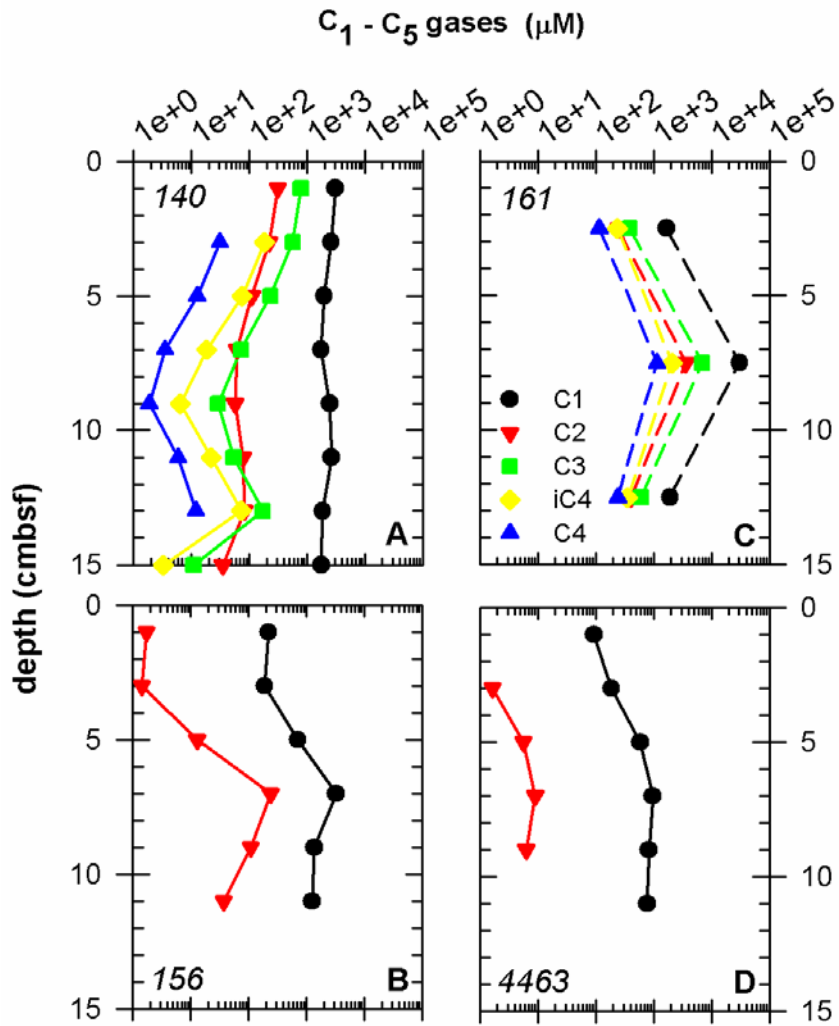


Figure 3.5.

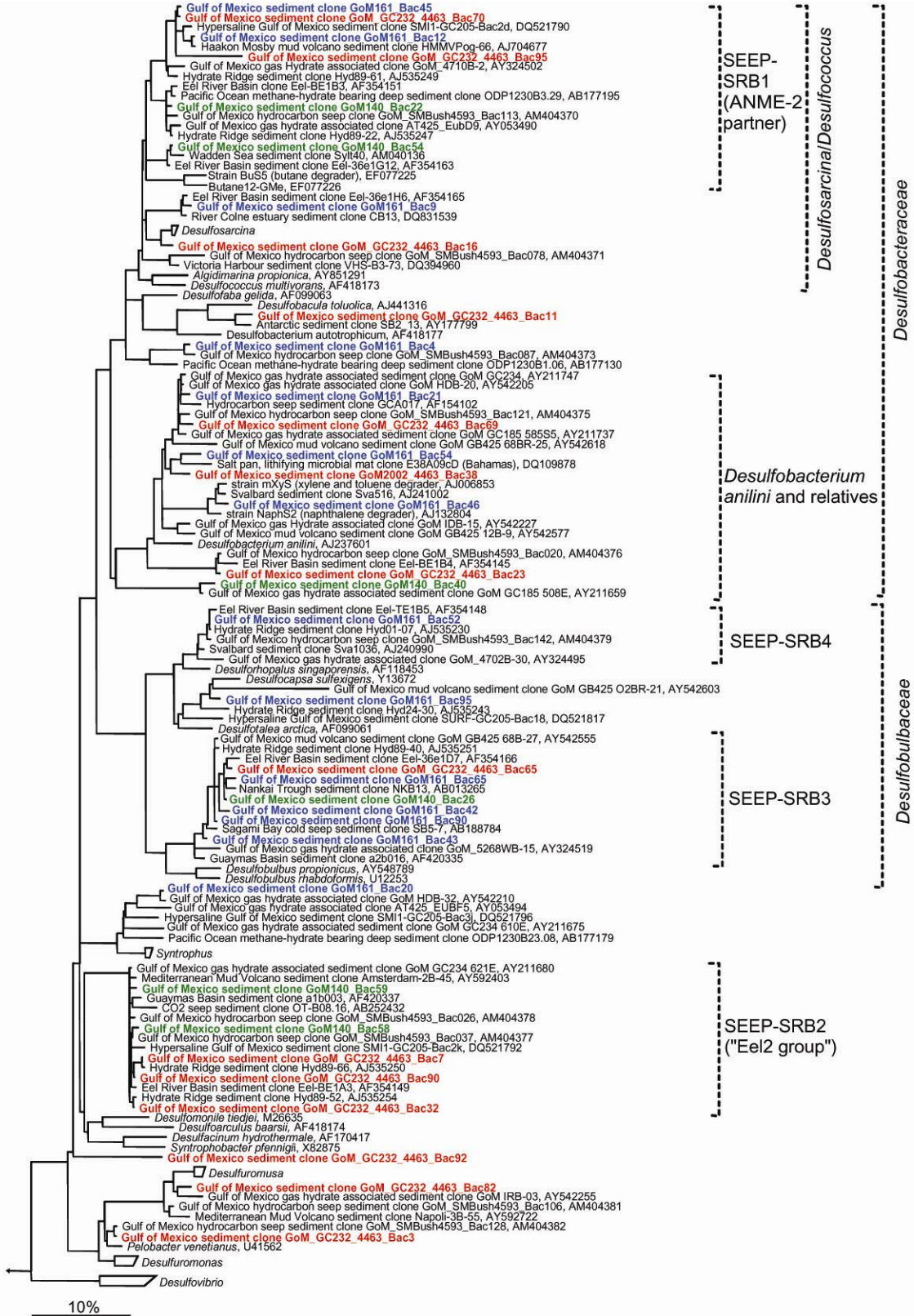
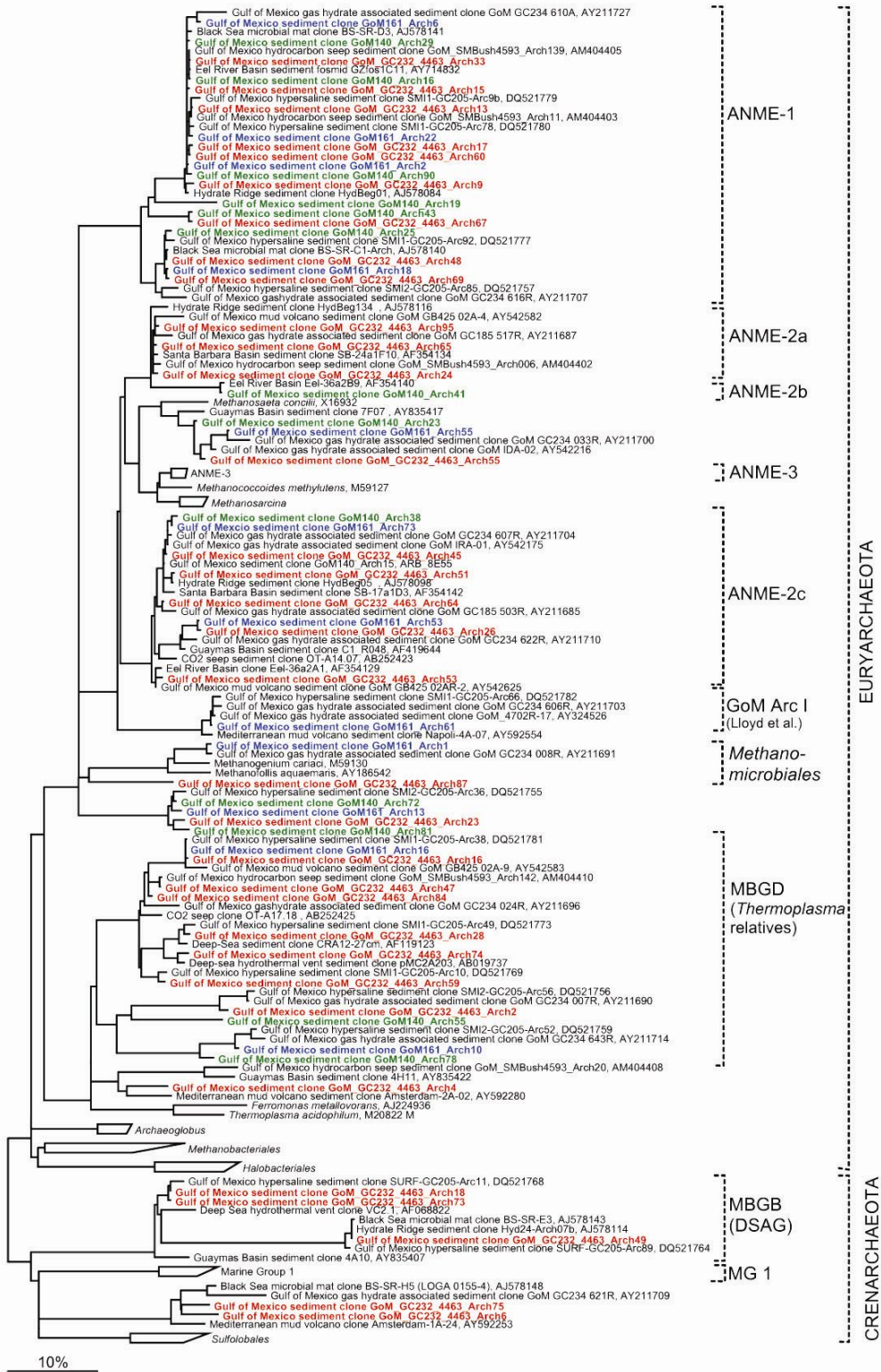


Figure 3.6.



References

- Aharon P. and Fu B. (2000) Microbial sulfate reduction rates and sulfur and oxygen isotope fractionations at oil and gas seeps in deepwater Gulf of Mexico. *Geochimica et Cosmochimica Acta* **64**, 233-246.
- Arvidson R. S., Morse J. W., and Joye S. B. (2004) The sulfur biogeochemistry of chemosynthetic cold seep communities, Gulf of Mexico, USA. *Marine Chemistry* **87**, 97-119.
- Boetius A., Ravensschlag K., Schubert C. J., Rickert D., Widdel F., Gieseke A., Amann R., Jørgensen B. B., Witte U., and Pfannkuche O. (2000) A marine microbial consortium apparently mediating anaerobic oxidation of methane. *Nature* **407**, 623-626.
- Bohrmann G., Schenck S., and participants S. C. (2004) RV SONNE 174 Cruise Report SO 174, OTEGA II: LOTUS OMEGA MUMM (ed. G. Bohrmann and S. Schenck). IFM-GEOMAR.
- Canfield D. E., Thamdrup B., and Hansen J. W. (1993) The anaerobic degradation of organic matter in Danish coastal sediments: Iron reduction, manganese reduction, and sulfate reduction. *Geochimica et Cosmochimica Acta* **57**, 3867-3883.
- Cordes E. E., Arthur M. A., Shea K., Arvidson R. S., and Fisher C. R. (2005) Modeling the mutualistic interactions between tubeworms and microbial consortia. *PLoS Biology* **3**(3), e77.
- Delong E. F. (1992) Archaea in coastal marine sediments. *Proceedings of the National Academy of Science U.S.A.* **89**, 5685-5689.
- Dhillon A., Teske A., Dillon J., Stahl D. A., and Sogin M. L. (2003) Molecular characterization of sulfate-reducing bacteria in the Guaymas Basin. *Applied and Environmental Microbiology* **69**(5), 2765-2772.
- Gelwicks J. T., Risatti J. B., and Hayes J. M. (1994) Carbon-isotope effects associated with acetoclastic methanogenesis. *Applied and Environmental Microbiology* **60**(2), 467-472.
- Hallam S. J., Girguis P. R., Preston C. M., Richardson P. M., and Delong E. F. (2003) Identification of methyl coenzyme M reductase A (*mcrA*) genes associated with methane-oxidizing archaea. *Applied and Environmental Microbiology* **69**(9), 5483-5491.
- Hallam S. J., Putnam N., Preston C. M., Detter J. C., Rokhsar D., Richardson P. M., and Delong E. F. (2004) Reverse methanogenesis: Testing the hypothesis with environmental genomics. *Science* **305**, 1457-1462.
- Heider J., Spormann A. M., Beller H. R., and Widdel F. (1999) Anaerobic bacterial metabolism of hydrocarbons. *FEMS Microbiology Reviews* **22**, 459-473.
- Hinrichs K.-U. and Boetius A. (2002) The anaerobic oxidation of methane: New insights in microbial ecology and biogeochemistry. In *Ocean Margin Systems* (ed. G. Wefer, D. Billett, D. Hebbeln, B. B. Jørgensen, M. Schlüter, and T. C. E. van Weering), pp. 457-477. Springer-Verlag.
- Jørgensen B. B. (1982) Mineralization of organic-matter in the sea bed - the role of sulfate reduction. *Nature* **296**(5868), 643-645.
- Joye S. B., Orcutt B. N., Boetius A., Montoya J. P., Schulz H., Erickson M. J., and Lugo S. K. (2004) The anaerobic oxidation of methane and sulfate reduction in sediments from at Gulf of Mexico cold seeps. *Chemical Geology* **205**(3-4), 219-238.

- Joye S. B., Samarkin V. A., Orcutt B. N., Hinrichs K.-U., MacDonald I. R., Meile C. D., Elvert M., and Montoya J. P. (in preparation) Deeply sourced brines fuel microbial activity along the seafloor in the Gulf of Mexico. *Science*.
- Kane M. D., Poulsen L. K., and Stahl D. A. (1993) Monitoring the enrichment and isolation of sulfate-reducing bacteria by using oligonucleotide hybridization probes designed from environmentally derived 16S rRNA sequences. *Applied and Environmental Microbiology* **59**, 682-686.
- Kennicutt M. C., Brooks J. M., and Denoux G. J. (1988) Leakage of deep reserved petroleum to the near surface of the Gulf of Mexico continental slope. *Marine Chemistry* **24**, 39-59.
- Kniemeyer O., Musat F., Sievert S. M., Knittel K., Wilkes H., Blumenberg M., Michaelis W., Classen A., Bolm C., Joye S. B., and Widdel F. (In press) Anaerobic oxidation of propane and butane by novel marine sulphate-reducing bacteria. *Nature*.
- Knittel K., Boetius A., Lemke A., Eilers H., Lochte K., Pfannkuche O., and Linke P. (2003) Activity, distribution, and diversity of sulfate reducers and other bacteria in sediments above gas hydrate (Cascadia Margin, Oregon). *Geomicrobiology Journal* **20**, 269-294.
- Knittel K., Lösekann T., Boetius A., Kort R., and Amann R. (2005) Diversity and Distribution of Methanotrophic Archaea at Cold Seeps. *Applied and Environmental Microbiology* **71**(1), 467-479.
- Krüger M., Treude T., Wolters H., Nauhaus K., and Boetius A. (2005) Microbial methane turnover in different marine habitats. *Palaeogeography, Palaeoclimatology, Palaeoecology* **227**, 6-17.
- Krzycki J. A., Kenealy W. R., DeNiro M. J., and Zeikus J. G. (1987) Stable isotope fractionation by *Methanosarcina barkeri* during methanogenesis from acetate, methanol, or carbon dioxide-hydrogen. *Applied and Environmental Microbiology* **53**, 2597-2599.
- Lane D. J., Pace B., Olsen G. J., Stahl D. A., Sogin M. L., and Pace N. (1985) Rapid determination of 16S ribosomal RNA sequences for phylogenetic analyses. *Proceedings of the National Academy of Science U.S.A.* **82**, 6955-6959.
- Lloyd K. G., Lapham L., and Teske A. (2006) An anaerobic-methane oxidizing community of ANME-1b archaea in hypersaline Gulf of Mexico sediments. *Applied and Environmental Microbiology* **72**(11), 7218-7230.
- Ludwig W., Strunk O., Westram R., Richter L., Meier H., Yadhukumar, Buchner A., Lai T., Steppi S., Jobb G., Förster W., Brettske I., Gerber S., Ginhart A., Gross O., Grumann S., Hermann S., Jost R., König A., Liss T., Lüssmann R., May M., Nonhoff B., Reichel B., Strehlow R., Stamatakis A., Stuckmann N., Vilbig A., Lenke M., Ludwig T., Bode A., and Schleifer K.-H. (2004) ARB: a software environment for sequence data. *Nucleic Acids Research* **32**, 1363-1371.
- MacDonald I. R. (2004) Gas hydrate in the Gulf of Mexico. In *RV SONNE Cruise Report SO174, GEOMAR Report 117* (ed. G. Bohrmann and S. Schenck), pp. 14-16. IFM-GEOMAR.
- MacDonald I. R., Bender L. C., Vardaro M., Bernard B., and Brooks J. M. (2005) Thermal and visual time-series at a seafloor gas hydrate deposit on the Gulf of Mexico slope. *Earth and Planetary Science Letters* **233**, 45-59.
- MacDonald I. R., Bohrmann G., Escobar E., Abegg F., Blanchon P., Blinova V., Bruckmann W., Drews M., Eisenhauer A., Han X., Heeschen K., Meier F., Mortera C., Naehr T., Orcutt B. N., Bernard B., Brooks J. M., and de Farago M. (2004) Asphalt volcanism and chemosynthetic life in the Campeche Knolls, Gulf of Mexico. *Science* **304**, 999-102.

- MacDonald I. R., Guinasso N. L., Ackleson S. G., Amos J., Duckworth R., Sassen R., and Brooks J. M. (1993) Natural oil slicks in the Gulf of Mexico visible from space. *Journal of Geophysical Research* **98**(C9), 16351-16364.
- MacDonald I. R., Guinasso N. L., Sassen R., Brooks J. M., Lee L., and Scott K. T. (1994) Gas hydrate that breaches the sea-floor on the continental slope of the Gulf of Mexico. *Geology* **22**, 699-702.
- MacDonald I. R., Reilly Jr. J. F., Best S. E., Venkataramaiah R., Sassen R., Amos J., and Guinasso N. L. (1996) Remote-sensing inventory of active oil seeps and chemosynthetic communities in the northern Gulf of Mexico. In *Hydrocarbon migration and its near-surface expression* (ed. D. Schumacher and M. A. Abrams), pp. 27-37. American Association of Petroleum Geologists.
- MacDonald I. R., Sager W. W., and Peccini M. B. (2003) Gas hydrate and chemosynthetic biota in mounded bathymetry at mid-slope hydrocarbon seeps: Northern Gulf of Mexico. *Marine Geology* **198**, 133-158.
- Massana R., Murray A., Preston C. M., and DeLong E. F. (1997) Vertical distribution and phylogenetic characterization of marine planktonic archaea in the Santa Barbara Channel. *Applied and Environmental Microbiology* **63**, 50-56.
- Meyerdierks A., Kube M., Lombardot T., Knittel K., Bauer M., Glöckner F. O., Reinhardt R., and Amann R. (2005) Insights into the genomes of archaea mediating the anaerobic oxidation of methane. *Environmental Microbiology* **7**(12), 1937-1951.
- Mills H. J., Hodges C., Wilson K., MacDonald I. R., and Sobecky P. A. (2003) Microbial diversity in sediments associated with surface-breaching gas hydrate mounds in the Gulf of Mexico. *FEMS Microbiology Ecology* **46**(1), 39-52.
- Mills H. J., Martinez R. J., Story S., and Sobecky P. A. (2004) Identification of members of the metabolically active microbial populations associated with *Beggiatoa* species mat communities from Gulf of Mexico cold-seep sediments. *Applied and Environmental Microbiology* **70**(9), 5447-5458.
- Muyzer G., Teske A., Wirsén C. O., and Jannasch H. W. (1995) Phylogenetic relationships of *Thiomicrospira* species and their identification in deep-sea hydrothermal vent samples by denaturing gradient gel electrophoresis of 16S rRNA fragments. *Archives of Microbiology* **164**, 165-172.
- Nauhaus K., Treude T., Boetius A., and Krüger M. (2005) Environmental regulation of the anaerobic oxidation of methane: a comparison of ANME-1 and ANME-II communities. *Environmental Microbiology* **7**(1), 98-106.
- Niemann H., Lösekann T., de Beer D., Elvert M., Nadalig T., Knittel K., Amann R., Sauter E., Schlüter M., Klages M., Foucher J.-P., and Boetius A. (2006) Novel microbial communities of the Haakon Mosby mud volcano and their role as a methane sink. *Nature* **443**, 854-858.
- Orcutt B. N., Boetius A., Elvert M., Samarkin V. A., and Joye S. B. (2005) Molecular biogeochemistry of sulfate reduction, methanogenesis and the anaerobic oxidation of methane at Gulf of Mexico cold seeps. *Geochimica et Cosmochimica Acta* **69**(17), 4267-4281.
- Orcutt B. N., Boetius A., Lugo S. K., MacDonald I. R., Samarkin V. A., and Joye S. B. (2004) Life at the edge of methane ice: microbial cycling of carbon and sulfur in Gulf of Mexico gas hydrates. *Chemical Geology* **205**(3-4), 239-251.

- Orcutt B. N., Samarkin V. A., Joye S. B., and Boetius A. (in preparation) On the relationship between methane production and consumption by anaerobic methanotrophs from cold seeps of the Gulf of Mexico.
- Orphan V. J., Hinrichs K.-U., Ussler W., III, Paull C. K., Taylor L. T., Sylva S. P., Hayes J. M., and Delong E. F. (2001) Comparative analysis of methane-oxidizing archaea and sulfate-reducing bacteria in anoxic marine sediments. *Applied and Environmental Microbiology* **67**(4), 1922-1934.
- Orphan V. J., House C. H., Hinrichs K.-U., McKeegan K. D., and Delong E. F. (2002) Multiple archaeal groups mediate methane oxidation in anoxic cold seep sediments. *Proceedings of the National Academy of Science U.S.A.* **99**, 7663-7668.
- Phelps C., Kerkhof L. J., and Young L. Y. (1998) Molecular characterization of sulfate-reducing consortium that mineralizes benzene. *FEMS Microbiology Ecology* **27**, 269-279.
- Rabus R., Nordhaus W., Ludwig W., and Widdel F. (1993) Complete oxidation of toluene under strictly anoxic conditions by a new sulfate-reducing bacterium. *Applied and Environmental Microbiology* **59**, 1444-1451.
- Raghoebarsing A. A., Pol A., van de Pas-Schoonen K. T., Smolders A. J. P., Ettwig K. F., Rijpstra W. I. C., Schouten S., Sinninghe Damste J. S., Op den Camp H. J. M., Jetten M. S. M., and Strous M. (2006) A microbial consortium couples anaerobic methane oxidation to denitrification. *Nature* **440**, 918-921.
- Rueter P., Rabus R., Wilkes H., Aeckersberg F., Rainey F. A., Jannasch H. W., and Widdel F. (2001) Anaerobic oxidation of hydrocarbons in crude oil by new types of sulfate-reducing bacteria. *Nature* **372**, 455-458.
- Sager W. W., MacDonald I. R., and Hou R. (2003) Geophysical signatures of mud mounds at hydrocarbon seeps on the Louisiana continental slope, northern Gulf of Mexico. *Marine Geology* **198**, 97-132.
- Sahling H., Rickert D., Lee R. W., Linke P., and Suess E. (2002) Macrofaunal community structure and sulfide flux at gas hydrate deposits from the Cascadia convergent margin, NE Pacific. *Marine Ecological Progress Series* **231**, 121-138.
- Sassen R., MacDonald I. R., Requejo A. G., Guinasso N. L., Kennicutt M. C., Sweet S. T., and Brooks J. M. (1994) Organic geochemistry of sediments from chemosynthetic communities, Gulf of Mexico slope. *Geo-Marine Letters* **14**, 110-119.
- Sassen R., McCabe C., Kyle J. R., and Chinn E. W. (1988) Deposition of magnetic pyrrhotite during alteration of crude oil and reduction of sulfate. *Organic Geochemistry* **14**, 381-392.
- Sassen R., Roberts H. H., Carney R., Milkov A. V., DeFreitas A., Lanoil B. D., and Zhang C. L. (2004) Free hydrocarbon gas, gas hydrate, and authigenic minerals in chemosynthetic communities of the northern Gulf of Mexico continental slope: relation to microbial processes. *Chemical Geology* **205**, 195-217.
- Shima S. and Thauer R. K. (2005) Methyl-coenzyme M reductase and the anaerobic oxidation of methane in methanotrophic Archaea. *Current Opinion in Microbiology* **8**, 643-648.
- Spormann A. M. and Widdel F. (2000) Metabolisms of alkylbenzenes, alkanes, and other hydrocarbons in anaerobic bacteria. *Biodegradation* **11**, 85-105.
- Teske A., Hinrichs K.-U., Edgecomb V., de Vera Gomez A., Kysela D., Sylva S. P., Sogin M. L., and Jannasch H. W. (2002) Microbial diversity of hydrothermal sediments in the Guaymas Basin: Evidence for anaerobic methanotrophic communities. *Applied and Environmental Microbiology* **68**(4), 1994-2007.

- Treude T. (2003) Anaerobic oxidation of methane in marine sediments. Ph.D. dissertation, University of Bremen.
- Treude T., Boetius A., Knittel K., Wallmann K., and Jørgensen B. B. (2003) Anaerobic oxidation of methane above gas hydrates at Hydrate Ridge, NE Pacific Ocean. *Marine Ecological Progress Series* **264**, 1-14.
- Treude T., Orphan V. J., Knittel K., Gieseke A., House C. H., and Boetius A. (In press) Consumption of methane and CO₂ by methanotrophic microbial mats from gas seeps of the anoxic Black Sea. *Applied and Environmental Microbiology*.
- Widdel F. and Rabus R. (2001) Anaerobic degradation of saturated and aromatic hydrocarbons. *Current Opinions in Biotechnology* **12**, 259-276.
- Zhou J., Brunns M. A., and Tiedje J. M. (1996) DNA recovery from soils of diverse composition. *Applied and Environmental Microbiology* **62**, 316-322.

CHAPTER 4

ON THE RELATIONSHIP BETWEEN METHANE PRODUCTION AND OXIDATION BY ANAEROBIC METHANOTROPHIC COMMUNITIES FROM COLD SEEPS OF THE GULF OF MEXICO¹

¹ Orcutt, B!, V. Samarkin, A. Boetius, S. Joye. In preparation for *Environmental Microbiology*.

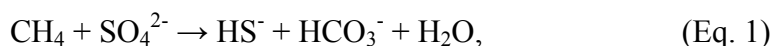
Abstract/Summary

The anaerobic oxidation of methane (AOM) in the marine subsurface is one of the most significant sinks for methane on Earth, yet our understanding of its regulation and dynamics is still incomplete. Relatively few groups of microorganisms consume methane in subsurface environments - namely the anaerobic methanotrophic archaea (ANME clades 1, 2, and 3), which are phylogenetically related to methanogenic archaea. AOM proceeds via a 'reversed' methanogenic pathway and the ANME are generally associated with sulfate reducing bacteria (SRB) as sulfate serves as the final electron acceptor for methane oxidation. Our comparative study explored the coupling of AOM with sulfate reduction (SR) and methane generation (MOG) in methanotrophic communities from Gulf of Mexico cold seep sediments that were naturally enriched with methane and other hydrocarbons. These sediments harbor a variety of ANME clades and SRB. Under an atmosphere of methane, AOM fuelled 50-100% of SR, even in sediment slurries containing petroleum-associated hydrocarbons and organic matter. In the presence of methane and sulfate, the investigated ANME communities produce methane at a small fraction (~10%) of the AOM rate. AOM, MOG and SR rates decreased significantly with decreasing concentration of methane, and in the presence of the SR inhibitor molybdate, but reacted differently to the MOG inhibitor 2-bromoethanesulfonate (BES). The addition of acetate, a possible breakdown product of petroleum *in situ* and a possible intermediate in AOM/SR syntrophy, did not suppress AOM activity, but stimulated microbial activity in oily sediment slurries.

Introduction

Biological activity is a major factor influencing methane seepage from ocean sediments. Though methanogenic archaea convert buried organic matter into methane in anoxic marine sediments, an estimated 90% (averaged globally) of methane is oxidized microbially, thus preventing the escape of methane from ocean sediments (HINRICHS and BOETIUS, 2002; REEBURGH, 1996). However, relatively little is known about this filtration process - the anaerobic oxidation of methane (AOM) - in terms of the biochemistry of the microorganisms involved and the factors influencing the efficiency of the process. Understanding the controls on AOM is critical for predicting the regulation of methane consumption in oceanic sediments.

Available data show that sulfate is the dominant oxidant for AOM in marine sediments according to the following net equation:



where methane oxidation is coupled to sulfate reduction (SR; (HOEHLER et al., 1994; NAUHAUS et al., 2002). Surprisingly, although the energy yield of this reaction under typical environmental conditions is meager (-20 to -40 kJ/mol), it appears to be shared in a syntrophic relationship between methane-consuming archaea and sulfate reducing bacteria (SRB) (BOETIUS et al., 2000; HOEHLER and ALPERIN, 1996; ORPHAN et al., 2001a; VALENTINE, 2002). The energy currency of this syntrophy remains unknown (NAUHAUS et al., 2002; SØRENSEN et al., 2001; VALENTINE, 2002). Recently discovered syntrophic consortia of methane-consuming archaea coupled with denitrifying bacteria (RAGHOEBARSING et al., 2006) suggest that syntrophy may be essential for AOM. The required spatial association of the syntrophic partners remains unclear, as some AOM-mediating ANMEs have been documented occurring as microbial mats, in attached consortia of various types (i.e. 'shell'- and 'mixed'-type), as well as without directly attached

partners (KNITTEL et al., 2005; ORCUTT et al., 2005; ORPHAN et al., 2002). Of the globally-distributed surficial sediment sites where AOM has been investigated, a limited diversity of microorganisms appear to be involved in sulfate-dependent AOM, namely the ANME-1, -2, and -3 clades of anaerobic methanotrophic archaea, which are distantly related to the *Methanosarcinales* clade of methanogenic archaea. The ANMEs are commonly associated with sulfate reducing δ -Proteobacteria related to the *Desulfosarcina*, *Desulfococcus*, and *Desulfobulbus* clades (KNITTEL et al., 2003; KNITTEL et al., 2005). The environmental parameters that may regulate the distribution of these groups are not well understood (KNITTEL et al., 2005; NAUHAUS et al., 2005; NIEMANN, 2005; ORCUTT et al., 2005).

Recent work has highlighted the close phylogenetic and functional similarities between ANMEs and methanogens and raise questions about the metabolic flexibility of ANMEs. Genes for enzymes typically associated with methanogenesis (MOG), many of which are easily reversible, were found in ANME metagenomic libraries (CHISTOSERDOVA et al., 2005; HALLAM et al., 2004; MEYERDIERKS et al., 2005). There is significant evidence that a modified form of methyl-coenzyme M reductase (*mcr*) – the final enzyme used by methanogens to produce methane - catalyzes the first step of the AOM reaction in ANMEs (KRÜGER et al., 2003; MEYERDIERKS et al., 2005; SHIMA and THAUER, 2005). Structural modifications of this *mcr* protein may overcome mechanistic inhibitions to allow for the activation of methane (SHIMA and THAUER, 2005). The modified *mcr* protein extracted from Black Sea microbial mats, which are enriched in ANME-1, performs MOG at 10% of the rate of AOM (KRÜGER et al., 2003; SHIMA and THAUER, 2005). This same ratio of rates of MOG to AOM was observed in sediments collected from a Gulf of Mexico cold seep (ORCUTT et al., 2005) and in *in vitro* ¹⁴C-radiotracer experiments with Black Sea microbial mats (TREUDE et al., In press) while a higher ratio (30%)

in Black Sea mats was interpreted based on the carbon isotopic composition of methane and bicarbonate (SEIFERT et al., 2006). Whether ANMEs mediate MOG for energy generation *in situ*, perhaps reversing the enzymatic pathway based on environmental cues, remains to be determined.

Attempts to isolate the microorganisms responsible for sulfate-dependent AOM have not been successful; thus, understanding the functioning of AOM and its coupling with other processes must rely on *in vitro* experiments with sediments and materials which are naturally enriched in methane cycling microbes. In this study, sediment from different methane-rich habitats that varied in water depth, methane flux, and availability of other carbon sources (i.e. oil) were collected and used for enrichment experiments to systematically investigate the coupling and interactions between AOM, SR and MOG in relation to various stimuli and inhibitors. These experiments allow us to address the following questions: (1) What is the relationship between AOM and MOG in methanotrophic sediments? and (2) Does the presence of alternate carbon substrates such as acetate or non-methane hydrocarbons decouple AOM and SR?

Materials and Methods

Study Sites and Sample Collection

Sediment samples used for these experiments were collected in October/November 2003 during cruise SO-174 aboard the *R.V. SONNE* in the Gulf of Mexico (GOM; Fig. 4.1) as described elsewhere (ORCUTT et al., In preparation). A brief description of the sites and cores retrieved is given in Table 4.1. Detailed geochemical descriptions of these sites are published

elsewhere (BOHRMANN et al., 2004; MACDONALD et al., 2004; ORCUTT et al., In preparation). Following recovery on deck, sediment cores were transferred to a 4 °C cold room and processed within a few hours. After collecting samples for geochemistry and other analyses, the remaining sediment was transferred under a stream of Argon gas via a metal spatula into 250 – 1000 ml glass bottles; bottles were then closed with butyl rubber stoppers and an open-hole screw cap. Samples were stored at 4 °C until further processing at the UGA laboratory.

Slurry Preparation and Sampling

To examine the impact of a variety of compounds on the rates and coupling of AOM, SR, and MOG, sediments from a variety of cold seep sites were slurried and amended with specific compounds. Three experiments were conducted: (1) comparison of rates in slurries amended with methane, methane plus acetate, or methane plus molybdate (molybdate is a specific inhibitor of sulfate reduction; (OREMLAND and CAPONE, 1988)) using sediment from all four sites; (2) comparison of rates in slurries amended with varying concentrations of methane using sediment from the shallow gas hydrate sites; and (3) comparison of rates in slurries incubated with or without added hydrogen and inhibitors (OREMLAND and CAPONE, 1988) of either SR (molybdate) or MOG (2-bromoethanesulfonate, BES) using sediment from a shallow gas hydrate site.

Slurries were generated in an anaerobic chamber (5% H₂/95% N₂ atmosphere, COY Labs) by mixing 1 volume of sediment with 3-4 volumes of anoxic artificial seawater media in 100 ml glass bottles. The anoxic media was prepared using sterile techniques and contained major sea salts with sulfate (28 mM), bicarbonate (30 mM), ammonium (5 mM), phosphate (1.5 mM), trace elements, vitamins, and sulfide (0.5-1 mM) (NAUHAUS et al., 2002; WIDDEL and

BAK, 1992). After mixing, appropriate slurries were amended with specific compounds by addition of a small volume of an anaerobic stock solution to achieve the following initial concentrations: sodium acetate, 50 μM ; 2-bromoethanesulfonate (BES), 5 mM; or sodium molybdate (Moly), 28 mM. Bottles were sealed with Teflon[®]-lined rubber stoppers and an open-hole screw cap and removed from the anaerobic chamber. Subsequently, the headspace of all bottles was purged by insertion of one 25G 5/8" sterile needle attached to a gas line and a similar needle for venting overpressure for 30 minutes with either N₂, CH₄, or a mixture of 5% H₂/95% N₂ depending on the treatment. A pure CH₄ headspace resulted in a porewater CH₄ concentration of 1.2 mM at the beginning of the experiments. For treatments that required a mixture of CH₄ and other gases, appropriate volumes of the headspace were replaced by some fraction of pure CH₄ gas. Bottles were then incubated inverted for several weeks (Table 4.1) in a 9 °C incubator with continuous shaking (60 rpm) with inversion every few days to resuspend sediment. No media exchange or methane replenishment occurred during the course of the incubation. The production of sulfide during this time period did not exceed a final concentration of 10 mM (data not shown), and is therefore not thought to interfere with the processes examined here (NAUHAUS et al., 2002).

Following incubation, bottles were returned to the anaerobic chamber for subsampling. After mixing, each individual bottle was opened and immediately sampled with a sterile 10 ml plastic syringe fitted with a 10 cm length of sterile plastic tubing. For methane concentration analysis, 2 ml of the slurry was transferred to a 6 ml glass headspace vial containing 2 ml of 1M NaOH solution; the vial was immediately sealed with a butyl rubber stopper and crimp seal. 1 ml of slurry was aliquoted to a sterile 15 ml plastic centrifuge tube for FISH preservation. The remaining slurry was transferred into a sterile 15 ml plastic centrifuge tube for subsequent

porewater extraction and analysis. Sediment porosity and density averaged 0.6 and 1.2 g cm⁻³, respectively, in the mixed sediments (data not shown).

Using the same sampling syringe, additional slurry was transferred in 2 ml aliquots to prepared reaction vessels for subsequent radiotracer injection for activity measurements using previously described techniques (ORCUTT et al., 2005). Briefly, reaction vessels consisted of cut-end 20 ml glass Hungate tubes closed at one end with a rubber stopper and open-hole screw cap and at the other by insertion of a rubber plunger. The slurry was introduced into reaction vessels via the sampling syringe and reaction vessels were subsequently closed without air bubbles. From each treatment, replicate samples (n=4; 3 for experimental, 1 for killed control) were collected for each analysis in the following order – AOM, SR, MOG.

After sampling, reaction vessels were removed from the anaerobic chamber and transferred to an 8°C incubator until further manipulation; geochemical samples were transferred to a 4°C refrigerator until further handling. Samples for FISH were mixed with 3x volumes of a buffered (1xPBS) 3.7% formalin solution and fixed for 1 hour at 4°C. Following fixation, samples were centrifuged at 4500 rpm for 20 minutes at 4°C, washed twice with 1xPBS, and subsequently stored in 2 ml 1:1 1xPBS:ethanol at -20°C. Samples for porewater analyses were centrifuged at 4500 rpm at 4°C for 15 minutes, supernatant was poured into a 10 ml plastic syringe fitted with a 0.2 µm syringe filter and filtered into a glass vial. Aliquots of the filtered porewater were transferred immediately to prepared 4 ml glass vials for the following analyses. Samples for anion (sulfate and chloride) concentration were mixed with 0.01% [v/v] concentrated HNO₃. Samples for sulfide analysis were fixed 1:1 [v/v] with 20% [w/v] zinc acetate solution. Vials for dissolved inorganic carbon (DIC) analysis were completely filled to reduce the possibility of gas flux in or out of the headspace before analysis (within 24 hours).

Analytical procedures and instrumentation for these geochemical analyses have been described previously (ORCUTT et al., 2005).

Microbial Activity Measurements

To measure AOM, SR and MOG rates, turnover of radiotracer compounds was evaluated in comparison to killed controls, which were fixed (see below) prior to isotope injection. For AOM, 100 μl of $^{14}\text{CH}_4$ dissolved in anoxic sterile milliQTM water (~ 15 nCi) was injected into each sample of the quadruplicate sets. SR samples were injected with 100 μl (~ 10 μCi) $\text{Na}^{35}\text{SO}_4$ dissolved in anoxic sterile milliQ water. Finally, samples for MOG analysis were injected with 100 μl (~ 5 μCi) $\text{NaH}^{14}\text{CO}_3$ dissolved in anoxic sterile milliQ water. Following isotope addition, reaction vessels were stored inverted in an 8°C incubator for 24 hours with gentle inversion for mixing every 2-4 hours until termination of the reactions by injection of fixative solutions. For AOM and MOG, samples were fixed by injecting 2 ml 2M NaOH solution directly into the reaction vessel followed by thorough mixing. For SR, samples were killed by injecting 5 ml 20% [w/v] zinc acetate solution followed by thorough mixing. Subsequent measurement of the activities of the various product and reactant pools in the radiotracer experiments and calculation of rates followed previous methods (ORCUTT et al., 2005). Analyses were done in triplicate; rates are presented as the mean of the samples \pm one standard deviation of the mean ($n=3$). All rates were normalized to the sediment volume of the slurry and are reported as $\text{nmol} (\text{CH}_4 \text{ or } \text{SO}_4^{2-}) \text{ cm}^{-3} \text{ d}^{-1}$.

Microbial community structure

The microbial community structure in the various slurry experiments was evaluated using techniques that target 16S rRNA. Some of the sediment contained significant quantities of oil, which inhibited detection of cells stained using mono-labeled fluorescence *in situ* hybridization probes (ORCUTT et al., 2005). Thus, signal-amplifying catalyzed reporter deposition fluorescence *in situ* hybridization (CARD-FISH) techniques were employed to determine the abundance and associations of microorganisms (PERNTHALER et al., 2002). Hybridization and cell counting procedures followed previous methods (ORCUTT et al., 2005) with the addition of a permeabilization treatment in proteinase K solution (incubation in 0.01 % [w/v] proteinase K, 0.1M Tris-HCl, 0.05M EDTA at 37°C for 1 hr followed by washing with phosphate buffered saline) to target archaeal cell walls (TEIRA et al., 2004). The CARD FISH probes used here included ANME1-350 (ORPHAN et al., 2001b) for the ANME1 clade of *Euryarchaeota* (50% formamide (FA) in hybridization buffer), EelMSX932 (BOETIUS et al., 2000) for the ANME2 clade of *Euryarchaeota* (50% FA), and DSS658 (MANZ et al., 1998) for the *Desulfosarcina* spp./*Desulfococcus* spp./*Desulfofrigus* spp./*Desulfofaba* spp. clades of sulfate reducing δ -Proteobacteria (55% FA).

Results

Community composition

The distribution of ANMEs and certain SRB groups were quantified using CARD-FISH (Table 4.2). Neither the community composition nor abundance of specific microbial groups as measured by CARD-FISH changed significantly in any of the treatments in these experiments (data not shown). Station 87 sediments contained a relatively low quantity (<10% of total cells)

of small (average 3 μm diameter) shell-type ANME2/DSS consortia as well as populations of ANME-1 rods (~20%) and free-living DSS cells. The ANME-1 rods typically occurred as double rod chains, although occasionally chains of 4 or more rods were also observed. ANME-1 rods were also abundant (~20%) in Station 140 sediments; very few small mixed consortia of ANME2/DSS were observed. Station 156 sediments contained abundant shell- and mixed-type consortia of ANME2/DSS ranging in size from 3 μm to >15 μm outer diameter; ANME-1 were not abundant in Station 156 sediment. Station 161 sediments were comprised of roughly 20% ANME-1 rods and small rod chains; a few small ANME2/DSS aggregates were also visible encased in a thick organic matrix with entrained oil.

Experiment 1 – Stations 87, 140, 156 and 161

Sediments originating from shallow gas hydrate sites (Stations 87 and 156) exhibited the highest potential rates of SR, AOM and MOG (Fig. 4.2). Sediment collected near surface breaching, oil-laden gas hydrate (Station 156) had significant rates ($70 \pm 8 \text{ nmol cm}^{-3} \text{ d}^{-1}$) of SR in the methane-free control; however, SR rates increased significantly when amended with methane or methane plus acetate (398 ± 33 and $651 \pm 37 \text{ nmol cm}^{-3} \text{ d}^{-1}$, respectively). In contrast, sediment from another gas hydrate site (Station 87) had low rates of SR ($9 \pm 2 \text{ nmol cm}^{-3} \text{ d}^{-1}$) in the methane-free control but again rates increased significantly when amended with methane or methane plus acetate (212 ± 33 and $392 \pm 53 \text{ nmol cm}^{-3} \text{ d}^{-1}$, respectively). The ratio of methane-dependent SR to AOM varied between 0.8-1.2 in the methane-only treatments. SR was completely inhibited by the addition of molybdate. AOM was not observed in methane-free controls but rates were substantial in the presence of methane or methane plus acetate ($265 \pm 33 \text{ nmol cm}^{-3} \text{ d}^{-1}$ with methane; $318 \pm 45 \text{ nmol cm}^{-3} \text{ d}^{-1}$ with methane and acetate; range of stations

156 and 87). Addition of molybdate inhibited >90% of AOM in slurries of stations 156 and 87. Addition of acetate to the shallow gas hydrate sediments with methane significantly increased SR but not AOM, indicating that the acetate had fueled an AOM-independent fraction of the SRB community. MOG rates in the shallow gas hydrate sediments were negligible in the control treatments but reached 20 ± 3 to 28 ± 4 $\text{nmol cm}^{-3} \text{d}^{-1}$, respectively, in methane and methane plus acetate amended treatments. Hence, MOG was roughly 10% of AOM in the carbon addition experiments. Rates of MOG were lower in the molybdate treatments by 70-80% but in these treatments MOG rates accounted for 40-50% of AOM rates.

Rates of SR in sediment from the deeper gas hydrate site (Station 161; 113 ± 26 to 142 ± 30 $\text{nmol cm}^{-3} \text{d}^{-1}$) were comparable to shallow gas hydrate sediments but were lower in sediments collected from the asphalt volcano site (Station 140; 11 ± 0.1 to 21 ± 4 $\text{nmol cm}^{-3} \text{d}^{-1}$ Fig. 4.2). Both AOM (13 ± 5 to 36 ± 11 $\text{nmol cm}^{-3} \text{d}^{-1}$) and MOG (0.9 ± 0.1 to 2.6 ± 0.2 $\text{nmol cm}^{-3} \text{d}^{-1}$) rates in these samples were lower than those measured in the shallow gas hydrate sites. Addition of acetate to these sediments did not significantly increase the rates of SR although both AOM and MOG rates were stimulated significantly by acetate (i.e. rates roughly doubled in the presence of acetate). Rates of MOG were 15-19% of AOM rates in sediments from the deeper hydrate site and 7% in sediment from the asphalt volcano. In asphalt volcano sediments (station 140) in the presence of methane, rates of AOM were consistently higher than SR, especially when acetate was added ($15 \pm 1\%$ to $60 \pm 30\%$ greater AOM than SR).

Experiment 2 – Station 156

The second experiment examined the effects of varied methane concentrations on microbial activity rates in shallow gas hydrate sediment (Station 156, Fig 3). Rates of SR, AOM

and MOG showed a positive linear trend with increasing methane concentration from 50-700 μM CH_4 . As in Experiment 1, SR occurred in sediments from Station 156 without the addition of methane. Subtracting this non-methane-based SR value ($70 \pm 8 \text{ nmol cm}^{-3} \text{ d}^{-1}$) from the carbon addition values gave SR rates comparable to the rates of AOM, with a ratio of SR to AOM varying from 0.9-1.2. MOG rates in the Station 156 treatments were $\sim 10\%$ of AOM rates at higher methane concentrations, increasing to 35% when methane concentrations were less than 50 μM .

Experiment 3 – Station 87

This experiment evaluated the response of microbial activity under conditions favoring methanogenesis or methanotrophy to elucidate the role of anaerobic methanotrophs in mediating MOG. To this end, slurries of shallow gas hydrate sediment (Station 87) were amended with or without hydrogen and inhibitors of either SR (molybdate) or MOG (2-bromoethanesulfonate, BES). SR occurred in these sediments without the presence of methane and when not inhibited by molybdate (rates 35 ± 10 to $38 \pm 4 \text{ nmol cm}^{-3} \text{ d}^{-1}$). Rates of SR significantly increased more than two-fold (89 ± 9 to $103 \pm 14 \text{ nmol cm}^{-3} \text{ d}^{-1}$) when incubated with methane (Fig. 4.4). In contrast, rates of AOM and MOG were essentially zero without the presence of added methane, even though the initial environmental conditions were favorable for methanogenesis from H_2/CO_2 . Some methane was measurable in the treatments without methane addition and may reflect endogenous methane which was not completely purged from the slurry at the beginning of the experiments; thus negligible rates of AOM were measured in the treatments without added methane (Fig. 4.4). AOM rates averaged $22.5 \pm 3 \text{ nmol cm}^{-3} \text{ d}^{-1}$ in treatments with methane or with methane plus BES (an inhibitor of MOG) but decreased significantly to $3 \pm 0.2 \text{ nmol cm}^{-3} \text{ d}^{-1}$

¹ when incubated with molybdate to block SR. MOG rates averaged $0.7 \pm 0.1 \text{ nmol cm}^{-3} \text{ d}^{-1}$ in the methane and methane plus BES treatments and increased to $1.8 \pm 0.1 \text{ nmol cm}^{-3} \text{ d}^{-1}$ when SR was blocked by molybdate. Notably, MOG was not significantly inhibited by addition of BES at the concentrations used in this experiment (5 mM).

Discussion

On the Coupling of AOM and SR in the presence of other carbon substrates

Significant rates of SR were supported by non-methane carbon substrates in the absence or presence of methane in the sediment slurries investigated here (Figs. 2-4). This was observed previously in field experiments (JOYE et al., 2004; ORCUTT et al., 2005). As AOM and methane-fueled SR were occurring at a ~1:1 ratio, the presence of other hydrocarbons and organic matter apparently had no effect on methane turnover. Most likely, different types of SRB utilize the different hydrocarbons and organic matter available in the sediments (see Table 4.1 for organic carbon weight percent in original sediments). Recently, a novel sulfate-reducing bacterium that grows on butane and propane was cultivated from similar GOM sediments, supporting the finding that endemic sulfate-reducing bacteria can grow anaerobically on non-methane hydrocarbons (KNIEMEYER et al., In press). This novel strain is closely related to the *Desulfosarcina*-grouped clade which is associated with ANME communities and often found at hydrocarbon seeps (KNITTEL et al., 2003; ORPHAN et al., 2001a). In our experiments, volatile alkanes such as butane and propane would have been stripped from the slurries during initial purging, but it is possible that they were produced from oil degradation over the course of the

incubation. It is unknown which non-methane substrates fueled SR in these sediments, although slurries did contain a significant proportion of endogenous oil.

Acetate is a probable breakdown product of petroleum-derived compounds *in situ*; surveys show that concentrations of acetate in oil-laden marine sediments are relatively high (ORCUTT et al., 2005; ORCUTT et al., In preparation). Acetate has also been proposed as a possible intermediate in AOM/SR syntrophy (NAUHAUS et al., 2002; SØRENSEN et al., 2001; VALENTINE, 2002), potentially being produced by the AOM-performing partner and subsequently consumed by the SRB-partner. Previous studies with methanotrophic communities from the Hydrate Ridge cold seeps or Black Sea microbial mats indicate that acetate does not have a stimulatory affect on SR in AOM/SR communities *ex situ* (NAUHAUS et al., 2005); however the availability of acetate for the Hydrate Ridge and Black Sea communities is unknown. In sediments naturally enriched in acetate (i.e. oil-laden Gulf of Mexico sediments), could this compound have a stronger influence on AOM/SR activity?

Acetate had differential effects on microbial activity depending on the endogenous microbial community present. In samples from shallow gas hydrate sites, which contained high quantities of ANME-2, acetate stimulated SR but not AOM or MOG (Fig. 4.2). In contrast, in samples from the deeper gas hydrate site or the asphalt volcano, where ANME-1 communities were more abundant than ANME-2, acetate stimulated both AOM and MOG but not SR (Fig. 4.2). Surprisingly, in station 140 sediments with a higher proportion of ANME-1 cells, AOM exceeded rates of SR when acetate and methane were added. Acetate addition did not cause a negative effect on AOM in any of the experiments, as would be expected from an intermediate in the syntrophic interaction between methanotrophs and SRB. These findings suggest that SRB in

the ANME-2-rich oil-laden sediments can take advantage of acetate whereas the SRB in sediments richer in ANME-1 cannot.

On the coupling of AOM and MOG

In agreement with field data (ORCUTT et al., 2005) and laboratory incubation of AOM-mediating microbial mats from the Black Sea (TREUDE et al., In press), the rate of MOG in most sediment slurries amended with methane was roughly 10% of the AOM rate (Figs. 2-4). In contrast to the shallow gas hydrate sites, which contained more ANME-2 than ANME-1, the deeper gas hydrate site and the asphalt volcano had only a few small ANME-2/DSS aggregates and more ANME-1 rods. It appears that both phylogenetic groups have roughly the same potential for MOG in proportion to AOM. The inhibition of SR by molybdate had a strong effect on both AOM and MOG, causing the rates to decrease to 10 and 20%, respectively, of the non-inhibited rates. The decrease in AOM rates would be expected if AOM was linked with SR, which was directly inhibited by molybdate; the decrease in MOG could be explained if MOG was performed by the indirectly-inhibited AOM-mediating microorganisms.

AOM, MOG and SR all increased with increasing CH₄ concentration (Fig. 4.3). This indicates that methane availability is a key factor driving microbial activity in these sediments. As observed in Experiment 3, neither AOM nor MOG occurred without the presence of methane, even though environmental conditions were favorable for MOG from H₂ and CO₂ (Fig. 4.4). Thus, MOG did not occur unless AOM occurred. Similar results have been observed with anaerobic methanotrophic microbial mats from the Black Sea in *ex situ* experiments (TREUDE et al., In press). One possible explanation for this observation is that the ANMEs perform AOM, which only happens when methane is present, and that some degree of enzymatic back-reaction

of methanogen-related enzymes occurs which results in the methane production (SHIMA and THAUER, 2005). Under the conditions tested, it does not appear that ANMEs ‘switch’ their metabolic mode to perform MOG for energy generation when AOM is not possible due to methane limitation.

Based on genomic and proteomic evidence indications that ANME perform methanogenesis using modified methanogenic enzymes (HALLAM et al., 2003; HALLAM et al., 2004; KRÜGER et al., 2003; MEYERDIERKS et al., 2005; SHIMA and THAUER, 2005), both MOG and AOM should be inhibited by the addition of 2-bromoethanesulfonate, a structural analogue to coenzyme M and inhibitor of the methyl-coenzyme M reductase complex (OREMLAND and CAPONE, 1988). In enrichment experiments with sediments from other cold seep habitats, addition of 1 mM BES inhibited sulfate reduction presumably linked to AOM (NAUHAUS et al., 2005). In our experiments, neither AOM nor MOG were significantly inhibited by a 5 mM addition of BES (Fig. 4.3). It is possible that the concentration of the BES inhibitor was too low to affect the microorganisms in these sediments (OREMLAND and CAPONE, 1988), although a lower concentration was effective for other AOM-communities (NAUHAUS et al., 2005). The AOM-mediating communities in Gulf of Mexico sediments may be differentially susceptible to BES compared to those from other environments; for instance, previous work with cultured methanogens shows that CO₂-reducing methanogens require much higher concentrations of BES for inhibition than do acetate-utilizing methanogens (OREMLAND and CAPONE, 1988; ZINDER et al., 1984). Likewise, slurry experiments with sediments from methane-rich, hypersaline environments show that much higher BES concentrations were required to inhibit methanogenesis (OREMLAND et al., 1982). It is also possible that the AOM and MOG-mediating microorganisms in the Gulf of Mexico sediments are resistant to BES. Studies with cultured

methanogens show that immunity to BES can be achieved by developing cell walls which are impermeable to the compound (SMITH, 1983; SMITH and MAH, 1981).

Conclusions

AOM is one of the largest methane consuming processes on Earth, yet our understanding of the regulation and mechanics of this process is still uncertain. To evaluate and correlate variations in methane-related microbial activity with community structure, carbon substrates, and stimulation or inhibition by various compounds, a series of enrichment experiments utilizing sediments from a four methane-rich cold seep environments were conducted. In combination with other environmental surveys (ORCUTT et al., 2005; TREUDE et al., 2005) and laboratory enrichment experiments (NAUHAUS et al., 2002; NAUHAUS et al., 2005; TREUDE et al., In press), this study suggests that SR and AOM are strongly coupled, and that other carbon sources added like petroleum-associated hydrocarbons or acetate will mainly fuel other parts of the microbial community independent of methane. Furthermore we can confirm that ANME communities are regularly responsible for some degree of methane production when they perform AOM. It does not appear that ANMEs 'switch' their metabolic mode to generate energy from MOG alone, indicating that the modified methanogenic enzymes they possess are adapted for methane consumption. Enzymatic studies with mutants designed to contain the genes for the modified methanogenic pathway enzymes could help resolve how MOG occurs in ANME and if it may be attributed to an enzymatic back reaction. Further kinetic studies of enriched ANME communities cycling carbon substrates of known and controlled stable isotopic composition would help resolve whether ANME-mediated-MOG impacts the stable isotopic signature of

compounds in the environment, which may effect the interpretation of environmental isotopic surveys.

Acknowledgements

This work would not have been possible without the support of the *R/F SONNE* cruise 174 shipboard team and chief scientist Gerhard Bohrmann. Funding for this research was provided by BMBF, the German Ministry of Research and Education, within the special program “Gas Hydrate in the Geosystem” (OTEGA II project), the American Chemical Society (PRF-36834-AC2), and the National Science Foundation (Life in Extreme Environments Program, OCE-0085549 (S.B.J.) and a Graduate Research Fellowship (B.O.)). We thank Imke Busse, Matthew Erickson and Tina Treude for their unending sampling effort at sea, Katrin Knittel for phylogenetic expertise, and other thoughtful reviewers for comments on this manuscript.

Figure Captions

Figure 4.1. Study sites in the Gulf of Mexico from SO-174. Map created using the Generic Mapping Tool available at www.aquarius.geomar.de

Figure 4.2. Microbial activity of (A) sulfate reduction (note break in scale bar); B) anaerobic oxidation of methane; and (C) methanogenesis measured in experiment 1. All panels have units indicated in panel B but different scales. Error bars represent 1 standard deviation of the mean (n=3). Asterisks indicate treatment was not conducted.

Figure 4.3. Rates of microbial activity in slurried sediment from Station 156 in relation to various methane concentrations. Solid black symbols, SR; open symbols, AOM; grey symbols, MOG. SR' in top panel indicates AOM-dependent SR rates. Error bars represent one standard deviation of the mean. MOG rates presented are 10x the measured rates so that all rates are on the same scale.

Figure 4.4. Rates of microbial activity in slurries amended with hydrogen and with (right) or without (left) methane. Units of rates in all panels equivalent to middle panel values although scales vary. Error bars represent one standard deviation of the mean (n=3).

Table 4.1. Site descriptions for the Gulf of Mexico sediments used in these experiments.

Stations	Exp.	Sample Description	Site Name	Coordinates (Lat./Long.)	Water depth (m)	Incubation period (d)	OC (wt%) ¹
87	1,3	orange <i>Beggiatoa</i> spp.	GC234	27°44.73 / 91°13.33	552	68	~2
156	1,2	white SOB ² , oily hydrate	GC185	27°46.95 / 91°30.47	546	29	~8
140	1	oil, hydrate, carbonate nodules, disturbed during retrieval	<i>Chapopote</i>	21°54.00 / 93°26.4	2902	68	10-20
161	1	white mat, oil, hydrate, carbonate nodules, disturbed during retrieval	GC415	27°33.48 / 90°58.86	950	68	0-12

1: OC, organic carbon weight percent (wt%) (ORCUTT et al., In preparation)

2: SOB: Sulfide oxidizing bacteria occurring as a 'mat' on the surface of the sediment.

Table 4.2. Abundance of ANME groups in sediments in these experiments as measured by catalyzed reporter deposition fluorescence in situ hybridization (CARD-FISH) with 16S rRNA specific probes.

Station	Cell density [cells cm⁻³]	ANME-1 [%]	ANME-2 [%]
87	3.2 x 10 ⁹	22	<10
140	1.7 x 10 ⁹	21	<1
156	9.6 x 10 ⁹	<1	~30
161	1.1 x 10 ⁹	17	<1

Figure 4.1.

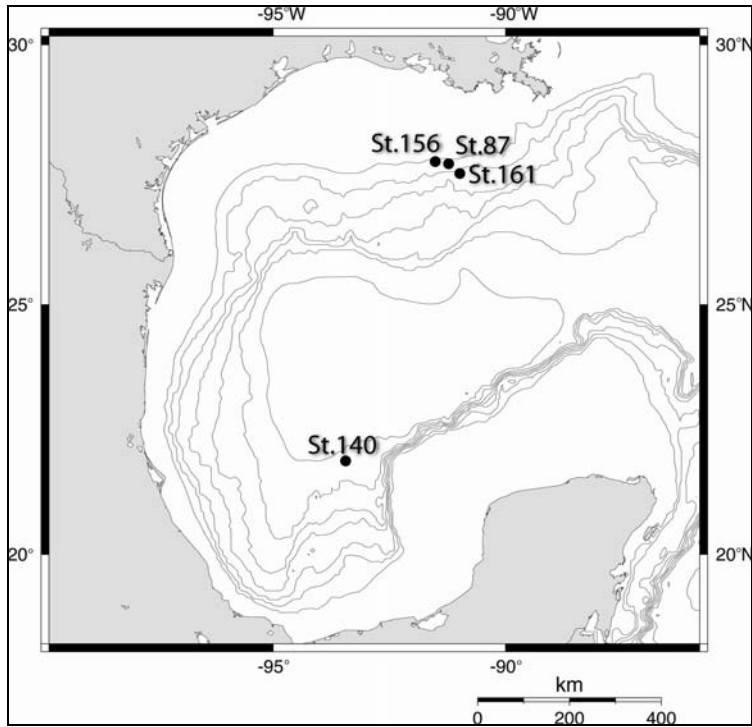


Figure 4.2.

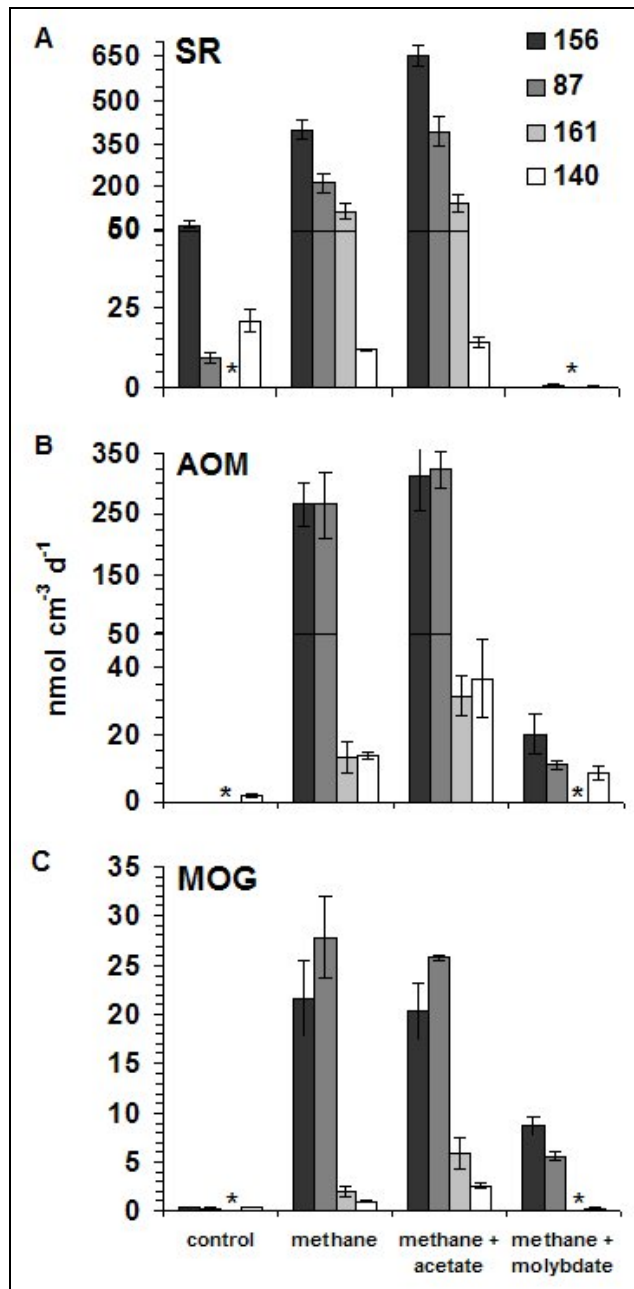


Figure 4.3.

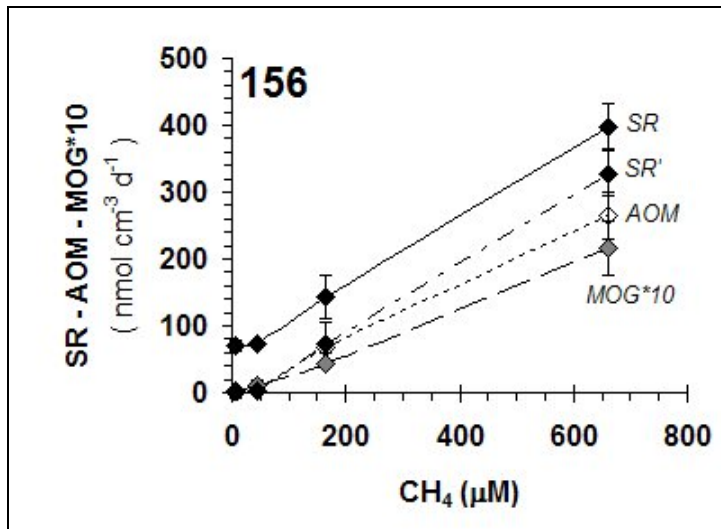
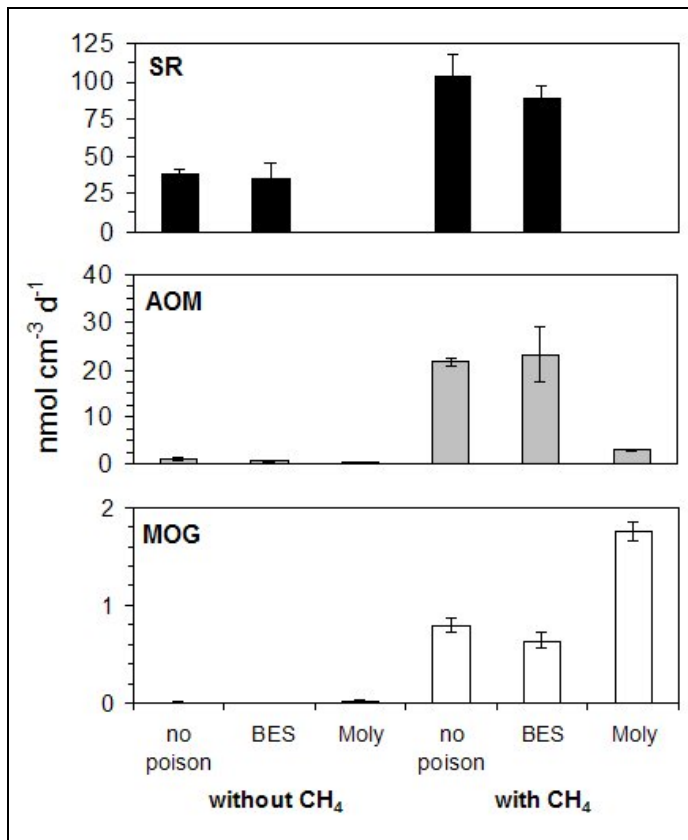


Figure 4.4.



References

- Boetius A., Ravensschlag K., Schubert C. J., Rickert D., Widdel F., Gieseke A., Amann R., Jørgensen B. B., Witte U., and Pfannkuche O. (2000) A marine microbial consortium apparently mediating anaerobic oxidation of methane. *Nature* **407**, 623-626.
- Bohrmann G., Schenck S., and participants S. C. (2004) RV SONNE 174 Cruise Report SO 174, OTEGA II: LOTUS OMEGA MUMM (ed. G. Bohrmann and S. Schenck). IFM-GEOMAR.
- Chistoserdova L., Vorholt J. A., and Lidstrom M. E. (2005) A genomic view of methane oxidation by aerobic bacteria and anaerobic archaea. *Genome Biology* **6**, 208.
- Hallam S. J., Girguis P. R., Preston C. M., Richardson P. M., and Delong E. F. (2003) Identification of methyl coenzyme M reductase A (*mcrA*) genes associated with methane-oxidizing archaea. *Applied and Environmental Microbiology* **69**(9), 5483-5491.
- Hallam S. J., Putnam N., Preston C. M., Detter J. C., Rokhsar D., Richardson P. M., and Delong E. F. (2004) Reverse methanogenesis: Testing the hypothesis with environmental genomics. *Science* **305**, 1457-1462.
- Hinrichs K.-U. and Boetius A. (2002) The anaerobic oxidation of methane: New insights in microbial ecology and biogeochemistry. In *Ocean Margin Systems* (ed. G. Wefer, D. Billett, D. Hebbeln, B. B. Jørgensen, M. Schlüter, and T. C. E. van Weering), pp. 457-477. Springer-Verlag.
- Hoehler T. M. and Alperin M. J. (1996) Anaerobic methane oxidation by methanogen-sulfate reducer consortium: geochemical evidence and biochemical considerations. In *Microbial Growth on C₁ compounds* (ed. M. E. Lidstrom and R. F. Tabita), pp. 326-333. Kluwer Academic Publishing.
- Hoehler T. M., Alperin M. J., Albert D. B., and Martens C. S. (1994) Field and laboratory studies of methane oxidation in an anoxic marine sediment - evidence for a methanogen-sulfate reducer consortium. *Global Biogeochemical Cycles* **8**, 451-463.
- Joye S. B., Orcutt B. N., Boetius A., Montoya J. P., Schulz H., Erickson M. J., and Lugo S. K. (2004) The anaerobic oxidation of methane and sulfate reduction in sediments from at Gulf of Mexico cold seeps. *Chemical Geology* **205**(3-4), 219-238.
- Kniemeyer O., Musat F., Sievert S. M., Knittel K., Wilkes H., Blumenberg M., Michaelis W., Classen A., Bolm C., Joye S. B., and Widdel F. (In press) Anaerobic oxidation of propane and butane by novel marine sulphate-reducing bacteria. *Nature*.

- Knittel K., Boetius A., Lemke A., Eilers H., Lochte K., Pfannkuche O., and Linke P. (2003) Activity, distribution, and diversity of sulfate reducers and other bacteria in sediments above gas hydrate (Cascadia Margin, Oregon). *Geomicrobiology Journal* **20**, 269-294.
- Knittel K., Lösekann T., Boetius A., Kort R., and Amann R. (2005) Diversity and Distribution of Methanotrophic Archaea at Cold Seeps. *Applied and Environmental Microbiology* **71**(1), 467-479.
- Krüger M., Meyerdiecks A., Glockner F. O., Amann R., Widdel F., Kube M., Reinhardt R., Kahnt R., Bocher R., Thauer R. K., and Shima S. (2003) A conspicuous nickel protein in microbial mats that oxidize methane anaerobically. *Nature* **426**, 878-881.
- MacDonald I. R., Bohrmann G., Escobar E., Abegg F., Blanchon P., Blinova V., Bruckmann W., Drews M., Eisenhauer A., Han X., Heeschen K., Meier F., Mortera C., Naehr T., Orcutt B. N., Bernard B., Brooks J. M., and de Farago M. (2004) Asphalt volcanism and chemosynthetic life in the Campeche Knolls, Gulf of Mexico. *Science* **304**, 999-102.
- Manz W., Eisenbrecher M., Neu T. R., and Szewzyk U. (1998) Abundance and spatial organization of gram negative sulfate-reducing bacteria in activated sludge investigated by in situ probing with specific 16S rRNA targeted oligonucleotides. *FEMS Microbiology Ecology* **25**, 43-61.
- Meyerdiecks A., Kube M., Lombardot T., Knittel K., Bauer M., Glöckner F. O., Reinhardt R., and Amann R. (2005) Insights into the genomes of archaea mediating the anaerobic oxidation of methane. *Environmental Microbiology* **7**(12), 1937-1951.
- Nauhaus K., Boetius A., Krüger M., and Widdel F. (2002) *In vitro* demonstration of anaerobic oxidation of methane coupled to sulfate reduction from a marine gas hydrate area. *Environmental Microbiology* **4**, 296-305.
- Nauhaus K., Treude T., Boetius A., and Krüger M. (2005) Environmental regulation of the anaerobic oxidation of methane a comparison of ANME-1 and ANME-II communities. *Environmental Microbiology* **7**(1), 98-106.
- Niemann H. (2005) Rates and signatures of methane turnover in sediments of continental margins. Doctoral Dissertation, University of Bremen.
- Orcutt B. N., Boetius A., Elvert M., Samarkin V. A., and Joye S. B. (2005) Molecular biogeochemistry of sulfate reduction, methanogenesis and the anaerobic oxidation of methane at Gulf of Mexico cold seeps. *Geochimica et Cosmochimica Acta* **69**(17), 4267-4281.

- Orcutt B. N., Knittel K., Samarkin V. A., Treude T., Boetius A., and Joye S. B. (In preparation) Impact of oil and higher hydrocarbons on microbial diversity, distribution and activity in Gulf of Mexico cold seep sediments.
- Oremland R. S. and Capone D. G. (1988) Use of 'specific' inhibitors in biogeochemistry and microbial ecology. *Advanced Microbial Ecology* **10**, 285-383.
- Oremland R. S., Marsh L., and Des Marais D. J. (1982) Methanogenesis in Big Soda Lake, Nevada: An alkaline, moderately hypersaline desert lake. *Applied and Environmental Microbiology* **43**, 462-468.
- Orphan V. J., Hinrichs K.-U., Ussler W., III, Paull C. K., Taylor L. T., Sylva S. P., Hayes J. M., and Delong E. F. (2001a) Comparative analysis of methane-oxidizing archaea and sulfate-reducing bacteria in anoxic marine sediments. *Applied and Environmental Microbiology* **67**(4), 1922-1934.
- Orphan V. J., House C. H., Hinrichs K.-U., McKeegan K. D., and Delong E. F. (2001b) Methane-consuming archaea revealed by directly coupled isotopic and phylogenetic analysis. *Science* **293**, 484-487.
- Orphan V. J., House C. H., Hinrichs K.-U., McKeegan K. D., and Delong E. F. (2002) Multiple archaeal groups mediate methane oxidation in anoxic cold seep sediments. *Proceedings of the National Academy of Science U.S.A.* **99**, 7663-7668.
- Pernthaler A., Pernthaler J., and Amann R. (2002) Fluorescence in situ hybridization and catalyzed reporter deposition for the identification of marine bacteria. *Applied and Environmental Microbiology* **68**(6), 3094-3101.
- Raghoebarsing A. A., Pol A., van de Pas-Schoonen K. T., Smolders A. J. P., Ettwig K. F., Rijpstra W. I. C., Schouten S., Sinninghe Damste J. S., Op den Camp H. J. M., Jetten M. S. M., and Strous M. (2006) A microbial consortium couples anaerobic methane oxidation to denitrification. *Nature* **440**, 918-921.
- Reeburgh W. S. (1996) "Soft Spots" in the global methane budget. In *Microbial Growth on C₁ Compounds* (ed. M. E. Lidstrom and R. F. Tabita), pp. 334. Kluwer Academic Publishers.
- Seifert R., Nauhaus K., Blumenberg M., Krüger M., and Michaelis W. (2006) Methane dynamics in a microbial community of the Black Sea traced by stable carbon isotopes *in vitro*. *Organic Geochemistry* **37**(10), 1411-1419.
- Shima S. and Thauer R. K. (2005) Methyl-coenzyme M reductase and the anaerobic oxidation of methane in methanotrophic Archaea. *Current Opinion in Microbiology* **8**, 643-648.

- Smith M. R. (1983) Reversal of 2-bromoethanesulfonate inhibition of methanogenesis in *Methanosarcina* sp. *Journal of Bacteriology* **156**, 516-523.
- Smith M. R. and Mah R. A. (1981) 2-Bromoethanesulfonate: A selective agent for isolating resistant *Methanosarcina* mutants. *Current Microbiology* **6**, 321-326.
- Sørensen K. B., Finster K., and Ramsing N. B. (2001) Thermodynamic and kinetic requirements in anaerobic methane oxidizing consortia exclude hydrogen, acetate, and methanol as possible electron shuttles. *Microbial Ecology* **42**, 1-10.
- Teira E., Reinthaler T., Pernthaler A., Pernthaler J., and Herndl G. J. (2004) Combining catalyzed reporter deposition-fluorescence in situ hybridization and microautoradiography to detect substrate utilization by bacteria and archaea in the deep ocean. *Applied and Environmental Microbiology* **70**(7), 4411-4414.
- Treude T., Krüger M., Boetius A., and Jørgensen B. B. (2005) Environmental control on anaerobic oxidation of methane in the gassy sediments of Eckernförde Bay (German Baltic). *Limnology and Oceanography* **50**(6), 1771-1786.
- Treude T., Orphan V. J., Knittel K., Gieseke A., House C. H., and Boetius A. (In press) Consumption of methane and CO₂ by methanotrophic microbial mats from gas seeps of the anoxic Black Sea. *Applied and Environmental Microbiology*.
- Valentine D. L. (2002) Biogeochemistry and microbial ecology of methane oxidation in anoxic environments: a review. *Antonie van Leeuwenhoek* **81**, 271-282.
- Widdel F. and Bak F. (1992) Gram-negative mesophilic sulfate-reducing bacteria. In *The Prokaryotes* (ed. A. Balows, H. G. Trüper, M. Dworkin, W. Harder, and K.-H. Schleifer), pp. 3352-3378. Springer.
- Zinder S. H., Anguish T., and Cardwell S. C. (1984) Selective inhibition by 2-bromoethanesulfonate of methanogenesis from acetate in a thermophilic anaerobic digester. *Applied and Environmental Microbiology* **47**, 1343-1345.

CHAPTER 5

LIFE AT THE EDGE OF METHANE ICE: MICROBIAL CYCLING OF CARBON AND SULFUR IN GULF OF MEXICO GAS HYDRATES¹

¹ Orcutt, B., A. A. Boetius, S.K. Lugo, I.R. MacDonald, V. Samarkin, S.B. Joye. 2004. *Chemical Geology* 205: 239-251. Reprinted here with permission from the publisher.

Abstract

The processes of methane oxidation and sulfate reduction were examined in sub-samples of gas hydrate associated materials collected along the Gulf of Mexico continental slope. Standard radiotracer techniques were used to determine rates of microbial activity in different layers of the hydrate environment, including outer sediment, interface sediment, worm-burrow sediment, interior hydrate and a mixture of hydrate and sediment. The anaerobic oxidation of methane (AOM) and sulfate reduction (SR) were observed in all hydrate samples examined and the rates of these processes showed similar spatial trends between different hydrate layers. Highest rates of both AOM and SR were observed at interface between the sediment and hydrate. AOM rates were about 3-11 $\text{nmol cm}^{-3} \text{d}^{-1}$ in worm burrow and interface sediments as compared to $<1 \text{ nmol cm}^{-3} \text{d}^{-1}$ in other hydrate material types. Rates of SR ranged from 59 - 490 $\text{nmol cm}^{-3} \text{d}^{-1}$ in worm burrow and interface sediments while rates in interior hydrate samples were an order of magnitude lower. These rates observed in hydrate materials are lower than rates from nearby methane-rich sediments at ambient temperatures. Nevertheless, our data show that active microbial populations inhabit all layers of the hydrate environment and suggest their activity may impact biogeochemical methane and sulfur cycling in this unique niche.

1. Introduction

Gas hydrates represent one of the largest and most dynamic reservoirs of organic carbon, in particular methane, on Earth (COLLETT and KUUSKRAA, 1998; KVENVOLDEN, 1993). Current estimates of the mass of carbon in global gas hydrate vary; however, the reservoir mass is probably between $10^{18} - 10^{19}$ g of carbon (COLLETT and KUUSKRAA, 1998; DICKENS, 2001; KVENVOLDEN, 1998). Data from geochemical models, paleontological analyses and stable carbon isotopes suggest that large changes in global hydrate inventories have contributed to rapid shifts in global climate in past periods of Earth history (DICKENS et al., 1995; HESSELBO et al., 2000; KENNETT et al., 2000; NORRIS and ROEHL, 1999). The largest fraction of the gas hydrate reservoir is buried beneath 200-300 m of sediment at the base of continental margins (KVENVOLDEN, 1993), where rates of methane oxidation may be presumed to be slow (HOEHLER et al., 2000). Gas hydrate deposits may also occur in the upper few meters of seafloor sediments (BROOKS, 1984; BROOKS et al., 1991; GINSBURG et al., 1999; GINSBURG et al., 1992; MACDONALD et al., 1994). In these settings, particularly when a hydrate deposit is exposed to seawater or covered by a thin drape of sediment, methane oxidation, dissolution of hydrate gases into seawater, and microbial alterations of gas hydrate would be expected to be much more active.

On a global scale the aerobic and anaerobic microbial oxidation of methane is estimated to consume 80-90% of the methane produced by natural and anthropogenic sources annually (REEBURGH, 1996; REEBURGH et al., 1993). However, rates of methane oxidation in hydrate environments are poorly documented (HINRICHS and BOETIUS, 2002). Microbial methane oxidation functions like a barrier in consuming upwardly diffusing hydrate-derived methane in the overlying sediments (HOEHLER et al., 2000) and in the overlying water column (VALENTINE et al., 2001). Methane oxidation could thus ameliorate or buffer climate impacts resulting from

slow hydrate dissociation. Rapid destabilization of hydrate may result in gas bubbling and floating of hydrates and is most likely not controlled by microbial methane oxidation. However, microbial consumption in and around hydrate affects hydrate stability, which depends not only on temperature and pressure, but also on methane concentration in the vicinity of hydrates. Sediment methane oxidation effectively sequesters hydrate carbon in the form of carbonates over longer time scales (MICHAELIS et al., 2002; SASSEN and MACDONALD, 1994) while water column oxidation may aid in sequestering methane-derived carbon in the planktonic food web as organic or inorganic carbon (KENNETT et al., 2000).

In marine sediments, microbial anaerobic oxidation of methane (AOM) and sulfate reduction (SR) proliferate near the methane-sulfate interface, where supplies of oxidant (sulfate, SO_4^{2-}) and reductant (methane, CH_4) are concurrently available. AOM and SR are hypothesized to be coupled in anoxic environments according to the following net reaction (HOEHLER et al., 1994; REEBURGH, 1980):



This coupling between AOM and SR has been documented in other methane rich sediments using enrichment and radiotracer methods (MICHAELIS et al., 2002; NAUHAUS et al., 2002).

To evaluate the activity of microorganisms in hydrates and hydrate-draping sediment, we obtained samples of intact hydrate and associated sediments and determined the magnitude and spatial distribution of AOM and SR using radiotracer methods. We hypothesized that rates of these processes would vary between different layers of the hydrate environment (outer sediment (OS), interface sediment (IS), sediment accumulated in hydrate worm burrows (WB), interior hydrate (IN), and a mixture of interface sediment and hydrate (MIX), see 2.1 Site Description and Fig. 5.1) due to geochemical and physical differences between the layers. These novel studies

indicate that spatial heterogeneity in both processes exists in the hydrate environments. Due to the presence of many other types of hydrocarbons in the hydrate environments in the Gulf of Mexico, which might also be used as microbial substrates, it is difficult to discern definitively whether AOM and SR are stoichiometrically coupled.

2. Materials and Methods

2.1. Site Description

Samples of solid hydrate and hydrate-draping sediment (Fig. 5.2) were collected during July 2001 and July 2002 from two sites (GC 234 and GC 232) along the continental slope in the northern Gulf of Mexico (see (JOYE et al., 2004) Fig. 5.1, for detailed map). Natural gas and oil continuously seep from the seafloor at these sites (MACDONALD et al., 1994) and near- or surface-breaching hydrates exist on the edge of the hydrate stability curve between 500-700m (5-7 MPa) and 7-8 °C. Gulf of Mexico hydrates occur as Structure II, being comprised of methane (70-85%) and higher alkanes (BROOKS, 1984; SASSEN et al., 1999; SASSEN and MACDONALD, 1994). Sediments around hydrates were predominantly clay-rich silts. At these sites, methane serves as the base of a complex chemosynthetic ecosystem by supporting both free-living and symbiotic bacteria (MACDONALD et al., 1989; MACDONALD et al., 1994). Hydrate deposits are often evident as prominent topographic mounds that can be several meters in height and up to 10 m in diameter (MACDONALD et al., 2002). The mounds comprise displaced sediments, as well as solid hydrate, and are colonized by chemosynthetic species of tube worms and mussels. Mats of giant sulfide-oxidizing bacteria cover exposed hydrate mounds, creating a living interface between the overlying water, nearby anoxic sediments and the solid hydrate surface. Polychaete “ice” worms (*Hesiocaeca methanicola*) create burrows in the hydrate surface and in the sediment

drape; burrows in the interior of the hydrate may subsequently fill with sediment (Fig. 5.2;(FISHER et al., 2000)).

2.2. Sample Collection

Samples of hydrate material were collected during multiple dives of the *Johnson Sea-Link* submersible operated by the *R/V Seward Johnson I* and *II* (Harbor Branch Oceanographic Institute, Fort Pierce, Florida). A hydrate “chipper” operated by the robot arm of the submersible removed contiguous sections of hydrate and the surrounding hydrate-drape sediments from hydrate mounds exposed at the seafloor. The sample material was placed into an insulated pressure-retaining hydrate recovery chamber. The hydrate chamber contained ambient bottom water. After collection, the chamber was sealed with a pressure-retaining lid equipped with a vent valve, which prevented significant over pressure within the chamber. The chamber is insulated with low-density plastic to prevent heat gain during recovery through warm surface waters; consequently, the chamber assured delivery of intact hydrate/sediment material to the surface with minimum degassing. Upon retrieval, the hydrate chamber was transferred quickly to a cold laboratory (8 °C in 2001, 4 °C in 2002) for processing.

Intact sections of hydrate and sediment material in the hydrate chamber were removed and placed in a liquid nitrogen-chilled sterile tub for sectioning with sterile instruments (Fig. 5.1). The outer 1-3 mm of material in contact with seawater in the hydrate collection chamber was carefully pared away to remove potentially contaminated material. Next, the following layers were separated using sterile instruments and were placed into separate sterile containers (150 mL I-chem[®] jars): outer sediment (OS): sediment more than a centimeter away from the hydrate surface; interface sediment (IS): sediments directly in contact with the hydrate; worm burrow sediment (WB): sediment from inside a worm burrow on the hydrate surface; interior hydrate

(IN): solid hydrate more than 5 cm from the surface that contained minimal (if any) sediment debris; and a mixture of sediment and hydrate chunks **(MIX)**: outer hydrate layer co-mingled with sediment material that was “frozen” into the hydrate matrix (Fig. 5.1). Samples from each layer were separated and transferred quickly to Ar-purged sterile glass I-chem[®] vials sealed with a Teflon-lined septa screw cap. Solid hydrate slowly sublimed in the vials at ambient surface pressure. Vial over pressure was relieved by inserting a vent needle into the septa or through sampling (see 2.3.). Samples remained at 8°C during manipulation and until subsequent processing. Results presented here represent data conducted from multiple hydrate collections at each study site.

In both years, vent gas escaping near hydrates was collected to compare the vent gas C₁-C₅ hydrocarbon composition to the hydrate C₁-C₅ hydrocarbon composition. Comparison of the molecular ratios of vent gas and solid hydrate allows evaluation of hydrate structure and may help elucidate microbial alteration of hydrate gases. Vent gas was collected into an inverted butyrate tube that was open at the bottom and sealed with a gas tight lid equipped with a sampling port. The tube, which was initially filled with water, was held over a stream of bubbles, which displaced the water and collecting into the tube. Upon surfacing of the submersible, gas samples were collected into He-purged, evacuated, crimp-sealed headspace vials.

2.3. Geochemical Measurements

To determine the molecular composition of hydrate samples, material was sectioned and stored as described above. When the hydrate sample began to sublime and degas, a vent needle was used to puncture the Teflon-lined sampling port. A gas volume of at least 200 mL vented from the jar and then a sub-sample of headspace gas was transferred from each vial into a He-flushed 60cc plastic syringe. This sub-sample was stored in replicate He-purged, evacuated 20-

mL headspace vials that were crimp-sealed with butyl rubber stoppers. Concentrations of C₁-C₅ hydrocarbons in hydrate and vent gas samples were determined on-board ship using a gas chromatograph (Shimadzu 14-A) equipped with a flame-ionization-detector. Individual gases were separated on a Haysep[®] DB column (100/120 mesh) by application of a temperature ramp. Peaks were quantified by comparison with a certified C₁-C₅ gas standard (Joye et al. this volume).

For the determination of major ions, sub-samples of hydrate material were transferred from the chilled tub into crimp-sealed, Ar-flushed headspace vials. The samples sublimed and the melt fluid was separated from particulate material by centrifugation. Supernatant was withdrawn into a sterile plastic syringe, and a filtered (0.2µm acrodisc[®]) 0.5-1.0 ml aliquot was fixed with 100µL of 50% H₃PO₄ or conc. HNO₃ in an Ar-flushed vial. Samples were stored at 4°C until analysis. Sulfate and chloride concentrations were determined by ion-chromatography (Dionex[®]) in comparison with both certified and lab standards (JOYE et al., 2004). Concentration values are reported as the average of multiple (n>3) analyses conducted on separate hydrate samples from the same site.

2.4. Bacterial Counts

Sub-samples of hydrate material were preserved by formaldehyde fixation for determination of microbial cell numbers using acridine orange direct counting (AODC, (HOBBIE et al., 1977)). The AODC method was chosen because it does not suffer from interference due to oil fluorescence, which is common in these hydrate samples, and which may have caused difficulties in cell identification in previous studies where a different method (e.g. DAPI) was used (LANOIL et al., 2001).

2.5. Methane oxidation rates

Rates of AOM in hydrate material were determined using a $^{14}\text{CH}_4$ tracer technique (JOYE et al., 1999; JOYE et al., 2004). Aliquots of material from specific hydrate layers were rapidly transferred under a stream of argon (to keep samples anoxic) from collection vials into either (1) Ar-flushed 8.5ml headspace vials crimp-sealed with butyl rubber stoppers or (2) glass tubes sealed at one end with a plunger and at the other with a rubber stopper. Hydrate material in serum vials was slurried by filling bottles with sterile filtered (0.2 μm), UHP CH_4/Ar (10/90) purged bottom water ($[\text{CH}_4] = 130 \mu\text{M}$, $[\text{SO}_4^{2-}] = 28 \text{ mM}$). Each sample set included 2 to 4 replicates of each treatment depending on amount of material available. At least one control, which was fixed immediately after isotope addition, was included with each sample set. 30-60 μL of dissolved $^{14}\text{CH}_4$ tracer (activity 1500 dpm μL^{-1} or $\sim 0.68 \text{ nCi } \mu\text{L}^{-1}$, dissolved in sterile, anoxic Milli-Q[®] water) was added to samples using a gas-tight syringe. Samples were incubated in the dark at 8°C for 24-48 hours. Experiments were terminated by replacing 1mL of the slurry volume with 1mL of anoxic 1N NaOH (to stop biological activity and fix generated $^{14}\text{CO}_2$ as bicarbonate). The displaced 1 mL of sample fluid was preserved in a 7 mL scint vial containing 1 mL anoxic 1N NaOH. All samples were stored at 4°C until analysis. For syringe incubations, experiment were terminated by transferring the sediment volume into a 20 mL glass vial containing 3 mL of 1N NaOH and sealing the vial with a Teflon-lined screw cap. The activities of $^{14}\text{CH}_4$ and $^{14}\text{CO}_2$ and the rate of AOM ($\text{nmol cm}^{-3} \text{ d}^{-1}$) were determined using previously described methods (JOYE et al., 1999; JOYE et al., 2004). Rates presented here were normalized to the original sample volume and are averages of replicate collections at each site.

2.6. Sulfate reduction rates

Sulfate reduction (SR) rates were determined using ^{35}S -techniques (CANFIELD et al., 1986; FOSSING and JØRGENSEN, 1989). In 2001, samples were slurried in the same way as AOM samples (see above). In 2002, additional samples were prepared without slurrying to evaluate SR rates at *in situ* SO_4^{2-} concentrations. Non-slurry samples were prepared in glass tubes sealed at both ends with butyl rubber stoppers. 30-60 μL of carrier-free $^{35}\text{SO}_4$ tracer (activity 88000 dpm μL^{-1} or ~ 40 nCi μL^{-1} , dissolved in sterile, anoxic Milli-Q[®] water) was added to the samples using a gas-tight syringe. Samples were incubated in the dark at 8 °C for 24-48 hours. Experiments were terminated by transferring each sample into 50ml centrifuge tubes (15 mL in 2001) containing 10 mL (7 mL in 2001) of 20% zinc acetate (ZnAc; to stop biological activity and preserve reduced ^{35}S -sulfide as Zn^{35}S). Samples were stored frozen until analysis on-shore. The radioactivity of SO_4^{2-} (the substrate) was determined by counting an aqueous sub-sample of the fixation solution after centrifugation and the radioactivity of H_2S (the product) was determined using a one-step hot chromous acid digestion. The SR rate ($\text{nmol cm}^{-3} \text{d}^{-1}$) was calculated using a published rate equation (CANFIELD et al., 1986; FOSSING and JØRGENSEN, 1989; JOYE et al., 2004) and normalized to original sample volume; values presented represent an average from replicate collections of hydrate material at a given site (as for AOM).

3. Results

3.1. Geochemistry

During the hydrate crystallization, certain gases are concentrated in the matrix resulting in differences between the source gas molecular composition and the hydrate molecular composition (Sloan 1990). As expected, ratios of hydrocarbon gases varied between vent gas and sublimed hydrate at GC232 and at GC234 (Table 5.1). Enrichment of $> C_2$ alkanes (e.g. ethane and propane) was observed at both sites, as expected for structure II hydrate. The GC232 vent gas was approximately 91% methane, whereas the GC232 hydrate was about 50% methane and a large fraction of ethane and propane. Compared to the GC232 vent gas, the GC234 vent gas contained less methane and more ethane and propane (Table 5.1). The GC234 hydrate material was similar in composition to the GC232 hydrate, however, the edge hydrate material and interior hydrate material exhibited slight differences in the percent methane (4% lower at the edge than in the interior).

Multiple analyses of hydrate and sediment material illustrated variable concentrations of major anions. Sulfate (SO_4^{2-}) and chloride (Cl^-) concentrations differed between hydrate layers (Table 5.2). The lowest SO_4^{2-} concentrations were observed in sediment-free IN (3.5 to 4 mM). The MIX samples exhibited a range of SO_4^{2-} values (5 to 9.5 mM). The WB sediment had the highest SO_4^{2-} concentration at 17.9 mM. The IS contained varying amounts of SO_4^{2-} , ranging from 5.5 to 12.4 mM. The OS averaged about 11.5 mM SO_4^{2-} . Similarly, Cl^- concentrations were lowest (~ 150 mM) in IN material and highest (~ 450 mM) in WB material. The Cl^- concentrations in the OS material averaged about 390 mM, in the MIX about 300 mM, and in the IS material from 230-400 mM. The SO_4/Cl ratio ranged between 0.02 and 0.04, which is less than the value (0.05) expected for seawater, suggesting some SO_4 consumption occurs under natural conditions.

3.2 Bacterial Numbers

In both years, hydrate-drape sediment material had higher cell counts than the interior hydrate material. Hydrate-drape material (OS, IS, and WB) contained an average of 1×10^9 cells cm^{-3} , while MIX material and IN had averages of $4 - 7 \times 10^8$ and $2 - 5 \times 10^7$ cells cm^{-3} , respectively. The hydrate-drape sediment material contained a variety of microbial morphotypes, a large fraction was rod-shaped, usually as double rods or in rod chains, similar to the morphologies described for ANME1 archaea (Orphan et al 2001, 2002; Fig. 5.3A). The morphology of interior hydrate microorganisms was dominated by such rod-shaped cells, usually occurring as double rod chains (Fig. 5.3B).

3.3. Methane oxidation rates

Anaerobic oxidation of methane was observed in all layers of hydrate but rates varied between layers (Table 5.2, Fig. 5.4). Highest AOM rates were observed in sediment material from the hydrate interface (i.e. worm burrow and interface sediment). In GC234 samples in 2001 (slurried), the IS exhibited the highest AOM rates ($11.2 \text{ nmol cm}^{-3} \text{ d}^{-1}$), an order of magnitude greater than rates observed in the other layers. Similarly, in 2002, the highest AOM rates were observed in material from the interface of the hydrate ($2.4 - 3.3 \text{ nmol cm}^{-3} \text{ d}^{-1}$ in WB and IS, respectively). Rates at the interface exceeded activity observed in the sediment-poor hydrate material (MIX and IN: 0.1 and $0.3 \text{ nmol cm}^{-3} \text{ d}^{-1}$, respectively) and in outer sediments (OS: $0.6 \text{ nmol cm}^{-3} \text{ d}^{-1}$). Hydrate samples from GC 232 displayed a similar distribution of rates: $10.7 \text{ nmol cm}^{-3} \text{ d}^{-1}$ in WB and $\leq 0.7 \text{ nmol cm}^{-3} \text{ d}^{-1}$ in MIX and IN. Significant variability in rates of AOM between replicate samples was observed in both years (Table 5.2) suggesting differences in the abundance of AOM-related microorganisms or in the cell-specific rates of microbial activity.

3.4. Sulfate reduction rates

Sulfate-reduction was observed in all hydrate sub-samples (Table 5.2, Fig. 5.4). The spatial distribution of SR was comparable to that of AOM with the highest rates occurring in hydrate-drape sediments but SR rates were usually an order of magnitude higher than AOM rates. High variability in SR rates was probably also related to variation in the abundance of sulfate reducing microorganisms in the samples. In the 2001 GC234 slurry experiments, the highest rates of SR were observed in the IS ($489.1 \text{ nmol cm}^{-3} \text{ d}^{-1}$). The OS and MIX material exhibited similar SR rates between $100 - 118 \text{ nmol cm}^{-3} \text{ d}^{-1}$ while the lowest rates were observed in the IN ($54.7 \text{ nmol cm}^{-3} \text{ d}^{-1}$). In the 2002 non-slurry experiments at both sites, the highest SR rates were observed in the hydrate-drape sediments (76 and $59 \text{ nmol cm}^{-3} \text{ d}^{-1}$ in OS and WB, respectively; Fig. 5.4) while lower rates were observed in the sediment-poor hydrate layers ($\sim 20 \text{ nmol cm}^{-3} \text{ d}^{-1}$ in MIX and $\leq 3.2 \text{ nmol cm}^{-3} \text{ d}^{-1}$ in IN).

4. Discussion

These data provide the first evidence of anaerobic oxidation of methane and sulfate reduction in gas hydrate materials and in hydrate-drape sediments (Table 5.2, Fig. 5.4). Our data clearly illustrate that active microbial populations are present in all layers of the hydrate (Fig. 5.1), particularly at the boundary between hydrate and the overlying hydrate-drape sediments. However, our data cannot distinguish whether the active microbial communities inside gas hydrate reside within the hydrate structure or within brine inclusions or sediment trapped within the hydrate lattice.

Rates of AOM and SR in hydrate-drape sediment ($0.3-11.2$ and $59 - 490 \text{ nmol cm}^{-3} \text{ d}^{-1}$, respectively) are lower than rates in associated sediments at these same sites in the Gulf (by a factor of 10 to 100, (JOYE et al., 2004)). The AOM rates in hydrate-drape sediments are

comparable to rates of AOM in other marine sediments (ALPERIN and REEBURGH, 1985; HOEHLER et al., 1994; IVERSEN and JØRGENSEN, 1985) but are lower than rates observed in methane-rich seep sediments (AHARON and FU, 2000; ARVIDSON et al., 2004; BOETIUS et al., 2000; BUSSMAN et al., 1999; JOYE et al., 2004). Hydrate-drape sediments may experience greater frequency of disturbance as nearby sediments and this might influence the accumulation of active microbial biomass at the hydrate-sediment interface. Fluctuating sediment distribution and varying geochemical conditions result from the dynamic nature of the hydrates themselves: time-lapse photographic evidence demonstrates growth and retreat of hydrates, sloughing off of draping sediment, as well as the variable distribution and activity of vacuolate sulfur bacteria and “ice worms” on the hydrate surface. However, nutrient and bioactive trace metal availability probably also play an important role in controlling microbial distribution and activity within and adjacent to gas hydrates. Understanding the environmental controls on microbial distribution and activity in hydrates and adjacent sediments requires further study.

Previously, comparison of the molecular isotopic composition of solid hydrate with that of vent gas showed isotopic enrichment of ^{13}C in hydrate-bound CH_4 , suggestive of microbial consumption of CH_4 within the hydrate (SASSEN et al., 1999). We observed depletion in the percent of CH_4 , relative to other hydrocarbons, in outer layers of the hydrate, relative to inner layers (at GC234), which could result *in situ* from CH_4 oxidation (as suggested by (SASSEN et al., 1999; SASSEN et al., 1998). Furthermore, deviation of the hydrate melt fluid from expected SO_4/Cl ratio (assuming no bias in the relative exclusion of these ions from the hydrate lattices during formation) is suggestive of the microbial consumption of SO_4^{2-} in these environments under *in situ* conditions.

Spatial patterns of CH_4 and SO_4^{2-} consumption are evident between the hydrate layers, with maximum rates of both processes occurring at the interface of sediment and hydrate (Table

5.2, Fig. 5.4). Microorganisms living at the edge of methane ice have simultaneous access to the source of dissolved CH₄ as well as to oxidants in the hydrate-drape sediment, which could enhance both AOM and SR rates. High flux rates of oxidants (SO₄²⁻) and reductants (methane, higher alkanes and oil) may result from the dissolution of hydrate and release of reductants across the hydrate boundary as well as the dynamic turnover of the oxidant pool at the hydrate surface via biological (i.e. sulfide oxidizing bacteria, “ice worms”; (FISHER et al., 1998; JOYE et al., 2004; NELSON et al., 1986; O'HARA et al., 1995)) and abiological (i.e. bubble-induced mixing; (O'HARA et al., 1995)) mixing. Microbial activity at the sediment/hydrate boundary thus creates a living interface in the hydrate ecosystem, potentially altering the flux of methane from these structures into the surrounding sediments and the over-lying water column (SUESS et al., 1999).

The normalized rates presented here (particularly the AOM rates) are likely to be conservative estimates of *in situ* rates. Our experiments were conducted at lower CH₄ concentrations (≤ 1 mM CH₄ compared to over 70 mM CH₄ under *in situ* conditions (5-7 MPa, 7 °C)) and much lower pressures (0.1 MPa) than experienced *in situ* (5-7 MPa). While slurring of sediment may increase activity, our data are nonetheless likely reflective of the general patterns of activity occurring *in situ* because the same spatial distribution of activity was observed in slurries and in whole sediment incubations. Although a similar spatial distribution of AOM and SR rates was observed in all samples, rates of SR were typically 2 to 3 orders of magnitude higher than the corresponding AOM rates (Table 5.2). In the slurry experiments, this offset can be explained in part by sulfate enrichment from the slurring process. The lack of stoichiometric (i.e., 1:1) balance between the two processes suggests that only a fraction of sulfate reduction is coupled directly to AOM. This loose coupling between SR and AOM is quite different from the efficient (1:1) coupling observed in other systems (MICHAELIS et al., 2002; NAUHAUS et al., 2002). However, in the GOM hydrocarbon basin, in addition to methane, oil and other

hydrocarbons are abundant, and these other C substrates serve as additional reductants (or substrates) to fuel sulfate reduction (HEIDER et al., 1999; JOYE et al., 2004; ZENGLER et al., 1999).

The rates of both AOM and SR measured in material from the interior hydrate exhibited significant variability in replicate samples (Table 5.2, Fig. 5.4). The most likely explanation for this variability is environmental heterogeneity. It is possible and likely that the separate samples of hydrate material collected during multiple dives were quite different with respect to each other. These differences arise from differing amounts of entrapped sediment particles or sea water, which may influence the distribution of microorganisms, the concentrations of substrates (especially) sulfate and thus may influence the measured activity. While activity of both AOM and SR are evident in material from the hydrate interior, rates of these processes on a volumetric basis are lower than those observed in the sediment-rich layers (Table 5.2, Fig. 5.4). The hydrate interior represents a very different physical and geochemical environment with observed lower biomass content than outer sediments (10^7 cells cm^{-3} in hydrate versus 10^9 cells cm^{-3} in hydrate-drape sediments). If process (AOM and SR) activities are corrected for microbial numbers per volume of material, the cell specific activities are comparable between the hydrate-drape sediments and the material from the interior hydrate. This indicates that the microorganisms residing in the interior regions hydrate have similar metabolic capabilities to microorganisms in the surrounding sediments. Microscopic evaluation of the hydrate material types revealed that microorganisms from the interior of the hydrate had similar morphologies (rod-shaped cells dominating) to microorganisms in hydrate-draping sediments (Fig. 5.3), which may suggest that these microorganisms are derived from trapped or migrating pore fluids or sediment grains.

The distribution and activity of microorganism in hydrates may be determined by similar factors that drive the distribution of microbes in sea ice. In sea ice, microbial communities are concentrated in pockets of brine fluid within the ice matrix (EICKEN, 1992). Sea ice microbial

communities may also create biofilms of “extracellular polymeric substances,” which could alter the physiochemical structure of their niche to promote continued growth (THOMAS and WHITE, 2002). Microorganisms residing within the interior hydrates may experience similar conditions and may exploit similar adaptations, e.g., focusing populations in certain regions and/or excreting mucous. Furthermore, as hydrates form, small channels or pockets of brine solution (a concentrated mixture containing salts, nutrients, and dissolved gases) may develop and sediments and their associated microbial populations, may be trapped within the frozen hydrate (BOHRMANN et al., 1998). In such zones, microbes could survive and even proliferate. The inclusion of sediment particles in the hydrate matrices may also offer interfacial oasis for microbial life. These hypothetical habitats may represent unexpected niches for novel microorganisms, although microscopic evaluation suggests that microorganisms from interior hydrate material are morphologically similar to those observed in the outer sediments. However, a difference between hydrates and other ice-structures (sea ice, glaciers, permafrost) is that hydrate ice contains an abundance of methane. This methane, if bioavailable, provides a powerful fuel for microbes and the availability of dissolved methane, oxidant and nutrients is likely higher at the interface between the hydrate and bottom sediment/water environment, making this the most microbially active portion of the hydrate environment.

The evidence of microbial activity in samples from the interior of a methane hydrate further illustrates the extreme and remote reaches of microbial life here on Earth. Further research - such as *in vitro* pressure experiments and molecular biological quantification and identification of microbial communities - in these systems is needed to evaluate the range and dynamics of microbial activity. Investigating the successful ecological strategies of hydrate-bound microbial life may lead to broader understanding of geomicrobiological interactions at life’s “extremes.” Detection of microbial life within frozen, submarine gas hydrates should

encourage continued study of life in other icy environments here on Earth (i.e. permafrost, glaciers, accretion ice; (PRISCU et al., 1999)), as these data will further our ability to evaluate such habitats as a proxies for life in ice on other planets.

Acknowledgements

We thank members of the LExEn 2001 and 2002 scientific parties for assistance on board ship, especially Matthew Erickson, who provided help with laboratory analyses. We thank the crews of the *R/V Seward Johnson I & II* and the pilots and crew of the deep submergence vehicle *Johnson Sea Link* for assistance with sample collection. Two anonymous reviewers provided valuable comments that improved our manuscript. Submersible operations support was provided by the National Undersea Research Program and the US Department of Energy. Support for this work was provided by the National Science Foundation (OCE-0085549), the American Chemical Society (PRF-36834-AC2), the German Federal Ministry for Education and Research (03G0554A) and the Max Planck Society. Additional support was provided by a Barry Goldwater scholarship and a University of Georgia recruiting fellowship (BNO) and by a sabbatical fellowship (SBJ) by the Hanse Institute for Advanced Study, Delmenhorst, Germany. This is publication number 19 of the GEOTECHNOLOGIEN program of BMBF and DFG.

Figure Captions.

Fig. 5.1. Layers of Gulf of Mexico gas hydrate used in these experiments. **(A)** Diagram depicting different layers, arrow on left indicates relative sediment content. Patterned line through diagram represents the sediment/hydrate interface, where free gas is released as the hydrate dissolves. Lower case labels indicate the location of samples described in the text. **(B)** Photo of recovered gas hydrate after outer sediment layer has been removed. Scale bar ~1 inch. **(C)** Cross-section through sample in **B**, dark areas indicate entrapped sediment and oily material. Ruler (in inches) for scale. **(D)** Photo of “MIX” layer with sediment frozen into hydrate; ruler (in cm and inches) for scale. **(E)** “Interior hydrate” sample, darker areas represent oily material. Ruler with 0.5 cm markings for scale. (Photo credits: I. R. MacDonald, 2002)

Fig. 5.2. An underwater photo of a surface-breaching hydrate. Arrows indicate worm burrows in the hydrate surface, and a *Beggiatoa* field is labeled at the lower left. (Photo credit: I. R. MacDonald, 2002)

Fig. 5.3. Microscopic images of microorganisms stained with AO from material from the (A) interface sediment, and (B) interior hydrate. Scale bars are 5 μm .

Fig. 5.4. Rates of AOM and SR in hydrate material collected from Gulf of Mexico hydrate sites in 2001 and 2002. SR rates (white columns) are plotted on the left axes; black error bars represent one standard deviation of the mean values. AOM rates (black columns) are plotted on the right axes; white error bars represent one standard deviation of the mean values. Note the differences in scale for both axes due to slurry conditions (see text). Sample types are given on

along the x-axis. **(A)** Rates determined in slurried material (see text) from GC234 in 2001; **(B)** rates from GC234 material in 2002; **(C)** rates from GC232 material in 2002. Note that SR rates in **B** and **C** were determined in non-slurried material while AOM rates were determined in slurried samples (see text).

Table 5.1. Average hydrocarbon gases (as percentages) of hydrate material and vent gas from GC232 and GC234. Mean values and standard deviations of the mean (in parentheses) are shown.

GC232			
Hydrocarbons	Vent Gas	Interior	Edge
number of samples =	3	7	3
Percentage	%	%	%
Methane (C ₁)	90.7 (0.1)	49.8 (1.5)	49.9 (5.5)
Ethane (C ₂)	5.2 (0.1)	15.9 (1.7)	18.2 (7.2)
Propane (C ₃)	1.1 (0.1)	25.1 (2.2)	22.3 (0.3)
<i>iso</i> -Butane (<i>iso</i> -C ₄)	0.1 (0.02)	6.1 (1.1)	4.7 (1.2)
Butane (C ₄)	1.4 (0.2)	2.8 (0.6)	4.5 (0.9)
Pentane (C ₅)	1.4 (0.1)	0.3 (0.3)	0.5 (0.1)

GC234			
Hydrocarbons	Vent Gas	Interior	Edge
number of samples =	5	6	4
Percentage	%	%	%
Methane (C ₁)	86.5 (0.2)	44.4 (4.7)	40.3 (1.6)
Ethane (C ₂)	6.9 (0.1)	12.1 (4.6)	9.3 (0.8)
Propane (C ₃)	4.2 (0.1)	26.8 (11.3)	36.4 (1.7)
<i>iso</i> -Butane (<i>iso</i> -C ₄)	0.6 (0.02)	8.4 (2.3)	11.2 (1.0)
Butane (C ₄)	1.5 (0.01)	2.8 (0.6)	2.3 (0.4)
Pentane (C ₅)	0.2 (0.01)	0.3 (0.1)	0.5 (0.01)

Table 5.2. Rates of AOM and SR in gas hydrate material collected from two sites in the Gulf of Mexico. Values are organized by experiment year, site and material type. Rates are expressed as an average of replicates ($n > 3$) from multiple collections of material in units of $\text{nmol cm}^{-3} \text{d}^{-1}$, standard deviation of the mean listed in parentheses. Average sulfate and chloride concentrations of original hydrate material also shown with standard deviation in parentheses.

Hydrate Sample	Code	AOM $\text{nmol cm}^{-3} \text{d}^{-1}$	SR $\text{nmol cm}^{-3} \text{d}^{-1}$	SO_4^{2-} mM	Cl^- mM
<u>GC234 in 2001</u>					
outer sediment	<i>OS</i>	0.34 (0.11)	100 (81.7)	11.0 ¹	382.9
interface sediment	<i>IS</i>	11.2 (1.9)	489 (76.2)	12.4	401.7
mixture	<i>MIX</i>	0.75 (0.42)	118 (58)	4.9	338.2
interior hydrate	<i>IN</i>	0.72 (0.66)	54.7 (36.6)	3.5	137.1
<u>GC234 in 2002</u>					
outer sediment	<i>OS</i>	0.60 (0.26)	76.2 (20.8)	12.3 (1.4)	397.2 (158.2)
interface sediment	<i>IS</i>	3.25 (1.7)	n.d. ²	5.5 (0.3)	231.1 (115.9)
worm burrow sediment	<i>WB</i>	2.43 (0.26)	n.d.	n.d.	n.d.
mixture	<i>MIX</i>	0.13 (0.09)	23.0 (1.0)	9.5 (1.0)	317.0 (111.0)
interior hydrate	<i>IN</i>	0.28 (0.26)	3.2 (4.1)	3.2 (2.1)	150.0 (142.4)
<u>GC232 in 2002</u>					
worm burrow sediment	<i>WB</i>	10.74 (0.21)	59.0 (7.8)	17.9 ³	451.4
mixture	<i>MIX</i>	0.74 (0.04)	18.8 (2.3)	6.6	285.8
interior hydrate	<i>IN</i>	0.36 (0.48)	0.6 (0.1)	4.0 (1.9)	158.5 (19.8)

¹ no replicates available for sulfate and chloride concentrations in 2001

² not determined

³ no replicates available for concentration

Fig. 5.1.

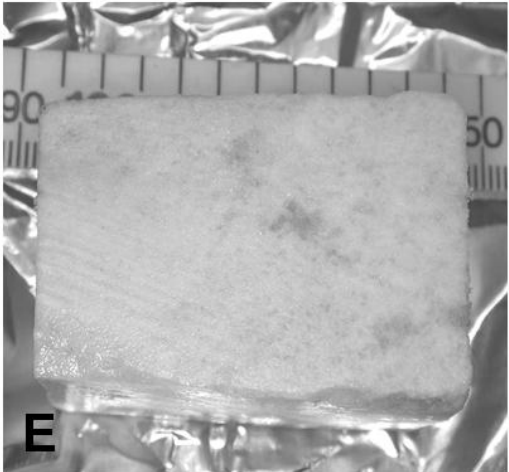
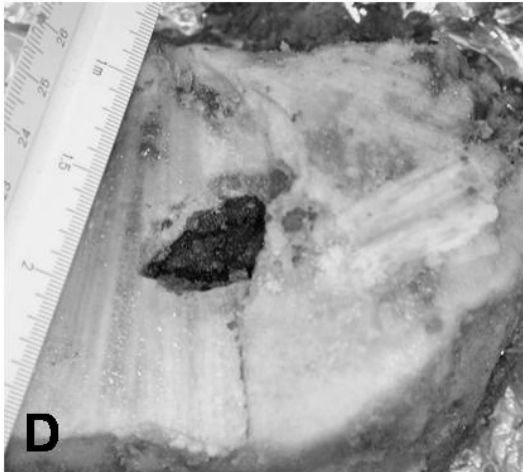
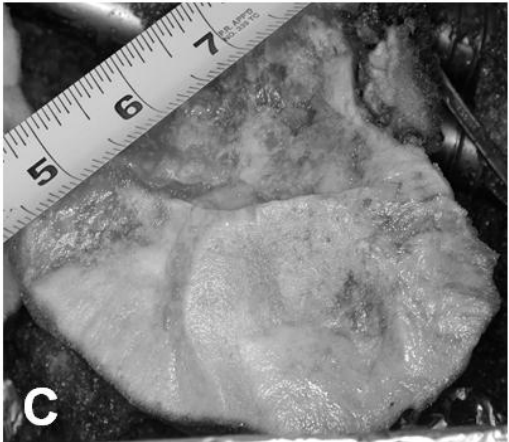
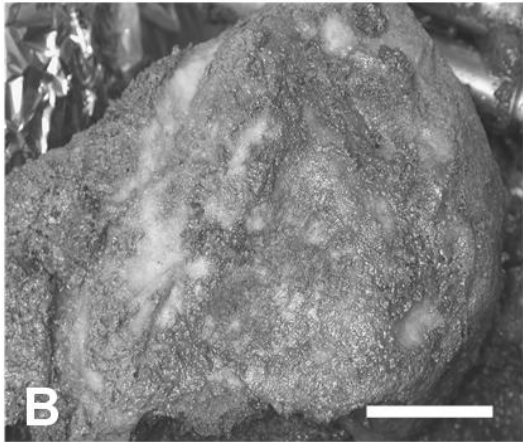
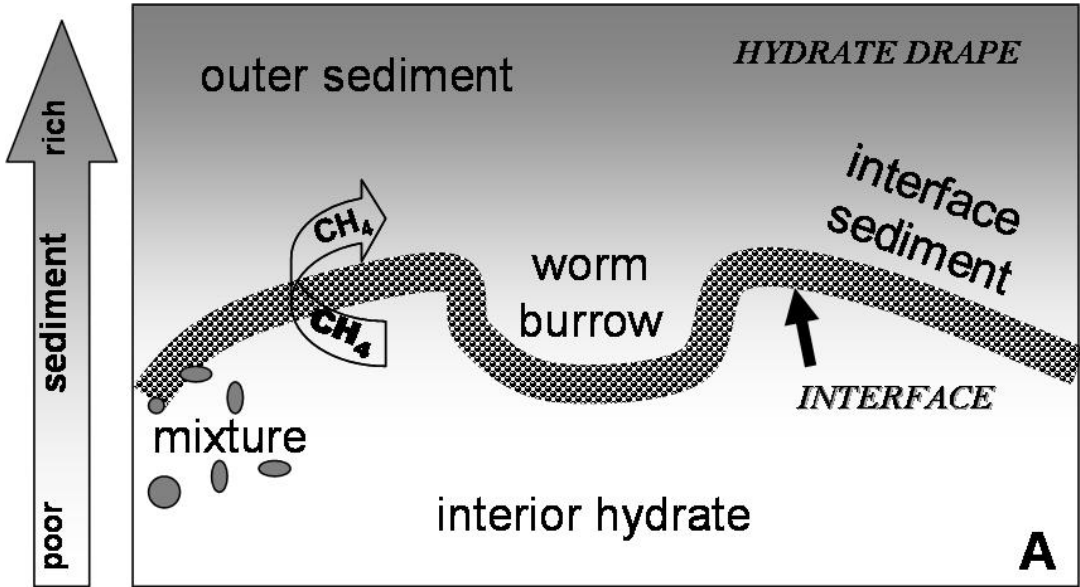


Fig. 5.2.



Fig. 5.3.

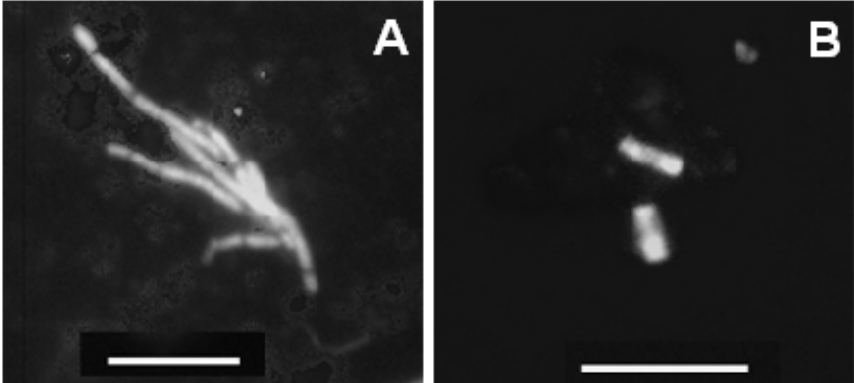
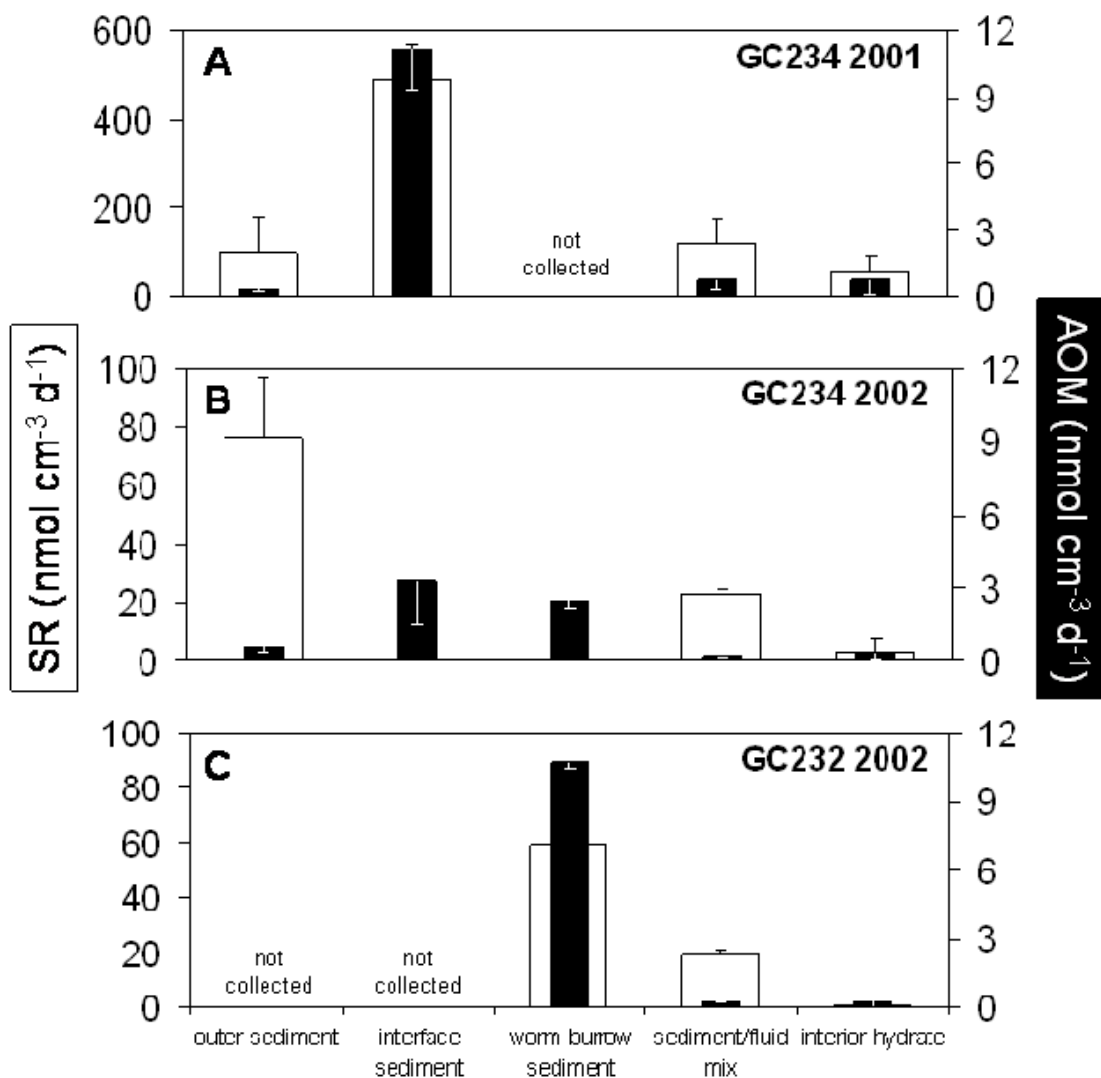


Fig. 5.4.



References

- Aharon P. and Fu B. (2000) Microbial sulfate reduction rates and sulfur and oxygen isotope fractionations at oil and gas seeps in deepwater Gulf of Mexico. *Geochimica et Cosmochimica Acta* **64**, 233-246.
- Alperin M. J. and Reeburgh W. S. (1985) Inhibition experiments on anaerobic methane oxidation. *Applied and Environmental Microbiology* **50**, 940-945.
- Arvidson R. S., Morse J. W., and Joye S. B. (2004) The sulfur biogeochemistry of chemosynthetic cold seep communities, Gulf of Mexico, USA. *Marine Chemistry* **87**, 97-119.
- Boetius A., Ravensschlag K., Schubert C. J., Rickert D., Widdel F., Gieseke A., Amann R., Jørgensen B. B., Witte U., and Pfannkuche O. (2000) A marine microbial consortium apparently mediating anaerobic oxidation of methane. *Nature* **407**, 623-626.
- Bohrmann G., Greinert J., Suess E., and Torres M. (1998) Authigenic carbonates from the Cascadia subduction zone and their relation to gas hydrate stability. *Geology* **26**(7), 647-650.
- Brooks J. M. (1984) Thermogenic gas hydrates in the Gulf of Mexico. *Science* **223**, 696-698.
- Brooks J. M., Field M. E., and Kennicutt M. C. (1991) Observations of gas hydrates in marine sediments, offshore northern California. *Marine Geology* **96**, 103-109.
- Bussman I., Dando P. R., Niven S. J., and Suess E. (1999) Groundwater seepage in the marine environment: role for mass flux and bacterial activity. *Marine Ecological Progress Series* **178**, 169-177.
- Canfield D. E., Raiswell R., Westrich J. T., Reaves C. M., and Berner R. A. (1986) The use of chromium reduction in the analysis of reduced inorganic sulfur in sediments and shale. *Chemical Geology* **54**, 149-155.
- Collett T. S. and Kuuskraa V. A. (1998) Hydrates contain vast store of world gas resources. *Oil and Gas Journal* **96**(19), 90-95.
- Dickens G. R. (2001) The potential volume of oceanic methane hydrates with variable external conditions. *Organic Geochemistry* **32**(10), 1179-1193.

- Dickens G. R., O'Neil J. R., Rea D. K., and Owen R. M. (1995) Dissociation of oceanic methane hydrate as a cause of the carbon isotopic excursion at the end of the Paleocene. *Paleoceanography* **10**(6), 965-971.
- Eicken H. (1992) The role of sea ice in structuring Antarctic ecosystems. *Polar Biology* **12**, 3-13.
- Fisher C. R., MacDonald I. R., Joye S. B., and Sassen R. (1998) The lair of the ice worm: a clathrate dwelling polychaete from the Gulf of Mexico. *1998 Ocean Sciences Meeting*.
- Fisher C. R., MacDonald I. R., Sassen R., Young C. M., Macko S. A., Hourdez S., Carney R., Joye S. B., and McMullin E. (2000) Methane ice worms: *Hesiocaeca methanicola* colonizing fossil fuel reserves. *Naturwissenschaften* **87**, 184-187.
- Fossing H. and Jørgensen B. B. (1989) Measurement of bacterial sulfate reduction in sediments - evaluation of a single-step chromium reduction method. *Biogeochemistry* **8**, 205-222.
- Ginsburg G. R., Milkov A. V., Solovyev V., Egorov A. V., Cherkashev G. A., Vogt P. R., Crane K., Lorenson T. D., and Khutorskoy M. D. (1999) Gas hydrate accumulation at the Haakon Mosby mud volcano. *Geo-Marine Letters* **19**(1/2), 57-67.
- Ginsburg G. R., Suseynov R., Dadashev A., Ivanova G., Kazantsev S., Solovyev V., Telepnev E., Askeri-Nasirov R., and Yesikov A. (1992) Gas hydrates of the southern Caspian Sea. *International Geological Reviews* **34**(8), 765-782.
- Heider J., Spormann A. M., Beller H. R., and Widdel F. (1999) Anaerobic bacterial metabolism of hydrocarbons. *FEMS Microbiology Reviews* **22**, 459-473.
- Hesselbo S. P., Groecke D. R., Jenkyns H. C., Bjerrum C. J., Farrimond P., Morgans Bell H. S., and Green O. R. (2000) Massive dissociation of gas hydrate during a Jurassic oceanic anoxic event. *Nature* **406**, 392-395.
- Hinrichs K.-U. and Boetius A. (2002) The anaerobic oxidation of methane: New insights in microbial ecology and biogeochemistry. In *Ocean Margin Systems* (ed. G. Wefer, D. Billett, D. Hebbeln, B. B. Jørgensen, M. Schlueter, and T. C. E. van Weering), pp. 457-477. Springer-Verlag.
- Hobbie J. E., Daley R. J., and Jasper S. (1977) Use of nucleopore filters for counting bacteria for fluorescence microscopy. *Applied and Environmental Microbiology* **33**, 1225-1228.
- Hoehler T. M., Alperin M. J., Albert D. B., and Martens C. S. (1994) Field and laboratory studies of methane oxidation in an anoxic marine sediment - evidence for a methanogen-sulfate reducer consortium. *Global Biogeochemical Cycles* **8**, 451-463.

- Hoehler T. M., Borowski W. S., Alperin M. J., Rodriguez N. M., and Paull C. K. (2000) Model, stable isotope, and radiotracer characterization of anaerobic oxidation in gas hydrate-bearing sediments of the Blake Ridge. In *Proceedings of the Ocean Drilling Program, Scientific Results*, Vol. 164 (ed. C. K. Paull, R. Matsumoto, P. J. Wallace, and W. P. Dillon), pp. 79. Ocean Drilling Program.
- Iversen N. and Jørgensen B. B. (1985) Anaerobic methane oxidation rates at the sulfate-methane transition in marine sediments from Kattegat and Skagerrak (Denmark). *Limnology and Oceanography* **30**, 944-955.
- Joye S. B., Connell T., Miller L. G., Oremland R. S., and Jellison R. (1999) Oxidation of ammonia and methane in an alkaline, saline lake. *Limnology and Oceanography* **44**, 178-188.
- Joye S. B., Orcutt B. N., Boetius A., Montoya J. P., Schulz H., Erickson M. J., and Lugo S. K. (2004) The anaerobic oxidation of methane and sulfate reduction in sediments from at Gulf of Mexico cold seeps. *Chemical Geology* **205**(3-4), 219-238.
- Kennett J. P., Cannariato K. G., Hendy J. L., and Behl R. J. (2000) Carbon isotopic evidence for methane hydrate instability during quaternary interstadials. *Science* **288**, 128-133.
- Kvenvolden K. A. (1993) Gas hydrates - geological perspective and global change. *Reviews of Geophysics* **31**, 173-187.
- Kvenvolden K. A. (1998) A primer on the geologic occurrence of gas hydrate. In *Gas hydrates: Relevance to World Margin Stability and Climate Change*, Vol. 137 (ed. J. P. Henriot and J. Mienert), pp. 9-30. Special Publication - Geological Society of London.
- Lanoil B. D., Sassen R., La Duc M. T., Sweet S. T., and Nealson K. H. (2001) *Bacteria* and *Archaea* physically associated with Gulf of Mexico gas hydrates. *Applied and Environmental Microbiology* **67**(11), 5143-5153.
- MacDonald I. R., Boland G. S., Baker J. S., Brooks J. M., Kennicutt M. C., and Bidigare R. R. (1989) Gulf of Mexico hydrocarbon seep communities II: spatial distribution of seep organisms and hydrocarbons at Bush Hill. *Marine Biology* **101**, 235-247.
- MacDonald I. R., Guinasso N. L., Sassen R., Brooks J. M., Lee L., and Scott K. T. (1994) Gas hydrate that breaches the sea-floor on the continental slope of the Gulf of Mexico. *Geology* **22**, 699-702.
- MacDonald I. R., Power D., Leifer I., Lane K., and Youden J. (2002) The remote sensing signature of hydrocarbon seeps and implications for carbon flux. *AGU Ocean Sciences Meeting*.

- Michaelis W., Seifert R., Nauhaus K., Treude T., Thiel V., Blumenberg M., Knittel K., Gieseke A., Peterknecht F., Pape T., Boetius A., Amann R., Jørgensen B. B., Widdel F., Peckmann J., Pimenkov N., and Gulin M. B. (2002) Microbial reefs in the Black Sea fueled by anaerobic methane oxidation. *Science* **297**, 1013-1015.
- Nauhaus K., Boetius A., Krüger M., and Widdel F. (2002) *In vitro* demonstration of anaerobic oxidation of methane coupled to sulfate reduction from a marine gas hydrate area. *Environmental Microbiology* **4**, 296-305.
- Nelson D., Revsbech N. P., and Jørgensen B. B. (1986) Microoxic-anoxic niche of *Beggiatoa* spp.: microelectrode survey of marine and freshwater strains. *Applied and Environmental Microbiology* **52**, 161-168.
- Norris R. D. and Roehl U. (1999) Carbon cycling and chronology of climate warming during the Paleocene/Eocene transition. *Nature* **401**, 775-778.
- O'Hara S. C. M., Dando P. R., Schuster U., Bennis A., Boyle J. D., Chiu F. T. W., Hathrell T. V. J., Niven S. J., and Taylor L. J. (1995) Gas seep induced interstitial water circulation: observations and environmental implications. *Continental Shelf Research* **15**, 931-948.
- Priscu J. C., Adams E. E., Lyons W. B., Voytek M. A., Mogk D. W., Brown R. L., McKay C. P., Takas C. D., Welch K. A., Wolf C. F., Kirshtein J., and Avci R. (1999) Geomicrobiology of subglacial ice above Lake Vostok, Antarctica. *Science* **286**, 2141-2144.
- Reeburgh W. S. (1980) Anaerobic methane oxidation: rate depth distributions in Skan Bay sediments. *Earth and Planetary Science Letters* **47**, 345-352.
- Reeburgh W. S. (1996) "Soft Spots" in the global methane budget. In *Microbial Growth on C₁ Compounds* (ed. M. E. Lidstrom and R. F. Tabita), pp. 334. Kluwer Academic Publishers.
- Reeburgh W. S., Whalen S. C., and Alperin M. J. (1993) The role of methylotrophy in the global methane budget. In *Microbial Growth on C₁ Compounds* (ed. J. C. Murrell and D. P. Kelly), pp. 1-14. Intercept Ltd.
- Sassen R., Joye S. B., Sweet S. T., DeFreitas A., Milkov A. V., and MacDonald I. R. (1999) Thermogenic gas hydrates and hydrocarbon gases in complex chemosynthetic communities, Gulf of Mexico continental slope. *Organic Geochemistry* **30**, 485-497.
- Sassen R. and MacDonald I. R. (1994) Evidence of structure H hydrate, Gulf of Mexico continental slope. *Organic Geochemistry* **23**, 1029-1032.
- Sassen R., MacDonald I. R., Guinasso N. L., Joye S. B., Requejo A. G., Sweet S. T., Alcalá-Herrera J., DeFreitas A., and Schink D. R. (1998) Bacterial methane oxidation in sea-floor gas hydrate: Significance to life in extreme environments. *Geology* **26**(9), 851-854.

Suess E., Torres M., Bohrmann G., Collier R. W., Greinert J., Linke P., Rehder G., Trehu A., Wallmann K., Winckler G., and Zuleger E. (1999) Gas hydrate destabilization: enhanced dewatering, benthic material turnover and large methane plumes at the Cascadia convergent margin. *Earth and Planetary Science Letters* **170**(1-2), 1-15.

Thomas D. N. and White G. S. (2002) Antarctic sea ice - a habitat for extremophiles. *Science* **295**(641-644).

Valentine D. L., Blanton D. C., Reeburgh W. S., and Kastner M. (2001) Water column methane oxidation adjacent to an area of active hydrate dissociation, Eel River Basin. *Geochimica et Cosmochimica Acta* **65**(16), 2633-2640.

Zengler K., Richnow H. H., Rossello-Mora R., Michaelis W., and Widdel F. (1999) Methane formation from long-chain alkanes by anaerobic microorganisms. *Nature* **40**, 266-269.

CHAPTER 6

*ARCHAEA AND BACTERIA AND THEIR ACTIVITY IN HYDRATE-BEARING DEEP SUBSURFACE SEDIMENTS OF HYDRATE RIDGE (CASCADIA MARGIN, ODP LEG 204)*¹

¹ Orcutt, B!, J.S. Lipp, K. Knittel, K.-U. Hinrichs, S.B. Joye, A. Boetius. In preparation for *Geochimica et Cosmochimica Acta*

Abstract

The process of anaerobic oxidation of methane (AOM) has been inferred in deep biosphere samples from geochemical profiles; however, the responsible microorganisms have not been identified. We applied a combination of tracer-based rate measurements of microbial activity and cultivation-independent DNA- and lipid-based microbiological and molecular tools to methane-rich deep biosphere sediments (Hydrate Ridge, Cascadia Convergent Margin, ODP Leg 204) to investigate the distribution, diversity and activity of microorganisms involved in AOM. In near-surface samples from the summit of southern Hydrate Ridge, highly ^{13}C -depleted archaeal and bacterial lipids indicate the incorporation of methane-derived carbon into microbial biomass and an important role of anaerobic methane-oxidizing (ANME), methane-assimilating prokaryotes in the top meter of sediment. Presumably due to the rapid depletion of sulfate, methane assimilation is less prevalent in deeper sediment layers, despite the high availability of methane throughout the hydrate stability zone. *Crenarchaeota* dominate a well-defined sulfate methane transition zone (SMTZ) where both AOM and sulfate reduction are active; isotopic evidence suggests that these microbes do not incorporate methane-derived carbon into their biomass. For the first time, archaea phylogenetically affiliated with the ANME group were detected in deeply buried sediments within the hydrate stability zone (54 m depth) together with low potential rates of AOM and elevated archaeal lipid concentrations. In these sulfate-containing sediments, ANME-1 sequences dominate the archaeal 16S rDNA clone library and co-occurred with 16S rDNA sequences related to sulfate-reducing bacteria commonly found at cold seeps (Seep-SRB2 branch).

Introduction

The relatively recent discovery of microbial life in the deep marine subsurface poses fundamental questions about the evolution and distribution of life, the spatial extent of active elemental (i.e. carbon) cycles within the Earth's upper crust, and the functioning of cell metabolism at low energy availability. Rough estimates based on available data suggest that the deep biosphere contains 55-85 % of Earth's microbial population (WHITMAN et al., 1998), representing between 10-30 % of Earth's total biomass (PARKES et al., 2000; WHITMAN et al., 1998), although growth rates of this community are thought to be extremely low (doubling time of 1000s of years; (D'HONDT et al., 2002; WHITMAN et al., 1998)). Relatively little is known about the metabolic processes, activities, diversity and distribution of this large microbial community, although recent reports have provided intriguing new theories. Available evidence suggests that prokaryotic activity and abundance are highest at interfaces (i.e. sulfate methane transition zones in the Peru Margin, (PARKES et al., 2000; PARKES et al., 2005); within sapropels with high organic carbon content (Mediterranean, (COOLEN et al., 2002; CRAGG et al., 1998; PARKES et al., 2000)); or areas with methane hydrate (Northern Hydrate Ridge, (CRAGG et al., 1996); Blake Ridge, (CRAGG et al., 1996; PARKES et al., 2000; WELLSBURY et al., 1997)). Whether such interfaces lead to niche formations and unique endemic species or if the geochemical conditions enhance the activity of serendipitous cosmopolitan communities is unclear but recent work further suggests that the microorganisms in these zones are phylogenetically distinct from those outside the interfaces (PARKES et al., 2005).

Our understanding of the microbial community structure in the deep marine subsurface is still in its infancy, however. Due to low cell densities in deep biosphere samples, standard methods to measure community composition (i.e. targeting DNA, rRNA or cellular material)

often operate at or near the limit of detection. Additionally, in order to calculate specific turnover and growth rates and identify key microorganisms in elemental cycling, it is important to distinguish viable from dormant, recently dead or ‘ancient’ microbial biomass. For example, real-time PCR and fluorescence in situ hybridization (FISH) techniques targeting 16S rRNA in deep biosphere samples from the Peru margin and Pacific Ocean suggested that *Bacteria* dominated the community composition (INAGAKI et al., 2006; MAUCLAIRE et al., 2004; SCHIPPERS and NERETIN, 2006; SCHIPPERS et al., 2005). However, in samples originating from the same sites, other researchers concluded that *Archaea* dominated the microbial community – using similar (i.e. FISH) and different methods (i.e. analysis of membrane lipids from intact cells, creation of 16S rRNA clone libraries from reversely transcribed extracted rRNA; (BIDDLE et al., 2006; SØRENSEN et al., 2004; SØRENSEN and TESKE, 2006)). Explaining the discrepancy in these findings is paramount in order to gain a clear understanding of the structure of the vast microbial community in the deep biosphere.

Although geochemical evidence indicates that consumption of methane co-occurs with sulfate reduction in deep biosphere samples (D’HONDT et al., 2002), it is not clear which microorganisms mediate these processes. In many sediment zones, methane could be the main energy source if adequate electron acceptors are present (BIDDLE et al., 2006). Microbial groups typically found in surficial methane-consuming zones (i.e. the ANME-1, -2, and -3 clades of anaerobic methanotrophic archaea and sulfate-reducing bacteria related to *Desulfosarcina/Desulfococcus* or *Desulfobulbus* spp.; (KNITTEL et al., 2003; KNITTEL et al., 2005)) are conspicuously absent from all 16S rRNA clone libraries constructed from deep biosphere samples to date, with the exception of one study conducted on capped borehole fluid collected one year after drilling, where ANME-1 related sequences were retrieved (LANOIL et al.,

2005). Instead, certain groups of Crenarchaeota, namely the Marine Crenarchaeotic Group I (MCGI) and the combined Marine Benthic Group B (MBGB)/Deep Sea Archaeal Group (DSAG), are present in a wide range of deep biosphere samples of methane-rich sediments (BIDDLE et al., 2006; INAGAKI et al., 2006; INAGAKI et al., 2003; SØRENSEN et al., 2004; SØRENSEN and TESKE, 2006; TESKE, 2006). With the exception of the recently cultivated ammonia-oxidizing Crenarchaea (KÖNNEKE et al., 2005), these clades contain no currently cultured organisms. Thus, there are few clues about their metabolic role(s) in the environment. However, the stable isotopic composition of whole cells and extracted lipid material in samples where these Crenarchaea are abundant are relatively heavy, with $\delta^{13}\text{C}$ values around -25‰ vs. PeeDee Belemnite, suggesting these crenarchaeotes do not incorporate methane-derived carbon into cellular material and are instead heterotrophic (BIDDLE et al., 2006). Despite their cosmopolitan distribution, SØRENSEN and TESKE (2006) report that the MBGB (and to a lesser extent the MCGI) are more active in the SMTZ, indicating they may benefit directly or indirectly from coupled AOM and sulfate reduction (SR).

Here, we provide new insight into the function, distribution, and diversity of the microbial community from the deep biosphere of Hydrate Ridge, a well-studied methane seep system on the Cascadia Convergent Margin (BOETIUS and SUESS, 2004; TREUDE et al., 2003; TYRON et al., 1999) and the focus of Ocean Drilling Program (ODP) Leg 204 (TRÉHU et al., 2006). During Leg 204, nine sites on the Oregon continental margin were cored and logged to determine the distribution and concentration of gas hydrates in an accretionary ridge and adjacent slope basin, to investigate the mechanisms that transport methane and other gases into the gas hydrate stability zone (GHSZ), to obtain constraints on physical properties of gas hydrates in situ and to reveal the identity and distribution of microbes involved in the subsurface

methane cycle (TRÉHU et al., 2006). The focus of the present work was to explore how the presence of deeply buried gas hydrates and/or free methane gas influences the structure and diversity of the microbial community at the Hydrate Ridge deep biosphere.

Materials and Methods

Study area and sample collection

Gas hydrate deposits of the Cascadia accretionary margin in the northeastern Pacific Ocean, formed by the subduction of the Juan de Fuca plate beneath North America, have been studied extensively (BOHRMANN et al., 1998; KASTNER et al., 1995; KULM et al., 1986; LEE and COLLETT, 2005; SUESS et al., 1999; TORRES et al., 2004; TREHU et al., 2003). Hydrate Ridge (HR) is an area with high methane and fluid flux on part of this active continental margin complex located off the coast of Oregon (LUFF and WALLMANN, 2003; TORRES et al., 2002; TYRON et al., 1999). Leg 204 of the Ocean Drilling Program (ODP) focused on the southern summit of HR (TRÉHU et al., 2004), where the high fluid flux rates support gaseous methane transport to the summit surface sediments and sustain rapid formation of gas hydrate (up to 10^2 mol m⁻² y⁻¹; (HEESCHEN et al., 2003; TORRES et al., 2004).

This investigation focused on two types of sites characterized by high and low gas hydrate content (Table 6.1; detailed site descriptions available in (TORRES et al., 2002; TRÉHU et al., 2004)). Samples from Sites 1249 and 1250 represent the most active regions of seafloor venting and sedimentary gas hydrate content; massive hydrate deposits (30-40% average pore volume) were indicated in the upper 20-40 m, followed by areas with 2-4% hydrate within the gas hydrate stability zone (GHSZ), extending down to the bottom simulation reflector (BSR;

Table 6.1). In contrast, Site 1251 samples originate from a slope basin east of the summit that is characterized by high sedimentation rates and low hydrate content (~1% in the GHSZ).

Core collection and sampling

Whole round core (WRC) sections of 30 cm length were collected shortly after core retrieval onboard using standard ODP protocols. WRC for microbiological analysis were capped and stored in gas-tight bags under a nitrogen atmosphere at 4 °C until laboratory analysis approximately four months later. Due to concerns over seawater contamination of subsurface samples, retrieved sediment that exhibited a “soupy” consistency, potentially indicating seawater-compromised sediment, were not collected shipboard for our shore-based analysis. Thus, sediments with high hydrate content, which would also display a “soupy” texture due to hydrate sublimation upon recovery, were unfortunately not available for analysis. At the home laboratory, bagged WRC were transferred into an anaerobic chamber (10% CO₂/90% N₂ atmosphere) and opened. All equipment or reagents used in subsequent manipulation of sample material were pre-combusted at 450 °C or autoclaved at 121 °C for 30 minutes to ensure sterile conditions. Sediment from the centermost parts of the WRC was used, avoiding the outermost sections which may have been in contact with seawater during drilling. Contamination checks using fluorescent microscopic beads and perfluorocarbon tracers confirmed that these samples had minimal exposure to seawater (TRÉHU et al., 2003). Geochemical data (SO₄, CH₄, Cl, ¹³C-DIC, ¹³C-CH₄) from these cores and sites has been published elsewhere and is presented here with permission (BOROWSKI, 2006; MILKOV et al., 2005; TRÉHU et al., 2003). The stable carbon isotopic composition of total organic carbon in select sediment samples was provided by Monika Segl (Research Center Ocean Margins, Bremen, Germany).

Rates of AOM and SR

To measure potential rates of microbial activity, AOM and SR were determined in sediment slurry incubations using radiotracers. In the anaerobic chamber, sediment from a WRC section was mixed 1:2 [v/v] with artificial sea water medium containing 1 mM methane, 28 mM sulfate and 0.5-1 mM sulfide (WIDDEL and BAK, 1992). Subsamples of the sediment slurry (2.5 ml) were aliquoted into replicate 10 ml glass serum vials; each vial was then filled to the brim with additional medium and subsequently closed with a butyl rubber stopper and aluminum crimp seal, excluding the introduction of any gas bubbles. For AOM analysis, triplicate samples from each slurry were each amended with 100 μ l of $^{14}\text{CH}_4$ dissolved in milliQ™ water (~20 nCi) and incubated in the dark at 12 °C for 2.5 months. At the end of the incubation period, sample material was transferred to 50 ml glass jars containing 25 ml of 1 M NaOH and sealed with rubber stoppers (TREUDE et al., 2003). For SR analysis, triplicate samples were each amended with 100 μ l of $^{35}\text{SO}_4^{2-}$ (~225 nCi); samples were fixed at the end of the incubation period in 20 ml of 20 % [w/v] zinc acetate solution. Control samples for both analyses were fixed immediately after tracer addition. Methods for measurement of activity, concentration of tracers in reactant and product pools and calculation of rates have been described elsewhere (KALLMEYER and BOETIUS, 2004; TREUDE et al., 2003). Calculated rates were considered robust only if the sample activities were greater than three times the standard deviation of the activity measured in control samples.

Catalyzed reporter deposition fluorescence in situ hybridization (CARD FISH) and total cell counting

During subsampling of the WRC for rate analyses (above), samples were also collected for phylogenetic and cell density measurements. 1 ml of sediment material was collected from the WRC with a cut-end plastic syringe and fixed for 1-4 hours with 9 ml of filtered, buffered 3.7% formalin in a 20 ml plastic vial. The sample was vortexed to homogenize the mixture and then a 1 ml aliquot of the fixed sample was removed, washed twice with PBS (10 mM sodium phosphate, 130 mM NaCl), and stored in 1:1 PBS:ethanol at -20 °C for FISH. The remaining fixed sample was frozen for subsequent cell counting. Catalyzed report deposition fluorescence in situ hybridization (CARD FISH) was performed on 1:500 diluted filter preparations following established protocols (KNITTEL et al., 2005; ORCUTT et al., 2005; PERNTHALER et al., 2002) using published probes EUB I-III for Bacteria, ARCH915 for Archaea, ANME1-350 for members of the ANME1 clade of Archaea, and MBGB280 and MBGB335 for members of the MBGB clade of Crenarchaeota (KNITTEL et al., 2005). CARD-FISH samples were counter-stained with DAPI. Cell densities were measured using acridine orange direct counting (AODC) on 1:500 diluted filter preparations using published protocols (HOBBIE et al., 1977; ORCUTT et al., 2005). This was the highest dilution possible to achieve acceptable cells/field-of-view densities (typically 0-1 cell per field) without substantial interference from background sediment material. At least 40 random fields-of-view were quantified for each filter preparation to generate an average cell density.

16S rRNA gene library construction

Approximately 150 g of sediment from each WRC was transferred to glass jars and frozen at -20 °C. Total DNA was extracted directly from frozen sediment samples (~10 g) following the method of ZHOU et al. (1996). Crude DNA was purified with the Wizard DNA

Clean-Up Kit (Promega, Madison, WI). Two 16S rDNA clone libraries were constructed: one for archaea using primer sets Arch20f (MASSANA et al., 1997) with Uni1392R (LANE et al., 1985) and ARCH20f/ARCH958R (DELONG, 1992), and one for bacteria using primers EUB008f (MUYZER et al., 1995) with EUB1492R (KANE et al., 1993)). PCRs were performed and products purified as described previously (RAVENSCHLAG et al., 1999). PCR products were purified with the QiaQuick PCR Purification Kit using the manufacturer's protocol (Qiagen, Hilden, Germany). Clone libraries were constructed in pGEM-T-Easy (Promega, Madison, WI, USA) or the pCR4 TOPO vector (Invitrogen, Karlsruhe, Germany) according to the manufacturer's recommendations. Sequencing was performed by *Taq* cycle sequencing with a model ABI377 sequencer (Applied Biosystems). The presence of chimeric sequences in the clone libraries was determined with the CHIMERA_CHECK program of the Ribosomal Database Project II (Center for Microbial Ecology, Michigan State University, <http://rdp.cme.msu.edu/html/analyses.html>). Potential chimeras were eliminated before phylogenetic trees were constructed. Sequence data were analyzed with the ARB software package (LUDWIG et al., 2004). The phylogenetic tree was calculated with the ODP 204 sequences from this project together with reference sequences which are available in the EMBL, GenBank and DDJB databases by performing neighbor-joining analysis with different sets of filters. In all cases, general tree topology and clusters were stable. For specific PCR amplification of the deltaproteobacterial SRB, PCR conditions were as described above using primer combinations given in Table 6.2.

Intact polar membrane lipid biomarker analysis

Intact polar lipids (IPL) were extracted from 48 g of frozen sediment from select samples using a modified Bligh and Dyer method in four steps as described previously (BIDDLE et al., 2006; STURT et al., 2004). Before extraction, a known quantity of C₁₆-PAF (1-O-hexadecyl-2-acetyl-sn-glycero-3-phosphocholine) was added as an internal standard to all samples. Total lipids were extracted four times with 200 ml of 2:1:0.8 [v/v] methanol/dichloromethane (DCM)/buffer, where the buffer in the first two steps was 50 mM phosphate buffer at pH 7.4 (targeting bacterial cells) and 50 mM trichloroacetate buffer (5% [w/v]) was used as buffer in the final two steps (targeting archaeal cells). After sonication for 10 min and centrifugation at 2000 rpm for 10 min after each addition of solvent, the combined supernatants were washed with water and the organic phase subsequently evaporated to dryness. A fraction of the total lipid extract was separated by liquid chromatography with 10 g activated silica (60 Mesh, Carl Roth GmbH, Germany; combusted at 450°C overnight, mixed with 0.5 ml water to achieve 5% deactivated gel) suspended in DCM into a non-polar fraction (200 ml DCM) and polar fraction containing glycolipids and phospholipids (200 ml acetone followed by 200 ml of methanol).

Lipid components in the polar fraction were separated according to head group polarity using high-performance liquid chromatography (HPLC) techniques described previously (BIDDLE et al., 2006; STURT et al., 2004). No more than 1 µg of lipid material was injected from each sample onto a LiChrospher[®] Diol column fitted with a guard column of the same material used in a ThermoFinnigan Surveyor HPLC system; flow rates and eluents were described previously (BIDDLE et al., 2006; STURT et al., 2004). Components were analyzed by mass spectrometric (up to MS³) experiments on a ThermoFinnigan LCQ DecaXP Plus Electrospray Ionization-Ion Trap multistage mass spectrometer in both positive and negative ion modes using conditions described previously (SCHUBOTZ, 2005; STURT et al., 2004). Identification of

compound classes of interest relied on characteristic ionization and fragmentation properties identified previously (SCHUBOTZ, 2005; STURT et al., 2004). IPL concentration was calculated based on the sample signal response relative to that of the internal standard. The method has a sensitivity of 1-10 ng IPL ml⁻¹ sediment which corresponds to 10⁵ - 10⁶ cells ml⁻¹ (K.-U. Hinrichs, J. Lipp, unpublished data).

Specific lipid classes representing archaeal and bacterial sources were collected separately from the polar fraction for subsequent manipulation and isotopic analysis by preparative HPLC with a LiChrosphere Si60 column (5 µm, 250x10 mm, Alltech, Germany) with a fraction collector following established parameters (BIDDLE et al., 2006). This method was employed to select for IPLs and avoid ether- and ester-bound alkyl moieties that might be present in the polar fraction. Archaeal IPLs (45-50 min. elution time) were treated with HI and LiAlH₄ for ether cleavage to produce isopranyl phytanyl or biphytanyl derivatives (BIDDLE et al., 2006). Bacterial IPLs (60-80 min. elution time) were mixed with an internal C_{19:0} fatty acid standard and were saponified with KOH in methanol followed by acidification to release fatty acid derivatives; methyl ester derivatives of the fatty acids were formed following treatment with BF₃-methanol (ELVERT et al., 2001). Abundance and identification of IPL derivatives was measured using a ThermoFinnigan Trace GC-MS using instrument parameters that have been defined previously (BIDDLE et al., 2006). The column was run with a flow rate of 1 ml min⁻¹ and a temperature program of 60 °C to 150 °C at 10 °C min⁻¹ in the first 10 min. followed by a further 4 °C min⁻¹ ramp to 310 °C and held at 310 °C for 35 minutes. Compound specific carbon isotopic analysis (δ¹³C) of IPL derivatives was measured on a Hewlett-Packard 5890 GC interfaced with a ThermoFinnigan MAT252 isotope-ratio-monitoring mass spectrometer utilizing parameters defined previously (BIDDLE et al., 2006).

Apolar lipids, which may be extracted from viable cells or “fossil” cell material, were also analyzed for qualitative and quantitative comparison to the IPL. The non-polar fraction of the total lipid extract (above) was subjected to asphaltene separation by ultrasonication in 0.5 mL of *n*-hexane for 10 min followed by filtration of the suspension in a pasteur pipette filled with glass wool to yield the maltene fraction. The pipette was then washed with 4 mL of DCM to dissolve the asphaltenes. The maltene fractions were then further separated into specific compound classes using SPE cartridges filters with 500 mg of aminopropyl packing material (Sigma Aldrich, Germany) following methods described previously (HINRICHS et al., 2000). Briefly, the cartridge was prepared (dried at 70 °C for 30 min, washed with five volumes of *n*-hexane), the maltene fraction was dissolved in 200 µL *n*-hexane and then transferred to the cartridge. Four fractions were eluted: hydrocarbons (4 ml *n*-hexane), ketones and esters (6 ml 3:1 *n*-hexane:DCM), alcohols (7 ml 9:1 DCM:acetone), and fatty acids (8 ml 2% formic acid in DCM). Following addition of alcohol (*n*-nonadecanol) and hydrocarbon (cholestane) internal standards with known concentrations and stable carbon isotopic composition, methylsilyl-derivatives of the alcohols were created with bis(trimethylsilyl)trifluoroacetamide and pyridine according to methods described previously (ORCUTT et al., 2005). After addition of internal fatty acid (*n*-nonadecanoic acid) and hydrocarbon (cholestane) standards with known concentrations and stable carbon isotopic composition, fatty acid methyl esters were formed and analyzed as described above.

Results

Geochemistry

At the summit sites 1249 and 1250, sulfate concentrations were very low near the surface, indicating consumption in the upper sediment layers (Figs. 1A and 2A, respectively). Porewater methane concentrations were elevated in and just below the layers of massive hydrate at these two sites, returning to background values (<1 mM) with depth (Figs. 1A and 2A). Both sites showed increases in salinity near the surface (Figs. 2B and 3B), likely due to rapid hydrate formation (TORRES et al., 2004). Dissolved inorganic carbon (DIC) isotopic compositions at these sites were relatively heavy with $\delta^{13}\text{C}$ values of 14-15‰ throughout the sampled depths (Figs. 1B and 2B). For comparison, seawater DIC $\delta^{13}\text{C}$ values are ~0 ‰ (CLAYPOOL et al., 2006). These values are consistent with high rates of biological methane formation by reduction of CO_2 (TORRES and RUGH, 2006). The sedimentary organic carbon had a $\delta^{13}\text{C}$ value between -23.5‰ and -25.4‰ (Fig. 6.3). Methane at Site 1249 had $\delta^{13}\text{C}$ values between -63 and -70‰, becoming heavier with depth. At site 1250, $\delta^{13}\text{C}$ of methane ranged from -65 to -70‰ above the BSR and became heavier (up to -60‰) below the BSR (MILKOV et al., 2005).

In contrast, at the eastern slope basin site (Site 1251), sulfate gradually decreased with depth, reaching lower (<1 mM) values at ~5.5 mbsf, roughly coinciding with the depth where porewater methane concentration increased (Fig. 6.4A). Additionally, dissolved sulfide showed a maximum concentration just above this zone, reaching 11.3 mM at 4.1 mbsf. Although the upper ~10 m of the sediment exhibited seawater salinity, deeper layers indicated porewater freshening from a deep source with a broad mixing zone between ~10 and 210 mbsf (Fig. 6.4B). From the surface down to ~6 mbsf, $\delta^{13}\text{C}$ values of porewater DIC were relatively light (around -14‰), and increased below that depth to ~12‰ below 25 mbsf (Fig 4B). The sedimentary organic carbon had $\delta^{13}\text{C}$ values of -22.5‰ at the surface and -23.2‰ at 5.5 mbsf (Fig. 6.3).

Methane had a $\delta^{13}\text{C}$ value of -75‰ at 5.2 mbsf and exhibited a general increase in $\delta^{13}\text{C}$ value with depth (CLAYPOOL et al., 2006).

AOM and SR activity

At Site 1249, AOM and SR activity was detectable in samples beneath the massive hydrate layer (Fig. 6.1C), although the rates were very low (0.01-0.05 $\text{nmol cm}^{-3} \text{d}^{-1}$) in comparison with rates measured in the surface sediments of HR (BOETIUS and SUESS, 2004; TREUDE et al., 2003) or at other surficial methane seeps (i.e. rates usually tens to thousands $\text{nmol cm}^{-3} \text{d}^{-1}$; (JOYE et al., 2004; ORCUTT et al., 2005)). The measured rates were at the lower limits of detection of the methods ($\sim 0.001 \text{ nmol cm}^{-3} \text{d}^{-1}$) and should be viewed as representing the range of activity over the incubation time (see Discussion). At Site 1250, AOM was only detected in the surficial sample and at relatively low rates (0.05 $\text{nmol cm}^{-3} \text{d}^{-1}$; Fig. 6.2C). Although highly variable between replicates, SR activity was detected at low levels ($>0.1 \text{ nmol cm}^{-3} \text{d}^{-1}$) in all samples investigated at this site (Fig. 6.2C). At Site 1251, the highest rates ($\sim 0.2 \text{ nmol cm}^{-3} \text{d}^{-1}$) of sulfate reduction were measured in the samples above 6 mbsf; below this depth SR was not detected (Fig. 6.4C). Very low rates ($<0.01 \text{ nmol cm}^{-3} \text{d}^{-1}$) of AOM were detected in a few samples above 10 mbsf but not at lower depths. The highest measured rates of AOM at this site were measured within the sulfate methane transition zone (SMTZ).

Microbial community structure investigated with DNA-based techniques

Averaged over all investigated sites, total cell densities measured with AODC were in the range of 1.2×10^7 to $1.6 \times 10^8 \text{ cells cm}^{-3}$ (Table 6.3), which is within the higher end of the expected range (PARKES et al., 2000). Due to the low number of cells per field-of-view densities

(typically 1 or no cells per field), quantification of the percentages of archaea and bacteria in the samples as measured by CARD FISH was not statistically robust; so, qualitative relative contributions to the microbial community structure were reported (Table 6.3). Archaea were detected using CARD FISH in all investigated samples except in one sample from 30.7 mbsf at Site 1249. Bacteria were also detected in all samples, and this group dominated the microbial community in a surficial sample from Site 1250 and in the same sample from Site 1249 where no Archaea were detected. Cells targeted by the ANME-1 CARD FISH probe were detected in sediment from Site 1249 54 mbsf (Fig. 6.5), although the probe was used at low specificity and detection was not robustly reproducible. No cells were identified with signal from the various CARD FISH probes designed to target the MBGB group of Crenarchaea; however, there were substantial difficulties in using the general DNA stain DAPI to identify cells in the deep biosphere sediments, as has been noted by other researchers (SCHIPPERS et al., 2005).

16S rRNA gene libraries were constructed for two samples which had relatively high cell densities: Site 1249 54 mbsf and Site 1250 24 mbsf. Seven different major bacterial phylogenetic groups were detected by analysis of 97 (Site 1249 54 mbsf) and 36 clones (Site 1250 24 mbsf), respectively (Table 6.4): *Alpha-*, *Beta-*, and *Gammaproteobacteria*, *Bacteroidetes*, *Firmicutes*, *Actinobacteria* and the candidate phylum of uncultivated organisms “JS1”. The diversity within the *Gammaproteobacteria* was high, with observed sequences belonging to several different genera including *Roseobacter* spp., *Pseudomonas* spp., and *Halomonas* (EILERS et al., 2000). *Gammaproteobacteria* as well as the *Firmicutes* and *Actinobacteria* are commonly observed in 16S rRNA gene library surveys and in cultivations of bacteria from deep biosphere sediments (D'HONDT et al., 2004; INAGAKI et al., 2006; TESKE, 2006; WEBSTER et al., 2006). At site 1249,

12 clones related to *Thiomicrospira*, sulfur oxidizers that are found in nearly all coastal surface sediments (BRINKHOFF et al., 1998) were retrieved.

The archaeal clone libraries contained 94 clones from Site 1249 (54 mbsf) and 86 clones from Site 1250 (24 mbsf). At Site 1249 the most abundant group of clones (60%) was affiliated with ANME-1 archaea (Fig. 6.6), microorganisms which have been shown to mediate AOM at different methane seep sites (HINRICHS et al., 2000; MICHAELIS et al., 2002; ORPHAN et al., 2001a; ORPHAN et al., 2001b). This is the first time that this group has been detected in deep subsurface sediments. The second most abundant archaeal clone group was the crenarchaeotal Marine Benthic Group B (MBGB; also referred to as the Deep Sea Archaeal Group, DSAG; (INAGAKI et al., 2006)) which was found at both sites with high numbers of clones (38 and 81 clones at Sites 1249 and 1250, respectively). MBGB sequences have been found at many methane-rich sediments, and it is speculated that this group is associated with methanotrophic communities or maybe involved in AOM (BIDDLE et al., 2006; KNITTEL et al., 2005). The third group of clone sequences detected in our studies was the crenarchaeotal group Marine Benthic Group C (MBGC). This group contains only sequences from uncultivated species so their physiology and ecological function remains completely unknown.

The detection of ANME-1 at Site 1249 led us to look further for potential sulfate-reducing partners that may have not been revealed with the general 16S rRNA gene survey. We performed specific PCRs for groups of SRB repeatedly found at methane-rich sites (Table 6.2): *Desulfosarcina/Desulfococcus* spp. which have been found in consortium with ANME-2 (BOETIUS et al., 2000) and ANME-1 (MICHAELIS et al., 2002), *Desulfobulbus* spp. which have been found in consortium with ANME-3 (NIEMANN et al., 2006), *Desulforhopalus* spp., the seep-endemic group SEEP-SRB2 (KNITTEL et al., 2003), and *Desulfovibrio* spp. From both samples,

sequences were obtained from the SEEP-SRB2 group and *Desulforhopalus*; however, no sequences were obtained from the known ANME partners *Desulfosarcina/Desulfococcus* or *Desulfobulbus* (Fig. 6.7). The sequences related to *Desulforhopalus* were most closely affiliated with the moderately psychrophilic species *Desulforhopalus vacuolatus* (95% sequence similarity) and the psychrophilic strain LSv22 isolated from Svalbard sediments (99% similarity; (KNOBLAUCH et al., 1999)). The SEEP-SRB2 sequences branched within the large cluster of more than 70 sequences from 12 different habitats. Although they are commonly detected in methane-rich sediments and generally co-occur with the ANME/DSS consortia, no organisms of this group have been cultivated; thus, assigning functional roles to the detected microorganisms is not possible.

Microbial community structure measured with lipid-based techniques

Confirming the results from CARD FISH and gene library methods, the IPL composition indicated that both Archaea and Bacteria are present and active in the deep biosphere of Hydrate Ridge, although the relative proportion of these domains varied between samples (Table 6.3). Bacterial IPLs were detectable in all samples except from 24 mbsf at Site 1250 and 5.5 mbsf at Site 1251 and were comprised of diacylglycerophospholipids with phosphoethanolamine (PE) and phosphoglycerol (PG) polar head groups. The PG headgroup-containing compounds were more abundant than the PE headgroup compounds except at Site 1250, 0.8 mbsf. Fatty acid methyl ester derivatives from the intact bacterial lipids in all samples revealed that the acyl chains consisted mainly of 16:1 ω 7c, 16:1 ω 5c, 16:0, 18:1 ω 9c, and 18:1 ω 7c, and 18:0 fatty acids. Of these fatty acids, 16:1 ω 5c became strongly enriched in a growing ANME/DSS culture (NAUHAUS et al., 2006), and appeared to be a specific biomarker of the SRB partner in AOM.

Although no bacterial IPLs were detected by HPLC analysis from Site 1250 24 mbsf and Site 1251 5.5 mbsf samples, concentration by preparative HPLC and subsequent derivatization revealed a small quantity (20-60 ng lipid/g_{sediment} versus 80-800 ng/g in other samples, data not shown) of polar fatty acids in these samples. With the exception of the sample from Site 1250, 0.8 mbsf, the carbon isotopic composition of the bacterial fatty acids from the summit sites ranged between -23‰ and -29‰. The Site 1250, 0.8 mbsf sample contained depleted 16:1 (-50‰), 16:0 (-42‰) and 18:1 (-39‰) fatty acids, indicating that the bacteria at this depth were incorporating ¹³C-depleted carbon compounds into biomass. At the eastern slope basin Site 1251, the stable carbon isotopic compositions of the fatty acids ranged from -29‰ to -35‰.

The archaeal IPL glyceroldialkylglyceroltetraethers (GDGT) with diglycosidic polar head groups were detected in all of the investigated sediments (Table 6.3). The detected GDGTs appeared to occur with two types of diglycosidic headgroups, distinguished on the mass spectrometer as having base peaks at ~ m/z 1640 (GDGT-A, two hexoses) or ~1660 m/z (GDGT-B, possibly containing a hexose and a modified sugar derivative, K.-U. Hinrichs and J. Lipp, unpublished data). Samples above 8 m were dominated by the GDGT-A group, with the exception of the sample from the SMTZ at Site 1251. Deeper samples were dominated by the GDGT-B group. Due to coelution on the HPLC, determination of the abundance of the various GDGT compounds was not possible. Biphytanes with 0-3 rings were revealed by HI/LiAlH₄ treatment to be the components of the alkyl chains in the GDGTs. The acyclic biphytane was the most abundant compound in all of the investigated samples, although the proportion of the other biphytanes varied. With the exception of the tricyclic biphytane, possibly derived from crenarchaeol, which had a δ¹³C value of -21‰, the biphytanes from the shallow Site 1250 sample were strongly depleted in ¹³C (δ values of -55 to -95‰), with the monocyclic biphytane

being the most depleted. The monocyclic biphytane derived from IPL in the Station 1250, 7.4 mbsf sample was also slightly depleted at -35‰. The remaining biphytanes extracted from the summit site samples had heavier $\delta^{13}\text{C}$ values ranging from -19‰ to -26‰. The IPL-derived biphytanes from the slope basin Site 1251 were on average even heavier at -22‰ to -23‰. In all samples, the tricyclic biphytane was the heaviest of the biphytanes. The shallow sample from Site 1250 was the only sample to contain intact polar diglycosidic archaeol diether (data not shown). The phytane derivative of the archaeol was also depleted in ^{13}C with a δ value of -54‰ (Table 6.3).

A variety of apolar compounds, which could derive from living or dead/fossil cells, were also detected in the samples (Table 6.3). As seen in the polar-derived fatty acids, the shallow Site 1250 sample (0.8 mbsf) had depleted 16:1 (-48‰) and 18:1 (-49‰) apolar fatty acids, indicating that the bacteria which synthesized these compounds were incorporating carbon substrates which were depleted in ^{13}C . No other sample contained depleted short-chain apolar fatty acids. The sample from Site 1250, 7.4 mbsf contained a fatty acid derivative of the acyclic biphytane which was slightly depleted in ^{13}C (data not shown). Otherwise, the apolar fatty acids observed in these samples had carbon isotopic compositions ranging from -20‰ to -31‰. ^{13}C -depleted apolar pentamethyleicosane (PMI, a compound often found in AOM-mediating communities (ELVERT et al., 2000; ELVERT et al., 1999) including those in the subsurface (BIAN et al., 2001)) was detected in all of the samples from Site 1250, with the strongest depletion occurring in the shallow sample (-95‰) and the weakest depletion in the deep 24 mbsf sample (-52‰). No other samples contained depleted PMI. Apolar archaeol was detected in all samples investigated, but only the archaeol from the 0.8 mbsf at Site 1250 exhibited ^{13}C depletion.

Discussion

Anaerobic methane-consuming communities in the deep biosphere of Hydrate Ridge

This is the first report of the occurrence of the anaerobic methanotrophic archaeal group ANME-1 in deep subsurface sediments. The ANME-1 group is well known from surficial environments such as the methanotrophic reefs of the Black Sea (MICHAELIS et al., 2002), coastal SMTZ zones (NIEMANN et al., 2005), shallow subsurface of cold seeps at Hydrate Ridge (KNITTEL et al., 2005), the Eel River Basin (HINRICHS et al., 1999; ORPHAN et al., 2001b; ORPHAN et al., 2002), the Gulf of Mexico (LLOYD et al., 2006; ORCUTT et al., 2005) and hydrothermal sediments in the Guaymas Basin (TESKE et al., 2002). Previous extensive studies of deep subsurface sediments with and without hydrates by INAGAKI et al. (2006) did not retrieve a single sequence belonging to anaerobic methanotrophs after analyzing several thousands of clones. In this study, multiple ANME-1 sequences were retrieved from a sample at 54 mbsf at Site 1249 that had low but measurable AOM rates; ANME-1 cells were also visually identified using a CARD FISH probe specific for the 16S rRNA of ANME-1 (Figs. 5, 6). The ANME-1 might co-occur with sulfate reducing bacteria of the SEEP-SRB2 and *Desulforhopalus* spp. clades (Fig. 6.7), although functional association between these microorganisms remains highly speculative. Although no polar or apolar lipid biomarkers extracted from the ANME-1 containing sediment were noticeably depleted in ^{13}C (Table 6.3), which would indicate the incorporation of methane-derived carbon into biomass, it is possible that the ANME-1 community was in very low abundance, and that any signature of methane incorporation into

biomass was diluted out by the input of the same biomarker compounds from other species – such as the *Crenarchaeota* - which do not incorporate methane-derived carbon into biomass.

An abundant AOM-mediating community of archaea and bacteria is evident in the shallow samples from summit Site 1250 based on ^{13}C -depleted polar and apolar lipid biomarkers (Table 6.3, Fig. 6.3). The potential rates of AOM and SR in this sediment are relatively low in comparison to surficial Hydrate Ridge sediments, which contain 10^9 - 10^{10} cells cm^{-3} sediment of which 90% are involved in AOM (KNITTEL et al., 2003; KNITTEL et al., 2005; TREUDE et al., 2003). Using biomarker/cell abundance ratios developed from surficial cold seep sediments, rough proportions of ANME and SRB populations in this sediment can be estimated. At Hydrate Ridge surficial sediments, ELVERT et al. (2003) determined a ratio of $0.9 \cdot 10^{-15}$ g $\text{C}_{16:1}$ fatty acid per SRB cell at depths where ANME-2/SRB aggregates were abundant. Comparing the density of ANME-1 cells in Black Sea mats ($\sim 5 \cdot 10^{10}$ cells gdw^{-1} ; (KNITTEL et al., 2005)) with abundances of archaeol (214 μg gdw^{-1} mat material; (BLUMENBERG et al., 2004)) allows a calculation of roughly $4.3 \cdot 10^{-15}$ g archaeol per ANME-1 cell, assuming that all of the archaeol originates from ANME-1 cells. Applying these ratios to the biomarker content of the Site 1250 0.8 mbsf sediment (Table 6.3) and assuming that these apolar compounds originate solely from SRB and ANME populations, an estimate of $1.7 \cdot 10^7$ ANME-1 cells cm^{-3} and $1.6 \cdot 10^8$ SRB cells cm^{-3} is calculated. These cell densities are higher by up to an order of magnitude than the cell density measured by AODC (Table 6.3) and may reflect the variable cell wall composition of surficial versus subsurface microorganisms, that the compounds are not species-specific, or, more likely, substantial contributions from fossil biomass. Note that intact, polar archaeol was not detected in this sample.

AOM in the deep biosphere of Hydrate Ridge

The total absence or extremely low measured rates of AOM in the methane-rich sediments of the Hydrate Ridge deep biosphere is surprising, given the availability of methane. It is possible that AOM in these systems is limited by the availability of the electron acceptor sulfate; the *in situ* concentrations of sulfate were below 2 mM (TRÉHU et al., 2003). Available data from enriched AOM-mediating communities from surficial methane-seep habitats indicate that sulfate-limitation of AOM can occur when sulfate is in the low mM range (TREUDE, 2003). However, the tracer incubation conditions provided higher levels of sulfate (>20 mM) and methane (>1 mM), which would have made AOM favorable. However, if the microorganisms which could mediate AOM were in very low abundance due to the unfavorable *in situ* conditions, and if the growth rates of these microorganisms are quite low (NAUHAUS et al., 2006), then it is not surprising that AOM activity could not be detected in some of the samples. With the concurrence of non-limiting sulfate concentrations and elevated methane, AOM is a likely energy providing process in some areas of the Hydrate Ridge deep biosphere.

Considering the free energy available from methane or organic carbon consumption in the Hydrate Ridge deep biosphere, and building on assumptions initially presented elsewhere (BIDDLE et al., 2006), AOM is estimated to provide a significant fraction of energy to the microbial community (Table 6.5). For instance, in the Site 1249 54 mbsf sample where the ANME-1 were detected, taking the first order rate constant measured in the $^{14}\text{CH}_4$ tracer AOM incubation assays of this study ($6.7 \cdot 10^{-6} \text{ hr}^{-1}$) and assuming that this rate constant is a reflection of the potential activity of the AOM community *in situ*, scaling the methane turnover to the theoretical soluble methane concentration *in situ* (~90 mM; from (MILKOV et al., 2003)) [*ex situ* measurements of methane can be low estimates because of methane degassing and hydrate

sublimation during sediment recovery], a potential *in situ* rate of AOM is estimated at $\sim 5 \cdot 10^{-6}$ mol cm⁻³ yr⁻¹ (Table 6.5). Given the free energy available from the AOM reaction at the *in situ* conditions, $8 \cdot 10^{-2}$ J cm⁻³ yr⁻¹ can be provided from the AOM reaction (Table 6.5). In comparison, the degradation of organic matter by SR or methanogenesis is estimated to yield $\sim 6.6 - 14.0 \cdot 10^{-5}$ J cm⁻³ yr⁻¹, assuming either hexadecane or sucrose as the model organic carbon for standard Gibbs free energy calculations (Table 6.5). Assuming instead that acetate were the model organic carbon compound, the calculation of energy yield using measured acetate values from LORENSEN et al. (2006) indicates that even less energy would be available overall from organic carbon degradation. Following these assumptions, AOM theoretically provides more energy than organic carbon degradation at all of the depths and sites investigated. Similarly, AOM could provide up to 23% of the energy required to maintain the microbial community, which may be a low estimate for two reasons: first, the maintenance energy calculation assumes that all of the cells measured by AODC are active (Table 6.5), and second, the *in situ* methane concentrations measured by pressure core samplers at the summit sites were actually higher than the theoretical methane solubility values (MILKOV et al., 2003). These estimated contributions of AOM to the total energy in the Hydrate Ridge deep biosphere are substantially higher than has been estimated based on methane fluxes for other deep biosphere sediments (BIDDLE et al., 2006).

A lower, more conservative estimate of the energy available from AOM can be found by assuming that the *in situ* rates are closer to those measured in the ¹⁴C tracer assays, even though these were conducted at much lower pressures (1 atm) and methane concentrations (~ 1.2 mM) than what would be expected *in situ*. If the *in situ* rates matched the experimental rates, then the free energy from AOM would range from ~ 10 to $564 \cdot 10^{-6}$ J cm⁻³ yr⁻¹ (Table 6.5). AOM at

these rates would only provide up to 0.3% of the required energy to maintain the observed microbial community. Organic carbon degradation would provide more energy than AOM at the shallower depths (<10 mbsf) including the SMTZ at Site 1251. However, the available free energy from both AOM and organic carbon degradation under these assumptions could only provide a very small fraction (<2%) of the total maintenance energy, as suggested previously (BIDDLE et al., 2006), suggesting that laboratory models of maintenance energies are not adequate for describing deep subsurface microbial communities.

Overall, the experimental rates (but not the derived potential *in situ* rates, Table 6.5) of SR and AOM activity measured in the Hydrate Ridge deep biosphere are comparable to rates measured or estimated at the Peru Margin deep biosphere sites (BIDDLE et al., 2006; PARKES et al., 2005) but lower than rates determined for the Blake Ridge deep biosphere (PARKES et al., 2000) or some areas of the Cascadia convergent margin (CRAGG et al., 1996). Low rates of metabolic activity at those sites were suggested to reflect low-energy conditions due to reductant limitation (PARKES et al., 2000). High rates of AOM activity were observed at other Cascadia convergent margin sediments with high measured gas hydrate content (CRAGG et al., 1996); the lower comparative rates of AOM in our samples may reflect the lower gas hydrate content of the specific sediments in this study which were collected below the zones of massive hydrate content. Additional support for the occurrence of AOM within the zone where ANME-1 were observed comes from the observation that methane has a slightly heavier $\delta^{13}\text{C}$ value around 50 mbsf compared to the zones above and below (CLAYPOOL et al., 2006), indicating that ^{12}C -methane has been preferentially removed by oxidation. In addition, the $\delta^{13}\text{C}$ of CO_2 is lowest in this particular horizon (MILKOV et al., 2005) and suggests a local source of ^{13}C -depleted CO_2 .

AOM at a deep SMTZ at Hydrate Ridge

Based on the chemistry and isotopic composition of sedimentary carbon and sulfur compounds in the eastern slope basin (i.e. Site 1251), AOM may be very minor or absent and the majority of sulfate may be consumed via organic carbon mineralization (BOROWSKI, 2006). At this site, rapid sedimentation rates and organic carbon delivery may limit the amount of methane which can diffuse to the SMTZ to support AOM (TORRES and RUGH, 2006). At site 1251 SMTZ, AOM was detected at low but measurable rates (Fig. 6.4C). Based on the composition of intact polar lipids extracted from the SMTZ, archaea dominated this habitat. However, no distinctly ^{13}C -depleted polar or apolar lipid biomarkers were detected in this sample. One possible explanation for this observation would be that the AOM-mediating community at the SMTZ incorporates non-methane carbon into biomass. This was suggested for other deep SMTZ which were dominated by members of the MBGB and MCG Crenarchaeota (BIDDLE et al., 2006). However, even in the subsurface sample at Hydrate Ridge where ANME-1 was detected (Site 1249, 24 mbsf), the bulk lipid biomarkers were also not depleted in ^{13}C , suggesting the isotopic signature of AOM-mediating populations at low abundance may not be resolved from the biomass of other organisms incorporating for example sedimentary organic matter. Alternatively, even ANME-1 may not incorporate methane-derived C under low-energy conditions.

Bacteria and Archaea observed in the deep biosphere of Hydrate Ridge

The data presented here indicate that both *Archaea* and *Bacteria* are present and active in the deep biosphere of Southern Hydrate Ridge in varying relative proportions of biomass and biodiversity. This supports previous findings that *Archaea* are important members of the

subsurface community (BIDDLE et al., 2006; MAUCLAIRE et al., 2004) as well as evidence from other researchers which show that *Bacteria* are also a major component of the deep biosphere (SCHIPPERS and NERETIN, 2006; SCHIPPERS et al., 2005). The presence of Marine Benthic Group B microorganisms in the Hydrate Ridge subsurface (Table 6.3, Fig. 6.6) is consistent with data from other recent studies on the microbial diversity of subsurface sediments where this group was found to be abundant with respect to clone frequencies (INAGAKI et al., 2006; SØRENSEN et al., 2004; SØRENSEN and TESKE, 2006) and lipid biomarker composition (BIDDLE et al., 2006). The observation of the seep endemic SEEP-SRB 2 sequences from Site 1249 where ANME-1 were detected is intriguing and requires further investigation. The metabolic role of this microbial group at surficial cold seeps is unknown but is speculated to be involved in hydrocarbon cycling (KNITTEL et al., 2003; ORCUTT et al., In preparation).

Conclusion and Outlook

Complimentary molecular biogeochemical techniques indicate that both *Archaea* and *Bacteria* are present in the subsurface of Hydrate Ridge. In contrast to the surface sediments, where high rates of AOM occur and anaerobic methanotrophs comprise > 90% of the microbial community (TREUDE et al., 2003), AOM in the deep subsurface of Southern Hydrate Ridge occurs at low rates and may be limited by the availability of the electron acceptor sulfate. Marine Benthic Group B microorganisms appear to dominate the archaeal community in subsurface sediments, similar to other hydrate bearing deep biosphere systems (INAGAKI et al., 2006). We also found that *Crenarcheota* dominate the microbial community in a sulfate methane transition zone, as reported for other deep biosphere sites (BIDDLE et al., 2006), but the isotope composition of their biomarkers does not show distinct signs of methane uptake. Only at the base

of the hydrate stability zone did we detect sequences commonly assigned to archaeal methane-oxidizers otherwise known from surficial cold seep systems and methane-sulfate transition zones. The finding of ANME-1 sequences in a deep biosphere sample is reported for the first time, although their abundance and activity was rather low. They co-occur with 16S rRNA genes of sulfate reducing bacteria in the same zone, which are common to cold seep systems, but have not been shown to form consortia.

Acknowledgements

This work would not have been possible without the support of the ODP Leg 204 shipboard team and chief scientists Gerhard Bohrmann, Marta Torres, and Anne Tréhu. This cruise was sponsored by the US National Science Foundation and participating countries in the Joint Oceanographic Institutions, Inc. The DFG provided funding for this research to A. Boetius (BO1650-3) and to K.-U. Hinrichs (Hi 616/4 and RCOM). We wish to acknowledge Melanie Summit and Mark Delwiche for their unending sampling effort at sea; Daniel Birgel and Marcus Elvert for biomarker analytical expertise; Imke Busse and Viola Beier for analytical assistance; Monika Segl for providing the isotopic composition of organic matter.

Figure Captions

Figure 6.1. Geochemical characteristics and microbial activity in sediments collected from Site 1249 at the summit of Southern Hydrate Ridge (ODP Leg 204). Depth scale in all panels same as indicated in panel A. (A) Sulfate (SO_4) and methane (CH_4) concentrations. (B) Chloride (Cl^-) concentration and stable carbon isotopic composition of dissolved inorganic carbon (^{13}C -DIC versus PDB; in per mil notation). (C) Sulfate reduction (SR) and rates of anaerobic oxidation of methane (AOM); error bars represent the standard deviation (n=3).

Figure 6.2. Geochemical characteristics and microbial activity in sediments collected from Site 1250 at the summit of Southern Hydrate Ridge (ODP Leg 204). Depth scale in all panels same as indicated in panel A. (A) Sulfate (SO_4) and methane (CH_4) concentrations. (B) Chloride (Cl^-) concentration and stable carbon isotopic composition of dissolved inorganic carbon (^{13}C -DIC versus PDB; in per mil notation). (C) Sulfate reduction (SR) and rates of anaerobic oxidation of methane (AOM); error bars represent the standard deviation (n=3).

Figure 6.3. Comparison of the stable carbon isotopic composition ($\delta^{13}\text{C}$) of sedimentary methane (black triangles), TOC (grey triangles) and DIC (open triangles) with select polar- (filled circles) and apolar- (open circles) derived lipid biomarkers for archaea, including biphytane with 0 rings (yellow circles), biphythane with 1 ring (red circles), biphythane with 3 rings (blue circles), and archaeol (green circles) extracted from Hydrate Ridge deep biosphere samples (ODP Leg 204).

Figure 6.4. Geochemical characteristics and microbial activity in sediments collected from Site 1251 on the eastern slope basin of Southern Hydrate Ridge (ODP Leg 204). Depth scale in all panels same as indicated in panel A. Note break in depth scale. (A) Sulfate (SO₄) and methane (CH₄) concentrations. (B) Chloride (Cl⁻) concentration and stable carbon isotopic composition of dissolved inorganic carbon (¹³C-DIC versus PDB; in per mil notation). (C) Sulfate reduction (SR) and rates of anaerobic oxidation of methane (AOM); error bars represent the standard deviation (n=3).

Figure 6.5. CARD FISH micrograph of ANME-1 cells in a sample from Site 1249, 54 mbsf. Scale in both panels is 10 μm. (A) DAPI-stained cells. (B) Cells with positive signal from the ANME-1 350 probe.

Figure 6.6. Phylogenetic tree showing the affiliations of Site 1249 54 mbsf, and 1250 24 mbsf, 16S rRNA gene sequences to selected sequences of the Archaea. The tree was calculated with nearly full-length sequences by neighbor-joining analysis in combination with filters, which consider only 50% conserved regions of the 16S rRNA gene of the Archaea. Groups containing sequences from site 1249 and 1250 samples are printed in boldface type. The scale bar gives 10% estimated sequence divergence.

Figure 6.7. 16S rRNA phylogenetic tree showing the affiliations of the detected groups of sulfate-reducing bacteria at Sites 1249, 54 mbsf and 1250, 24 mbsf, to selected sequences of the *Deltaproteobacteria*. The tree was calculated with nearly full-length sequences by neighbor-joining analysis in combination with filters, which consider only 50% conserved regions of the

16S rRNA gene of the *Deltaproteobacteria*. Groups containing sequences from site 1249 and 1250 samples are labeled grey. The scale bar gives 10% estimated sequence divergence.

Figure 8. Flowchart illustrating the variety of lipid compounds and their derivatizations in Hydrate Ridge deep biosphere (ODP Leg 204).

Table 6.1. Southern Hydrate Ridge (ODP Leg 204) site characteristics

Site	Description	Latitude	Longitude	Water depth (m)	BSR depth (m)
1249	Summit	44°35.17'N	125°8.84'W	775-788	115
1250	Summit	44°35.17'N	125°9.01'W	792-807	112
1251	Slope basin	44°34.21'N	125°4.44'W	1210	193

Table 6.2. Primers used for specific amplification of SRB.

Target Group	Primer set	T_m^a	Reference
<i>Desulfosarcina/Desulfococcus</i> spp.	GM3/DSS658	52	(MANZ et al., 1998; MUYZER et al., 1995)
<i>Desulforhopalus</i> spp.	GM3/DSR651	52	(MANZ et al., 1998; MUYZER et al., 1995)
<i>Desulfovibrio</i> spp.	GM3/DSV698	52	(MANZ et al., 1998; MUYZER et al., 1995)
<i>Desulfobulbus</i> spp.	GM3/660	52	(DEVEREUX et al., 1992; MUYZER et al., 1995)
<i>Desulfobulbus</i> spp.	DBB121/DBB1237	66	(DALY et al., 2000)
SEEP-SRB2	SEEP-SRB2-138F ^b /EUB1492R	44	This study, (KANE et al., 1993)

a: T_m, annealing temperature

b: SEEP-SRB2-138F: TTG GTT TGG AAT AAC CCG

Table 6.3. Composition of bacterial and archaeal apolar and polar lipids and relative composition of microbial community as measured by FISH in Hydrate Ridge deep biosphere sediments (ODP Leg 204). Unusually ¹³C-depleted lipid compounds highlighted in bold font.

		mbsf	Site 1249		Site 1250			Site 1251	
			30.7	54.1	0.8	7.4	24	0.95	5.5
Apolar	PMI	ng/g _{sediment} (δ ¹³ C)	7 (-35)	5 (n.d.)	22 (-95)	14 (-63)	14 (-52)	9 (n.d.)	7 (n.d.)
	crocetane		n.d.	n.d.	25 (-82)	n.d.	n.d.	n.d.	n.d.
	archaeol*		27 (-28)	74 (-32)	71 (-43)	62 (-32)	161 (-35)	31 (-25)	17 (-31)
	16:1 fatty acid		n.d.	n.d.	146 (-48)	n.d.	n.d.	83 (-29)	n.d.
	16:0 fatty acid		23 (-30)	23 (n.d.)	142 (-35)	430 (-25)	40 (n.d.)	355 (-25)	8 (n.d.)
	18:1 fatty acid		n.d.	n.d.	61 (-49)	n.d.	n.d.	114 (-27)	n.d.
	18:0 fatty acid		48 (-28)	42 (-27)	65 (-24)	386 (-24)	42 (-26)	317 (-24)	18 (n.d.)
IPL	GDGT-A	ng/g _{sediment}	158	165	328	234	184	459	93
	GDGT-B		208	538	150	145	242	525	143
	PG-headgroup		1423	264	153	86	n.d.	1328	n.d.
	PE-headgroup		404	82	330	n.d.	n.d.	896	n.d.
IPL derivatives	phytane	% (δ ¹³ C)	n.d.	n.d.	3 (-54)	n.d.	n.d.	n.d.	n.d.
	biphytane (0-ring)		54 (-24)	63 (-26)	54 (-55)	58 (-24)	52 (-25)	57 (-22)	55 (-22)
	biphytane (1-ring)		7 (-25)	11 (-22)	22 (-95)	9 (-35)	10 (-27)	6 (n.d.)	5 (-23)
	biphytane (2-ring)		17 (-22)	14 (-25)	14 (-69)	14 (-26)	18 (-22)	16 (-23)	17 (-23)
	biphytane (3-ring)		23 (-22)	13 (-19)	7 (-21)	19 (-24)	20 (-20)	21 (-22)	23 (-22)
	16:1 fatty acid		31 (-28)	23 (-25)	42 (-50)	7 (-25)	23 (-29)	29 (-31)	13 (-31)
	16:0 fatty acid		17 (-29)	26 (-26)	36 (-42)	35 (-25)	30 (-27)	37 (-30)	48 (-29)
	18:1 fatty acid		44 (-27)	41 (-24)	17 (-39)	22 (-25)	35 (-28)	30 (-31)	21 (-35)
18:0 fatty acid	4 (-27)	10 (-24)	5 (n.d.)	36 (-23)	12 (-26)	4 (-29)	18 (-34)		
AODC cells ml ⁻¹			2.9E+07	3.9E+07	1.2E+07	4.4E+07	1.1E+08	6.0E+07	3.7E+07
Archaea (FISH)			-	+	+	n.m.	+	n.m.	+
Bacteria (FISH)			++	+	++	n.m.	+	n.m.	+

n.d. – not detected; n.m. – not measured; * Target compound co-eluted on irMS with isomeric compound and thus has a mixed signal

Table 6.4. Overview of 16S rRNA gene sequences obtained from Site 1249 54 mbsf and Site 1250 24 mbsf using general archaeal and bacterial primers.

	Phylogenetic group	1249 54 mbsf	1250 24 mbsf
Bacteria	Alphaproteobacteria	0	2
	Betaproteobacteria	0	1
	Gammaproteobacteria	97	24
	Bacteroidetes-Chlorobium	0	2
	JS1	0	3
	Firmicutes	0	2
	Actinobacteria	0	2
Archaea	ANME-1	56	0
	Marine benthic group B	38	81
	Marine benthic group C	0	5

Table 6.5. Rates of AOM and OC degradation activity and corresponding energy yields and requirements for microbial communities in the Southern Hydrate Ridge deep biosphere sediments (ODP Leg 204).

Site	Depth	AOM rate, exp. ^a	AOM rate, <i>in situ</i> potential ^b	OC degradation rate ^c	$\Delta G_{\text{AOM}}^{\text{d}}$	$\Sigma \Delta G_{\text{AOM, exp.}}^{\text{e}}$	$\Sigma \Delta G_{\text{AOM, in situ}}^{\text{f}}$	$\Sigma \Delta G_{\text{OC_MOG}}^{\text{g}}$	$\Sigma \Delta G_{\text{OC_SR}}^{\text{g}}$	Maintenance energy ^h	Fraction energy AOM ⁱ
		mbsf	$10^{-9} \text{ mol C cm}^{-3} \text{ yr}^{-1}$		kJ mol^{-1}	$10^{-6} \text{ J cm}^{-3} \text{ yr}^{-1}$				%	
1249	31	17.2	986	1.8	-32.7	564	32,000	41/101	70/135	213,000	0.3/15
	54	7.5	5,282	1.0	-15.2	114	80,000	24/60	42/80	354,000	0.03/23
1250	0.8	12.8	788	84.6	-16.2	208	13,000	1,980/4,909	3,385/6,517	71,000	0.3/18
	7	0.4*	35*	11.6	-27.7	10*	970*	272/674	465/895	290,000	0.003/0.3
	24	0.4*	37*	3.6	-28.4	10*	1,054*	85/211	145/280	810,000	0.001/0.1
1251	0.5	0.4*	33*	300.9	-32.3	12*	1,060*	7,042/17,500	12,037/23,172	473,000	0.002/0.2
	5.5	2.8	175	45.8	-20.2	56	3,540	1,072/2,658	1,833/3,629	244,000	0.02/1.5

^a Rate estimated from potential activity experiments conducted at 1 atm pressure, this study

^b Rate of AOM estimated using the substrate turnover rate measured in this study and the theoretical soluble CH₄ concentration at depth *in situ* (MILKOV et al., 2003).

^c OC degradation rate calculated using diagenetic model of (MIDDELBURG, 1989), rate = TOC • $k \cdot \rho_{\text{sed}} / m_c$, where TOC is the sedimentary organic carbon content (1.5% at all sites; from (TRÉHU et al., 2003)), ρ_{sed} is the mean density of the sediment (TRÉHU et al., 2003), and m_c is 12.011 g C mol⁻¹. k is the decay constant for the sediment depth determined by $k = 0.16 \cdot (a + t)^{-0.95}$ (MIDDELBURG, 1989), where a is the assumed initial reactivity of the organic matter (500 yr) and t is the age of the sediment at depth, which was calculated from the measured sedimentation rates at the sites (9, 15, and 60 cm kyr⁻¹ at Sites 1249, 1250, and 1251, respectively; (TRÉHU et al., 2003)).

^d Free energy yield of the AOM reaction (ΔG_{AOM}) at *in situ* temperatures and activities calculated by $\Delta G_{\text{AOM}} = \Delta G_{\text{AOM}}^{\circ} + R \cdot T \cdot \ln((\gamma[\text{HCO}_3^-] \cdot \gamma[\text{HS}^-]) / (\gamma[\text{CH}_4] \cdot \gamma[\text{SO}_4^{2-}]))$, where $\Delta G_{\text{AOM}}^{\circ}$ is the standard free energy yield of the AOM reaction (-32.9 kJ/mol; calculated using free energy of formation values from (STUMM and MORGAN, 1981); R is the universal gas constant (8.314 J mol⁻¹ K⁻¹); T is the *in situ* temperature (TRÉHU et al., 2003); γ represents the activity coefficients for the various species assuming an ionic strength of seawater (MILLERO and PIERROT, 1998); [HCO₃⁻] is the concentration of bicarbonate as calculated from published alkalinity and pH values (TRÉHU et al., 2003); [CH₄] is the concentration of methane (MILKOV et al., 2005); [SO₄²⁻] is the concentration of sulfate (TRÉHU et al., 2003); and [HS⁻] is the concentration of sulfide (BOROWSKI, 2006).

^e Energy produced from AOM rates measured in the experiments in this study based on the free energy available from the AOM reaction

^f Energy produced from potential *in situ* rates of AOM based on the free energy available from the AOM reaction.

- ^g Energy produced from estimated OC carbon degradation rates based on assumed free energy yields of methanogenesis ($\Sigma\Delta G_{OC_MOG}$) or sulfate reduction ($\Sigma\Delta G_{OC_SR}$) with organic carbon represented by either hexadecane (first value; $\Delta G_{OC_MOG} = -23.4$ kJ/mol electron donor; $\Delta G_{OC_SR} = -40$ kJ/mol; (ZENGLER et al., 1999)) or sucrose (second value; $\Delta G_{OC_MOG} = -58$ kJ/mol; $\Delta G_{OC_SR} = -77$ kJ/mol; (BERNER, 1980)).
- ^h Energy required to support the quantified microbial community (this study) calculated as described in (BIDDLE et al., 2006) using the model of (HARDER, 1997) where the maintenance energy equals the product of number of cells cm^{-3} , the cellular carbon content (19 fg C cell⁻¹), the constant $4.99 \cdot 10^{12}$ kJ (g dry weight cell)⁻¹ d⁻¹ for anaerobic bacteria, and the exponent of an assumed activation energy of -69.4 kJ mol⁻¹ divided by the universal gas constant and the *in situ* temperature.
- ⁱ Fraction of the total maintenance energy that can be supplied by AOM at the experimental AOM rates (first value) or the potential *in situ* rates (second value)
- * no AOM was measured using tracer at these depths, values are calculated assuming AOM rate is at the detection limit of the method (1 pmol cm^{-3} d⁻¹).

Figure 6.1.

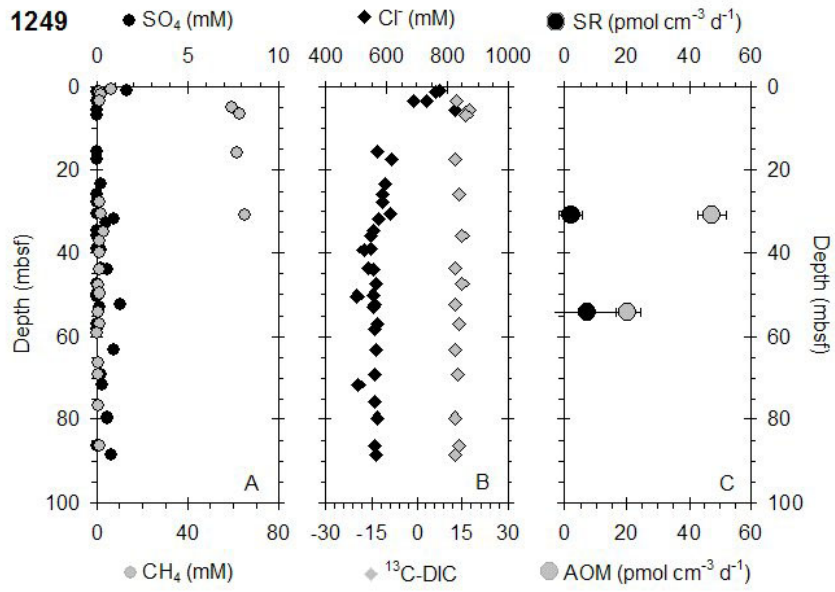


Figure 6.2.

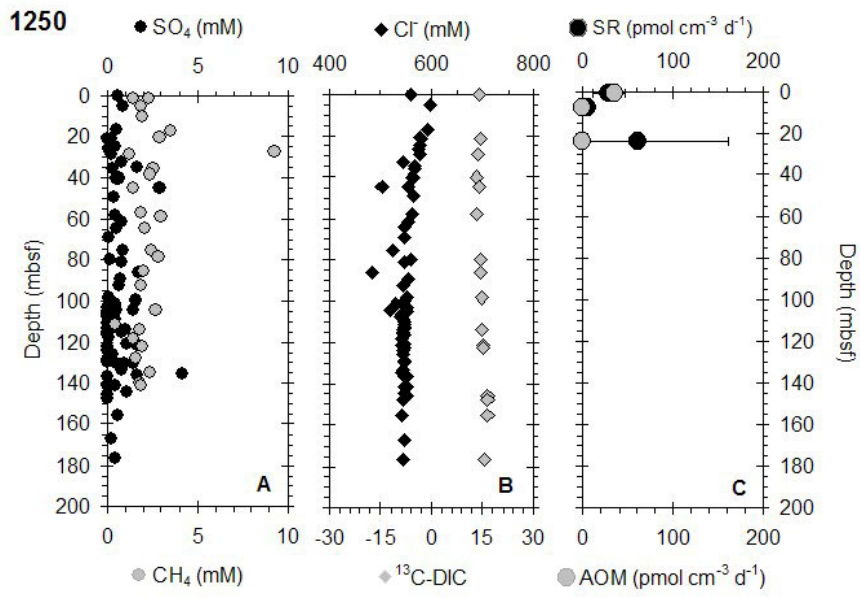


Figure 6.3.

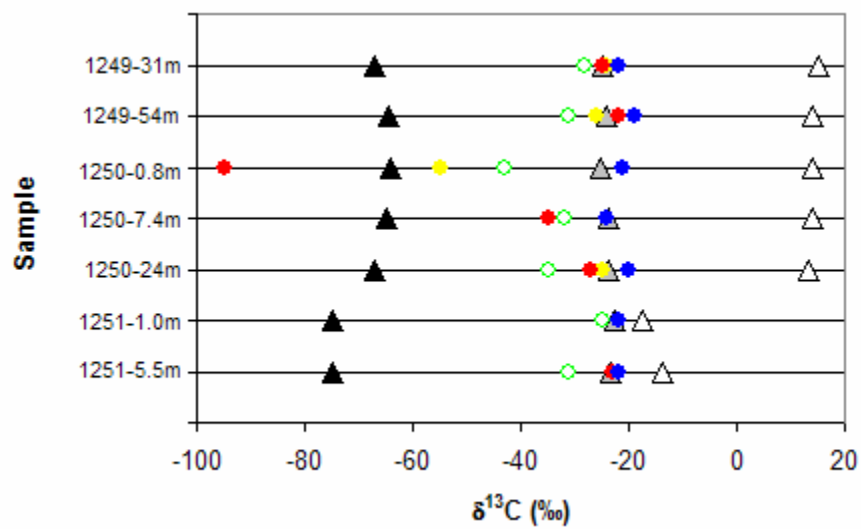


Figure 6.4.

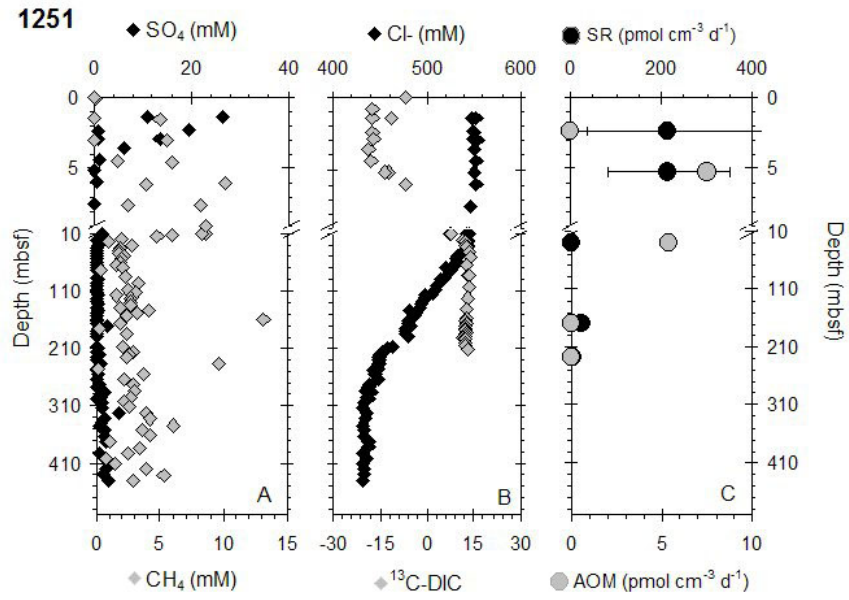


Figure 6.5.

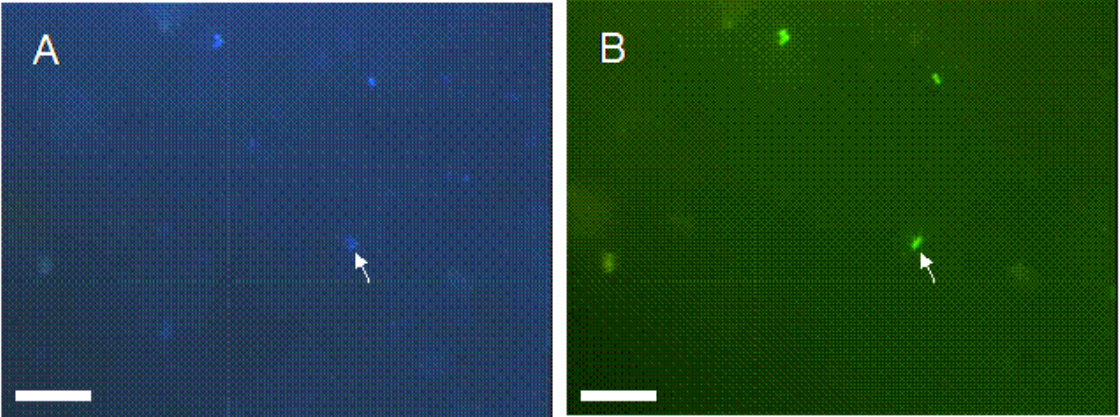


Figure 6.6.

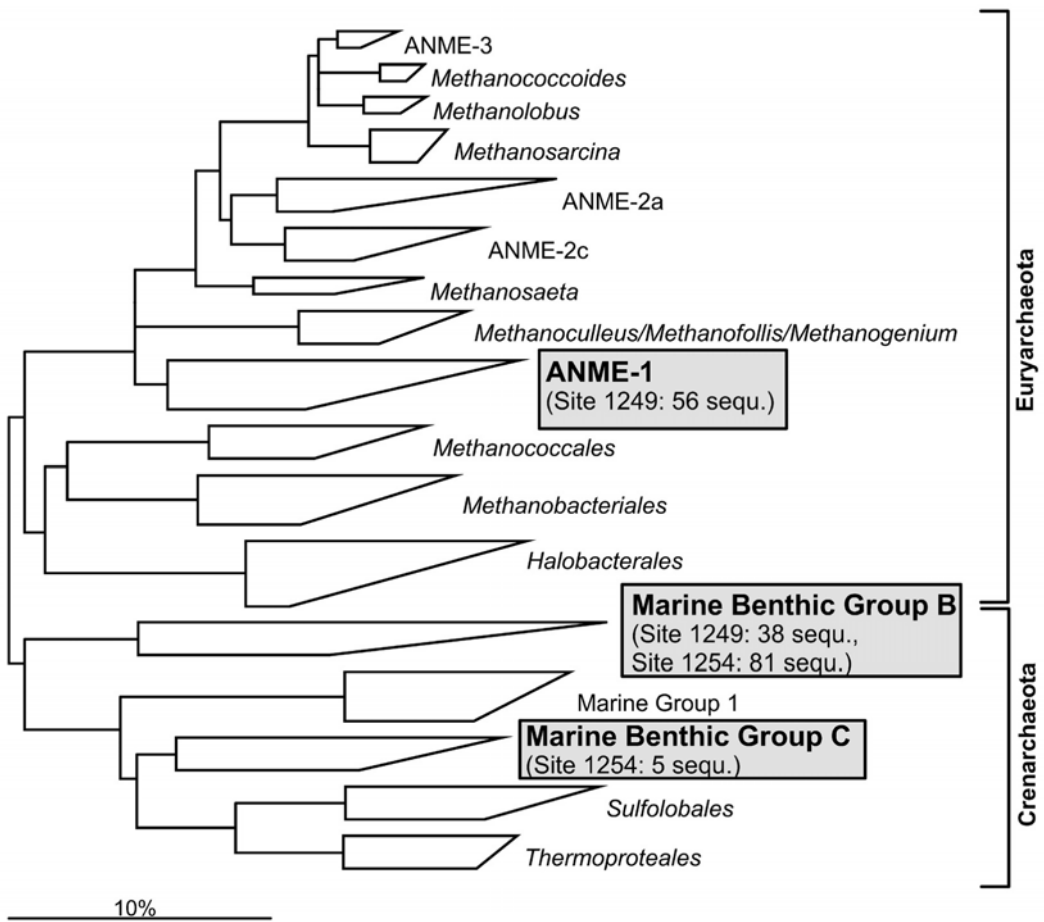
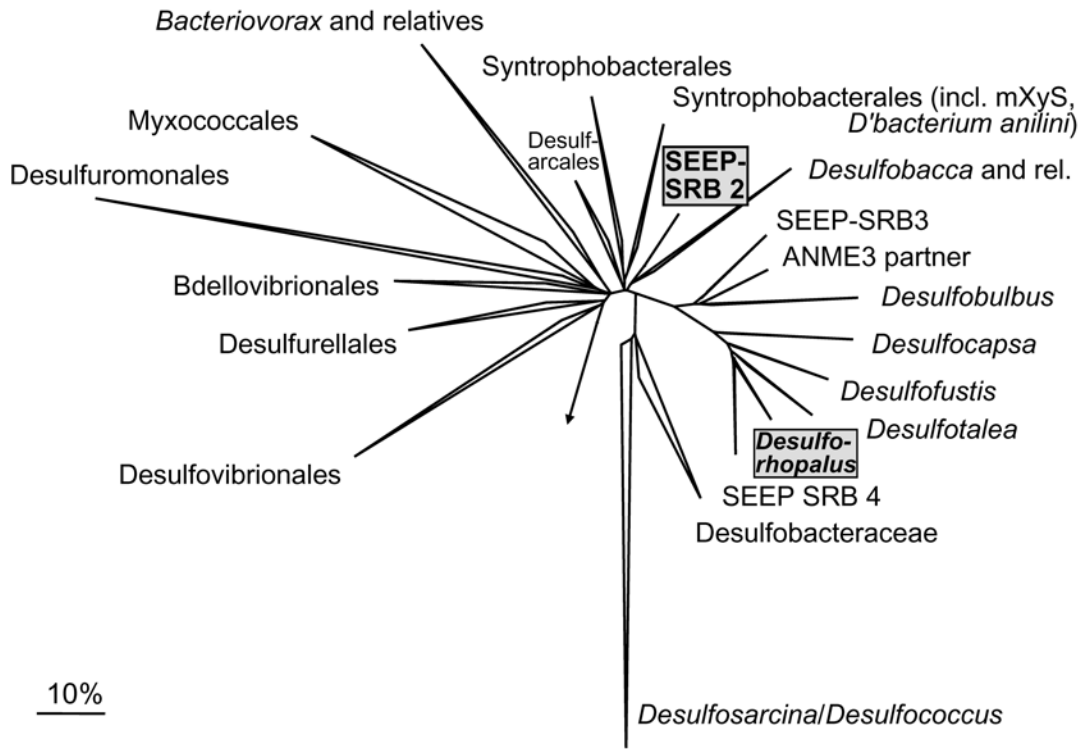


Figure 6.7.



References

- Berner R. A. (1980) *Early Diagenesis: A Theoretical Approach*. Princeton University Press.
- Bian L. Q., Hinrichs K.-U., Xie T. M., Brassell S. C., Iversen H., Fossing H., Jørgensen B. B., and Hayes J. M. (2001) Algal and archaeal polyisoprenoids in a recent marine sediment: Molecular isotopic evidence for anaerobic oxidation of methane. *Geochemistry, Geophysics, Geosystems* **2**, 2000GC000112.
- Biddle J. F., Lipp J. S., Lever M., Lloyd K. G., Sørensen K. B., Anderson K., Fredricks H. F., Elvert M., Kelly T. J., Schrag D. P., Sogin M. L., Brenchley J. E., Teske A., House C. H., and Hinrichs K.-U. (2006) Heterotrophic Archaea dominate sedimentary subsurface ecosystems off Peru. *Proceedings of the National Academy of Science U.S.A.* **103**(10), 3846-3851.
- Blumenberg M., Seifert R., Reitner J., Pape T., and Michaelis W. (2004) Membrane lipid patterns typify distinct anaerobic methanotrophic consortia. *Proceedings of the National Academy of Science U.S.A.* **101**(30), 11111-11116.
- Boetius A., Ravensschlag K., Schubert C. J., Rickert D., Widdel F., Gieseke A., Amann R., Jørgensen B. B., Witte U., and Pfannkuche O. (2000) A marine microbial consortium apparently mediating anaerobic oxidation of methane. *Nature* **407**, 623-626.
- Boetius A. and Suess E. (2004) Hydrate Ridge: a natural laboratory for the study of microbial life fueled by methane from near-surface gas hydrates. *Chemical Geology* **204**.
- Bohrmann G., Greinert J., Suess E., and Torres M. (1998) Authigenic carbonates from the Cascadia subduction zone and their relation to gas hydrate stability. *Geology* **26**(7), 647-650.
- Borowski W. S. (2006) Data report: Dissolved sulfide concentration and sulfur isotopic composition of sulfide and sulfate in pore waters, ODP Leg 204, Hydrate Ridge and vicinity, Cascadia Margin, offshore Oregon. In *Proceedings of the Ocean Drilling Program, Scientific Results*, Vol. 204 (ed. A. M. Tréhu, G. Bohrmann, M. Torres, and F. S. Colwell), pp. 1-13 [Online]. Ocean Drilling Program.
- Brinkhoff T., Santegoeds C., Sahm K., Kuever J., and Muyzer G. (1998) A polyphasic approach to study the diversity and vertical distribution of sulfur-oxidizing Thiomicrospira species in coastal sediments of the German Wadden Sea. *Applied and Environmental Microbiology* **64**, 4650-4657.

- Claypool G. E., Milkov A. V., Lee Y.-J., Torres M., Borowski W. S., and Tomaru H. (2006) Microbial methane generation and gas transport in shallow sediments of an accretionary complex, Southern Hydrate Ridge (ODP Leg 204), offshore Oregon, USA. In *Proceedings of the Ocean Drilling Program, Scientific Results, Volume 204* (ed. A. Tréhu, G. Bohrmann, M. Torres, and F. S. Colwell), pp. 1-52 [Online]. http://www-odp.tamu.edu/publications/204_SR/VOLUME/CHAPTERS/113.PDF. Ocean Drilling Program.
- Coolen M. J. L., Cypionka H., Sass A. M., Sass H., and Overmann J. (2002) Ongoing modification of Mediterranean Pleistocene sapropels mediated by prokaryotes. *Science* **296**(5577), 2407-2410.
- Cragg B. A., Law K. M., Cramp A., Parkes R. J., Robertson A. H. F., Emeis K.-C., Richter C., and Camerlenghi A. (1998) The response of bacterial populations to sapropels in deep sediments of the Eastern Mediterranean (Site 969). In *Proceedings of the Ocean Drilling Program. Scientific Results. Leg 160*, Vol. 160 (ed. O. D. Program), pp. 303-307. Texas A&M University.
- Cragg B. A., Parkes R. J., Fry J. C., Weightman A. J., Rochelle P. A., and Maxwell J. R. (1996) Bacterial populations and processes in sediments containing gas hydrates (ODP Leg 146:Cascadia Margin). *Earth and Planetary Sciences* **139**, 497-507.
- Daly K., Sharp R. J., and McCarthy A. J. (2000) Development of oligonucleotide probes and PCR primers for detecting phylogenetic subgroups of sulfate-reducing bacteria. *Microbiology-UK* **146**, 1693-1705.
- Delong E. F. (1992) Archaea in coastal marine sediments. *Proceedings of the National Academy of Science U.S.A.* **89**, 5685-5689.
- Devereux R., Kane M. D., Winfrey J., and Stahl D. A. (1992) Genus- and group-specific hybridization probes for determinative and environmental studies of sulfate-reducing bacteria. *Systematic Applied Microbiology* **15**, 601-609.
- D'Hondt S., Jørgensen B. B., Miller D. J., Batzke A., Blake R., Cragg B. A., Cypionka H., Dickens G. R., Ferdelman T. G., Hinrichs K.-U., Holm N. G., Mitterer R., Spivack A. J., Wang G., Bekins B., Engelen B., Ford K., Gettemy G., Rutherford S., Sass H., Skillbeck C. G., Aiello I. W., Guerin G., House C. H., Inagaki F., Meister P., Naehr T., Niituma S., Parkes R. J., Schippers A., Smith D. C., Teske A., Wiegel J., Naranjo Padilla C., and Acosta J. L. S. (2004) Distributions of microbial activities in deep seafloor sediments. *Science* **306**, 2216-2221.
- D'Hondt S., Rutherford S., and Spivack A. J. (2002) Metabolic activity of subsurface life in deep-sea sediments. *Science* **295**, 2067-2070.

- Eilers H., Pernthaler J., Glöckner F. O., and Amann R. (2000) Succession of pelagic marine bacteria during enrichment: a close look at cultivation-induced shifts. *Applied and Environmental Microbiology* **66**(11), 3044-3051.
- Elvert M., Boetius A., Knittel K., and Jørgensen B. B. (2003) Characterization of specific membrane fatty acids as chemotaxonomic markers for sulfate-reducing bacteria involved in anaerobic oxidation of methane. *Geomicrobiology Journal* **20**, 403-419.
- Elvert M., Greinert J., Suess E., and Whiticar M. J. (2001) Carbon isotopes of biomarkers derives from methane-oxidizing microbes at Hydrate Ridge, Cascadia convergent margin. In *Natural Gas Hydrates: Occurrence, Distribution, and Dynamics*, Vol. 124 (ed. C. K. Paull and W. P. Dillon), pp. 115-129. American Geophysical Union.
- Elvert M., Suess E., Greinert J., and Whiticar M. J. (2000) Archaea mediating anaerobic methane oxidation in deep-sea sediments at cold seeps of the eastern Aleutian subduction zone. *Organic Geochemistry* **31**, 1175-1187.
- Elvert M., Suess E., and Whiticar M. J. (1999) Anaerobic methane oxidation associated with marine gas hydrates: super-light C-isotopes from saturated and unsaturated c-20 and c-25 irregular isoprenoids. *Naturwissenschaften* **86**, 295-300.
- Harder J. (1997) Species-independent maintenance energy and natural population sizes. *FEMS Microbiology Ecology* **23**, 39-44.
- Heeschen K., Trehu A., and Collier R. W. (2003) Distribution and height of methane bubble plumes on the Cascadia margin characterized by acoustic imaging. *Geophysical Research Letters* **30**(1643-1646).
- Hinrichs K.-U., Hayes J. S., Sylva S. P., Brewer P. G., and Delong E. F. (1999) Methane-consuming archaeobacteria in marine sediments. *Nature* **398**, 802-805.
- Hinrichs K.-U., Summons R. E., Orphan V. J., Sylva S. P., and Hayes J. M. (2000) Molecular and isotopic analysis of anaerobic methane-oxidizing communities in marine sediments. *Organic Geochemistry* **31**, 1651-1701.
- Hobbie J. E., Daley R. J., and Jasper S. (1977) Use of nucleopore filters for counting bacteria for fluorescence microscopy. *Applied and Environmental Microbiology* **33**, 1225-1228.
- Inagaki F., Nunoura T., Nakagawa T., Teske A., Lever M., Lauer A., Suzuki M., Takai K., Delwiche M. E., Colwell F. S., Nealson K. H., Horikoshi K., D'Hondt S., and Jørgensen B. B. (2006) Biogeographical distribution and diversity of microbes in methane hydrate-bearing deep marine sediments on the Pacific Ocean Margin. *Proceedings of the National Academy of Science U.S.A.* **103**(8), 2815-2820.

- Inagaki F., Suzuki M., Takai K., Oida H., Sakamoto T., Aoki K., Nealson K. H., and Horikoshi K. (2003) Microbial communities associated with geological horizons in coastal subseafloor sediments from the Sea of Okhotsk. *Applied and Environmental Microbiology* **69**(12), 7224-7235.
- Joye S. B., Orcutt B. N., Boetius A., Montoya J. P., Schulz H., Erickson M. J., and Lugo S. K. (2004) The anaerobic oxidation of methane and sulfate reduction in sediments from at Gulf of Mexico cold seeps. *Chemical Geology* **205**(3-4), 219-238.
- Kallmeyer J. and Boetius A. (2004) Effects of temperature and pressure on sulfate reduction and anaerobic oxidation of methane in hydrothermal sediments of Guaymas Basin. *Applied and Environmental Microbiology* **70**(2), 1231-1233.
- Kane M. D., Poulsen L. K., and Stahl D. A. (1993) Monitoring the enrichment and isolation of sulfate-reducing bacteria by using oligonucleotide hybridization probes designed from environmentally derived 16S rRNA sequences. *Applied and Environmental Microbiology* **59**, 682-686.
- Kastner M., Sample J. C., Whiticar M. J., Hovland M., Cragg B. A., and Parkes R. J. (1995) Geochemical evidence for fluid flow and diagenesis at the Cascadia convergent margin. In *Proceedings of the Ocean Drilling Program, Scientific Results*, Vol. 146 (ed. B. Carson, G. K. Westbrook, R. J. Musgrave, and E. Suess), pp. 375-384. Ocean Drilling Program.
- Knittel K., Boetius A., Lemke A., Eilers H., Lochte K., Pfannkuche O., and Linke P. (2003) Activity, distribution, and diversity of sulfate reducers and other bacteria in sediments above gas hydrate (Cascadia Margin, Oregon). *Geomicrobiology Journal* **20**, 269-294.
- Knittel K., Lösekann T., Boetius A., Kort R., and Amann R. (2005) Diversity and Distribution of Methanotrophic Archaea at Cold Seeps. *Applied and Environmental Microbiology* **71**(1), 467-479.
- Knoblauch C., Jørgensen B. B., and Harder J. (1999) Community size and specific sulfate reduction rates of psychrophilic sulfate reducing bacteria in arctic marine sediments: evidence for high activity at low temperature. *Applied and Environmental Microbiology* **65**, 4230-4233.
- Könneke M., Bernhard A. E., de la Torre J., Walker C. B., Waterbury J. B., and Stahl D. A. (2005) Isolation of an autotrophic ammonia-oxidizing marine archaeon. *Nature* **437**, 543-546.
- Kulm L. D., Suess E., Moore J. C., Carson S., Lewis B. T., Ritger S. D., Kadko D. C., Thornburg T. M., Embley R. W., Rugh W. D., Massoth G. J., Langseth M. G., Cochrane G. R., and

- Scamman R. L. (1986) Oregon subduction zone: venting, fauna, and carbonates. *Science* **231**, 561-566.
- Lane D. J., Pace B., Olsen G. J., Stahl D. A., Sogin M. L., and Pace N. (1985) Rapid determination of 16S ribosomal RNA sequences for phylogenetic analyses. *Proceedings of the National Academy of Science U.S.A.* **82**, 6955-6959.
- Lanoil B. D., La Duc M. T., Wright M., Kastner M., Neelson K. H., and Bartlett D. (2005) Archaeal diversity in ODP legacy borehole 892b and associated seawater and sediments of the Cascadia Margin. *FEMS Microbiology Ecology* **54**, 167-177.
- Lee M. W. and Collett T. S. (2005) Gas hydrate and free gas saturations estimated from velocity logs on Hydrate Ridge, offshore Oregon, USA. In *Proceedings of the Ocean Drilling Program, Scientific Results Volume 204* (ed. A. Trehu, G. Bohrmann, M. Torres, and F. S. Colwell), pp. 1-25 [Online].
- Lloyd K. G., Lapham L., and Teske A. (2006) An anaerobic-methane oxidizing community of ANME-1b archaea in hypersaline Gulf of Mexico sediments. *Applied and Environmental Microbiology* **72**(11), 7218-7230.
- Lorensen T. D., Colwell F. S., Delwiche M. E., and Dougherty J. (2006) Data report: Acetate and hydrogen concentrations in pore fluids associated with a large gas hydrate reservoir, southern Hydrate Ridge, offshore Oregon, USA. In *Proceedings ODP, Scientific Results, 204*, Vol. 204 (ed. A. M. Tréhu, G. Bohrmann, M. Torres, and F. S. Colwell), pp. 1-20. Ocean Drilling Program.
- Ludwig W., Strunk O., Westram R., Richter L., Meier H., Yadhukumar, Buchner A., Lai T., Steppi S., Jobb G., Förster W., Brettske I., Gerber S., Ginhart A., Gross O., Grumann S., Hermann S., Jost R., König A., Liss T., Lüssmann R., May M., Nonhoff B., Reichel B., Strehlow R., Stamatakis A., Stuckmann N., Vilbig A., Lenke M., Ludwig T., Bode A., and Schleifer K.-H. (2004) ARB: a software environment for sequence data. *Nucleic Acids Research* **32**, 1363-1371.
- Luff R. and Wallmann K. (2003) Fluid flow, methane fluxes, carbonate precipitation and biogeochemical turnover in gas hydrate-bearing sediments at Hydrate Ridge, Cascadia Margin: Numerical modeling and mass balances. *Geochimica et Cosmochimica Acta* **67**(18), 3403-3421.
- Manz W., Eisenbrecher M., Neu T. R., and Szewzyk U. (1998) Abundance and spatial organization of gram negative sulfate-reducing bacteria in activated sludge investigated by in situ probing with specific 16S rRNA targeted oligonucleotides. *FEMS Microbiology Ecology* **25**, 43-61.

- Massana R., Murray A., Preston C. M., and Delong E. F. (1997) Vertical distribution and phylogenetic characterization of marine planktonic archaea in the Santa Barbara Channel. *Applied and Environmental Microbiology* **63**, 50-56.
- Mauclaire L., K. Z., Meister P., and McKenzie J. (2004) Direct *in situ* detection of cells in deep-sea sediment cores from the Peru Margin (ODP Leg 201, Site 1229). *Geobiology* **2**, 217-223.
- Michaelis W., Seifert R., Nauhaus K., Treude T., Thiel V., Blumenberg M., Knittel K., Gieseke A., Peterknecht F., Pape T., Boetius A., Amann R., Jørgensen B. B., Widdel F., Peckmann J., Pimenkov N., and Gulin M. B. (2002) Microbial reefs in the Black Sea fueled by anaerobic methane oxidation. *Science* **297**, 1013-1015.
- Middelburg J. L. (1989) A simple rate model for organic matter decomposition in marine sediments. *Geochimica et Cosmochimica Acta* **53**(7), 1577-1581.
- Milkov A. V., Claypool G. E., Lee Y.-J., and Sassen R. (2005) Gas hydrate systems at Hydrate Ridge offshore Oregon inferred from molecular and isotopic properties of hydrate-bound and void gases. *Geochimica et Cosmochimica Acta* **69**(4), 1007-1026.
- Milkov A. V., Claypool G. E., Lee Y.-J., Xu W., Dickens G. R., Borowski W. S., and Party O. L. S. (2003) In situ methane concentrations at Hydrate Ridge, offshore Oregon: New constraints on the global gas hydrate inventory from an active margin. *Geology* **31**(10), 833-836.
- Millero F. J. and Pierrot D. (1998) A chemical equilibrium model for natural waters. In *Aquatic Geochemistry*, v.4, pp. 153-199.
- Muyzer G., Teske A., Wirsén C. O., and Jannasch H. W. (1995) Phylogenetic relationships of *Thiomicrospira* species and their identification in deep-sea hydrothermal vent samples by denaturing gradient gel electrophoresis of 16S rRNA fragments. *Archives of Microbiology* **164**, 165-172.
- Nauhaus K., Albrecht M., Elvert M., Boetius A., and Widdel F. (2006) *In vitro* cell growth of marine archaeal-bacterial consortia during anaerobic oxidation of methane. *Environmental Microbiology* doi:10.1111/j.1462-2920.2006.01127.x.
- Niemann H., Elvert M., Hovland M., Orcutt B. N., Judd A., Suck I., Gutt J., Joye S. B., Damm E., Finster K., and Boetius A. (2005) Methane emission and consumption at a North Sea gas seep (Tommeliten area). *Biogeosciences* **2**(4), 335-351.
- Niemann H., Lösekann T., de Beer D., Elvert M., Nadalig T., Knittel K., Amann R., Sauter E., Schlüter M., Klages M., Foucher J.-P., and Boetius A. (2006) Novel microbial

- communities of the Haakon Mosby mud volcano and their role as a methane sink. *Nature* **443**, 854-858.
- Orcutt B. N., Boetius A., Elvert M., Samarkin V. A., and Joye S. B. (2005) Molecular biogeochemistry of sulfate reduction, methanogenesis and the anaerobic oxidation of methane at Gulf of Mexico cold seeps. *Geochimica et Cosmochimica Acta* **69**(17), 4267-4281.
- Orcutt B. N., Knittel K., Samarkin V. A., Treude T., Boetius A., and Joye S. B. (In preparation) Impact of oil and higher hydrocarbons on microbial diversity, distribution and activity in Gulf of Mexico cold seep sediments.
- Orphan V. J., Hinrichs K.-U., Ussler W., III, Paull C. K., Taylor L. T., Sylva S. P., Hayes J. M., and Delong E. F. (2001a) Comparative analysis of methane-oxidizing archaea and sulfate-reducing bacteria in anoxic marine sediments. *Applied and Environmental Microbiology* **67**(4), 1922-1934.
- Orphan V. J., House C. H., Hinrichs K.-U., McKeegan K. D., and Delong E. F. (2001b) Methane-consuming archaea revealed by directly coupled isotopic and phylogenetic analysis. *Science* **293**, 484-487.
- Orphan V. J., House C. H., Hinrichs K.-U., McKeegan K. D., and Delong E. F. (2002) Multiple archaeal groups mediate methane oxidation in anoxic cold seep sediments. *Proceedings of the National Academy of Science U.S.A.* **99**, 7663-7668.
- Parkes R. J., Cragg B. A., and Wellsbury P. (2000) Recent studies on bacterial populations and processes in sub seafloor sediments: a review. *Hydrogeology Journal* **8**, 11-28.
- Parkes R. J., Webster G., Cragg B. A., Weightman A. J., Newberry C. J., Ferdelman T. G., Kallmeyer J., Jørgensen B. B., Aiello I. W., and Fry J. C. (2005) Deep sub-seafloor prokaryotes stimulated at interfaces over geologic time. *Nature* **436**, 390-394.
- Pernthaler A., Pernthaler J., and Amann R. (2002) Fluorescence in situ hybridization and catalyzed reporter deposition for the identification of marine bacteria. *Applied and Environmental Microbiology* **68**(6), 3094-3101.
- Ravenschlag K., Sahm K., Pernthaler J., and Amann R. (1999) High bacterial diversity in permanently cold marine sediments. *Applied and Environmental Microbiology* **65**, 3982-3989.
- Schippers A. and Neretin L. N. (2006) Quantification of microbial communities in near-surface and deeply buried marine sediments on the Peru continental margin using real-time PCR. *Environmental Microbiology* **doi:10.1111/j.1462-2920.2006.01019.x**.

- Schippers A., Neretin L. N., Kallmeyer J., Ferdelman T. G., Cragg B. A., Parkes R. J., and Jørgensen B. B. (2005) Prokaryotic cells of the deep sub-seafloor biosphere identified as living bacteria. *Nature* **433**, 861-864.
- Schubotz F. (2005) Investigation of Intact Polar Lipids of Bacteria Isolated from the Deep Marine Subsurface. Masters, University of Bremen.
- Sørensen K. B., Lauer A., and Teske A. (2004) Archaeal phylotypes in a metal-rich and low-activity deep subsurface sediment of the Peru Basin, ODP Leg 201, Site 1231. *Geobiology* **2**, 151-161.
- Sørensen K. B. and Teske A. (2006) Stratified communities of active archaea in deep marine subsurface sediments. *Applied and Environmental Microbiology* **72**(7), 4596-4603.
- Stumm W. and Morgan J. J. (1981) *Aquatic Chemistry: An Introduction Emphasizing Chemical Equilibria in Natural Waters*. John Wiley & Sons.
- Sturt H. F., Summons R. E., Smith K., Elvert M., and Hinrichs K.-U. (2004) Intact polar membrane lipids in prokaryotes and sediments deciphered by high-performance liquid chromatography/electrospray ionization multistage mass spectrometry - new biomarkers for biogeochemistry and microbial ecology. *Rapid Communications in Mass Spectrometry* **18**, 617-628.
- Suess E., Torres M., Bohrmann G., Collier R. W., Greinert J., Linke P., Rehder G., Trehu A., Wallmann K., Winckler G., and Zuleger E. (1999) Gas hydrate destabilization: enhanced dewatering, benthic material turnover and large methane plumes at the Cascadia convergent margin. *Earth and Planetary Science Letters* **170**(1-2), 1-15.
- Teske A. (2006) Microbial communities of deep marine subsurface sediments: Molecular and cultivation surveys. *Geomicrobiology Journal* **23**, 357-368.
- Teske A., Hinrichs K.-U., Edgecomb V., de Vera Gomez A., Kysela D., Sylva S. P., Sogin M. L., and Jannasch H. W. (2002) Microbial diversity of hydrothermal sediments in the Guaymas Basin: Evidence for anaerobic methanotrophic communities. *Applied and Environmental Microbiology* **68**(4), 1994-2007.
- Torres M., McManus J., Hammond D. E., de Angelis M. A., Heeschen K., Colbert S. L., Tyron M. D., Brown K. M., and Suess E. (2002) Fluid and chemical fluxes in and out of sediments hosting methane hydrate deposits on Hydrate Ridge, OR. I: hydrological provinces. *Earth and Planetary Science Letters* **201**, 525-540.
- Torres M. and Rugh W. D. (2006) Data report: Isotopic characterization of dissolved inorganic carbon in pore waters, Leg 204. In *Proceedings of the Ocean Drilling Program, Scientific*

Results, Volume 204, Vol. 204 (ed. A. Tréhu, G. Bohrmann, M. Torres, and F. S. Colwell). Ocean Drilling Program.

- Torres M., Wallmann K., Trehu A., Bohrmann G., Borowski W. S., and Tomaru H. (2004) Gas hydrate growth, methane transport, and chloride enrichment at the southern summit of Hydrate Ridge, Cascadia margin off Oregon. *Earth and Planetary Science Letters* **226**, 225-241.
- Tréhu A., Bohrmann G., Torres M., and Colwell F. S. (2006) Proceedings of the Ocean Drilling Program, Scientific Results, 204. Ocean Drilling Program.
- Tréhu A., Long P. E., Torres M., Bohrmann G., Rack F. R., Collett T. S., Goldberg D. S., Milkov A. V., Riedel M., Schulteiss P., Bangs N. L., Barr S. R., Borowski W. S., Claypool G. E., Delwiche M. E., Dickens G. R., Gracia E., Guerin G., Holland M., Johnson J. E., Lee Y.-J., Liu C.-S., Su X., Teichert B., Tomaru H., Vanneste M., Watanabe M., and Weinberger J. L. (2004) Three-dimensional distribution of gas hydrate beneath southern Hydrate Ridge: constraints from ODP Leg 204. *Earth and Planetary Science Letters* **222**, 845-862.
- Tréhu A. M., Bohrmann G., Rack F. R., Torres M., and al. e. (2003) Proceedings of the Ocean Drilling Program, Initial Reports, Leg 204 [Online] http://www-odp.tamu.edu/publications/204_IR/204ir.htm. Ocean Drilling Program.
- Treude T. (2003) Anaerobic oxidation of methane in marine sediments. Ph.D. dissertation, University of Bremen.
- Treude T., Boetius A., Knittel K., Wallmann K., and Jørgensen B. B. (2003) Anaerobic oxidation of methane above gas hydrates at Hydrate Ridge, NE Pacific Ocean. *Marine Ecological Progress Series* **264**, 1-14.
- Tyron M. D., Brown K. M., Torres M., Trehu A., McManus J., and Collier R. W. (1999) Measurements of transience and downward fluid flow near episodic methane gas vents, Hydrate Ridge, Cascadia. *Geology* **27**(1075-1078).
- Webster G., Parkes R. J., Cragg B. A., Newberry C. J., Weightman A. J., and Fry J. C. (2006) Prokaryotic community composition and biogeochemical processes in deep seafloor sediments from the Peru Margin. *FEMS Microbiology Ecology* **58**, 65-85.
- Wellsbury P., Goodman K., Barth T., Cragg B. A., Barnes S. P., and Parkes R. J. (1997) Deep marine biosphere fuelled by increasing organic matter availability during burial and heating. *Nature* **388**, 573-576.

- Whitman W. B., Coleman D. C., and Wiebe W. J. (1998) Prokaryotes: The unseen majority. *Proceedings of the National Academy of Science U.S.A.* **95**, 6578-6583.
- Widdel F. and Bak F. (1992) Gram-negative mesophilic sulfate-reducing bacteria. In *The Prokaryotes* (ed. A. Balows, H. G. Trüper, M. Dworkin, W. Harder, and K.-H. Schleifer), pp. 3352-3378. Springer.
- Zengler K., Richnow H. H., Rossello-Mora R., Michaelis W., and Widdel F. (1999) Methane formation from long-chain alkanes by anaerobic microorganisms. *Nature* **40**, 266-269.
- Zhou J., Brunns M. A., and Tiedje J. M. (1996) DNA recovery from soils of diverse composition. *Applied and Environmental Microbiology* **62**, 316-322.

CHAPTER 7

CONSTRAINTS ON MECHANISMS AND RATES OF ANAEROBIC OXIDATION OF METHANE BY ANME-2 CONSORTIA¹

¹ Orcutt, B!, C. Meile. In preparation for *Biogeosciences*

Abstract

Anaerobic oxidation of methane (AOM) is the main process responsible for the removal of methane generated in Earth's subsurface environments. However, the biochemical mechanism of AOM, performed by methanotrophic archaea and sulfate reducing bacteria, remains elusive. Explicitly resolving the observed spatial arrangement of the microbes, potential intermediates involved in the electron transfer between the methane oxidizing and sulfate reducing partners are investigated via a consortia-scale reaction transport model that integrates experimental data with thermodynamic and kinetic controls on microbial activity. The results show that neither hydrogen, acetate, nor formate is exchanged fast enough via diffusion to achieve measured rates of metabolic activity. Higher rates of intermediate production lead to increased diffusive fluxes, but the build-up of the exchangeable species causes the energy yield of AOM to drop below that required for ATP production. A mechanism other than the diffusive exchange of intermediate metabolites to translocate electrons from the inner core to the outer shell or the environment may play an important role in the functioning these microbial aggregates.

1. Introduction

Methane, a potent greenhouse gas produced in anoxic regions of the ocean's subsurface, is largely prevented from entering the overlying water column and reaching the atmosphere by the activity of microorganisms living in marine sediments. Geochemical evidence indicates that the net consumption of methane (CH₄) in these anoxic environments is linked to the consumption of sulfate (SO₄²⁻) according to (BARNES and GOLDBERG, 1976; DEVOL et al., 1984; HOEHLER et al., 1994; IVERSEN and JØRGENSEN, 1985; REEBURGH, 1976):



Results from DNA- and lipid-based investigations indicate that the consumption of sulfate and methane is mediated via a syntrophic relationship between sulfate-reducing bacteria (SRB) and methanotrophic archaea (ANME, after ANaerobic METHanotroph; (BOETIUS et al., 2000; ELVERT et al., 1999; HINRICHS et al., 2000; HOEHLER et al., 1994; ORPHAN et al., 2001), and three distinct phylogenetic clades of ANMEs and multiple SRB groups have been identified which may be involved with this process (KNITTEL et al., 2003).

Attempts to isolate these microorganisms in culture so far have been unsuccessful (NAUHAUS et al., 2002a) and significant gaps remain in understanding the biochemical mechanism of AOM, including on how the processes of AOM and sulfate reduction (SR) are linked to one another (HOEHLER et al., 1994; NAUHAUS et al., 2002a; SØRENSEN et al., 2001; VALENTINE and REEBURGH, 2000). The concentrations of potential intermediates involved in electron exchange, produced during methane oxidation and consumed during sulfate reduction (Table 7.1), likely play a significant role in regulating consortia energetics, as high concentrations thermodynamically favor SR but lower the energy yield for the ANME. Thus, a consortia relying on these two processes for energy production can only function within a certain

range of concentrations of the intermediate compound, unless production and consumption are spatially separated enough to allow for a sufficient concentration difference between regions of active AOM and SR. Based on free energy yields in a setting with diffusive exchange of intermediates between an ANME and a nearby SRB cell, SØRENSEN et al. (2001) suggested that hydrogen and acetate are not feasible intermediates at low (tens of μM) methane concentrations modeled, representative of shallow water environments. Arguing for lower *in situ* maintenance energy requirements of the consortia, STROUS AND JETTEN (2004) found that acetate is a thermodynamically favorable intermediate in settings with abundant methane ($>10\text{ mM}$, such as seep environments), while exchange of formate is thermodynamically feasible at lower methane concentrations.

Here we re-evaluate thermodynamic and kinetic constraints on the function of an ANME/SRB consortia by modeling the potential intermediate exchange scenarios on the scale of the consortia. By explicitly resolving the spatial arrangement of the consortia, we (i) investigate the thermodynamic feasibility of a number of proposed intermediates, (ii) study the impact of aggregate size on the overall process energetics, (iii) compare the effect of different SRB to ANME ratios, (iv) assess the role of minimum energy requirements for the functioning of the consortia and (v) consider the potential for a pathway reversal of the archaea. These intrinsic microbial factors are discussed in the environmental contexts with and without a significant feedback from AOM. Finally, model results at the consortia scale are compared with available rate data.

2. Model implementation

2.1. Consortia arrangement

While a variety of spatial arrangements of the syntrophic partners has been described (KNITTEL et al., 2005; ORPHAN et al., 2001; ORPHAN et al., 2002), one of the predominant AOM-mediating communities of ANME/SRB consortia are found in a spherical arrangement in which SRB form a shell around an inner core of archaea belonging to the ANME-2 cluster, spatially separating SR from AOM (Fig. 7.1). From a survey on “shell-type” consortia sizes, cell sizes, and ANME:SRB abundance ratios, which were determined via 16S rRNA-based fluorescence in situ hybridization methods (BOETIUS et al., 2000; KNITTEL et al., 2003; KNITTEL et al., 2005; NAUHAUS et al., 2006; ORPHAN et al., 2001), a few trends emerged (Table 7.2). First, ANME-2 and SRB cells identified in these consortia tend to be 0.5 and 0.4 μm in diameter, respectively. Second, the ratio of the radius of the zone of ANME to the entire aggregate remains close to 0.73. Dividing the shell volumes by the respective average cell volumes leads to 3 SRB cells for every 1 ANME cell. In the model, the aggregate is placed into an environment of radius r_{env} set to at least twice the aggregate radius (Fig. 7.1).

2.2. Governing equations

The concentration of any chemical species (C_i) is subject to diffusion within the free fluid fraction of the consortia and production/consumption reactions:

$$\frac{\partial C}{\partial t} = \nabla \cdot (D \nabla C) + R \quad (\text{Eq. 2})$$

where t is time, D is the in-situ diffusion coefficient, and R equals the net of production and consumption terms of species i , representing methane (CH_4), dissolved inorganic carbon, sulfide, sulfate (SO_4^{2-}) and the exchangeable species, (i.e. H_2 , formate or acetate). pH is assumed constant at 8, and all sulfide and dissolved inorganic carbon was assumed to be in the form of HS^- and HCO_3^- . The domain is represented by a quadrant of a sphere cross-section rotating about

a vertical axis and mirrored horizontally. The model is, implemented in the finite element simulation environment COMSOL[®] and solved at steady state using a direct solver (UMFPACK).

At the outer edge of the model domain, an “environmental” concentration is imposed for all species. In simulations in which the consortium is considered the main source for the exchangeable species, a no gradient condition for the exchangeable species is imposed at the outer domain boundary.

Diffusion coefficients in aqueous solution (D_{aq}) are obtained from literature values, assuming a temperature of 8°C (Table 7.3). Aggregates *in situ* are typically embedded in a thick organic matrix (KNITTEL et al., 2005; ORPHAN et al., 2001). Estimating its effect on diffusion from experiments with EPS, the diffusion coefficient is reduced by a factor f_{eps} , set to 0.25 for organic ions and to 0.6 for inorganic ions and gases (STEWART, 2003). Taking into account tortuosity (θ^2), the *in situ* diffusion coefficient is defined as:

$$D = f_{eps} D_{aq} / \theta^2 \quad (\text{Eq. 3})$$

where θ^2 is set to 2.5. Assuming densest spherical packing of spherical cells with a free volume fraction of 26% (MARTIN et al., 1997), comparison to tortuosity datasets (BOUDREAU, 1997) suggests this may result in an overestimate of the effective diffusion coefficient, but leads to values of effective diffusion coefficients at the lower end of the range determined experimentally in microbial mats (WIELAND et al., 2001).

2.3. Reactions and Rate Laws

The reactions in AOM and SR zone can be generalized as follows:





where EX represents the intermediate species which acts as the electron carrier between AOM and SR (Table 7.1). AOM occurs exclusively within the inner sphere of ANME in the aggregate while SR is restricted to the outer shell of the aggregate. The rate laws contain both kinetic and thermodynamic factors and a Monod-type dependence on the substrates of each reaction:

$$R_{\text{AOM}} = k_{\text{AOM}} * B_{\text{ANME}} * [\text{CH}_4]/(\text{KmCH}_4 + [\text{CH}_4]) * F_{\text{TAOM}} \quad (\text{Eq. 6})$$

$$R_{\text{SR}} = k_{\text{SR}} * B_{\text{SRB}} * [\text{EX}]/(\text{KmEX} + [\text{EX}]) * [\text{SO}_4^{2-}]/(\text{KmSO}_4 + [\text{SO}_4^{2-}]) * F_{\text{TSRI}} \quad (\text{Eq. 7})$$

In the above equations, R_{AOM} and R_{SR} are the AOM and SR rates (in units of $\text{nmol cm}^{-3} \text{d}^{-1}$), respectively; k_{AOM} and k_{SR} the cell specific rate constants of AOM and SR, respectively ($\text{nmol cell}^{-1} \text{d}^{-1}$); B_{ANME} and B_{SRB} the cell densities of ANME in the inner core and SRB within the outer shell of the consortium (cells cm^{-3}), respectively; $[C_i]$ represents the concentration of species i ; KmCH_4 , KmEX and KmSO_4 the Monod rate constants for methane, the exchangeable species and sulfate, respectively; and F_{TAOM} and F_{TSRI} the “thermodynamic potential” factor for AOM and SR, respectively (JIN and BETHKE, 2003). Baseline values of various parameters are presented in Table 7.4. All cells are assumed to have the same turnover potential such that k_{AOM} and k_{SR} are population specific constants.

The thermodynamic potential factors (F_{TX} , where X represents either AOM or SR) reflect that there must be sufficient free energy available from the reactions to fuel ATP synthesis and cell maintenance. For instance, if the concentration of the intermediate species would make AOM energetically unfavorable, regardless of the availability of methane for consumption, methane oxidation is assumed not to take place. F_{TX} is defined as:

$$F_{\text{TX}} = \max(0, 1 - \exp(f_x / (\chi RT))) \quad (\text{Eq. 8})$$

where χ , the number of ATP synthesized per reaction, equals 1, R is the universal gas constant (8.314 J K⁻¹ mol⁻¹) and T is the absolute temperature (281.15 K). f_X represents the thermodynamic driving force for reaction X , relating the free energy yield of reaction X to the energy required to synthesize ATP (JIN and BETHKE, 2003) and is determined as:

$$f_X = -\Delta G_X - m\Delta G_{ATP} \quad (\text{Eq. 9})$$

Here, ΔG_X is the free energy yield of reaction X under in situ conditions, i.e.

$$\Delta G_X = \Delta G_X^0 + RT \ln\left(\prod a_i^{v_i}\right) \quad (\text{Eq. 10}).$$

ΔG_X^0 is the standard free energy yield of reaction X , determined from the free energy of formation of the species involved in the reactions (Table 7.3), a_i represents the activity of species i , computed based on the activity coefficients given in Table 7.3, and v_i are the stoichiometric coefficients. m in Eq. 9 is the number of ATP synthesized per electron transferred. Explicit measurements of m for AOM do not exist, as no pure cultures of AOM-mediating microorganisms can be manipulated for such as study. Available genomic data indicate that AOM may occur via a reversal of the enzymatic process of methanogenesis (HALLAM et al., 2003; HALLAM et al., 2004; KRÜGER et al., 2003), thus we estimate m based on available data from methanogenic archaea, presented by DUPPENMEIER (2002). In methanogenesis, the final enzymatic step catalyzed by methyl coenzyme A reductase creates a heterodisulfide of coenzymes B and S. The cleavage of this heterodisulfide by oxidoreductases fuels electron transport in the cell, which is accompanied by proton translocation (4 H⁺/2 e⁻) and drives ATP synthesis. Thus, there is 1 ATP synthesized per 2 electrons transported, and $m = 1/2$. ΔG_{ATP} in equation 9 represents the threshold energy limit for growth, which is often assumed to be the energy required to synthesize ATP. Assuming ~60 kJ/mol ATP to form ATP from ADP and phosphate and that three protons are translocated per ATP produced (SCHINK, 1997; THAUER et

al., 1977), this energetic limit is on the order of 20 kJ/mol H⁺, though it has been shown experimentally that some methanogens can survive with a free energy yield of 12-16 kJ/mol H⁺ (JACKSON and MCINERNEY, 2002). Even lower threshold energy limits of 4 kJ/mol H⁺ have been proposed (as reviewed in (DALE et al., 2006)). In our model, a range of $m\Delta G_{ATP}$ values from 0-20 kJ/mol H⁺ is considered. Note that Eq. 8 restricts the value of F_{TX} to the range between 0 and 1 and hence does not allow for a back reaction.

3. Results and Discussion

To quantify thermodynamic and kinetic influences on the rates of AOM performed by the ANME/SRB shell-type consortia, model simulations were conducted in which poorly constrained parameter values were varied systematically. Unless indicated otherwise, hydrogen is considered as the exchangeable species, as the high stoichiometric dependence of the rates of AOM and SR on hydrogen (Table 7.1) may promote significant concentration gradients at the consortia scale. To facilitate comparison of model results for different parameterizations, volume averages for the inner ANME core or the outer SRB shell are presented. Simulations that result in conditions with drastic changes at or below the scale of individual cell sizes, e.g. complete thermodynamic inhibition of AOM within one cell diameter distance from the zone of SR, are not included in the analysis. As our simulations consistently indicated much stronger thermodynamic challenges for the ANME compared to the SRB, the presentation of the results highlights the sensitivity of F_{TAOM} towards poorly constrained process parameters.

3.1. Substrate affinity

In the absence of experimental data on the nature of and kinetic properties related to the intermediate species, the impact of substrate affinity on AOM rates and thermodynamic limitations are investigated over a range of characteristic values: measured hydrogen concentrations in or around the zone of AOM typically range from 0.1- 1 nM (FINKE, 2003; HOEHLER et al., 1994; HOEHLER et al., 1998), and in a recent model to describe AOM in coastal marine sediments, DALE et al. (2006) estimated a half saturation constant K_{mH_2} of 10 nM and identified this as a parameter that significantly impacted R_{AOM} .

Performing simulations for a 25 μm outer diameter (OD) consortia under no gradient conditions, a high K_m value for hydrogen such as that used by DALE et al. (2006) leads to H_2 concentrations that preclude ATP production unless k_{SR} is 10x higher than k_{AOM} (Fig. 7.2). Additionally, at this K_m , only when k_{AOM} is 10^{-10} $\text{nmol cell}^{-1} \text{d}^{-1}$ or lower can the average F_{TAOM} approach unity. Average F_{TAOM} does not approach unity until the average hydrogen concentration is less than 1 nM. It should be noted that in these simulations with the $K_m = 10$ nM and at low ratios of k_{SR}/k_{AOM} , the outer edge of the ANME sphere still maintains a high F_{TAOM} even though the majority of the sphere has an F_{TAOM} close or equal to zero, suggesting shutdown of AOM. As the limits on hydrogen consumption for the SRB decrease (i.e. lower K_m), the F_{TAOM} increases towards 1 for all combinations of k_{AOM} and k_{SR} .

3.2. Aggregate size and distribution

For a given set of parameters, F_{TAOM} is closer to unity in the smaller consortia than in the larger ones (Fig. 7.3). For example, under conditions of no flux of hydrogen at the environmental boundary when both k_{AOM} and k_{SR} equal 10^{-9} $\text{nmol cell}^{-1} \text{d}^{-1}$, and the K_{mH_2} is 1 nM, F_{TAOM} is unity for the 4 μm consortia, ~ 0.6 for the 12 μm consortia, and ~ 0.4 for the 25 μm

consortia (Fig. 7.3). Additionally, at these k -values, F_{TAOM} is homogenous in the smaller consortia, while in the larger ones F_{TAOM} is only above zero in a very narrow band next to the contact with the SRB shell (not shown). Despite the small spatial scales, as the consortia grows larger in size, hydrogen cannot diffuse out of the inner core fast enough or that some of the areas of production are too far away from the SRB to be consumed. This leads to a build up of hydrogen that shuts AOM down in the most of the ANME core for settings with lower exchange area to ANME volume ratios.

For typical aggregate density of 10^7 per cm^3 , aggregates are likely $>10 \mu\text{m}$ apart. Over the range of expected distances to the environmental boundary, however, there is little difference in the trend in F_{T} , even when imposing high hydrogen concentrations - assumed to be maintained by processes external to the aggregates - at the outer domain boundary (Fig. 7.4). Even when imposing smaller aggregate distances, on the order of $1 \mu\text{m}$, F_{TAOM} is only slightly diminished (data not shown), indicating that the distribution of aggregates in otherwise homogeneous sediments does not influence our findings.

3.3. Sensitivity towards transport parameters and speciation

The impact of the organic matrix on diffusion transport is poorly known, and removing the impact of EPS on diffusion lessened thermodynamic limitation (i.e. higher F_{TAOM} without EPS; not shown). However, even for organic ions with a low value of f_{eps} , the magnitude of the change was not large enough to significantly modify the overall trend of thermodynamic limitation preventing a rate of AOM that matches expected values (see below). As k_{AOM} values increase, the exchangeable species production exceeds the speed at which it can diffuse to the SR zone for removal, thus leading to a situation where no free energy is available for AOM.

Additionally, regulation of solution pH may cause deviations from the assumed constant pH and affect the speciation of chemical species. At a pH of 8, bicarbonate and hydrogen sulfide are the dominant forms of dissolved organic carbon (DIC) and sulfide. As the *in situ* pH is not known, simulations were performed for pH ranging from 3 to 11, considering both the impact on hydrogen ion concentrations and speciation of DIC and sulfide on free energy. Taking into account the different species constituting of DIC and total sulfide had its largest impact on reaction energies at high pH values (i.e. higher F_{TAOM} when $pH > 10$) although the magnitude of the change was slight (<10%; data not shown). Furthermore, the limited set of chemical species considered in the model may also lead to an overestimate of free metabolites. To obtain an estimate of this effect, speciation calculations considering acetate and formate in seawater were performed, indicating free acetate and formate to be >70% of the total concentrations. Furthermore, an order-of-magnitude reduction of the free intermediate concentrations in the calculation of ΔG did lead to a similar overall trend in F_{TAOM} for each of the exchangeable species, even though complexation slightly lessened the thermodynamic limitation (not shown).

3.4. Can ANME “switch” metabolic modes to produce methane for energy generation?

Experimental evidence suggests that some ANME might perform methanogenesis under *in situ* conditions, although at a lower relative rate than that of AOM (ORCUTT et al., 2005; TREUDE et al., In press). To test whether environmental conditions and consortia dynamics may induce oscillatory modes of metabolism or whether the radiotracer data more likely reflects a spurious back reaction, the model was modified to allow the ANME to “switch” metabolic modes from methanotrophy to methanogenesis based on their local environment. In the absence of experimental data it is for simplicity assumed that the rate of methanogenesis proceeds at an

intrinsic rate comparable to the one of methanotrophy and is also subject to thermodynamic constraints:

$$R_{MG} = k_{AOM} B_{ANME} F_{TMG} \quad (\text{Eq. 11})$$

where F_{TMG} is defined by Eq. 8 with $f_X = -f_{AOM}$.

Under no gradient conditions at the domain boundary, the hydrogen concentration within the consortia never reaches a high enough steady state value to make methanogenesis favorable, regardless of size in the entire range considered ($3 \mu\text{m} < r_{\text{agg}} < 25 \mu\text{m}$; not shown). At high values of k_{AOM} , AOM is basically shut down because of hydrogen production, but H_2 concentrations never build up enough to cause a switch to methanogenesis.

In contrast, when environmental concentrations of hydrogen are imposed, hydrogen concentration in the AOM zone can reach values sufficiently high for reverse methanotrophy to become energetically feasible (Fig. 7.5). However, at environmental hydrogen concentrations typical of AOM zones (0.1-1 nM), methanogenesis is not favorable; conditions are favorable for AOM, although once k_{AOM} reaches 10^{-7} nmol/cell/d, the zone of activity (i.e where $F_{TAOM} > 0$) is smaller than the diameter of an ANME cell and is therefore considered unrealistic. When the outside hydrogen concentration is 10 nM, a value more typical for deeper methanogenic sedimentary zones or possible in highly reduced fluids, the steady state hydrogen concentration within the consortia is high enough to permit methanogenesis. When the k_{AOM} is 10^{-9} nmol/cell/d, methanogenesis is favorable for $k_{SR} \leq k_{AOM}$ ($F_T < 0$; Fig. 7.5) while for $k_{SR} \sim 1-10 \times k_{AOM}$, hydrogen concentrations in the inner core neither favor AOM nor MOG; once k_{SR} exceeds $10 \times k_{AOM}$, hydrogen concentrations are brought down to levels that make AOM favorable. A similar trend is observed when $k_{AOM} = 10^{-8}$ nmol/cell/d, although AOM becomes favorable for k_{SR} only 2x greater than k_{AOM} . Additionally, F_T approaches unity when k_{SR} is $10 \times k_{AOM}$ when

k_{AOM} equals 10^{-8} nmol/cell/d; for the 10^{-9} nmol/cell/d conditions, an F_T of unity is not reached until k_{SR} is 100x k_{AOM} (not shown). At higher k_{AOM} values, the zone of activity becomes smaller than the diameter of an ANME cell. Note that at no instance is methanogenesis and methanotrophy observed simultaneously within the ANME core.

3.5. What is the exchangeable species ?

The concentration of acetate in systems with AOM varies over a wide range from 100's of nM to 100's of μ M. When considering acetate as an intermediate species under no gradient conditions, the concentration of acetate does not build up enough within the aggregate to make MOG favorable (Fig. 7.6). At a k_{AOM} of 10^{-8} nmol cell⁻¹ d⁻¹, AOM is barely favorable for the larger aggregate and moderately favorable for the smaller aggregate. When imposing the environmental acetate concentration at domain boundary, AOM is energetically not favorable, except at concentrations lower than one might expect to find in situ (i.e. 10 nM), where AOM is slightly favorable, but never reaches an F_{TAOM} of 1 under the conditions tested. Additionally, when the k_{AOM} value exceeds 10^{-8} nmol cell⁻¹ d⁻¹, AOM gets restricted to a zone immediately adjacent to the SRB only. Considering the production of both acetate and hydrogen (0.5 and 2 per methane consumed, Table 7.1) by the ANME in the inner core, both of which are consumed in the SRB shell (VALENTINE and REEBURGH, 2000), yielded similar results.

Another potential candidate for the exchangeable species in the AOM/SR syntrophy is formate. As for hydrogen and acetate, under no gradient conditions for formate at the environmental boundary, the concentration of formate never builds up enough within the consortia to allow MOG to be favorable. The F_{TAOM} (and thus R_{AOM}) patterns of formate and

acetate are highly similar under the no gradient and forced conditions tested, which is likely a reflection of the similarities in transport properties.

Previous examinations of the syntrophic AOM/SR consortia indicate that methane availability may determine which compounds can be feasible electron shuttles (SØRENSEN et al., 2001; STROUS and JETTEN, 2004). At lower methane concentrations (1 mM) the model predicts lower F_{TAOM} lead to higher thermodynamic limitation of AOM; however, the overall trend was similar and the F_T values did not vary substantially when using the lower methane concentration (not shown).

3.6. Comparison to rate measurements

Model simulations are compared to a data set measured in ANME-2/SRB consortia enriched from Hydrate Ridge (NAUHAUS et al., 2006). In this experiment, a near ten-fold increase in AOM-mediating community abundance corresponded to a ~ten-fold increase in the rate of activity; at the end of the experiment the rate of activity in the enrichment was measured at approximately 2.5×10^5 nmol (gram wet sediment, gws)⁻¹ d⁻¹. To compare model simulations with experimental values, the methane consumption for a given size aggregate is multiplied by the number of aggregates in that size class in 1 gram of sediment at the end of the experiment (Table 7.5). This approach takes into account the potential for reduced AOM rates in the center of larger aggregate and considers the relative contribution of that size aggregate to the total rate. For example, a rate of AOM calculated for a 25 µm OD consortium is multiplied by the density of this size class of aggregates (4.4×10^8 aggregates gram dry weight⁻¹, Table 7.5) and assuming that this aggregate size class contributes ~70% of the total rate, with the remaining 30% being contributed by other size classes.

The highest k_{AOM} value that leads to a positive F_{TAOM} in a zone wider than a cell diameter is on the order of 10^{-8} nmol/cell/d, in both the small and large aggregate (Figs. 3, 6). This value is roughly an order of magnitude smaller than the value estimated from experimental measurements assuming abundant substrate and no thermodynamic limitation (Table 7.4). The modeled rate of activity is therefore lower than what was measured in the experiment: Even if all ANME behaved like those in the 3 μm OD consortia, the highest possible rate was ~ 20 x lower than what was measured; if all ANME behaved like those in the 25 μm OD consortia, the highest possible rate was ~ 200 x lower than the measured value. Note that these simulations were run at a low energy threshold stringency of $m\Delta G_{ATP}$ equaling 4 kJ/mol. If a higher energy threshold were used (i.e. $m\Delta G_{ATP}$ of 20 kJ/mol), AOM would be even less favorable.

4. Conclusions

Model simulations indicate that all investigated compounds have the potential to sustain a syntrophic AOM/SR relationship. However, neither hydrogen nor acetate nor formate can be exchanged between the ANME and SRB at a high enough rate to achieve rates that resemble measured bulk values., because increasing rate constants causes the exchangeable species builds up in the inner core faster than it can be removed by diffusion and consumption by the SRB. Thus, thermodynamic limitations set in and prevent high rates of AOM. Examining the impact of poorly constrained parameters, including transport coefficients, the effect of chemical speciation, methane concentration and pH revealed that these parameters affect the thermodynamic constraints of AOM, though not to a large enough degree to substantially change this finding.

A number of factors may cause this observed discrepancy between model estimates and measured rates, including intrinsic variations in cell specific rates across consortia sizes, substantial modification of the local chemical environment through active cross-membrane transport (e.g. proton pumps), or that hydrogen, acetate or formate are not the intermediate species. Alternatively, a more complex geometry than the one considered may facilitate contact between the syntrophic partners, or other physiological adaptations, including a network of nanowire-like structures (REGUERA et al., 2006), that allows for a more efficient exchange between ANME and SRBs may alleviate the identified thermodynamic constraints.

Acknowledgements

We would like to thank Antje Boetius and Katja Nauhaus for sharing raw experiment data on consortia dynamics and Samantha Joye for helpful discussion. This work was supported by a National Science Foundation Graduate Research Fellowship to B.O. and a fellowship from the Hanse Institute for Advanced Studies fellowship to C.M. that provided hospitality and financial support in Delmenhorst, Germany. C.M. also acknowledges partial support by the Office of Science of the United States Department of Energy (DE-FG02-05ER25676).

References

- Barnes R. O. and Goldberg E. D. (1976) Methane production and consumption in anaerobic marine sediments. *Geology* **4**, 297-300.
- Boetius A., Ravensschlag K., Schubert C. J., Rickert D., Widdel F., Gieseke A., Amann R., Jørgensen B. B., Witte U., and Pfannkuche O. (2000) A marine microbial consortium apparently mediating anaerobic oxidation of methane. *Nature* **407**, 623-626.
- Boudreau B. P. (1997) *Diagenetic models and their implementation*. Springer-Verlag.
- Dale A. W., Regnier P., and van Cappellen P. (2006) Bioenergetic controls on anaerobic oxidation of methane (AOM) in coastal sediments: A theoretical analysis. *American Journal of Science* **306**, 246-294.
- Devol A. H., Anderson J. J., Kuivila K., and Murray J. W. (1984) A model for coupled sulfate reduction and methane oxidation in the sediments of Saanich Inlet. *Geochimica et Cosmochimica Acta* **48**, 993-1004.
- Duppenmeier U. (2002) Redox-driven proton translocation in methanogenic Archaea. *Cellular Molecular Life Science* **59**, 1513-1533.
- Elvert M., Suess E., and Whiticar M. J. (1999) Anaerobic methane oxidation associated with marine gas hydrates: super-light C-isotopes from saturated and unsaturated c-20 and c-25 irregular isoprenoids. *Naturwissenschaften* **86**, 295-300.
- Finke N. (2003) The role of volatile fatty acids and hydrogen in the degradation of organic matter in marine sediments. Doctoral, University of Bremen.
- Girguis P. R., Cozen A. E., and Delong E. F. (2005) Growth and population dynamics of anaerobic methane-oxidizing archaea and sulfate-reducing bacteria in a continuous-flow bioreactor. *Applied and Environmental Microbiology* **71**(7), 3725-3733.
- Girguis P. R., Orphan V. J., Hallam S. J., and Delong E. F. (2003) Growth and methane oxidation rates of anaerobic methanotrophic archaea in a continuous-flow bioreactor. *Applied and Environmental Microbiology* **69**(9), 5472-5482.
- Hallam S. J., Girguis P. R., Preston C. M., Richardson P. M., and Delong E. F. (2003) Identification of methyl coenzyme M reductase A (*mcrA*) genes associated with methane-oxidizing archaea. *Applied and Environmental Microbiology* **69**(9), 5483-5491.

- Hallam S. J., Putnam N., Preston C. M., Detter J. C., Rokhsar D., Richardson P. M., and Delong E. F. (2004) Reverse methanogenesis: Testing the hypothesis with environmental genomics. *Science* **305**, 1457-1462.
- Hinrichs K.-U., Summons R. E., Orphan V. J., Sylva S. P., and Hayes J. M. (2000) Molecular and isotopic analysis of anaerobic methane-oxidizing communities in marine sediments. *Organic Geochemistry* **31**, 1651-1701.
- Hoehler T. M., Alperin M. J., Albert D. B., and Martens C. S. (1994) Field and laboratory studies of methane oxidation in an anoxic marine sediment - evidence for a methanogen-sulfate reducer consortium. *Global Biogeochemical Cycles* **8**, 451-463.
- Hoehler T. M., Alperin M. J., Albert D. B., and Martens C. S. (1998) Thermodynamic control on hydrogen concentrations in anoxic sediments. *Geochimica et Cosmochimica Acta* **62**, 1745-1756.
- Iversen N. and Jørgensen B. B. (1985) Anaerobic methane oxidation rates at the sulfate-methane transition in marine sediments from Kattegat and Skagerrak (Denmark). *Limnology and Oceanography* **30**, 944-955.
- Jackson B. E. and McNerney M. J. (2002) Anaerobic microbial metabolism can proceed close to thermodynamic limits. *Nature* **415**, 454-456.
- Jin Q. and Bethke C. M. (2003) A new rate law describing microbial respiration. *Applied and Environmental Microbiology* **69**(4), 2340-2348.
- Knittel K., Boetius A., Lemke A., Eilers H., Lochte K., Pfannkuche O., and Linke P. (2003) Activity, distribution, and diversity of sulfate reducers and other bacteria in sediments above gas hydrate (Cascadia Margin, Oregon). *Geomicrobiology Journal* **20**, 269-294.
- Knittel K., Lösekann T., Boetius A., Kort R., and Amann R. (2005) Diversity and Distribution of Methanotrophic Archaea at Cold Seeps. *Applied and Environmental Microbiology* **71**(1), 467-479.
- Krüger M., Meyerdiecks A., Glockner F. O., Amann R., Widdel F., Kube M., Reinhardt R., Kahnt R., Bocher R., Thauer R. K., and Shima S. (2003) A conspicuous nickel protein in microbial mats that oxidize methane anaerobically. *Nature* **426**, 878-881.
- Martin I., Dozin B., Quarto R., Cancedda R., and Beltrame F. (1997) Computer-based technique for cell aggregation analysis and cell aggregation in in vitro chondrogenesis. *Cytometry* **28**, 141-146.

- Millero F. J. and Pierrot D. (1998) A chemical equilibrium model for natural waters. In *Aquatic Geochemistry*, v.4, pp. 153-199.
- Nauhaus K., Albrecht M., Elvert M., Boetius A., and Widdel F. (2006) *In vitro* cell growth of marine archaeal-bacterial consortia during anaerobic oxidation of methane. *Environmental Microbiology* doi:10.1111/j.1462-2920.2006.01127.x.
- Nauhaus K., Boetius A., Krueger M., and Widdel F. (2002a) *In vitro* demonstration of anaerobic oxidation of methane coupled to sulfate reduction from a marine gas hydrate area. *Environmental Microbiology* **4**, 296-305.
- Nauhaus K., Boetius A., Krüger M., and Widdel F. (2002b) *In vitro* demonstration of anaerobic oxidation of methane coupled to sulfate reduction from a marine gas hydrate area. *Environmental Microbiology* **4**, 296-305.
- Orcutt B. N., Boetius A., Elvert M., Samarkin V. A., and Joye S. B. (2005) Molecular biogeochemistry of sulfate reduction, methanogenesis and the anaerobic oxidation of methane at Gulf of Mexico cold seeps. *Geochimica et Cosmochimica Acta* **69**(17), 4267-4281.
- Orphan V. J., Hinrichs K.-U., Ussler W., III, Paull C. K., Taylor L. T., Sylva S. P., Hayes J. M., and Delong E. F. (2001) Comparative analysis of methane-oxidizing archaea and sulfate-reducing bacteria in anoxic marine sediments. *Applied and Environmental Microbiology* **67**(4), 1922-1934.
- Orphan V. J., House C. H., Hinrichs K.-U., McKeegan K. D., and Delong E. F. (2002) Multiple archaeal groups mediate methane oxidation in anoxic cold seep sediments. *Proceedings of the National Academy of Science U.S.A.* **99**, 7663-7668.
- Reeburgh W. S. (1976) Methane consumption in Cariaco Trench waters and sediments. *Earth and Planetary Science Letters* **28**, 337-344.
- Reguera G., Nevin K. P., Nicoll J. S., Covalla S. F., Woodard T. L., and Lovley D. R. (2006) Biofilm and nanowire production leads to increased current in *Geobacter sulfurreducens* fuel cells. *Applied and Environmental Microbiology* **72**(11), 7345-7348.
- Schink B. (1997) Energetics of syntrophic cooperation in methanotrophic degradation. *Microbial Molecular Biology Review* **61**, 262-280.
- Sørensen K. B., Finster K., and Ramsing N. B. (2001) Thermodynamic and kinetic requirements in anaerobic methane oxidizing consortia exclude hydrogen, acetate, and methanol as possible electron shuttles. *Microbial Ecology* **42**, 1-10.

- Stewart P. S. (2003) Diffusion in biofilms. *Journal of Bacteriology* **185**(5), 1485-1491.
- Strous M. and Jetten M. S. M. (2004) Anaerobic oxidation of methane and ammonium. *Annual Reviews of Microbiology* **2004**(58), 99-117.
- Stumm W. and Morgan J. J. (1981) *Aquatic Chemistry: An Introduction Emphasizing Chemical Equilibria in Natural Waters*. John Wiley & Sons.
- Thauer R. K., Jungermann K., and Decker K. (1977) Energy conservation in chemotrophic anaerobic bacteria. *Microbiological Reviews* **41**, 100-180.
- Treude T., Orphan V. J., Knittel K., Gieseke A., House C. H., and Boetius A. (In press) Consumption of methane and CO₂ by methanotrophic microbial mats from gas seeps of the anoxic Black Sea. *Applied and Environmental Microbiology*.
- Valentine D. L. and Reeburgh W. S. (2000) New perspectives on anaerobic methane oxidation. *Environmental Microbiology* **2**(5), 477-484.
- Wieland A., de Beer D., Damgaard L. R., Kühl M., and van Dusschoten D. (2001) Fine-scale measurement of diffusivity in a microbial mat with nuclear magnetic resonance imaging. *Limnology and Oceanography* **46**(2), 248-259.

Table 7.1. Potential coupled reactions of AOM and SR discussed elsewhere in the literature, (SØRENSEN et al., 2001; VALENTINE and REEBURGH, 2000) and the corresponding standard free energy yield of the reactions, estimated using data from (STUMM and MORGAN, 1981).

<u>Reaction couples</u>	<u>ΔG° (kJ/mol)</u>
<u>Hydrogen transfer</u>	
$\text{CH}_4 + 3\text{H}_2\text{O} \rightarrow \text{HCO}_3^- + \text{H}^+ + 4\text{H}_2$	229.1
$\text{SO}_4^{2-} + 4\text{H}_2 + \text{H}^+ \rightarrow \text{HS}^- + 4\text{H}_2\text{O}$	-262.0
<u>Acetate transfer</u>	
$\text{CH}_4 + \text{HCO}_3^- \rightarrow \text{CH}_3\text{COO}^- + \text{H}_2\text{O}$	14.8
$\text{SO}_4^{2-} + \text{CH}_3\text{COO}^- \rightarrow 2\text{HCO}_3^- + \text{HS}^-$	- 47.7
<u>Formate transfer</u>	
$\text{CH}_4 + 3\text{HCO}_3^- \rightarrow 4\text{HCOO}^- + \text{H}^+ + \text{H}_2\text{O}$	154.0
$\text{SO}_4^{2-} + 4\text{HCOO}^- + \text{H}^+ \rightarrow 4\text{HCO}_3^- + \text{HS}^-$	-186.9
<u>Hydrogen and Acetate transfer</u>	
$2\text{CH}_4 + 2\text{H}_2\text{O} \rightarrow \text{CH}_3\text{COO}^- + 4\text{H}_2 + \text{H}^+$	243.9
$4\text{H}_2 + \text{SO}_4^{2-} + \text{H}^+ \rightarrow \text{HS}^- + 4\text{H}_2\text{O}$	-262.0
$\text{CH}_3\text{COO}^- + \text{SO}_4^{2-} \rightarrow \text{HS}^- + 2\text{HCO}_3^-$	- 47.7

Table 7.2. Survey of available data on AOM/SR-mediating consortia sizes, cell sizes, and cell ratios.

Reference	consortia size, diameter (μm)	inner core diameter (μm)	layers of SRB in outer shell	outer shell width (μm)	# ANME cells in aggregate	# SRB cells in aggregate	SRB:ANME ratio
(NAUHAUS et al., 2006)	3	2.2	1	0.4	63	189	3
(NAUHAUS et al., 2006)	6	4.4	2	0.8	504	1513	3
(NAUHAUS et al., 2006)	12	8.8	4	1.6	4034	12100	3
(NAUHAUS et al., 2006)	18	13.2	6	2.4	13616	40839	3
(NAUHAUS et al., 2006)	25	18.6	8	3.2	38094	106261	3
(KNITTEL et al., 2005)	7.6	5.6	2.5	1	1040	3045	2.9
(BOETIUS et al., 2000)	3.2	2.3	~1	0.45	72	238	3.3

Table 7.3. Properties of compounds considered in the model.

Compound	D_{aq} at 8°C ^a Units: [cm ² d ⁻¹]	ΔG formation ^b [kJ/mol]	Activity coefficients ^c <i>unitless</i>	Boundary value ^d [mM]
hydrogen (H ₂)	1.217	17.55	1	10 ⁻⁷ – 10 ⁻⁵
bicarbonate (HCO ₃ ⁻)	0.326	-586.9	0.642	2
methane (CH ₄)	0.462	-34.4	1	19
hydrogen sulfide (HS ⁻)	0.478	12.1	0.604	1
formate (HCOO ⁻)	0.420	-351	0.604	10 ⁻⁶ – 10 ⁻⁴
acetate (CH ₃ COO ⁻)	0.329	-369.4	0.642	10 ⁻⁵ – 10 ⁻³
sulfate (SO ₄ ²⁻)	0.296	-744.6	0.152	20

^a diffusion coefficients from (BOUDREAU, 1997)

^b Free energy of formation values from (STUMM and MORGAN, 1981). G_f^0 of H⁺ and H₂O are 0 and -237.1 kJ/mol, respectively.

^c Activity coefficients (γ) calculated as $\log \gamma_i = (-0.51 * z_i^2 * \sqrt{\mu_i}) / (1 + (\alpha_i * (\sqrt{\mu_i}) / 305))$, where z_i represents the charge of species i , μ_i represents the ionic strength of solution (set to seawater, 0.72), and α_i represents the ionic size of the species i (MILLERO and PIERROT, 1998).

^d applicable in imposed concentration simulations; concentrations derived from growth experiments (NAUHAUS et al., 2006).

Table 7.4. Model parameters

Parameter	Description	Values	Units
KmCH ₄	Half-saturation constant for methane in AOM	1	mM
KmEX	Half-saturation constant for exchangeable species in SR	10 ⁻⁷ to 10 ⁻³	mM
KmSO ₄	Half-saturation constant for sulfate in SR for SRB	1	mM
R _{AOM}	Rate of AOM	Eq. 6	nmol cm ⁻³ d ⁻¹
R _{SR}	Rate of SR	Eq. 7	nmol cm ⁻³ d ⁻¹
R _{AOMsed}	Rate of AOM in sediment	calculated (see text)	nmol gws ⁻¹ d ⁻¹
R _{SRsed}	Rate of SR in sediment	calculated (see text)	nmol gws ⁻¹ d ⁻¹
k _{AOM}	Per cell turnover rate of methane by ANME	varied ^a	nmol cell ⁻¹ d ⁻¹
k _{SR}	Per cell turnover rate of sulfate by SRB	varied ^a	nmol cell ⁻¹ d ⁻¹
B _{ANME}	Cell density of ANME in inner core of consortia ^b	1.1 x 10 ¹⁶	cells l ⁻¹
B _{SRB}	Cell density of SRB in outer shell of consortia ^b	2.2 x 10 ¹⁶	cells l ⁻¹
FT _{AOM}	Thermodynamic factor of AOM	0 to 1	unitless
FT _{SR}	Thermodynamic factor of SR	0 to 1	Unitless
mΔG _{ATP}	Minimum energy threshold	4-22	kJ mol ⁻¹

^a An estimate for rate constants was obtained from data in NAUHAUS et al. (2006), assuming no substrate or thermodynamic limitations; cell specific rate in this experiment result in k_{AOM} ~ 10⁻⁷ – 10⁻⁶ nmol d⁻¹ cell⁻¹ and are comparable to estimates from other data sets (10⁻¹⁰ to 10⁻⁵; (GIRGUIS et al., 2005; GIRGUIS et al., 2003; KNITTEL et al., 2005; NAUHAUS et al., 2002b; ORCUTT et al., 2005).

^b The number of cells within an aggregate was obtained by dividing the volume of the inner core and the outer shell by an estimate of the respective cell volumes and assuming densest even packing (NAUHAUS et al., 2006), which resulted in 11.1 cells μm⁻³ in the inner core and 22.2 cells μm⁻³ in the outer shell, respectively (B_{ANME} and B_{SRB}).

Table 7.5. Consortia size and abundance measured in ANME/SRB aggregates (agg.) enriched from Hydrate Ridge sediment at the beginning (Beg.) and end of the experiment (NAUHAUS et al., 2006).

$\mu\text{m OD}$	# ANME agg. ⁻¹	agg.*10 ⁶ gws ⁻¹		% ags		cells gws ⁻¹		% cells	
		Beg.	End	Beg.	End	Beg.	End	Beg.	End
3	63	40.6	436.9	75	76	2.56 x 10 ⁹	2.75 x 10 ¹⁰	3	2
6	504	8.22	57.7	15	10	4.15 x 10 ⁹	2.91 x 10 ¹⁰	5	2
12	4034	2.98	32.9	5	6	1.20 x 10 ¹⁰	1.33 x 10 ¹¹	13	9
18	13615	1.21	18.1	2	3	1.65 x 10 ¹⁰	2.46 x 10 ¹¹	18	17
25	38094	1.47	25.9	3	5	5.60 x 10 ¹⁰	9.87 x 10 ¹¹	61	69

Figure captions

Figure 7.1. AOM and SR mediating consortia. ANME (red) and SRB (green) consortium from Eel River Basin methane-seep sediments surrounded in a layer of exopolymeric saccharide (yellow), modified from (ORPHAN et al., 2002). The modeled geometrical arrangement is indicated by the white circles. The upper shaded quadrant denotes the model domain (with an inner aggregate radius r^* , an outer radius of the aggregate r and an environmental radius r_{env}), employing axial symmetry around the vertical axis, mirrored on the horizontal midsection plane denoted by the dotted horizontal line.

Figure 7.2. Values of F_{TAOM} in a 25 μm OD aggregate for various combinations of k_{AOM} and k_{SR} (units of $\text{nmol cell}^{-1} \text{d}^{-1}$) when K_{mH_2} equals 10 nM or 0.1 nM.

Figure 7.3. Values of F_{TAOM} for various combinations of k_{AOM} and k_{SR} when K_{mH_2} equals 1 nM and the size of the consortia is 4, 12 or 25 μm OD.

Figure 7.4. Values of F_{TAOM} for a 3 μm OD consortia when K_{mH_2} for SRB is 0.1 nM, H_2 equals 10 nM at the environmental boundary placed at $r_{env} = 2$ or 10 μm . The contour surfaces are highly similar; thus, the surface for the 10 μm condition is transparent and overlain on the 2 μm condition and the arrows distinguish the difference between the two.

Figure 7.5. Values of F_T for a 3 μm OD consortia when K_{mH_2} for SRB is 0.1 nM and the environmental concentration of hydrogen is forced to be 0.1, 1 or 10 nM, respectively. F_T varies between -1 and 0 when $\Delta G_{\text{methanogenesis}} (= -\Delta G_{AOM})$ is more negative than the minimum energy

quantum required for ATP production and methanogenesis becomes active. In an intermediate range, both forward and backward reaction are not feasible and the archaea are considered inactive ($F_{\text{TMG}} = F_{\text{TAOM}} = 0$), while at more negative ΔG_{AOM} , methane gets oxidized, indicated by F_{T} ranging from 0 to 1 (Eq. 8).

Figure 7.6. Values of F_{TAOM} for a 25 μm OD aggregate (left) and a 3 μm OD aggregate (right) under no gradient conditions when $K_{\text{mAc}} = 1, 10$ or 100 nM.

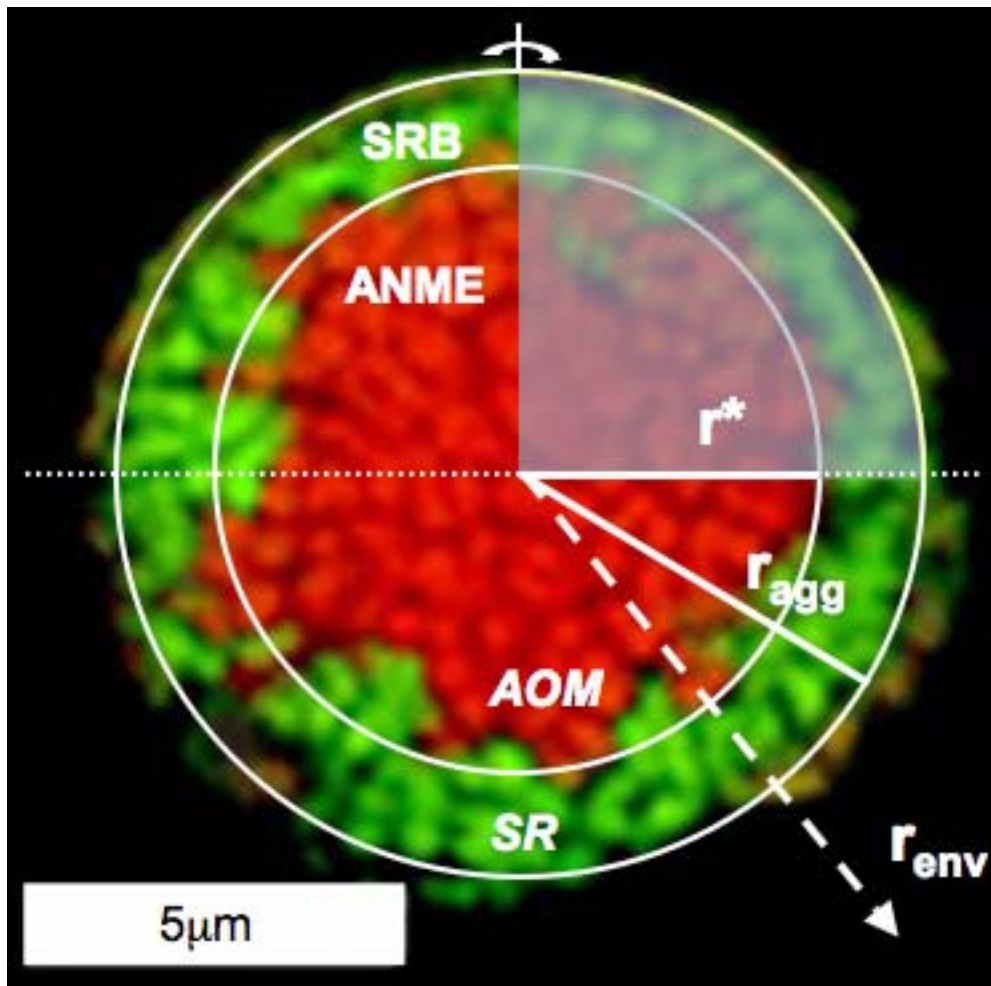


Figure 7.1.

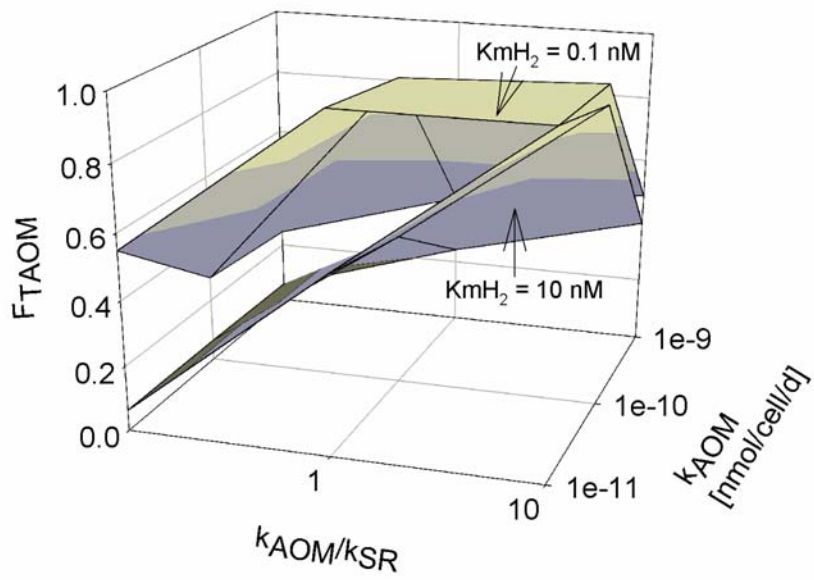


Figure 7.2.

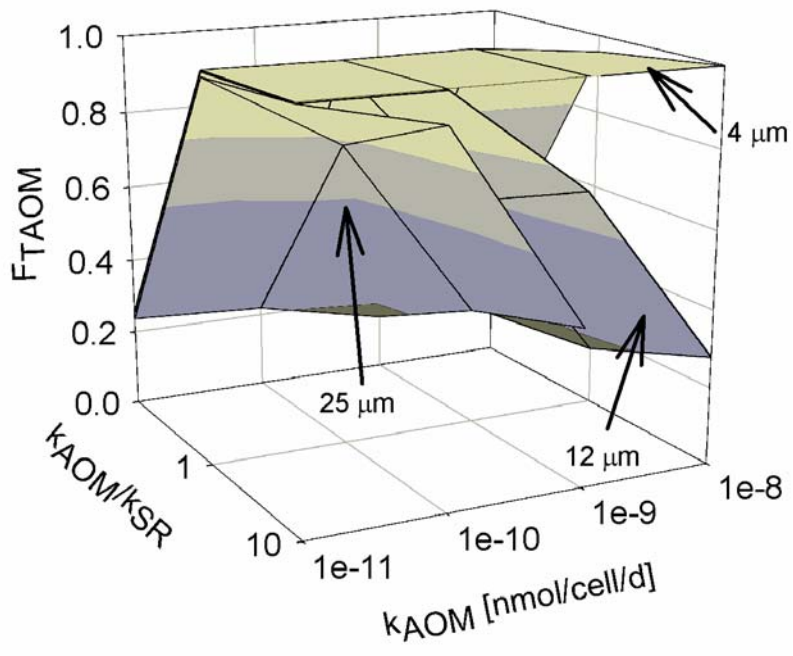


Figure 7.3.

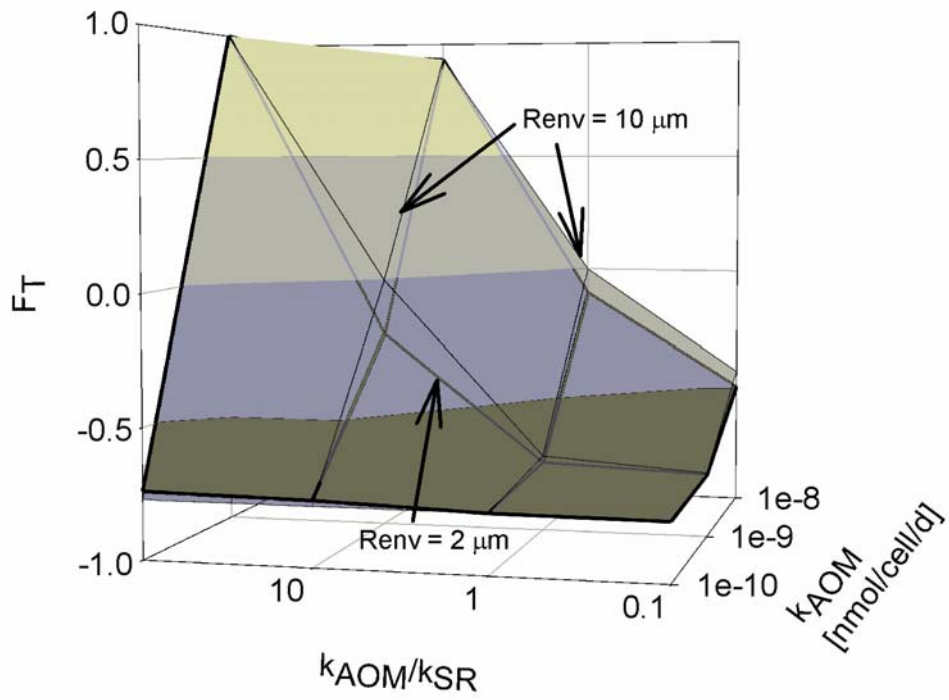


Figure 7.4.

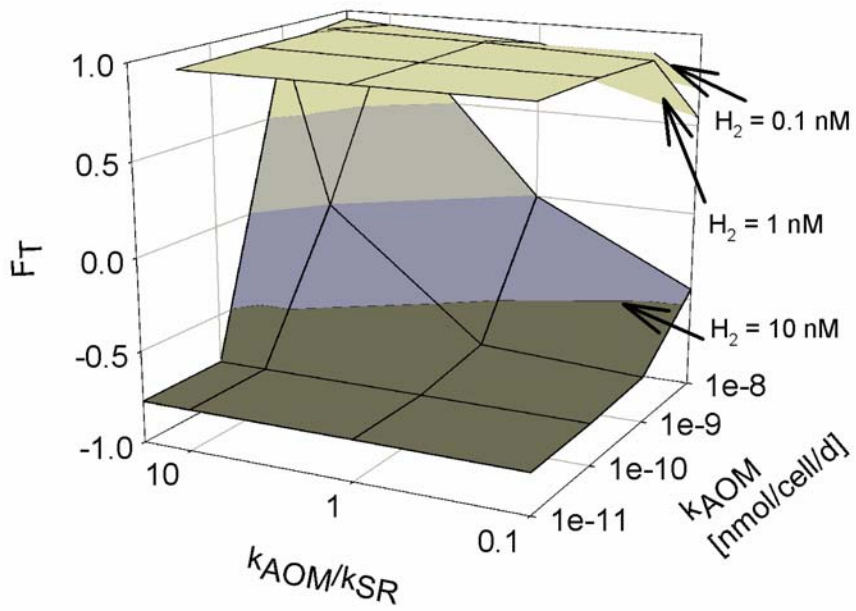


Figure 7.5.

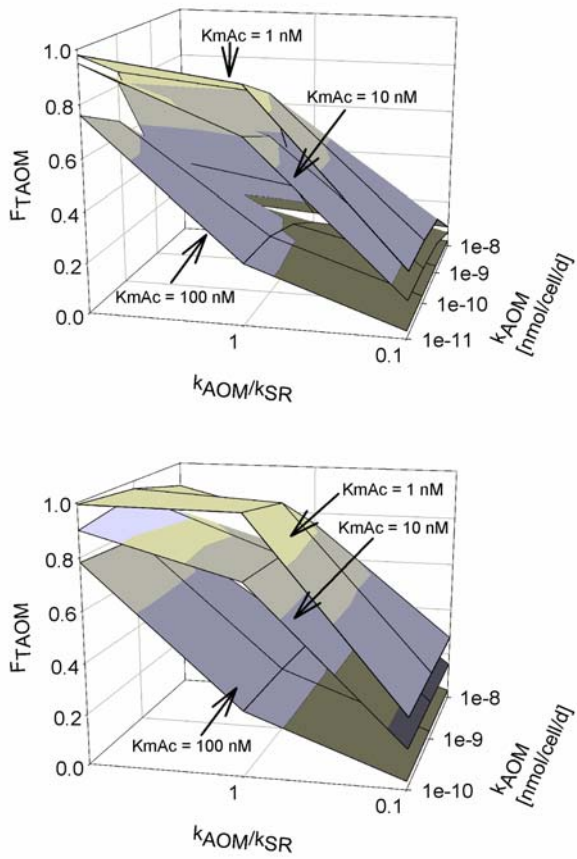


Figure 7.6.

CHAPTER 8

CONCLUSIONS

This dissertation began by exploring the intrigues of microbially-mediated methane cycling in anaerobic marine environments. After demonstrating the global importance of the anaerobic oxidation of methane (AOM) as a process that largely prevents the release of sedimentary methane, a greenhouse gas, to the hydrosphere and atmosphere, the current state of knowledge and theories on the microbial biogeochemistry and molecular ecology of AOM and associated processes were defined. Inspired by the insights brought to AOM research by application of methods from the molecular ecological tool-kit, I sought to investigate AOM-mediating communities found in two uncharacterized methane-rich systems – the Gulf of Mexico and the deep biosphere of Hydrate Ridge – using a multidisciplinary approach that combined biogeochemical, molecular ecological (DNA- and lipid-based), and modeling techniques.

To determine how the microbial methane filter operated in these systems, I set out to ascertain how AOM was coupled to other biogeochemical processes and which factors influenced the diversity and distribution of AOM-mediating microbes. Through these endeavors, my colleagues and I confirmed that the ANME-1 and -2 clades of methanotrophic archaea are responsible for AOM in surficial sediments in the Gulf of Mexico (Chapters 2, 3, & 4) and were the first to demonstrate that the ANMEs are also involved in the production of methane, although at a fraction of the rate of AOM (Chapters 2, 3 & 4). Our work was the first to directly document microbial activity within gas hydrate material collected from the Gulf of Mexico,

which suggests that microbial activity may impact the biogeochemical cycling of methane within the unique gas hydrate niche (Chapter 5). Active populations of both *Bacteria* and *Archaea* were observed in a methane-rich deep biosphere environment (Chapter 6), in contrast to previous studies which suggest that one or the other domain is dominant. In methane-rich areas of the deep subsurface, ANME were detected for the first time in an area where sulfate levels were elevated, although AOM may be limited in the deep biosphere by the availability of sulfate coupled with slow growth rates. *Crenarchaeota* likely play an important role in methane cycling elsewhere in the deep subsurface although it does not appear that they incorporate methane-derived carbon into biomass (Chapter 6). Unlike at other cold seeps which have been studied to date, sulfate reduction (SR) in Gulf of Mexico surficial sediments is often uncoupled from AOM and is also fueled by other endogenous hydrocarbons and petroleum derivatives (Chapters 2, 3, & 4); the identity of the microorganisms which mediate sulfate-dependent hydrocarbon oxidation *in situ* is unclear but likely includes members of the seep-endemic *Deltaproteobacteria* sulfate reducing bacterial clades (Chapter 3). Modeling approaches to determine the potential intermediate compound exchanged within consortia of ANME and SRB to sustain AOM and SR revealed that hydrogen, acetate and formate cannot sustain rates of activity that match measured values due to diffusion-limited removal of the intermediate compound (Chapter 7).

These investigations also highlight future avenues of exploration in AOM research. Although the involvement of ANME communities in methane production activity was repeatedly observed, the mechanism of this occurrence is unclear. By exploiting the recently available environmental genomic libraries from anaerobic methane oxidizing communities, gene products which are potentially involved in the AOM reaction or closely related to known methanogenic pathways could be experimentally tested for methanotrophic or methanogenic activity.

Similarly, biochemical pathways related to the production or consumption of the still unknown intermediate of AOM might be elucidated by coupling enrichment experiments with functional gene or protein expression. Detection of microbial activity within methane hydrate offers intriguing speculation that successful ecological strategies for living in ice may be possible in other icy locations such as permafrost or perhaps on other planets. Future research with gas hydrate using *in vitro* pressure experiments is needed to evaluate the range and dynamics of microbial activity. Our detection of anaerobic methanotrophic archaea in the deep biosphere of Hydrate Ridge in similar settings where other researchers did not find them highlights the methodological-related difficulties in understanding microbial distribution and activity in the deep marine subsurface, the largest habitat for microbial life on Earth, a supports the need for developing robust methods among the deep biosphere research community. These investigations will provide deeper understanding of the mechanistic foundation of AOM, a globally significant sink for the greenhouse gas methane.